

Proteomic Pattern in Pre-eclampsia

Thesis Submitted to AcSIR
for the Award of the Degree of

Doctor of Philosophy

In

BIOLOGICAL SCIENCES



By

Sheon Mary Samji

10BB11J26130

Under the guidance of

Dr. Ashok P. Giri (Research supervisor)

Dr. Mahesh J. Kulkarni (Research co-supervisor)



Biochemical Sciences Division
CSIR-National Chemical Laboratory
Pune 411008, India

2017



सीएसआईआर - राष्ट्रीय रासायनिक प्रयोगशाला

(वैज्ञानिक तथा औद्योगिक अनुसंधान परिषद)

डॉ. होमी भाभा मार्ग, पुणे - 411 008. भारत



CSIR - NATIONAL CHEMICAL LABORATORY

(Council of Scientific & Industrial Research)

Dr. Homi Bhabha Road, Pune - 411 008. India

CERTIFICATE

This is to certify that the work incorporated in this Ph.D thesis entitled “**Proteomic Pattern in Pre-eclampsia**” submitted by **Ms. Sheon Mary Samji** to the Academy of Scientific and Innovative Research (AcSIR) in fulfilment of the requirement for the award of the degree of **Doctor of Philosophy**, embodies original research work under our guidance. We further certify that this work has not been submitted to any other University or institution in part or full for the award of any degree of diploma. Research material obtained from other sources has been duly acknowledged in the thesis. Any text, illustration, table, etc., used in the thesis from other sources have been duly cited and acknowledged.

Sheon Mary Samji
(Student)

Dr. Mahesh J. Kulkarni
(Research co-supervisor)

Dr. Ashok P. Giri
(Research supervisor)

Date: 1st March 2017

Place: Pune

Dedicated to all the mothers...

*I will protect you
Until you are grown
And then I will let you fly free
But loving you
That is for always...*

-Charlotte Gray

Table of Contents

Declaration by Research Scholar -----	11
Acknowledgement -----	13
List of Tables -----	16
List of Figures -----	17
List of Accompanying Material -----	19
Definitions/Abbreviations-----	20
Preface -----	22
Chapter 1 Introduction -----	26
1.1 Human placenta -----	26
1.2 Pregnancy complications-----	26
1.3 Pre-eclampsia -----	26
1.4 Definition and diagnosis -----	26
1.5 Prevention and management-----	29
1.6 Pathophysiology and etiological factors -----	29
1.6.1 Placental hypoxia -----	29
1.6.2 Oxidative stress-----	30
1.6.3 Angiogenic factors -----	31
1.6.4 Immunological factors-----	32
1.6.5 Renin-angiotensin system-----	32
1.6.6 Genetics and epigenetics -----	33
1.7 Proteomics: need and origin -----	34
1.8 Developments in proteomics: In relation to protein identification-----	36
1.9 Application of proteomics in the field of disease identification and biomarker development -----	37
1.10 Proteomics in pregnancy -----	38
1.11 Proteomic approaches in pre-eclampsia -----	39
1.11.1 Changes in body fluid proteins in PE pathogenesis -----	40
1.11.2 Placental proteome in PE pathogenesis -----	44
1.11.3 Cell lines for PE studies and their application in proteomic analysis ---	45
1.11.4 Autoantibodies in PE pathogenesis: Can they serve as biomarkers? ----	45
1.11.5 PTMs in pre-eclampsia-----	46
Chapter 2 Biochemical insights into the pathophysiology of pre-eclampsia through placental proteomics- Part 1 (gel based proteomics) -----	48
2.1 Background -----	48
2.2 Material and Methods -----	49

2.2.1	Sample collection -----	49
2.2.2	Protein extraction and two dimensional gel electrophoresis (2DE)-----	50
2.2.3	In-gel digestion and nano LC-MS ^E protein identification -----	50
2.2.4	Western blot analysis -----	51
2.2.5	RNA extraction and qPCR -----	52
2.2.6	Statistical Analysis -----	52
2.2.7	Gene Ontology Analysis -----	52
2.3	Results and Discussion -----	53
2.3.1	Proteomic profiling of normal and pre-eclamptic placentas -----	53
2.3.2	Gene ontology of differential expressed proteins revealed numerous biological processes affected that are related to the etiological factors of pre-eclampsia -----	55
2.3.3	Validation of differentially expressed protein-----	60
Chapter 3 Biochemical insights into the pathophysiology of pre-eclampsia through placental proteomics- Part 2 (gel free proteomics) -----		70
3.1	Background -----	70
3.2	Materials and methods-----	70
3.2.1	Sample collection -----	70
3.2.2	Protein extraction from placental tissue-----	71
3.2.3	In-solution trypsin digestion and preparation for LC-MS -----	71
3.2.4	Label-free analysis MS ^E of placental tissue proteome -----	71
3.2.5	Gene ontology and protein-protein network-----	73
3.2.6	Plasma proteome SWATH TM analysis -----	73
3.2.7	Multiple Reaction Monitoring (MRM) analysis of plasma sample -----	75
3.2.8	Western Blot and Real-Time PCR -----	76
3.2.9	Experimental design and statistical rationale-----	76
3.3	Result and Discussion -----	77
3.3.1	Placental proteome profiling of normotensive and pre-eclamptic patients -----	77
3.3.2	Gene ontology identifies biological processes relevant to pathophysiology of pre-eclampsia -----	82
3.3.3	Plasma proteome profiling of normotensive and pre-eclamptic patients	89
Chapter 4 Placental pathophysiology in pregnant hypertensive rodent model -----		102
4.1	Background -----	102
4.1.1	Rat placenta -----	102
4.1.2	Hypertensive rodent model-SHRSP -----	102
4.2	Material and Methods -----	104

4.2.1	Sample collection -----	104
4.2.2	Protein extraction -----	104
4.2.3	In-solution digestion -----	105
4.2.4	Label-free analysis in LTQ orbitrap -----	105
4.2.5	Gene ontology and protein interaction network -----	106
4.3	Results and Discussion -----	106
4.3.1	Comparison of placental proteome of WKY and SHRSP -----	106
4.3.2	Gene ontology of differentially expressed protein -----	110
4.3.3	Comparison of human pre-eclamptic and SHRSP placental physiology -----	113
Chapter 5 Investigation of urinary peptidome over pregnancy in rodent model of hypertension -----		116
5.1	Introduction -----	116
5.2	Materials and Methods -----	117
5.2.1	Animals -----	117
5.2.2	Urinary biochemistry -----	118
5.2.3	Histology -----	118
5.2.4	Urinary peptidomics -----	119
5.2.5	Liquid chromatography- tandem mass spectrometry (LC-MS/MS) for peptide sequencing -----	120
5.2.6	Quantitative PCR for uromodulin expression -----	121
5.2.7	Western blot for Umod -----	122
5.2.8	N-deglycosylation of Umod -----	122
5.2.9	Purification of Umod and polymerization assay -----	122
5.2.10	Protease prediction -----	122
5.2.11	Statistical analysis -----	123
5.3	Results and Discussion -----	123
5.3.1	The SHRSP exhibits altered water and electrolyte balance during pregnancy -----	123
5.3.2	The SHRSP exhibits increased urinary protein and metabolite excretion during pregnancy -----	123
5.3.3	The SHRSP Kidney is increased in Size Relative to the WKY but does not Exhibit Histological Abnormalities -----	125
5.3.4	The urinary peptidome is altered during pregnancy and between WKY and SHRSP -----	129
5.3.5	Umod expression is increased in the urine and kidney of SHRSP during pregnancy -----	130
5.3.6	C-terminal Umod peptides found to be more abundant at GD12 and GD18 in SHRSP urine -----	133

5.3.7	Polymerization-incompetent Umod is increased in pregnant SHRSP -	135
5.3.8	Nifedipine treated pregnant SHRSP showed only polymerization-competent Umod -----	137
	List of References -----	139
	Appendix -----	157

Declaration by Research Scholar

I hereby declare that I am the sole author of this thesis entitled “**Proteomic Pattern in Pre-eclampsia**” submitted by me for the degree of Doctor of Philosophy to Academy of Scientific and Innovative Research (AcSIR) and is a record of the research performed by myself with exception to few experiments. The work in chapter 2 and 3 was performed in National Chemical Laboratory (Pune, MS, India) and the human samples were collected from Bharati hospital (Pune, MS, India), with the help Dr. Savita Mehendale and provided to us by Dr. Sadhana Joshi and Dr. Anvita Kale from Interactive Research School in Health Affairs (IRSHA) (Pune, MS, India). The study was approved by the Institutional Ethical Committee of Bharati Vidyapeeth Deemed University Medical College, Ref No BVU/EXAM 5608/2009-10 dated 19/2/2010. Written consent was only for participation in the study and the identity of the patients is kept confidential. The SWATH-MS and MRM experiments in Chapter 3 was conducted in Sciex Ltd (Gurgaon, HR, India) with the help of Dr. Dipankar Malakar. Rest of the mass spectrometry experiments mentioned in chapter 2, 3, 4 and 5 was performed by myself. All the mass spectrometry data analysis was carried out using licensed software except for the Transomics™ software which was provided to us on trial basis by Water Cooperation (Bangalore, KA, India).

The work reported in chapter 3 and 4 was conducted in Institute of Cardiovascular and Medical Sciences, University of Glasgow, Scotland, UK, during my tenure as visiting researcher through Commonwealth Split-Site Scholarship (2015-2016) under the supervision of Prof. Christian Delles. The animal experiments were conducted after my successful completion of personal license for animal handling course conducted by the ScotPiL Training Committee. The animals were maintained by the animal husbandry staff of Biological services, University of Glasgow (Ms. Christini and Mr. Charlie) and sacrificed by me or Dr. Heather Small (University of Glasgow) under the supervision of Dr. Delyth Graham. Urinary electrolyte and metabolite analysis in chapter 5 were carried out by Elaine Butler. Kidney sections in chapter 5 were scanned using the Leica Aperio slide scanner by Clare Orange (University Pathology Unit). The mass spectrometry analysis in chapter 4 and 5 was conducted in the Department of Chemistry, University of Glasgow, under the supervision of Dr. Willam Mullen. The urinary peptidomics data analysis in chapter 5 was done by me in Mosaiques Diagnostics and Therapeutics AG (Hannover, Germany), under the supervision of Dr. Justyna Siwy and Prof. Harald Mischak.

This work is original and has not been submitted previously for any higher degree and was supervised by Dr. Ashok Giri and Dr. Mahesh Kulkarni.



Sheon Mary Samji

Date: 1st March, 2017

Acknowledgement

During my journey as a Ph.D. student, I have come across a world of excitement, joy, surprises and difficulties. It was not easy to grow alone and make a place for oneself in this expedition. This was made possible with the continuous support of several people. First and foremost, I would like to express my sincerest gratitude to my research guides Dr. Ashok Giri and Dr. Mahesh Kulkarni, for their valuable guidance, tremendous support, and scientific inputs. I am one of the students who can proudly say that I could not have imagined having anyone else in their role as my advisors. This feat was possible only because of their unconditional support, collaboration and the intellectual freedom they had given me during my research in CSIR-National Chemical Laboratory (NCL). Ashok (as he prefers us calling him) is more like a friend, always encouraging and supportive in research as well as in extracurricular activities. He had always made our work environment more flexible and favorable to our need as a research student, and more experience oriented. He would never say no to our new ideas and encourage us to face new challenges. He would always urge us to learn from our mistakes and inspire us with his research experiences. Dr. Mahesh Kulkarni is my co-advisor, who have always given me an opportunity to come up with new ideas and supported me immensely. His cabin and lab door were always open for me for discussion and work and would like to express my thanks for always considering me as one of his students. His friendly, cheerful and '24 hour reachable' attitude have always made things easier and interesting.

I owe my deepest gratitude to Dr. Sadhana Joshi and her team from Interactive Research School in Health Affairs (IRSHA), Pune, India, for her continuous support and coordination in providing us the samples. Discussions with Dr. Sadhana, Dr. Prabhakar Ranjekar and Prof. Sahebarao Mahadik have been insightful in carrying forward this project. I would especially like to thank Dr. Savita Mehendale, other physicians, nurses and nurse aids in the Gynaecology unit at Bharti hospital.

I would like to thank Director, CSIR-NCL and Head of Department Biochemical Sciences, Dr. Archana Pundle and former head Dr. Vidya Gupta for providing the infrastructure and lab facilities. I appreciate the feedback offered by my DAC chairperson Dr. Anu Raghunathan and the current and former DAC members Dr. Archana Pundle, Dr. Bhushan Chaudari, Dr. C. G. Suresh and Dr. Vidya Gupta. Advice

and comments given by Dr. Vidya Gupta have been a great help. A special mention to Dr. Dipankar Malakar, Sciex Ltd, India who taught and helped me run few mass spectrometry experiments in their facility. I am also thankful to Dr. Ravi Kulkarni, Symbiosis Centre for Information Technology, Pune for his time spent in teaching me all the statistics used in my research. Also, would like to thank Waters Cooperation, Bangalore, India, especially Dr. Rakesh K S, Mr. Rajeev Bharadwaj, Mr. Ashutosh Kulkarni and rest of the team for their support provided to us with Synapt HDMS and software. I am grateful to CSIR for their generous support and funding for my Ph.D. I thank Department of Biotechnology, India for the project funding. Also, would like to thank Commonwealth Commission UK for the Split-Site Scholarship.

My heartfelt appreciation goes to Prof. Christian Delles from University of Glasgow (UoG) to mentor me during my research in Glasgow as a Commonwealth scholar. I am grateful for his invaluable support, encouragement, critical inputs and suggestions during my tenure. I acknowledge him for having faith in me and to give me the freedom for executing my ideas. I am thankful to Dr. Willam Mullen (Bill) from UoG for allowing me to use the MS instruments and his lab. His jokes, smiley face and coffees always helped me through difficult times. I would also like to thank Bill's colleagues Dr. Bahareh Mansoorian and Dr. Emma Carrick for patiently teaching me Capillary Electrophoresis-Mass Spectrometry. I express my gratitude to Dr. Delyth Graham from UoG for her time to supervise me during my animal handling course. Special thanks to my friends Dr. Katriona Brooksbank, Dr. Daniele Kerr and Dr. Gemma Currie from UoG for all the useful discussions, guidance and fun time. I owe a very important debt to Dr. Heather Small from UoG for being my lab-mate, office-mate and a true friend. Her generous support helped me to learn many new things, especially the work culture in a different country. She inspires me in many ways. Thanks Heather for everything!

Special thanks to all the labmates from Plant Molecular Biology (PMB) group. I received generous support from the three pillars of PMB Dr. Vidya Gupta, Dr. Ashok Giri, and Dr. Narendra Kadoo. The seven years in PMB was great and influential years of my career. I would like to thank my seniors: Dr. Vaijayanti Tamhane, Dr. Hemlata Kotkar, Dr. Vishal Dawkar, Dr. Bhushan Dholika, Dr. Ashwini Rajwade, Dr. Gayatri Gurjar, Dr. Hemangi Chidley, Dr. Rasika Bhagwat, Dr. Yashwant Kumar, Dr. Ramya Dixit and Dr. Purushottam Lomate. I am grateful to all my lab members Amey, Ashish, Rahul, Neha K., Neha M., Manasi, Medha, Priya, Nishi, Nena, Nikhil, Ram, Ajit, Tejas,

Pranjali, Sonal, Bal Krishna, Sucheta, Smriti, Nidhi, Rakesh, Yojana, Ranjit, Saleem, Ramesha, Gopal, Radhika, Amol K, Amol J, Uma and all other lab members. Also, I would like to thank my former project partner Gouri Patil and all the trainees who worked with me, special mention to Nupur, Sophia, Padmaja, Sayali and Vivek. Cheers to my PMB family!

It is a pleasure to thank all my friends from Dr. Mahesh Kulkarni's group (MJK proteomics group). A special mention to Jagadeeshaprasad M. G. (Jaggi) who has spent sleepless day and nights with me repairing and maintaining mass spectrometry. I have greatly benefited from discussions with Shweta, a great friend, and researcher. Time spend with her has been insightful. My gratitude is extended to other MJK group members, Gouri, Reema, Kedar, Dr. Arvind, Dr. Hemangi, Dr. Suresh, Dr. Yogesh, Dr. Sneha, Aarti, Rubina, Swami, Dr. Sandeep, Rashmi, Shakuntala, Prachi, and Rajeshwari.

To my dearest friends, Aditi (Bagdi, the road runner), Amey (Bhide, the singer), Ashish (Ashu, the pacifier), Gouri (Gou mata, the enthul!), Rahul (Duli, the confused), Reema (Reemu(ji), the teacher), Sachin (Chinya, the smiley) and Tejas (Teju, the player), you should know that your support and encouragement was worth more than I can express on paper. Thank you all for lunches, tea-breaks, bday parties, dramas and advice – you were always there with a word of encouragement or listening ear. Honest thanks to my batchmates Ruchria, Deepak, Ashish and Sayali for all the information, course work, CSIR-800 and AcSIR document preparation. Wholehearted thanks to few of my Masters friend Aditi, Prachi, Aditya, Chetan, Hemant, Veena, Trupti, Tejashri and Seema.

I owe a lot to my parents and sister who encouraged and helped me at every stage of my personal and academic life and longed to see this achievement come true. My hard-working parents have sacrificed their lives for my sister and myself and provided unconditional love and care. A good support system is important to surviving and staying sane in research, and I owe this to my husband, mother-in-law and father-in-law. My husband has been a true and great supporter and has unconditionally loved me during my good and bad times. I love you all dearly!

*Above all, I owe it all to Almighty God for granting me the wisdom, health, and strength to undertake this research task and enabling me to its completion. **“The steps of a man are established by the Lord, and he delights in his way. When he falls, he will not be hurled headlong, because the Lord is the One who holds his hand.”** Pslams37:23-24*

List of Tables

Table 1.1 Features of human placenta-----	27
Table 2.1 LC-MS ^E identification of differentially expressed proteins in normal versus pre-eclamptic pregnancies -----	57
Table 3.1 List of Differentially expressed proteins-----	79
Table 3.2 List of peptide and MRM transitions pairs used to detect protein -----	91
Table 4.1 Comparison between rat and human placenta -----	103
Table 4.2 Comparison of candidate proteins in human and rat -----	114

List of Figures

Figure 1.1 Postulated molecular mechanisms that lead to pre-eclampsia-----	30
Figure 1.2 Proteomics strategies for studying PE -----	39
Figure 2.1 Representative 2DE SDS PAGE-----	54
Figure 2.2 Magnified images of differentially expressed protein spots identified by PDQuest software -----	56
Figure 2.3 REVIGO scatterplot of biological processes GO terms of differentially expressed genes-----	58
Figure 2.4 Validation of Annexin A6 in placenta -----	61
Figure 2.5 Tubulointerstitial nephritis antigen-like protein Western blot analysis -	63
Figure 2.6 2DE gel with the zoomed out image of the region of spots of vimentin	65
Figure 2.7 Vimentin Western blot analysis-----	66
Figure 2.8 Caspase cleaving sites and various fragments of vimentin -----	68
Figure 3.1 Placental proteome-----	78
Figure 3.2 Protein- protein interaction network -----	83
Figure 3.3 Gene ontology and protein-protein interaction networks of differentially expressed proteins-----	87
Figure 3.4 Interaction between apolipoprotein A-I, apolipoprotein A-II, hemopexin and haptoglobin analyzed by STRING 9.1 -----	90
Figure 3.5 MRM transition plots for individual peptides-----	93
Figure 3.6 Total intensity count of all 120 sample runs (MRM)-----	94
Figure 3.7 Coefficient of variation versus retention time of MRM runs -----	94
Figure 3.8 Relative abundance of (A) apolipoprotein A-I, (B) apolipoprotein A-II, (C) hemopexin and (D) haptoglobin in plasma of normotensive and pre-eclamptic patients -----	95
Figure 3.9 Validation of transferrin receptor-1 in placenta tissue-----	99
Figure 4.1 Blood pressure profile in the normotensive WKY rat and the SHRSP rats -----	104
Figure 4.2 Rat placental proteome -----	107
Figure 4.3 Volcano plot for rat placental proteome -----	108
Figure 4.4 Heat map of differentially expressed protein -----	109
Figure 4.5 Protein interaction network from STRING-----	111
Figure 4.6 Gene ontology biological process enrichment -----	112
Figure 4.7 Venn diagram with comparison of differentially expressed protein between human and rat model-----	113
Figure 5.1 Pregnant SHRSP exhibit altered water and electrolyte balance-----	124
Figure 5.2 Pregnant SHRSP have altered urinary albumin and metabolite levels	125

Figure 5.3 Kidney size is increased in non-pregnant and pregnant (GD18) SHRSP relative to WKY -----	126
Figure 5.4 Glomeruli distribution is altered in non-pregnant and pregnant (GD18) SHRSP relative to WKY -----	127
Figure 5.5 The SHRSP does not show histological abnormalities in the glomeruli or vessels of the kidney-----	128
Figure 5.6 Schematic flowchart representing peptidomics data analysis and identification of peptide markers-----	131
Figure 5.7 Urinary uromodulin peptides are increased in the SHRSP relative to WKY in a pregnancy-dependent manner -----	132
Figure 5.8 Increase in uromodulin in SHRSP validated in urine and kidney tissue -----	133
Figure 5.9 Schematic representation of rat UMOD structure -----	134
Figure 5.10 Protease prediction -----	135
Figure 5.11 Two forms of uromodulin -----	136
Figure 5.12 Nifedipine significantly inhibits blood pressure elevation in the SHRSP -----	138

List of Accompanying Material

All the supplemental data is provided along with this thesis in the form of soft copy in CD attached to the last page.

Supplemental data 1: PLGS protein identification data including MW, pI, number of peptides, PLGS score, coverage, modifications, MS/MS fragmentation, and sequence of peptides. (.xlsx) (Chapter 2)

Supplemental data 2: Gene ontology terms of differentially expressed proteins from gel-based proteomics. (pdf) (Chapter 2)

Supplemental data 3: Normalisation calculations of Western blot band intensities with housekeeping protein. (.xlsx) (Chapter 3)

Supplemental data 4: List of peptides and proteins identified by Transomics™ in gel-free proteomics. (.xlsx) (Chapter 3)

Supplemental data 5: Gene ontology enrichment of differentially expressed proteins from gel-free proteomics. (.xlsx) (Chapter 3)

Supplemental data 6: List of 41 proteins with secreted gene ontology term from DAVID analysis. (pdf) (Chapter 3)

Supplemental data 7: List of plasma proteins from SWATH analysis. (.xlsx) (Chapter 3)

Supplemental data 8: Quantile-Quantile plot for test of normality for MRM transitions. (pdf) (Chapter 3)

Supplemental data 9: List of differentially expressed proteins of rat placental proteome. (.xlsx) (Chapter 4)

Supplemental data 10: Proteasix prediction of proteases that cleave uromodulin. (.xlsx) (Chapter 5)

Definitions/Abbreviations

2-DE	Two-dimensional electrophoresis
AF	Amniotic fluid
AGE	Advanced glycation end
AMIDA	Autoantibody mediated identification of antigens
Apo	Apolipoprotein
Bingo	Biological Networks Gene Ontology tool
C	Normotensive
CBB	Coomassie Brilliant Blue
DAVID	Database for Annotation, Visualization and Integrated Discovery
DIGE	Difference Gel Electrophoresis
FDR	False Determination Rate
GD	Gestational day
GWAS	Genome-wide association studies
HDL	High-density lipoprotein
HELLP	Hemolysis, Elevated Liver enzymes and Low Platelet
Hp	Haptoglobin
Hx	Hemopexin
ICAT	Isotope coded affinity tagging
IPG	Immobilized pH gradient
IRE	Iron regulatory element
IRP	Iron regulatory protein
LC	Liquid chromatography
LFQ	Label-free quantitation
MRM	Multiple Reaction Monitoring
MS	Mass spectrometry
MS/MS	Tandem Mass spectrometry
NHBPEP	National High Blood Pressure Education Program
NP	Non-pregnant
PCA	Principal component analysis
PDI	Protein disulfide isomerases
PE	Pre-eclampsia
PLGS	ProteinLynx Global Server
PTM	Post translational modification
RAS	Renin-angiotensin system
Rt	Retention time
SDS-PAGE	Sodium dodecyl sulphate-polyacrylamide gel electrophoresis
sFLT-1	Soluble fms-like tyrosine kinase-1

SHRSP	Stroke prone spontaneously hypertensive rat
SILAC	Stable isotope labeling by amino acids in cell culture
SPANOVA	Split-plot Factorial multivariate analysis of variance
SRM	Selective reaction monitoring
STRING	Search Tool for the Retrieval of Interacting Genes/Proteins
SWATH	Sequential window acquisition of all theoretical fragment ion spectra
Tfr	Transferrin receptor
Umod	Uromodulin
UPLC	Ultra performance liquid chromatography
VEGF	Vascular endothelial growth factor
WKY	Wistar-Kyoto

Preface

Pregnancy is a complex state involving physiological changes in various maternal organs to support the development of fetus and these changes determine the overall success of a pregnancy. Yet a continuum of complications are associated with pregnancy such as unexplained miscarriage, pre-eclampsia (PE) and intrauterine growth restriction, pre-term labour with intact membranes, premature rupture of the membranes and stillbirth, caused by either changes in intrauterine environment, impaired trophoblast invasion and maternal nutrition. PE is a hypertensive disorder characterized by the new onset of hypertension of $>140/90$ mmHg and proteinuria after the 20th week of gestation. Worldwide 10 million women develop PE of which >76000 women die per year. In the present study, we explored placental proteome of pre-eclamptic women and pregnant hypertensive rodent model. Pre-eclamptic women's plasma from different gestational weeks were used to validate potential protein markers. While, in case of rodent model urine was used to predict the potential peptide markers.

PE appears to be a multi-factorial, multi-organ disorder; wherein the origin is the insult to the placenta and abate when delivered. Elucidation of placental physiology and biochemistry with respect to PE is thus essential for its prevention, prediction, and clinical care. Although compartmentalization of different biological aspects of this disorder can help in understanding the pathophysiology, it is crucial to visualize the overall scenario. Proteome research of various biological samples such as plasma, amniotic fluid, urine, placental tissue, trophoblast cell line has been studied in PE for biomarker discovery. However, the capacity of unbiased proteomic analysis to elucidate the pathophysiology of PE is not explored. Therefore, we studied placental proteome, the subset of etiological factors and molecular mechanisms involved pathophysiology of PE using two proteomic approaches: (i) gel-based two-dimensional electrophoresis (ii) gel-free label-free proteomics

Chapter 2. Biochemical insights into the pathophysiology of pre-eclampsia through placental proteomics - Part 1 (gel based proteomics)

Total of 55 protein spots were differentially expressed, in which 26 were upregulated and 29 were downregulated in pre-eclamptic placenta. Gene ontology and enrichment

analysis of these differentially expressed proteins showed that they belong to many biological processes related to the etiological factors of pre-eclampsia. These processes include apoptosis, inflammation, oxidative stress, hypoxia, cell activation and cytoskeleton modelling. To obtain more insight into the pathophysiology of pre-eclampsia, candidate proteins were validated by Western blot and/or gene expression analysis. We report two novel proteins, tubulointerstitial nephritis antigen-like 1 protein, a matricellular protein and a pro-angiogenic factor to be downregulated, and annexin A6 upregulated in the pre-eclamptic placenta. We show that few vimentin fragments are significantly upregulated in pre-eclamptic tissue, with no significant difference in the 57kDa parent fragment. These fragments are the result of apoptosis occurring during pregnancy.

Chapter 3. Biochemical insights into the pathophysiology of pre-eclampsia through placental proteomics - Part 2 (gel free proteomics)

Comparison of the placental proteome of normotensive (n=25) and pre-eclamptic (n=25) patients by gel-free proteomic techniques, identified a total of 2145 proteins in the placenta of which 180 were differentially expressed (>1.3 fold, $p<0.05$). Gene ontology enrichment analysis of biological process suggested that the differentially expressed proteins belonged to various physiological processes such as angiogenesis, apoptosis, oxidative stress, hypoxia, placental development, which are implicated in the pathophysiology of pre-eclampsia. Some of the differentially expressed proteins were monitored in the plasma by multiple reaction monitoring (MRM) analysis, which showed an increase in Apolipoprotein AI and AII in gestational week 26-30th (2-fold, $p<0.01$) while haptoglobin and hemopexin decreased in gestational week 26-30th and 40th week/at delivery (1.8 fold, $p<0.01$) in pre-eclamptic patients.

Chapter 4. Placental pathophysiology of pregnant hypertensive rodent model

The stroke-prone spontaneously hypertensive rat (SHRSP) obtained by selective inbreeding of the Wistar-Kyoto (WKY) strain is a well-characterized model of cardiovascular disease in general and of maternal chronic hypertension. The placental proteome was extracted from these rat model and compared to pre-eclamptic women's placenta. Comparison of SHRSP and WKY identified a total of 1318 protein, were 363 are differentially expressed. Protein interaction networks and gene ontology analysis

identified major biological process such as apoptosis, inflammation, oxidative stress, cell adhesion and migration. The proteins identified in pregnant hypertensive rat proteome were compared to pre-eclamptic women and showed 30% similarity. The major candidate protein studied in human such as apolipoprotein, haptoglobin, hemopexin, transferrin receptor-1, tubulointerstitial nephritis antigen-like 1 protein, annexin A-6 were also to be differentially regulated in these hypertensive rodent models.

Chapter 5. Investigation of urinary peptidome during pregnancy in rodent model of hypertension

The kidney is centrally involved in blood pressure regulation and undergoes extensive changes during pregnancy. Hypertension during pregnancy may result in an altered urinary peptidome which could be used to indicate new targets of therapeutic or diagnostic interest. Capillary electrophoresis-mass spectrometry was conducted to interrogate the urinary peptidome in SHRSP and WKY at three time points: pre-pregnancy and gestational days (GD) 12 and 18. The comparison within and between the WKY and SHRSP peptidome at all time points detected 123 differentially expressed peptides (fold change > 1.5; $p < 0.05$). Sequencing of these peptides identified fragments of collagen alpha-chains, albumin, pro-thrombin, actin, serpin A3K, pro-epidermal growth factor and uromodulin. Uromodulin peptides showed a pregnancy-specific alteration in SHRSP with a 7.8 ($p < 0.01$) and 8.8 ($p < 0.05$) fold increase at GD12 and GD18 respectively, relative to the WKY. Further investigation revealed that these peptides belonged to the polymerization-inhibitory region of uromodulin. Two forms of uromodulin (polymerization-competent and incompetent) were found in urine from both WKY and SHRSP; where the polymerization incompetent form was increased in a pregnancy-specific manner in SHRSP. Nifedipine treated pregnant SHRSP showed only polymerization-competent uromodulin indicating that calcium may be mechanistically involved in uromodulin polymerization. This study highlights, for the first time, a potential role of uromodulin and its polymerization in hypertensive pregnancy

Chapter 1

Introduction

Contents of this chapter is published as review article in *Proteomics Clinical Applications*, 2012, vol 6, 79-90.

Chapter 1 Introduction

1.1 Human placenta

The placenta of humans is chorioallantoic i.e. derived from the chorion and allantois, and haemochorial structural organisation where the maternal blood is in direct contact with the chorion which encapsulates the fetal vasculature. A full term, delivered placenta is flat disc-like, round to oval organ, with an average diameter of 22cm, average thickness (at the center) of 2.5cm and average weight of 470g. Table 1.1 summaries the features of human placenta.

1.2 Pregnancy complications

Pregnancy is a complex state involving physiological changes in various maternal organs to support the development of fetus and these changes determine the overall success of a pregnancy. Yet a continuum of complications are associated with pregnancy such as placental abruption (1), unexplained miscarriage(2), pre-eclampsia (PE) and intrauterine growth restriction (IUGR) (3), pre-term labour with intact membranes (4), premature rupture of the membranes (5)and stillbirth (6), caused by either changes in intrauterine environment, impaired trophoblast invasion and maternal nutrition.

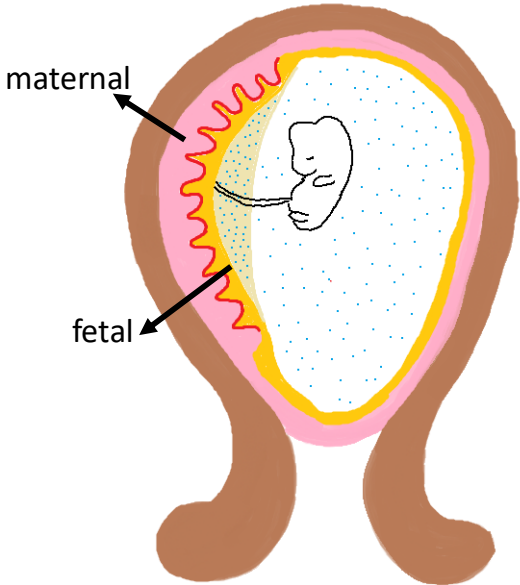
1.3 Pre-eclampsia

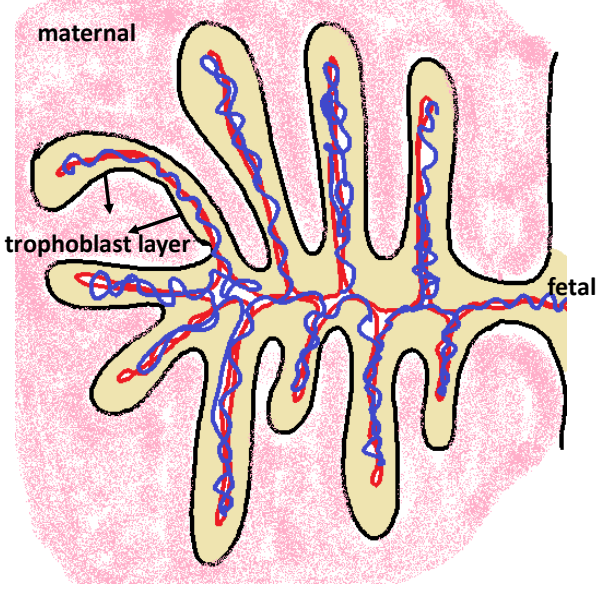
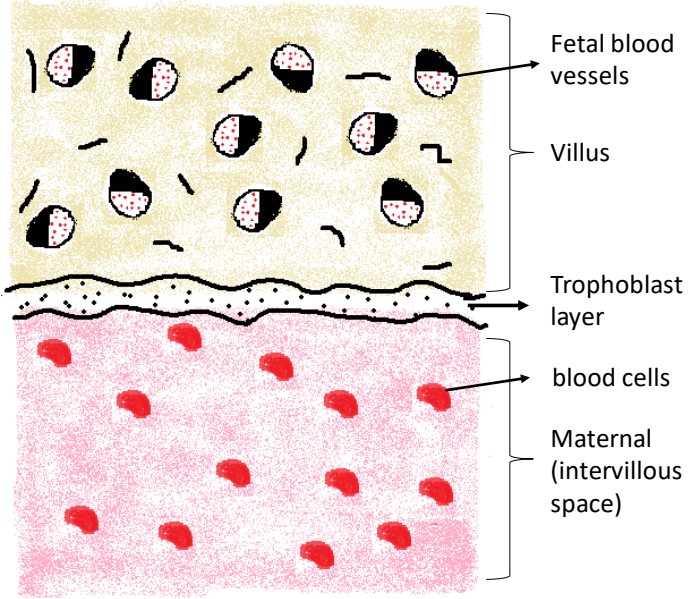
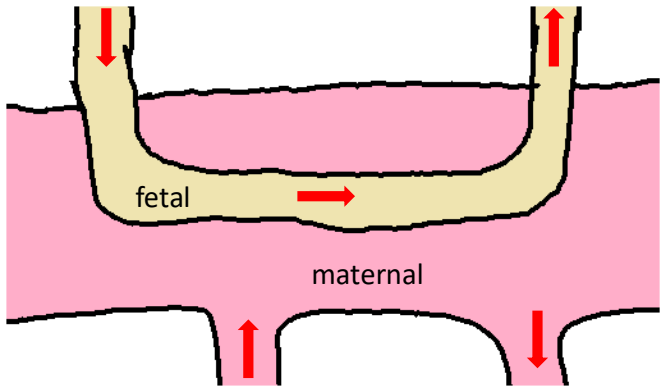
1.4 Definition and diagnosis

Pre-eclampsia (PE) is a unique hypertensive disorder in pregnancy that complicates approximately 5 to 7% of pregnancies and is associated with significant fetal/neonatal morbidity and mortality (7). In 2000, the National High Blood Pressure Education Program (NHBPEP) Working Group (8) defined the criteria for diagnosis of pre-eclampsia as 1) systolic blood pressure ≥ 140 mmHg and/or diastolic blood pressure ≥ 90 mmHg that occurs after 20 weeks of gestation in a woman with previously normal blood pressure and 2) proteinuria defined as urinary excretion of 0.3g protein or higher in a 24hr urine specimen. PE untreated can lead to eclampsia or Hemolysis, Elevated Liver enzymes and Low Platelet count (HELLP) syndrome. As per the task force report

issued by American College of Obstetricians and Gynecologists, in the absence of proteinuria, new onset of hypertension with new onset of either thrombocytopenia/ renal insufficiency/ impaired liver function/ pulmonary edema/ cerebral or visual symptoms are also suggested to be used as diagnostic criteria for pre-eclampsia (9). The known risk factors for PE include pre-existing hypertension, diabetes, autoimmune diseases like hypothyroidism, family history of PE, obesity and increased maternal age (10-14). Ten million women per year develop preeclampsia worldwide, and about 76000 women die each year from pre-eclampsia (15).

Table 1.1 Features of human placenta

Feature	Description	Figure
Placental shape: placenta discoidalis	Maternofetal interdigitation as a single disk-like zone	 <p>The diagram illustrates a cross-section of a discoid placenta. It shows a central fetal cavity containing a fetus, surrounded by a layer of chorionic tissue. The outer boundary is the maternal blood supply. The maternal and fetal sides are shown interdigitating, forming a single, continuous disk-like zone. Labels 'maternal' and 'fetal' with arrows point to these respective layers.</p>
Maternofetal interdigitation: Villous type	Tree-like branching pattern of the chorion, resulting in the placental villous tree and are directly surrounded by maternal blood	

Feature	Description	Figure
		 <p>The diagram shows a cross-section of a placental villus. The maternal side (top) is pink and contains red and blue blood vessels. The fetal side (bottom) is yellow and contains red and blue blood vessels. A central layer, labeled 'trophoblast layer', separates the maternal and fetal blood. The villus is labeled 'maternal' at the top and 'fetal' at the bottom.</p>
<p>Maternofetal barrier: hemochorial</p>	<p>The maternal vessels are eroded and finally completely destroyed by the invasive trophoblast.</p> <p>Number of trophoblastic epithelial layer: Hemodichorial (first trimester) hemomonochorial (at term)</p>	 <p>This diagram illustrates the hemochorial barrier. At the top, fetal blood vessels (black and red) are shown within a villus. Below the villus is a thin layer of trophoblast cells. The maternal side (bottom) shows maternal blood cells (red) in the intervillous space. Labels include 'Fetal blood vessels', 'Villus', 'Trophoblast layer', 'blood cells', and 'Maternal (intervillous space)'.</p>
<p>Maternal and fetal blood vessel arrangement</p>	<p>Multivillous flow exchanger</p>	 <p>The diagram shows a U-shaped fetal blood vessel (yellow) with red arrows indicating flow from the maternal side (bottom) to the fetal side (top). The maternal blood (pink) is shown in the intervillous space. Labels include 'fetal' and 'maternal'.</p>

1.5 Prevention and management

Many strategies have been employed in research in past 20yrs research to prevent pre-eclampsia. However, no intervention till date have proven effective. According to WHO recommendations, some of the strategies to prevent pre-eclampsia are: calcium, vitamin D, C and E supplementation; magnesium sulfate, antihypertensive drugs, aspirin treatments; induction of labor and bedrest (16). There is a pressing need to better understand the mechanisms of the disease, with the ultimate goal of preventing the disorder especially since the incidence of PE and rates of adverse outcomes are increasing (17-19).

1.6 Pathophysiology and etiological factors

PE involves changes in both placental and maternal physiology. Placentation is the process by which the placental trophoblast invades the uterine wall by cytotrophoblast invasion of the spiral arteries in the deciduas and the myometrium (20). The trophoblast invasion requires change in cell adhesion molecules' expression of extravillous trophoblast to transform into endothelial cell type, which is known as "pseudovasculogenesis" (21). In women destined to develop PE, inadequate spiral artery remodelling occurs due to absence of pseudovasculogenesis, leading to poor placental development, disturbed angiogenesis, placental ischemia/hypoxia and release of several circulatory factors, which subsequently causes maternal endothelial dysfunction, maternal clinical signs of hypertension and proteinuria (22). The etiological factors leading to inadequate trophoblast invasion and endothelial dysfunction have been enigmatic. The pathways in Figure 1.1 and molecular mechanisms mentioned below leading to PE have been debated for decades.

1.6.1 Placental hypoxia

Hypoxia is a state of reduced oxygen pressure below a critical threshold, which restricts the function of organs, tissues or cells (23). In the early placental development, hypoxic condition is required for vasculogenesis and angiogenesis. Angiogenic factors like vascular endothelial growth factor (VEGF) are regulated acutely by the local oxygen concentration (24). Hypoxia induces transcription of several hypoxia-inducible gene including angiogenic factors and anti- angiogenic receptors leading to disrupted

angiogenesis and endothelial dysfunction (25, 26). Conversely, it is also proposed that altered angiogenic factors cause poor trophoblast invasion subsequently leading to placental hypoxia (27). It is still unclear whether placental hypoxia is the cause or result of inadequate trophoblast invasion and subsequent endothelial dysfunction.

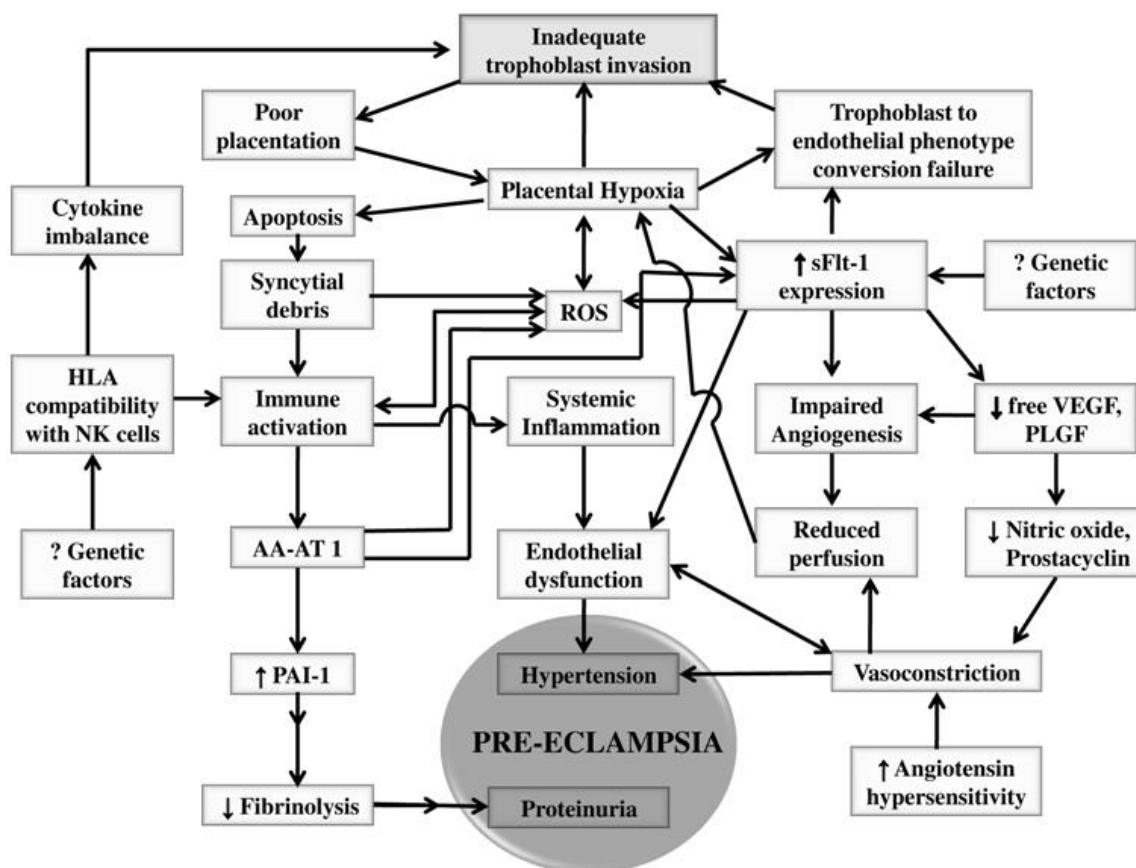


Figure 1.1 Postulated molecular mechanisms that lead to pre-eclampsia
(This figure is from author's own published article)

1.6.2 Oxidative stress

Oxidative stress results from increased production of reactive oxygen species (ROS) or a significant decrease in the capability of antioxidant defence. Reports indicate that failure of the tissues to adapt to the transition in intraplacental oxygenation may cause placental oxidative stress resulting in poor placental perfusion in PE (28, 29). It has also been proposed that poor trophoblast invasion leading to hypoxia and/or apoptosis results in release of syncytiotrophoblast debris causing increased oxidative stress in women with PE (30). Other reports indicate that endothelial dysfunction in PE may be

due to increased placental oxidative stress and reduced antioxidant defence pathways specifically involving glutathione peroxidases (31, 32). Elevated levels of oxidative stress markers like superoxide radicals (33), lipid peroxides and isoprostanes (34) have been reported in preeclamptic placenta. Our recent studies in women with PE at the end of pregnancy have shown that reduced antioxidants and increased oxidative stress are associated with reduced DHA levels (35).

1.6.3 Angiogenic factors

Recent discoveries concerning the pathogenesis of PE emphasize the emerging role of angiogenic factors as potential mediators of the clinical signs and symptoms of PE. Vasculogenesis and angiogenesis are considered to be central processes in the development of the placenta and are mediated by two families of ligands, namely VEGFs, angiopoietins, and their tyrosine kinase receptors VEGFR1/Flt-1 and VEGFR2/KDR in fetal and placental angiogenesis (36-38). Placental development is regulated by a local balance between pro- and antiangiogenic factors. Alterations in these pathways in early gestation could contribute to inadequate cytotrophoblast invasion in PE (39). Soluble Flt-1 (sFlt-1) antagonizes both VEGF and placental growth factor (PlGF) by binding them in the circulation and preventing interaction with their endogenous receptors (40). Circulating sFlt-1 levels are relatively low in early pregnancy and begin to rise in the third trimester and reflect a physiologic antiangiogenic shift in the placental environment towards the end of pregnancy, corresponding to completion of the vasculogenic phase of placental growth.

It is believed that hypoxia in PE leads to increased production of sFlt-1 in placental trophoblasts (4, 41) and is suggested to be the major source of circulating sFlt-1 (42). Others believe that hypoxia may not be the only or main stimulus to release sFlt-1; and emphasize the role of inflammatory mechanisms (43). Our study speculates that altered placental long chain poly unsaturated fatty acids result in altered membrane lipid fatty acid composition leading to shedding of sFlt-1 in circulation in PE (44).

sFlt-1 level has been reported to increase prior to the onset of the clinical disease in women with PE and has been shown to correlate with the severity and the time of the onset of the disease (45-47). Increased serum sFlt-1 and decreased PlGF levels are

associated with blood pressure, renal and endothelial dysfunction, trophoblast deportation, as well as with a shorter duration of pregnancy, fetal growth restriction and early onset of PE. Studies suggest that dysregulation of angiogenic factors and sFlt-1 play an important role in the pathogenesis of PE although the results are inconsistent (45, 48, 49). Our earlier studies suggest that dysregulation of angiogenic factors may be associated with maternal oxidative stress leading to poor birth outcomes due to PE (50). Further it has been suggested that sFlt-1 and PlGF could together serve as predictors of PE (51).

1.6.4 Immunological factors

PE is associated with increased immune response. Factors such as history of PE, change in paternity (52), donor spermatozoa (53) increase immune response in PE. Cytokines produced by immune and non-immune cells at the fetal-maternal interface play an important role in trophoblast invasion. Many pro- and anti-inflammatory cytokines expressions are altered in PE (54), which could be the result of placental damage or abnormal antigenic interaction between fetal antigen and maternal immune system. Trophoblast cells express HLA-C which interacts with maternal killer immunoglobulin-like receptors (KIR) of decidual NK cells. HLA-C and KIR show polymorphism, and depending on interaction between HLA and KIR allotypes, NK cells release stimulatory and inhibitory angiogenic cytokines and chemokines (55, 56). Pregnancy with HLA-C2 allotype fetus and KIR AA genotype is at higher risk of PE, thus showing paternal specificity in PE (57). Maternal circulating factors such as ficolin bind to apoptotic trophoblasts and induce innate immunity through cytokine activation(58). Further, shedding of syncytiotrophoblast cell debris as a result of apoptosis activates neutrophils, monocytes and NK cells that initiate inflammation and lead to increased oxidative stress and endothelial dysfunction which are associated with PE.

1.6.5 Renin-angiotensin system

During normal pregnancy, the components of renin-angiotensin system (RAS) undergo major changes including elevated levels of renin, angiotensin (Ang), aldosterone and decreased angiotensin-converting enzyme (ACE) with increase in chymase (non ACE Ang II producing enzyme)(59), contributed by the local uteroplacental RAS system.

Level of Ang II, an octapeptide vasoconstrictor, is high in normal pregnancy, yet its vascular response is low. However, it was reported that Ang II sensitivity is increased in PE. This could be explained firstly by heterodimerization of angiotensin receptors (AT1) with bradykinin receptors (60) and secondly, by the presence of AT1 receptor agonistic autoantibody (AA-AT1) (61). AA-AT1 is proposed to induce ROS intracellularly through activation of NADPH oxidase (62). It also stimulates plasminogen activator inhibitor (PAI)-1 synthesis leading to reduced fibrinolysis, less extracellular matrix and shallow trophoblast invasion. Reduced fibrinolysis increases fibrin deposition in glomeruli leading to decreased filtration capacity of kidney, thus contributing to proteinuria (63). Zhou *et al* proposed that AA-AT1 stimulates overproduction of sFlt-1, thus contributing in altered angiogenesis in PE (64).

1.6.6 Genetics and epigenetics

Almost 50 candidate genes are involved in the susceptibility to develop PE, out of which 8 genes such as those encoding for renin-angiotensin system, inherited thrombophilias, vasodilation related genes and pro-inflammatory cytokine genes were studied extensively (65). Several imprinted genes are critical for placental development and function. One such gene is STOX1 which is subjected to imprinting with preferential expression of the maternal allele, contains missense mutations and is hence suggested to have a role in trophoblast dysfunction in PE (66, 67). Epigenetic dysregulation can affect the placenta, impairing its size, function and predisposing to placental pathologies (68). Altered placental gene expression is reported in various pregnancy complications like IUGR, SGA babies and PE (69, 70).

Micronutrients like folic acid and vitamin B₁₂ are known to induce changes in DNA methylation and gene expression. Alterations in one carbon cycle during pregnancy may alter key methylation reactions. DNA methylation is critical for developmental changes in gene regulation and any changes that take place during this critical period will result in altered imprinting of genes which will be transferred to the next generation. Recent reports suggest epigenetic mechanisms such as CpG methylation and histone modifications are likely to play an important role in disease (71). Our studies report disturbed one carbon metabolism and altered global placental DNA methylation patterns in women with pregnancy complications (72-74).

1.7 Proteomics: Need and origin

The word protein is derived from the Greek adjective “πρωτεῖνες” (proteios) meaning ‘primary’. It was first coined by Jöns Jakob Berzelius in a letter written to Gerhardus Johannes Mulder on July 10, 1838. Mulder’s chemical analysis of silk, fibrin, egg and serum albumin led to the discovery of protein(75). The work done by James B. Sumner on enzyme isolation (76), Linus Pauling on protein structure (77), Walter Kauzmann on protein denaturation and folding (78, 79) and other investigators led to better knowledge of protein. The turning point in protein study came in 1950’s after the determination of amino acids sequence of insulin by Frederick Sanger (80) and stepwise cleavage and identification of amino acids sequence in a protein by Pehr Edman (81). Meanwhile in 1977, Sanger sequenced the first viral genome ϕ X174 bacteriophage (82) and at the same time Maxam-Gilbert established their work on DNA sequencing by chemical method, which became the stepping stone for DNA sequencing of other genomes (83). Thereby, starting the new era of “genomics” by the late 90’s. The study of protein became silent in these years because of the tedious, time consuming techniques for protein sequencing.

In 1996, the Human Genome Project started with the assumption that total genes can also give the picture of total protein. Completion of Human Genome Project in 2001 enriched the database and estimated about 30,000 genes in human genome, which showed no linearity with the protein number suggested to be more than 2,00,000. Beadle and Tatum’s one gene- one enzyme concept (84) was valid for prokaryote, where 100% of gene encodes for one protein per gene, but in many higher eukaryotes more than 50% of gene encode for more than one protein. For example, the Drosophila Down syndrome cell adhesion molecule (DScam) gene is a rich gene that exhibits 38,016 spliced variants (85).The quest of exploring life did not end with genomics, as it represented only the first level of complexity. The genome is the blueprint of the cell, but when it comes to biological functioning of the cell, protein plays an important role. A genome of the cell remains constant regardless of time, developmental stage, cell type and environmental condition, but the same is not true about a proteome of the cell. A protein maybe born according to cell type, stage or environmental condition, and during its lifetime, it undergoes several changes like post-translational modifications, compartmentalization, interaction and degradation. Unfavourable environmental

conditions turn on a gene, but turning on the gene is usually through a signalling pathway by some proteins which first encounter the environmental condition.

The static genome couldn't explain the dynamic nature of proteome, the next level of complexity. The term "proteome" was first described as the protein complement of genome (86). This definition however didn't explain the dynamic nature of protein contributed by the different patterns of gene expression, protein polymorphism, post transcription and post translational modifications. Thus, proteomics involves study of proteome at a given time of the cell and also includes protein expression profiling, protein-protein interactions, protein mining, post translational modifications, functional and structural studies of protein.

Protein chemistry had evolved long time before proteomics, but it dealt with only one protein at a time. Methods like separation and purification of protein, determination of specific activity, amino acids sequence, biochemical properties, 3D structure, regulation and artificial synthesis, were developed in protein chemistry which gave a platform for development of proteomics. Proteomics in turn focussed on all the proteins in a cell, that required large scale sequencing and identification which was made possible by development in two-dimensional electrophoresis, mass spectroscopy and protein microarray.

The development in the proteomics could not have happened without the progress of genomics and completion of sequencing of genome of many organisms which provides a rich source of data for identification of proteins. Proteomics in turn helps in functional annotation of genome. As proteomics directly focuses on gene product, it is said to be complementary to genomics (87). Yet genomics and proteomics provide limited information of phenotype and low molecular weight molecules are the closest link to phenotype. Metabolome is the linker between the genome and proteome. Metabolomics is the comprehensive, qualitative, and quantitative study of all small molecules in an organism (88). Metabolite profiling, metabolite fingerprinting and metabonomics are the three approaches to metabolomics which generate tremendous amount of information and gives a snapshot of the metabolite state of the cell.

1.8 Developments in proteomics: In relation to protein identification

The breakthrough in proteomics came with development of two-dimensional gel electrophoresis (2DE) and development in mass spectrometry. O'Farrell's combined method approach of isoelectric focussing and SDS-PAGE has become the basis of the modern 2DE. Advancement in 2DE happened due to (i) Development of first and second dimension, (ii) Development in staining methods, and (iii) Development in bioinformatics tools for detection and statistical analysis of spots. On the other hand, advancement in mass spectrometry especially with the development of soft ionization techniques such as ESI and MALDI, as well as improved resolutions in mass analysers such as TOFs, ORBITRAPs, FTs have intensified protein identification and characterization in proteomic research, which otherwise was difficult with conventional Edman sequencing. One of the fastest methods for protein identification using MS is by peptide mass fingerprinting where the masses of proteolytic peptide fragment is matched to the peptide masses from database. Peptide mass redundancy and posttranslational modifications of protein are the factors that affect the success of protein identification by peptide mass fingerprinting (89). These limitations are overcome by fragmentation of the peptide by tandem mass spectrometry (MS/MS). Mere protein identification will not answer the dynamic nature of proteins; the protein expression level as well as post translational modifications need to be analyzed. 2DE is the widely used quantitative proteomics approach. However, LC-MS based approaches are also emerging as a method of choice for quantitative proteomic analysis. LC-MS based quantitative methods such as stable isotope labelling in cell culture (SILAC), isotope coded affinity tagging (ICAT), trypsin-catalyzed ^{18}O labelling, isobaric tags for relative and absolute quantitation (iTRAQ) or semi quantitative label free methods have emerged as powerful techniques for studying differential protein expression (90). Mass spectrometry has played a great role as a discovery tool in clinical proteomics for biomarker and drug discovery but has not been able to overcome the limitations for diagnostic applications such as analysing hundreds of samples per day (91). Protein microarray technology on the other hand can be used as a diagnostic tool as well as for protein identification and relative quantification.

1.9 Application of proteomics in the field of disease identification and biomarker development

The recent advance in proteomic technology has led to its popularity in the clinical and pharmaceutical communities. One of the most common challenges faced in this field is the drug discovery and novel biomarker discovery for human diseases. A disease biomarker can be a diagnostic or prognostic marker, or proteins that correspond to the molecular mechanisms of disease, or help in identifying the drug target. Proteome of a tissue or bio fluid undergoes tremendous change in a diseased state. These changes may be at the level of protein expression such as up- or down-regulation, presence or absence of certain proteins; post translational modification of specific proteins which is not reflected in genomic studies. Many biomarkers are predicted for different human diseases such as cancer (PSA, CA125, CEA, CA15-3, etc (92)), Alzheimer's (Cerebrospinal fluid tau and CSF-Abeta42 (93)); cardiovascular diseases (troponinI and troponin T for myocardial infarction and brain natriuretic peptide for heart failure (94)). Though many candidate biomarkers have been identified using proteomic techniques, yet they have not found their route to clinical diagnostic application because of unfulfillment of certain criteria like selectivity, sensitivity and efficacy.

Analysing the human body fluids has become an attractive and promising approach for biomarker discovery in human diseases because of easy accessibility and minimum cost. Body fluids are rich source of protein and include serum, plasma, urine, sweat, cerebrospinal fluid, nipple aspirate, saliva, amniotic fluid, vaginal secretions, semen, synovial fluid, tears and bronchoalveolar lavage fluid (95). As a result of secretion and leakage of protein from variety of tissues into plasma; it becomes best choice for most of the disease diagnosis and prognosis, but several high abundant proteins, sample preparation and handling makes plasma proteome analysis challenging task. Tissue proteome profiling has been done by investigators to identify candidate markers which can be a foundation for identifying biomarker in the body fluid.

Biomarker identification faces many challenges such as many of protein biomarkers are low abundant proteins. Unlike genomic studies, the absence of protein PCR makes it difficult to amplify the low abundant protein. Thus different strategies are used by researchers to tackle this problem, most of which is related to the selective purification,

prefractionation and enrichment of the low abundant protein from the complex heterogeneous body fluid samples. Diseases like cancer are divided into stages; detection of these diseases in early stages increases the survival of the individual. Currently identified biomarkers do not reflect the early physiology and pathology of the disease. Early biomarker detection of some diseases is not feasible because of no clinical symptoms of onset of disease or difficulty in obtaining early stage samples. Many researchers are looking into animal models for the solution of this problem. Changes in protein isoform ratio can be a potent biomarker. Ratio of these protein isoform may sometime appear as biomarker, but may be a false positive result. As these ratios may be the property of the individual and not of a disease state or disease progression (96). Within sample variation is seen because of polymorphisms which add ups to the challenges faced in biomarker development.

1.10 Proteomics in pregnancy

Pregnancy is a physiological state involving several processes like proliferation, differentiation, apoptosis etc. that require dynamic change in protein expression. Most of our understanding of mammalian pregnancy has come from the research done on animal models and cell line cultures. Proteomics has recently stepped into this field with the aim to understand the consortium of proteins involved in pregnancy and its related complications. Proteomic analyses of pregnancy-related biological fluids involve maternal blood plasma or serum, follicular fluid, amniotic fluid, umbilical cord blood and urine. Follicular fluid (FF) constitutes the *in vivo* microenvironment of the oocyte that resembles the blood plasma. FF has revealed significant information regarding identification of reliable markers for oocyte maturation and quality (97), which aids in the selection of appropriate oocyte for *in vitro* fertilization (IVF). Amniotic fluid (AF) contains large amounts of proteins secreted by the amnion epithelial cells, maternal and fetal circulation, fetal and placental tissue, reflecting the physiology and pathology (if any) of the growing fetus. Prenatal diagnosis of many fetal abnormalities uses AF samples for conventional techniques like *amniocentesis* (98). Proteomic analysis of AF has helped in identifying many putative biomarkers for pregnancy-associated pathologies, such as premature rupture of amnion, intra amniotic infection, Down syndrome, Trisomy 13 and 18, pre-eclampsia, preterm delivery and fetoplacental hypoxia (99). Maternal blood is mostly used by investigators for

identification of potential biomarkers in pregnancy-related complications as it is easily accessible and available. In contrast, the neonatal blood is difficult to access as it is obtained by venipuncture of newborn and thus, is mostly obtained from umbilical cord blood (UCB). Protein profiling of UCB exhibits the physiological changes in the neonate and also aids in detecting novel biomarkers for fetal abnormalities (100).

1.11 Proteomic approaches in pre-eclampsia

PE is a highly potent life threatening syndrome; whose pathophysiology is poorly understood. Although biochemical pathways including hypoxia, oxidative stress, altered renin-angiotensin system, altered angiogenesis, immune response, inflammatory pathways have been independently implicated in development of PE, there is a pressing need to understand the disorder more comprehensively. Moreover, there are no markers to detect the PE in early stages of pregnancy. Preeclamptic patients tend to become hypertensive at the end of the second trimester and show symptoms of proteinuria. The specific diagnosis for PE relies on uteroplacental Doppler ultrasound technique as a preliminary screening test (101). PE can be better managed by identifying early stage biomarker(s). In this context, proteomics has recently stepped into preeclamptic studies to understand the molecular mechanisms, identify early biomarkers for diagnosis and develop intervention strategies to prevent and manage the disease. Various approaches used to study pre-eclampsia are depicted in Figure 1.2.

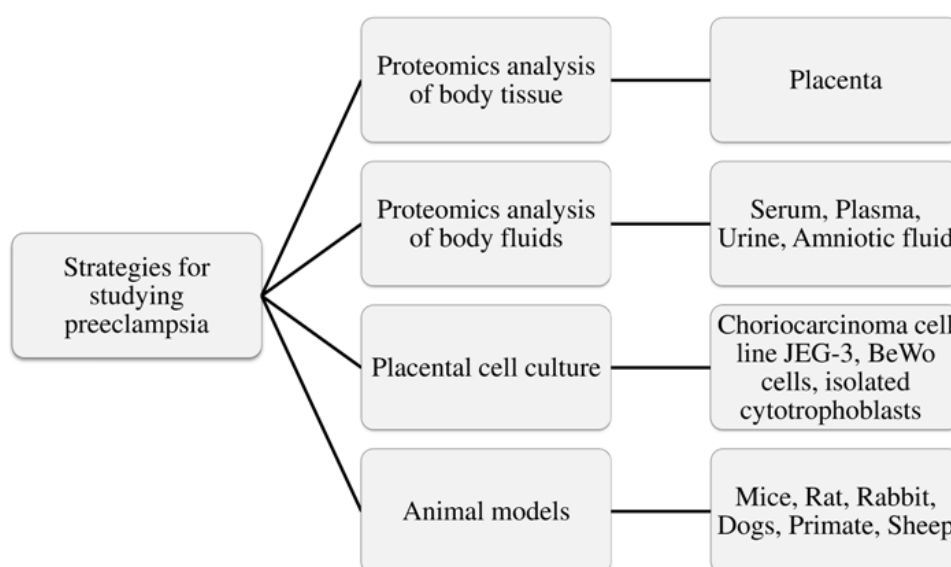


Figure 1.2 Proteomics strategies for studying PE

Proteomics studies on PE have been carried out on both animal models as well as in clinical samples of PE patients. Considerable efforts have been made to establish an animal model for PE, including uteroplacental ischemia, chronic NO synthase inhibition, adriamycin nephropathy, transgenic expression of human renin-angiotensin system, sFlt-1 and inflammatory models (102). Most of these animal models exhibit only some aspects of this syndrome, however the need for development of a model exhibiting the full spectra of the syndrome still remains.

1.11.1 Changes in body fluid proteins in PE pathogenesis

Proteinuria is one of the symptoms for clinical diagnosis of PE, wherein either protein amount in urine or spot protein-creatinine ratio of patients are monitored (103, 104). However, these quantitative methods are not clinically useful to predict the maternal and fetal complications in early stages of pregnancy (105). Proteome profiling of urine has led to identification of proteins for diagnosis and prognosis of PE. SELDI and tandem MS based characterisation of urine proteome was able to identify serine protease inhibitor A1 (SERPINA1) and albumin fragments, 10 weeks before clinical manifestation of PE, which could discriminate PE from hypertensive proteinuric disease. The study showed 21 amino acid C-terminus fragment of SERPINA1 was associated with severe forms of pre-eclampsia. The fragmentation pattern and misfolding of SERPINA1 is more related to PE compared to the high levels of circulating SERPINA 1 in other acute inflammatory conditions(106). SERPINS are a superfamily of proteins involved in various biological functions including inflammation, complement activation, blood pressure regulation, angiogenesis and fibrinolysis (107). Expression and epigenetic studies of placental SERPIN showed alteration under preeclamptic conditions (108). SERPINA1 (α -1-antitrypsin) is an inhibitor of elastase secreted by neutrophils at the site of inflammation. Elastase also plays a role in implantation and extracellular remodelling for placentation and its plasma level is known to be elevated in preeclamptic condition (109). The level of SERPINA3 (α -1-antichymotrypsin) also an inhibitor of elastase is known to be elevated in PE plasma as well as amniotic fluid and is postulated to be compensatory regulatory mechanism to inhibit ongoing platelet activation prior to the onset of clinical PE (110-

112). The urinary SERPINA8 (angiotensinogen) downregulation was identified by iTRAQ coupled with 2-D LC-MS/MS, which corresponds to the dysregulation of RAS system in preeclamptic condition (113).

Elevated SERPIN expression may be a compensatory mechanism in response to the imbalanced proteolytic activity prior to the development of PE. This is evident in studies done by Blumenstein *et al* on aberrant proteolytic processing of vitronectin and high molecular weight kininogen (HK) prior to onset of PE (week 20) (114). Vitronectin and HK are markers of fibrinolytic activity and neutrophil activation. These mechanisms are known to be associated with the pathophysiology of PE. In a recent study of urinary proteomics, fibrinogen α chain, collagen α chain and uromodulin fragments were predicted to be a marker for 28th gestational week, but they show lack of detectability in early gestational period (115). The role of protease and its inhibitors in pathophysiology of PE warrants further investigation.

Over expression or fragmentation of fibrinogen is associated with hypercoagulability in PE which is supported by proteomic study of plasma and urine (111, 115-117). Increased fibrinogen γ promotes platelet aggregation and leukocytes adhesion to the endothelium. Platelet activation is also reflected by increased clusterin in plasma of PE. Proteomic studies at clinical stage of PE with gestational age 32.2 ± 2.6 , showed a group of overexpressed spots, which was identified as clusterin by MALDI-TOF-MS, further the relative expression of serum clusterin was validated by immunoassay (118). Clusterin is a multifunctional protein that is shown to be up-regulated in placenta of PE than in control, and it is mainly localized in the syncytiotrophoblasts and villous endothelial cells (119). Data reveals that serum clusterin level can be used as a clinical marker, yet it alone cannot be used as potent marker for PE as overexpression of clusterin is also seen in renal disease, atherosclerosis, Alzheimer's, myocardial infarction and cancers (118, 120, 121). Increased clusterin levels in PE may reflect oxidative stress, endothelial cell injury or renal dysfunction.

Plasma or serum proteome profile can reflect the physiological changes occurring in PE. Circulating angiogenic and antiangiogenic factors such as sFlt-1, VEGF, PlGF in maternal blood have been explored as a potential marker for PE since the last decade (122-126). sFlt-1 and sEng increases in serum in PE, and binding of these neutralises

the free antiangiogenic factors to VEGF and PlGF thus reducing its serum concentration. Apart from angiogenic and antiangiogenic factors, histidine rich glycoprotein was also found to cause angiogenic imbalance during early onset of PE (116, 127). These studies have used ELISA for identification and quantification of angiogenic factors. Although angiogenic factors have a role in PE, the data relating to angiogenic factors as early marker are inconsistent, mainly because of the differences in methodology and sample heterogeneity.

Plasma proteomic profiling using 2D-MS techniques have led to identification of candidate markers for clinical as well as preclinical stages of PE. Maternal serum proteomic profile of clinical and preclinical PE groups using 2D-LC MS/MS and label free quantification identified differentially expressed proteins between these groups. In Clinical PE, fibronectin, pappalysin-2, choriogonadotropin- β , apolipoprotein C-III, cystatin-C, VEGFR-1, and endoglin were more abundant, while matrix metalloproteinase-9 (MMP-9) was significantly lower compared to normotensive women. In preclinical PE, differentially expressed proteins included placental, vascular, transport, matrix, and acute phase proteins, while angiogenic and antiangiogenic proteins were not significant (128). Several other pregnancy specific or pregnancy-enriched proteins such as PAPP-A (pregnancy-associated plasma protein-A), PSG1 (pregnancy-specific β -1 glycoprotein 1) and PSG9 also show significant increase in PE plasma, however they are also associated with other pregnancy complications (129). The role of some of these proteins in pathophysiology of PE needs to be explored.

Investigations to find markers to distinguish between severe, mild, early and late onset of PE were attempted. Using proteomic approach, combining SDS-PAGE, in-gel digestion and MS/MS, Zhang *et al* analyzed 16 plasma samples each from severe early onset PE and healthy gestational age matched pregnant women, showed lower level of complement component C4A and higher level of apolipoprotein A-1 in severe early onset PE than severe late PE patients. Similar results were also observed when Jar cells were cultured under hypoxia and normoxia conditions (130). In a gel-free approach, using in-solution digestion followed by LC-MS/MS of serum proteins from severe PE and normal pregnant women, showed differential expression of α 2-HS-glycoprotein (AHS2G), retinol binding protein 4 (RBP4) and α -1-micro-globulin/bikunin (AMB1P)

and Insulin like growth factor binding protein-acid labile subunit (IGFBP-ALS), these candidate proteins are involved in insulin regulation and were validated with a quantitative mass spectrometric method, selective reaction monitoring (SRM) and ELISA (131). SELDI-TOF MS showed significant increase in haemoglobin level in cerebrospinal fluid (CSF) in case of severe PE than in mild PE and normotensive (132). Study done by immunoassay methods suggests several other potent markers such as PIGF, leptin to be present in CSF of PE patients (133, 134). PE is a multisystem disorder thus presence of these proteins in CSF relates to the severity of PE rather than an early biomarker.

Advanced proteomic techniques such protein array technologies provide rapid screening of complex samples. Changes in plasma protein profile by ProteinChip technology, identified five significantly up-regulated proteins in PE plasma (135). Peptide ligand library affinity chromatography coupled with LC MS/MS is useful to capture and identify low abundant protein biomarker. This method efficiently identified 31 up-regulated and 20 down-regulated proteins involved in complement and coagulation response, acute inflammatory and defence response, lipid metabolism, extracellular matrix remodelling and protease inhibitor activity. Western blot analysis confirmed upregulation chorionic somatomammotropin hormone (CSH), AHSG, and downregulation of transthyretin (TTR) and RBP4. CSH is a low abundant protein of plasma and is secreted by syncytiotrophoblast, is known to have lipolytic activity and may be the major contributor of free fatty acid in preeclamptic maternal circulation (136). TTR is a transporter of thyroxine and RBP4, is also found to be up-regulated in its monomeric and oxidised form in amniotic fluid of preeclamptic women (112).

Proteomic analysis of amniotic fluid has been done for preterm birth (137, 138) and it is now extended to study PE. Proapolipoprotein A-1 and SBBI42 were identified as proteomic marker in amniotic fluid that can differentiate PE from chronic hypertension and normotensive control (139). Proapolipoprotein A-1 is the propeptide which is cleaved to mature apolipoprotein A-1, whose level is significantly high in PE than in normotensive controls. This correlates with the abnormal lipid profile seen in preeclamptic conditions, and may also contribute to endothelial dysregulation.

1.11.2 Placental proteome in PE pathogenesis

Many researchers have considered placental tissue for proteomic studies to identify a candidate marker which can be further analyzed in plasma. It has been found that the symptoms of PE disappear as soon as the placenta is delivered, thus emphasizing the importance of placenta in development of PE (140). Comparative analysis of placental proteome of PE and normotensive subjects has resulted in identification of several differentially expressed proteins. Studies on placental proteome profile changes in preeclamptic conditions using 2-D followed by MALDI-TOF MS/MS showed that differentially expressed proteins belongs to different classes of proteins including, stress-related/ chaperone proteins (HSP 60, HSP gp96, Hsc-70, HSP 27), antioxidants (Glutathione S transferase, Cu/Zn-superoxide dismutase, peroxiredoxin 2 and 3), endoplasmic reticulum protein (ERp 29, protein disulfide isomerase), transport protein (apolipoprotein A-1, chloride intracellular channel 3, transthyretin), cytoskeletal protein (actin γ 1 propeptide, tropomyosin α -3 chain), apoptosis related protein (Voltage dependent anion channel, Cathepsin D)(141-144). Quantitative proteomic approach using iTRAQ labelling to study secretome of placenta under both normoxic and hypoxic condition, identified 45 differentially expressed proteins, which included significant upregulation of an inflammatory component interleukin-8 under hypoxia (145).

As poor trophoblast invasion is one of the factor in development of PE, trophoblast proteome profile of normotensive and PE patient have been reported. This also focuses on the highly purified sub-proteome, thus reducing the complexity of the sample to be studied. Various proteins were found to be differentially expressed in placental trophoblasts. Proteomic analysis of highly purified cytotrophoblast (99.99%) identified three clusters of proteins: (i) peroxiredoxin 6, glutathione S-transferase, ezrin, aldosereductase; (ii) Hsp60, Hsp70, proteasome a subunit, protein disulfide isomerase; (iii) phosphoglycerate mutase I, triose- phosphate isomerase. These clusters of proteins demonstrate the reduced cytotrophoblast antioxidant defense to increased oxidative stress during preeclamptic conditions (146). Decreased antioxidant defence of trophoblast was also indicated by decreased peroxiredoxin 2. Proteomic analysis of placenta also identified ER resident protein (PDI, ERp60, ERp44) and mitochondrial protein (dihydrolipoyl dehydrogenase, delta3,5-delta2,4-dienoyl-CoA isomerise,

TIM21-like protein) to be related to pathogenesis of pre-eclampsia (147). However, in another study of proteome of placental trophoblast cells isolated by laser capture microdissection, showed upregulation of molecular chaperone (HSP27, 78kDa glucose-regulated protein, prohibitin) in response to oxidative stress in PE, along with upregulation of protein involved in apoptosis(annexin A5 and A2) and downregulation of titin and calnexin (148).

1.11.3 Cell lines for PE studies and their application in proteomic analysis

The unavailability of placenta during the onset of disease makes it difficult to study the early stages of PE in placenta. Cell cultures that mimic the PE conditions *in vitro* may overcome the problem of availability of placental tissue to some extent. As hypoxia is one of the major causes of PE, efforts have been made to study the role of low oxygen on placental cell culture. Hypoxia was found to change protein expression pattern in various cell lines such as cytotrophoblasts and BeWo (149, 150). One such up-regulated protein was neurokinin B, which is known to inhibit normal response to hypoxia (151). Similarly, hypoxia was found to induce apoptosis in JAR cells along with increased expression of Bcl-x, caspase-3 and 9, HSP-70, PTEN and Bag-1 whereas Bad, panJHK/SAPK-1, Bcl-2, Bid and Caspase-8 were decreased (152). Although several proteomics studies on PE have been reported, there is need to understand the disease better in order to elucidate the molecular mechanisms, identify drug targets for the treatment and discover early biomarker for the diagnosis and management of the disease.

1.11.4 Autoantibodies in PE pathogenesis: Can they serve as biomarkers?

Abnormal expression, aberrant degradation, post translational modification such as glycosylation, nitration, misfolding of proteins can lead to immune response as these proteins will be considered as non-self or antigens. In case of PE, many circulating factors from placenta, cell debris, fetal DNA come into maternal circulation which triggers immune response and autoantibody production. One of the first autoantibody suggested to be used as diagnostic tool to predict PE was autoantibodies to angiotensin II type I receptor (AT1-AA) which binds to the peptide AFHYESQ of second

extracellular loop of the AT1 receptor (61), but AA-AT1 are also found in normotensive pregnant women with IUGR and uncomplicated pregnancy (153), kidney transplant recipients suffering from severe vascular rejection and malignant hypertension (154).

Immunoproteomics –based technologies such as gel-based (PROTEOMEX) and gel free immunoproteomics (SEREX), inverse immunoproteomics for antigen profiling: AMIDA (autoantibody mediated identification of antigens) or immunocapture MS, can be used a tools for biomarker discovery (155, 156).

1.11.5 PTMs in pre-eclampsia

Mapping of PTMs in pre-eclampsia is still in its early stages. The studies on PTMs related to PE have been carried out by traditional method. PTMs such as glycation and nitration are reported in PE, as they are fingerprints of oxidative injury, which is one of the major contributors of endothelial dysfunction in PE. The advanced glycation end (AGE) and its receptor (RAGE) system was shown to be up-regulated in PE by methods such as immunohistochemistry, western blot and ELISA (157-159). Increase in ROS and RNS in pre-eclampsia, leads to peroxynitrite formation resulting in nitration of tyrosine residue of protein. Nitration of P2X₄ purinergic receptor, phospho-p38 mitogen-activated protein kinase (MAPK), Y132, Y245, and Y258 has been reported (160). S-nitrosylation (SNO, covalent adduction of an NO moiety to cysteines) of placental proteins is also altered by pre-eclampsia (161). Another example of post translational modification due to oxidative stress was seen in cysteine residue of monomeric TTR, where it is oxidized to glycine or cysteic acid at position 10, this leads to aggregation of TTR in PE (112). Dysregulation of O-linked glycosylation also occurs in pre-eclampsia, evident by increased deglycosylation of apolipoprotein E, which is postulated to contribute to vascular damage (162). Phosphorylation of protein is also observed in preeclamptic condition, such as increases in serine phosphorylation of HSP27 in response to oxidative stress, decrease in tyrosine phosphorylation of VEGFR-2 in response to overexpression of sFlt-1 and serine phosphorylation of insulin receptor substrate -1 and -2 leading to insulin resistance in preeclamptic patients (163-165). Further investigation of PTMs in PE using advanced proteomic techniques can be useful to increase our knowledge of PE pathophysiology as well as can contribute to pool of markers for PE.

Chapter 2

Biochemical insights into the pathophysiology of pre-eclampsia through placental proteomics- Part 1 (gel based proteomics)

Contents of this chapter is published as research article in Clinical proteomics, 2017,
DOI : 10.1186/s12014-017-9144-2

Chapter 2 Biochemical insights into the pathophysiology of pre-eclampsia through placental proteomics- Part 1 (gel based proteomics)

2.1 Background

The breakthrough in proteomics came with development of two-dimensional gel electrophoresis (2DE). O'Farrell's method of 2D SDS PAGE became the basis of the modern 2DE. Development in 2DE took place in three stages over a period of time: (i) Development of first and second dimension, (ii) Development in staining methods, and (iii) Development in bioinformatics tools for detection and statistical analysis of spots.

Choice of staining method in 2DE depends on sensitivity of detection, compatibility with MS, ease of use and cost. The very popular staining methods of protein include the Coomassie Brilliant Blue (CBB) and Silver staining. Both these methods have undergone massive changes with respect to their sensitivity and processing time. The conventional CBB R-250 staining has a sensitivity range of 200-500 ng (166) and recent development shows 12 ng (167). Colloidal CBB G-250 shows 30 ng per band sensitivity (168), and modification of this method the blue silver staining shows sensitivity 10 ng per band (169). Silver staining is far more sensitive than CBB staining, which can detect protein at nanogram level. The classical silver staining interferes with mass spectrometric analysis because of presence of glutaraldehyde and silver (170). This problem was overcome by MS-compatible silver staining which was however less sensitive and gave higher background. Another method gaining popularity in protein detection because of its high sensitivity and linear dynamic range is the fluorescent staining. There are two approaches of fluorescent staining: (i) pre-electrophoretic staining using fluorescently labelled compounds like dansyl chloride, fluorescamine (4-phenyl-[furan-2(3H), 1-phthalan]-3, 3'-dione), o-phthaldialdehyde (OPA), and 2-methoxy-2, 4-diphenyl-3([2H])-furanone (MDPF), monobromobimane and the cyanine-based dyes (CyDyes; Amersham biosciences) (171). CyDyes have given rise to a method termed as Difference Gel Electrophoresis (DIGE), in which Cy3 and Cy5 with same mass and charge but different excitation and emission wavelength are used to label two different protein samples prior to electrophoresis (172). Recently Cy2 has been used as an internal standard to improve normalization of data and quantitative

comparison of samples (173). (ii) Post-electrophoretic staining involves protein staining with a fluorescent dye after electrophoresis. Most dominantly used dye under this category is the ruthenium-based SYPRO Ruby with a detection limit of 1-2 ng protein per spot (174). The limitation of fluorescent staining is the cost of dyes and requirement of suitable imaging device.

The third and final step in 2DE is image analysis and spot detection, which is done using commercially available 2DE-image analysis software packages such as PDQuest (Biorad), Melanie (GeneBio), ImageMaster (GE healthcare), Delta2D, Progenesis, REDFIN. These software consist of sets of algorithms for image normalization, cropping, background subtraction, spot detection, land marking, matching spots and quantification. Some of these programs have options for automated spot excision. Despite these improvements in image analysis, we still require manual intervention.

2.2 Material and Methods

2.2.1 Sample collection

All samples were collected from Department of Obstetrics and Gynaecology, Bharati Hospital, Pune, Maharashtra, India with informed consent from the patient and was approved by the Bharati Vidyapeeth Medical College Institutional Ethical Committee. The study excludes women with indication of chronic hypertension, type1 or 2 diabetes mellitus, renal or liver diseases and seizure disorder. Patients were classified under PE if they showed systolic and diastolic blood pressures greater than 140 and 90 mmHg, respectively, with presence of proteinuria (>1+ or 300 mg/24 hrs) on a dipstick test and was confirmed by repeated recording of the blood pressure with an interval of 6 hrs. Appendix 1 shows the maternal characteristics. Placental tissues from normotensive and pre-eclamptic pregnancies were collected immediately after delivery. Small sections of tissues were cut out from placental cotyledons and rinsed with phosphate buffered saline to wash off the blood, snap frozen in liquid nitrogen and stored in -80°C until further use.

2.2.2 Protein extraction and two dimensional gel electrophoresis (2DE)

100 mg frozen placental tissue was pulverized, and dissolved in lysis buffer (7M urea, 2M thiourea, 4% 3-[(3-Cholamidopropyl) dimethylammonio]-1- propanesulfonate, 2% Dithiothreitol), vortexed for 5 min at 24°C±2 and sonicated for 2 min on ice. The homogenate was centrifuged (25,000 rpm, 45 min, 24°C±2), and supernatant used as source of placental proteins. Protein estimation was performed with Quick start Bradford reagent (Bio-Rad Laboratories, Hercules, CA, USA).

Total 18 placental tissues were analyzed by random pooling of equal amount of protein from 6 normotensive (C) or 6 pre-eclamptic (PE) placentas, respectively. Two technical replicates each of three pools of normotensive were compared with three pools of PE protein samples using 2DE. Immobilized pH gradient (IPG) strips 4-7, 11 cm were passively rehydrated using 200 µg samples solubilized in 200 µL rehydration buffer (7M urea, 2M thiourea, 4% CHAPS, 2% DTT and 1% ampholyte). The first dimension electrophoresis was performed using Protean IEF Cell (Bio-Rad). The isoelectric focusing was performed at the following voltage gradients: first step at 250V for 2 h, second step at 8000V for 4 h and third step at 20,000 Vh. The strips were reduced and alkylated by equilibrating for 20 min in buffer I (6M urea, 0.375M Tris-HCl buffer pH 6.8, 2% SDS, 20% Glycerol and 2% DTT) and 20 min in buffer II (6M urea, 0.375M Tris-HCl buffer pH 6.8, 2% SDS, 20% Glycerol and 2.5% Iodoacetamide). After IEF, the strips were placed on 12% Tris-Glycine SDS-PAGE gels for the second-dimension electrophoresis. Gels were stained with Coomassie Brilliant Blue R-250 and images were scanned on GS-800 Densitometer and analyzed for spot intensity data by PDQuest software (Bio-Rad). The number of spots was calculated based on the criteria that the spots were present in duplicate gels in each group with at least 1.5 fold differences.

2.2.3 In-gel digestion and nano LC-MS^E protein identification

Protein spots excised from 2DE were de-stained by 50 mM ammonium bicarbonate containing 50% acetonitrile (ACN), followed by reduction by 10 mM DTT for 60 mins at 56°C and alkylation in 55mM iodoacetamide for 45 mins in dark condition. Proteins were digested overnight with mass spectrometric grade trypsin (Promega, Madison,

WI, USA) at 37°C. Peptides were extracted in 50% ACN containing 2% formic acid, vacuum-dried and stored at -80°C until use.

Digested peptides were analyzed in LC-MS^E using a NanoAcquity ultra performance liquid chromatography (UPLC) system coupled to a SYNAPT high definition mass spectrometer (Waters, Milford, MA, USA). The nano-LC separation was performed on a C18 reversed phase column (1.7 µm particle size) with an internal diameter of 75 µm and length of 250 mm (Waters). The binary solvent system that was used, comprised 99.9% water and 0.1% formic acid (mobile phase A) and 99.9% acetonitrile and 0.1% formic acid (mobile phase B). LC-MS^E data were processed and searched using ProteinLynx Global Server 2.4 (PLGS) software (Waters). UniProtKB H.sapiens proteome (UP000005640), including only reviewed sequences (47,869) from UniprotKB/SwissProt (updated version of H.sapiens proteome, 2008) was used to search against the MS data. The inclusion criteria of selection for accurate identification was (i) minimum two peptides, (ii) sequence coverage more than 20%, (iii) PLGS score, (iv) MS/MS fragmentation (v) two miss cleavage, and (vi) FDR 1%. A fixed modification included carbamidomethyl C and variable modifications such as oxidation M, deamidation N and deamidation Q. Automatic setting of PLGS were used for mass accuracy of precursor and fragment ions. For each protein identified, number of unique peptides for a given protein was calculated using PepServe bioinformatics tool. The dataset (PASS00711) was uploaded to publicly accessible PeptideAtlas database (www.peptideatlas.org, Institute for Systems Biology, Seattle, WA).

2.2.4 Western blot analysis

Placental protein (10µg per lane) from normotensive (n=25) and pre-eclamptic (n=25) was separated on 10% SDS-PAGE. Multi-strip Western blotting protocol was performed as mentioned in Edita A. et al, 2007 (175). All 50 individual protein samples (7-gels) were transferred to one single PVDF membrane (Millipore Corporation, Billerica, MA, USA) and blocked overnight at 4°C in 5% skimmed milk or 2% bovine serum albumin. Primary and secondary antibodies incubation was performed as per manufacturer's instructions (Santa Cruz Biotechnology, Santa Cruz, CA, USA). The antibodies used are as follows: anti-vimentin, anti-transferrin receptor, anti-annexin A6, anti-tubulointerstitial nephritis antigen-like and anti-betaactin. Detection was

performed by chemiluminiscent ECL reagent (GE Healthcare, Little Chalfont, BUX, UK) and signals were detected with CCD imaging system (Syngene, Cambridge, UK) camera. Analysis of total signal intensity of Western blot bands was performed with Image Studio Lite version 4.0 (Li-Cor Biosciences, Lincoln, NE, USA) using local background subtractions.

2.2.5 RNA extraction and qPCR

Total RNA extraction from placental tissue was performed using RNeasy Plus Mini kit (Qiagen, Valencia, CA, USA) according to manufacturer's protocol. Two micrograms of total RNA were used for preparation of cDNA using High-Capacity cDNA Reverse Transcription kit (Applied Biosystems, Foster City, CA, USA) according to manufacturer's protocol. Total of 45 individual cDNA samples consisting of 18 PE and 27 normotensive samples were used for further qPCR. qPCR was performed in 7900 HT Fast Real time system using SYBR green chemistry using SYBR green Real-time PCR Master mixes (Applied Biosystems). The following gene-specific primers were used: AnnexinA6: sense (5'AGTTGAATGTGCTGGGCGGG3'), antisense (5'ATGGGTGGTGAATGGATGGGAAG3') and housekeeping gene betaActin: sense (5'CCATCGTCCACCGCAAAT3'), antisense (5'GCTGTACCTTCACCGTTC3'). All measurements were performed in triplicates and conditions used were as follows: 95°C for 10 min, 40 cycles of 95°C for 3 sec, 60°C for 30 sec. Relative quantitation was performed using Data AssistTM Software (Applied Biosystems).

2.2.6 Statistical Analysis

Analysis of statistical significance of differential expressed protein 2DE protein spots and Western blot protein bands were carried out using one-tailed Student's t-test. Analyzes were performed using SPSS/Pc package software version 18.0 (Chicago, IL, USA) and results were considered statistically significant if $p \leq 0.05$.

2.2.7 Gene Ontology Analysis

Gene ontology annotation of differentially expressed genes was performed using UniProt/ QuickGO and functional enrichment analysis was performed using DAVID

(176). REVIGO was used to summarise and visualize the enriched gene ontology terms for biological process (177).

2.3 Results and Discussion

A vast amount of research carried out till date on pre-eclampsia is still not enough to elucidate its origin, nor cure or manage or identify an ideal biomarker. Large-scale comprehensive basic research like proteomics gives insight into such a multi-factorial disorder. We had extensively reviewed the different proteomics techniques used to study pre-eclampsia (2). In this study, we not only found many known proteins to be involved in pre-eclampsia but also new sets of DEP which might be related to few etiological factors of pathophysiology of pre-eclampsia. Molecular chaperones, cytoskeleton binding proteins, ER proteins, ion transport regulators and intermediate filament proteins have certain normal functions in a cell or tissue. However, these proteins are the key to disturbance or imbalance in the cell under any diseased state.

2.3.1 Proteomic profiling of normal and pre-eclamptic placentas

In a typical 2DE gels over 228 protein spots were detected in placental protein extracts, of which 55 protein spots were differentially expressed. Figure 2.1 shows representative pre-eclamptic and normotensive Coomassie blue stained gels with marking of differentially expressed protein spots. Differentially expressed protein spots were identified by nano LC-MS/MS, and the computed MW/pI, Uniprot accession number was obtained by referring to human proteome database from Uniprot, using ProteinLynx Global Server (PLGS) software (Supplementary data 1). Table 2.1 shows the identified proteins with their molecular weight and isoelectric point, fold change with *p* value, and Figure 2.1 represents the respective spots' zoomed image.

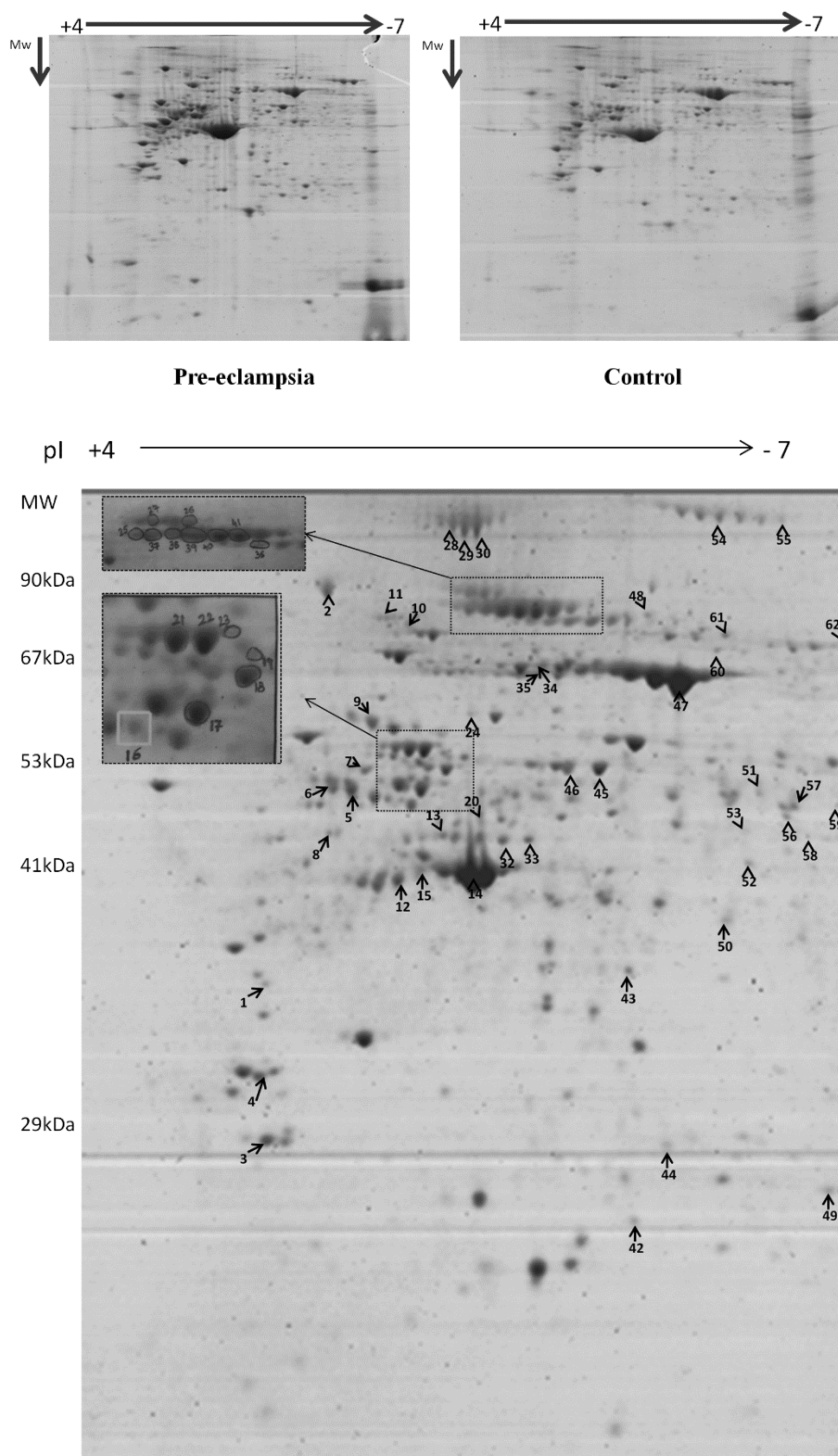


Figure 2.1 Representative 2DE SDS PAGE

Gel of pre-eclamptic and normotensive Coomassie blue stained gels and protein spot numbered on the images

Based on the inclusion criteria, we identified 27-up-regulated and 28-down-regulated protein spots in PE compared to normotensive placenta. It was notable that 9-protein spots were up-regulated more than 2-fold in PE, while 7-protein spots were up-regulated more than 2-fold in normotensive placental tissue with high confidence ($p \leq 0.05$). Several of these protein spots were identified as isoforms with differences in molecular weight and isoelectric point. These may be due to splicing or post translational modifications or in-vivo proteolysis or fragmentation. For example, actin cytoplasmic 1 or 2 (spot # 12, 13, 14, 15); alpha-1 antitrypsin (spot # 5, 6, 9); collagen alpha 1 VI chain (spot # 28, 29, 30); fibrinogen beta chain (spot # 50, 53, 56, 57, 59); fibrinogen gamma chain (spot # 36, 37, 38, 39, 40, 41); serum albumin (spot # 42 and 47) and vimentin (spot # 5, 6, 8, 17, 18, 19, 21, 22) were some of these proteins. Multiple proteins for single spots were also identified by LC-MS/MS, due to co-migration of proteins. Further to identify biological relevance of these DEP in PE, we performed gene ontology enrichment.

2.3.2 Gene ontology of differential expressed proteins revealed numerous biological processes affected that are related to the etiological factors of pre-eclampsia

The gene ontology terms for biological processes, molecular functions and cellular components of differentially expressed proteins are summarized in Supplemental data 2. A majority of these proteins participate in fundamental biological process such as cellular process (20%), metabolic process (17%), cellular component organization (14%), development process (12%), localization (9%), and other process like reproduction, immune response, apoptosis, and cell adhesion (28%). Functional enrichment results of biological processes from DAVID were visualized in REVIGO, wherein the redundancy in GO terms was removed. REVIGO scatterplot shows the enriched biological processes such as response to hypoxia, regulation of apoptosis, focal adhesion assembly, inflammatory response, response to metal ion and protein folding (Figure 2.3).

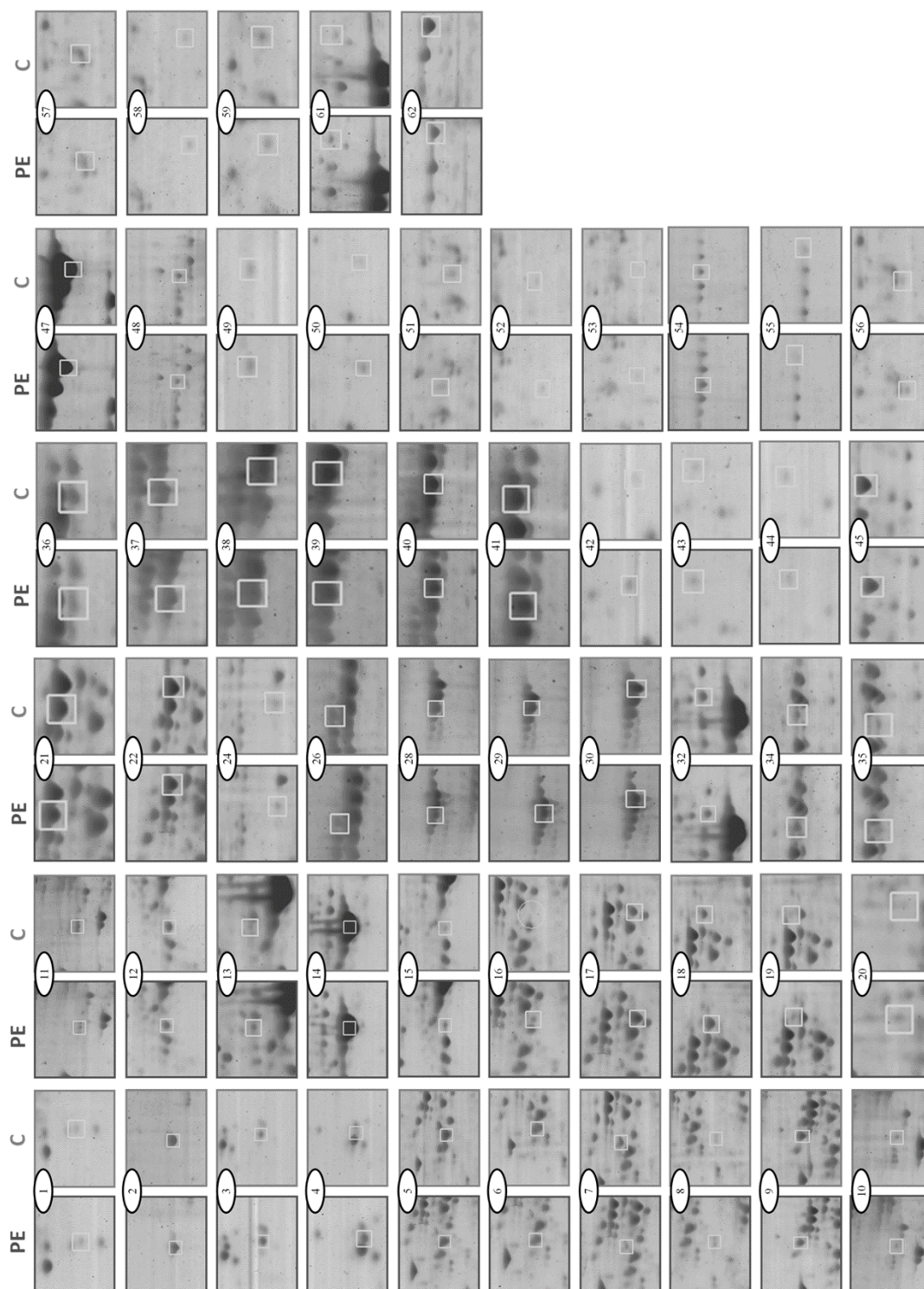


Figure 2.2 Magnified images of differentially expressed protein spots identified by PDQuest software

Placental proteome extracts (n=36) from 3 pre-eclamptic and 3 normotensive randomly pooled group (pool of 6 individuals) was analyzed by two dimensional electrophoresis in two technical replicates followed by image analysis with PDQuest software.

Table 2.1 LC-MS^E identification of differentially expressed proteins in normal versus pre-eclamptic pregnancies

Protein identification was done using PLGS and the number of unique peptides identified using PepServe software. In the column with fold change, ↑ represents up regulation and ↓ represents down regulation. () consists of total peptide identified by PLGS which includes more than twice identification of same peptide.

Spot No.	Accession No.	Protein description	MW	pI	Sequence coverage (%)	Unique peptide(Total peptide identified)	Fold change PE/C	p value
1	P09493-3	Isoform 3 of Tropomyosin alpha 1 chain	32855	4.5	33.1	(17)	1.5↑	0.0312
	P09493-9	Isoform 9 of Tropomyosin alpha 1 chain	32716	4.5	30.6	(15)		
	P09493-8	Isoform 8 of Tropomyosin alpha 1 chain	32796	4.5	30.3	(14)		
2	P14625	Endoplasmic	92411	4.6	63.6	22(198)	1.8↓	0.0072
	P63104	14 3 3 protein zeta delta	27727	4.5	64.1	6(46)		
3	Q04917	14 3 3 protein eta	28201	4.6	28.5	3(15)	1.6↑	0.0494
	P61981	14 3 3 protein gamma	28284	4.6	23.9	2(15)		
	P67936	Tropomyosin alpha 4 chain	28504	4.5	22.2	3(8)		
4	P01009	Alpha 1 antitrypsin	46707	5.2	59.6	12(103)	2.5↑	0.2892
	P08670	Vimentin	53619	4.9	70.4	13(49)		
5	P01009	Alpha 1 antitrypsin	46707	5.2	54.8	15(84)	1.7↓	0.0139
	P08670	Vimentin	53619	4.9	78.1	16(82)		
6	P07437	Tubulin beta chain	49638	4.6	73.9	4(55)	1.9↓	0.0005
7	P08670	Vimentin	53619	4.9	56.9	13(43)	1.8↑	0.0006
8	P01009	Alpha 1 antitrypsin	46707	5.2	65.1	16(91)	1.5↓	0.2874
9	P21980	Protein glutamine gamma glutamyltransferase 2	77279	4.9	33.9	11(25)	2.1↓	0.004
10	P08238	Heat shock protein HSP 90 beta	83212	4.8	58.1	8(96)	1.7↓	0.0052
	P07900	Heat shock protein HSP 90 alpha	84606	4.7	52.9	7(80)		
11	P60709	Actin cytoplasmic 1	41709	5.1	69.3	(42)	2.8↓	0.0151
12	P63261	Actin cytoplasmic 2	41765	5.2	22.4	(10)	2.7↑	0.021
13	P60709	Actin cytoplasmic 1	41709	5.1	80.8	(115)	3.0↓	0.156
	P63261	Actin cytoplasmic 2	41765	5.2	80.8	(155)		
14	P60709	Actin cytoplasmic 1	41709	5.1	72.8	(52)	1.8↑	0.313
	P68032	Actin alpha cardiac muscle 1	41991	5.1	65.8	(50)		
15	Q15084	Protein disulfide isomerase A6	48091	4.8	29.8	8(10)	3.1↑	NI
16	P08670	Vimentin	53619	4.9	82.8	19(141)	2.9↑	0.0001
	Q15084	Protein disulfide isomerase A6	48091	4.8	48.6	8(16)		
17	P08670	Vimentin	53619	4.9	86.9	21(115)	1.7↑	0.0084
	P17661	Desmin	53503	5.0	61.1	16(49)		
18	P08670	Vimentin	53619	4.9	80.7	20(115)	2.7↑	0.0203
	P02774	Vitamin D binding protein	52929	5.2	61.6	8(48)		
19	P17661	Desmin	53503	5.0	58.1	9(51)	3.1↑	0.003277
	Q8NBS9	Thioredoxin domain containing protein 5	47598	5.6	45.8	10(38)		
20	P08670	Vimentin	53619	4.9	90.3	21(179)	1.5↓	0.0033
21	P08671	Vimentin	53619	4.9	92.9	19(201)	1.8↓	0.207
22	P10809	60 kDa heat shock protein mitochondrial	61016	5.6	75.9	22(74)	1.6↑	0.358
23	O43707	Alpha actinin 4	104788	5.1	81.6	25(112)	3.2↓	0.0414
	P12109	Collagen alpha 1 VI chain	108461	5.1	61.7	27(138)		
24	Q05707-3	Isoform 3 of Collagen alpha 1 XIV chain	183037	5.0	26.0	(35)	1.5↓	0.0014
	Q9Y4L1	Hypoxia up regulated protein 1	111266	5.0	38.8	11(30)		
25	P35579	Myosin 9	226390	5.3	32.6	22(83)	1.6↑	0.0014
	P12109	Collagen alpha 1 VI chain	108461	5.1	53.9	21(120)		
26	P12109	Collagen alpha 1 VI chain	108461	5.1	51.0	21(114)	2.0↓	0.007
27	Q12905	Interleukin enhancer binding factor 2	43035	5.0	38.7	8(11)	1.5↓	0.006
28	P08133	Annexin A6	75825	5.3	81.9	30(131)	1.8↑	0.0372
	P08133-2	Isoform 2 of Annexin A6	72378	5.3	78.0	29(128)		
29	P11142	Heat shock cognate 71 kDa protein	70854	5.2	64.6	10(64)	1.8↑	0.0653
	Q03252	Lamin B2	67647	5.1	62.5	(62)		
30	P08107	Heat shock 70 kDa protein 1A 1B	70009	5.3	52.1	(42)	1.7↓	0.0504
	P08133-2	Isoform 2 of Annexin A6	72378	5.3	45.4	13(28)		
31	P02679	Fibrinogen gamma chain	51478	5.2	60.9	(69)	1.8↑	0.1693
	P02679-2	Isoform Gamma A of Fibrinogen gamma chain	49464	5.6	69.1	(55)		
32	P55072	Transitional endoplasmic reticulum ATPase	89265	5.0	81.9	(133)	1.5↓	0.205
	P02679-2	Isoform Gamma A of Fibrinogen gamma chain	49464	5.6	73.7	(112)		
33	O43707	Alpha actinin 4	104788	5.1	61.0	(65)	1.7↑	0.0133
	P55072	Transitional endoplasmic reticulum ATPase	89265	5.0	42.9	(27)		
34	P02679-2	Isoform Gamma A of Fibrinogen gamma chain	49464	5.6	70.0	(108)	1.5↓	0.0654
	O43707	Alpha actinin 4	104788	5.1	68.7	(80)		
35	P55072	Transitional endoplasmic reticulum ATPase	89265	5.0	36.6	(28)	1.5↓	0.0654
	P01023	Alpha 2 macroglobulin	163187	6.0	22.9	(32)		
36	P35609	Alpha actinin 2	103788	5.2	19.2	(15)	1.5↓	0.0654
	P02679-2	Isoform Gamma A of Fibrinogen gamma chain	49464	5.6	60.9	(122)		
37	O43707	Alpha actinin 4	104788	5.1	61.5	(66)	1.5↓	0.0654
	P01023	Alpha 2 macroglobulin	163187	6.0	34.9	(36)		
38	P12814-2	Isoform 2 of Alpha actinin 1	102644	5.2	33.5	(29)	1.5↓	0.0654
	P55072	Transitional endoplasmic reticulum ATPase	89265	5.0	57.1	(37)		
39	P35609	Alpha actinin 2	103788	5.2	25.7	(19)	1.5↓	0.0654
	Q08043	Alpha actinin 3	103176	5.2	21.2	(19)		
40	P02679-2	Isoform Gamma A of Fibrinogen gamma chain	49464	5.6	60.2	(108)	1.5↓	0.0373

	P55072	Transitional endoplasmic reticulum ATPase	89265	5.0	44.9	(40)		
	P01023	Alpha 2 macroglobulin	163187	6.0	25.1	(31)		
42	P02768	Serum albumin	69321	5.9	29.6	7(53)	12.5↑	0.1838
43	P07195	L lactate dehydrogenase B chain	36615	5.6	62.3	12(75)	3.3↑	0.1789
44	P30040	Endoplasmic reticulum resident protein 29	28975	7.3	56.7	9(44)	2.0↑	0.1654
45	P49189	4 trimethylaminobutyraldehyde dehydrogenase	53767	5.6	39.7	8(30)	2.3↓	0.0218
47	P02768	Serum albumin	69321	5.9	86.7	(260)	3.5↓	0.0001
48	P06396-2	Isoform 2 of Gelsolin	80590	5.5	60.9	20(84)	1.6↓	0.3942
49	P30041	Peroxisomal protein 6	25019	6.0	83.0	10(61)	2.4↑	0.1195
50	P02675	Fibrinogen beta chain	55892	8.3	51.3	11(92)	2.4↑	0.2181
	Q15257-2	Isoform 1 of Serine threonine protein phosphatase 2A activator	36751	5.9	49.8	11(24)		
	P37837	Transaldolase	37516	6.4	38.3	9(19)		
51	Q9GZM7	Tubulointerstitial nephritis antigen-like	52352	6.5	40.3	6(43)	1.6↓	0.0042
52	P23526	Adenosylhomocysteinase	47685	5.9	45.4	14(70)	2.4↑	0.0101
53	P02675	Fibrinogen beta chain	55892	8.3	30.3	6(15)	3.0↑	0.0657
54	P12110	Collagen alpha 2 VI chain	108511	5.8	28.9	(65)	2.6↑	0.0038
55	P12110	Collagen alpha 2 VI chain	108511	5.8	34.2	(70)	2.6↑	0.155
56	P50395	Rab GDP dissociation inhibitor beta	50630	6.1	83.1	6(76)	1.5↑	0.2353
	P02675	Fibrinogen beta chain	55892	8.3	65.2	14(78)		
57	P02675	Fibrinogen beta chain	55892	8.3	71.1	14(106)	2.0↓	0.1012
58	P61163	Alpha centractin	42586	6.2	72.3	10(57)	2.7↑	0.0058
	P27361	Mitogen activated protein kinase 3	43108	6.3	55.1	9(35)		
59	P02675	Fibrinogen beta chain	55892	8.3	78.8	14(92)	1.6↓	0.0293
	Q9NVA2	Septin 11	49367	6.4	32.9	4(18)		
61	P06396-2	Isoform 2 of Gelsolin	80590	5.5	50.3	18(82)	3.2↑	0.0013
	P02786	Transferrin receptor protein 1	84818	6.2	38.4	22(48)		
62	P02787	Serotransferrin	77013	6.8	60.0	17(171)	2.2↓	0.0165

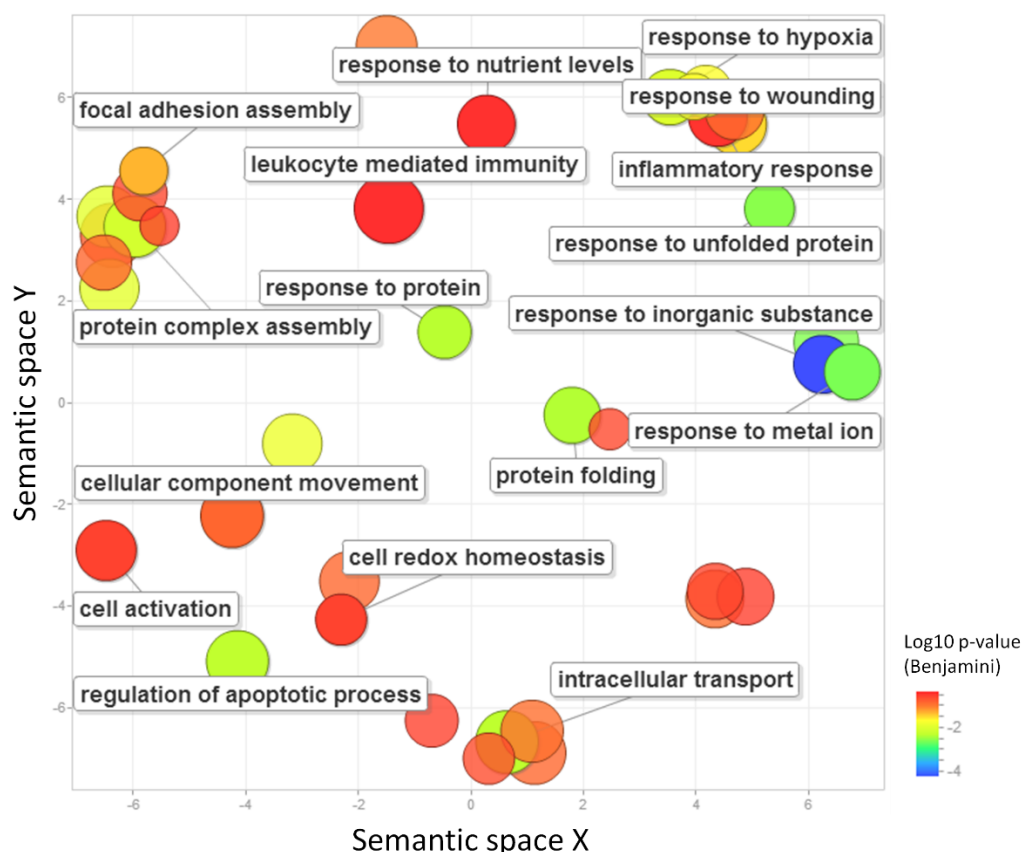


Figure 2.3 REVIGO scatterplot of biological processes GO terms of differentially expressed genes

The color of an individual circles represents the enrichment Benjamini p -value and size represents the frequency of occurrence of the GO term. Semantic space represents the semantic similarity; where similar GO terms cluster together.

DEP showed 14.1% molecular chaperones, which included increased expression in PE of 60 kDa HSP mitochondrial (spot # 24), heat shock cognate 71 kDa protein (spot # 34), HSP70 kDa 1A1B (spot # 35) and 14-3-3 gamma and zeta/delta proteins (spot # 3). Decreased expression in PE of HSP90 AA1 and HSP90 AB1 (spot # 11), endoplasmic reticulum chaperone protein (spot # 2) and hypoxia up-regulated protein-1 (spot # 28) was also evident. Up regulation of Hsp60 and Hsp70 under oxidative stress is known to protect the cells from apoptotic stress (178). However, the Hsp90s i.e. cytoplasmic HSP90AA1 and HSP90AB1, and endoplasmic HSP90B1 (Endoplasmic reticulum chaperone protein) showed down regulation in PE. Hsp90s are required for the proper functioning of steroid receptors and also plays a role in induction of VEGF and NOS, thus related to angiogenesis. Hypoxia up-regulated protein 1 (HYOU1), which also belongs to the family of Hsp70, known to have cytoprotective role under hypoxia condition and also inhibits apoptosis (179), was observed to be down-regulated in PE. Apoptosis is a major event in pathophysiology of pre-eclampsia, up regulation of certain anti-apoptotic protein may be the consequence or secondary effect of the pre-eclamptic condition, while differential expression of certain protein such as down regulation of protein glutamine gamma glutamyltransferase 2 (TGM2) and up regulation of Serine/threonine protein phosphatase 2A activator (PPP2R4) can lead to apoptosis. Oxidative stress or hypoxia may rapidly increase the intracellular Ca^{2+} level; in such conditions down regulation of Ca^{2+} -dependent TGM2 enzyme causes increase in cell death (180).

Alpha-actinin family of proteins, alpha-actinin-1 (spot # 40), alpha-actinin -2 (spot # 39, 40) alpha-actinin -3 (spot # 40) and alpha-actinin-4 (spot # 26, 38, 39, 40) were observed to be down-regulated in pre-eclamptic group. These proteins are actin-binding proteins and have various functions in different cell types such as platelet activation and degranulation, blood coagulation, hypoxia and apoptosis. Down regulation of non-muscle alpha actinin-4 is shown to reduce cell invasion properties of many cancer cell lines (181). Alpha actinin-4 also plays role in inflammation, cell migration and tissue modeling by interacting and modulating plasminogen activator inhibitor type-1 (182).

The endoplasmic reticulum stress related proteins such as endoplasmic reticulum chaperone protein, hypoxia up-regulated protein-1, transitional endoplasmic reticulum ATPase (spot # 38, 39) were down-regulated, and protein disulphide isomerase A6 (spot # 16, 17) and thioredoxin domain containing protein 5 (spot # 20) were up-regulated in pre-eclamptic group.

Elevated endoplasmic reticulum stress is evident in pre-eclamptic placenta, as reviewed in (183). ER stress can lead to imbalance in cellular redox regulation and accumulation of unfolded proteins in ER which triggers the unfolded protein response (UPR). This launches three transmembrane signaling cascades namely PERK and ATF4, ATF6 and IRE1 α signaling, which initially tries to restore the ER homeostasis; however, failure of restoration leads to activation apoptosis signaling. Protein disulphide isomerase A6 (PDIA6), an ER stress related protein was seen to be overexpressed in PE in our data. It is an IRE1 α attenuator that limits the excessive UPR (184). Thioredoxin domain containing protein-5 (Erp46) or also known as endoPDI, which is highly expressed in ER of endothelial cells, was identified to be up-regulated in PE. EndoPDI is induced under hypoxia conditions and known to protect cells from apoptosis and also induce angiogenesis (185, 186). While these proteins help in protecting the cells from ER stress, others namely endoplasmin, HYOU1 and transitional endoplasmic reticulum ATPase (Valosin-containing protein) can induce ER stress if abnormally expressed. Transitional endoplasmic reticulum ATPase down regulation can induce ER stress via promoting ubiquitin-proteasome system (UPS) degradation of resident and transient ER proteins; a process known as ER-associated degradation (ERAD) which is a component of UPR (187). Endoplasmin (HSP90B1/GRP94/GRP96) plays critical role in folding of proteins in ER, such as Toll-like receptors and integrins (188). HYOU1 (ORP150) acts as quality controller of proteins in ER in response to environmental stress (189). Ozawa et al showed that HYOU1 modulates the intracellular VEGF transport, colocalization study of these two proteins suggests its role in promotion of angiogenesis (190). And for the first time we report two novel proteins tubulointerstitial nephritis antigen-like 1 protein, a pro-angiogenic factor to be down-regulated and annexin A6 up-regulated in pre-eclamptic placenta.

2.3.3 Validation of differentially expressed protein

Western blot was performed for validation of 2DE data of few proteins that were differentially expressed and have potential role in pathophysiology of pre-eclampsia. For Western blot analysis one up-regulated proteins in PE (Annexin A6), one down-regulated protein in PE (Tubulointerstitial nephritis antigen-like protein) was selected. Vimentin was selected for fragmentation pattern study in these placental tissues.

2.3.3.1 Annexin A6 overexpression in pre-eclampsia

ANXA6 unlike other annexins is less explored in pre-eclampsia. ANXA6 is specifically localized at the apical and basal membrane of the placental syncytiotrophoblast. It is known to regulate the electrophysiological properties of the Maxi Chloride channels. ANXA6 was up-regulated in PE by 1.8-fold (spot # 34, 35) in 2DE analysis (Figure 2.2, Table 2.1), which was also reflected in Western blot analysis as it showed 1.5-fold (p value 0.017) increase in expression in PE (Figure 2.4).

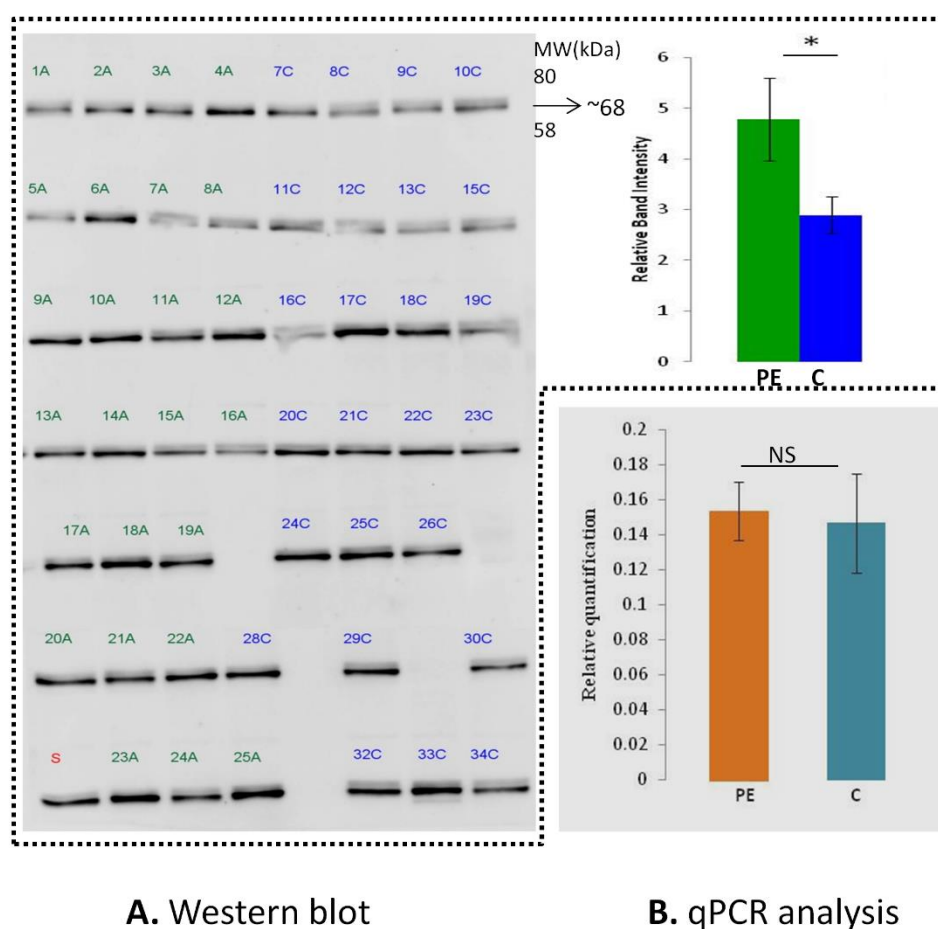


Figure 2.4 Validation of Annexin A6 in placenta

A) Western blot. In the image, PE samples are marked with green (1 to 25A) and normotensive with blue (7 to 34C), and standard sample (S) made by pooling all the individual sample is marked in red. The graph represents relative intensity of normotensive (blue) and pre-eclamptic pregnancies (green) normalized to beta-actin. B) qPCR analysis. The graph represents relative quantification of normal (blue) and pre-eclamptic pregnancies (orange) normalized to beta-actin (supplemental data 3). The bar represents mean \pm SE of 25 each individuals of normal and pre-eclamptic placenta ($*p < 0.05$, $**p < 0.01$, $***p < 0.001$, NS- not significant).

ANXA6 is a 68kDa Ca^{2+} regulated phospholipid-binding and membrane-binding protein. It contributes in various cellular processes such as membrane organization, cholesterol hemostasis, plasma membrane repair, cytoskeleton components and T-cell activation (191). Irrespective of the gestational age, ANXA6 is expressed in all cell types of placental villi (192). Placental immunohistochemistry data in Human Protein Atlas shows ANXA6 expression level as 40 to 55% in trophoblastic cells, 5 to 35% in endothelial cells and 20 to 50% in other cell types. Our data shows that ANXA6 is up-regulated in pre-eclamptic placental tissue. Koese et al, 2013 showed that ANXA6 promotes protein kinase C α (PKC α) mediated EGFR inactivation (193). EGFR signaling plays a role in cell growth, differentiation and angiogenesis; also it is central to trophoblast invasion and the inhibition of the apoptosis (194). We hypothesize that up regulation of ANXA6 plays a role in invasion and apoptosis of trophoblast through EGFR signaling, which is one of the major molecular mechanisms in pathogenesis of pre-eclampsia.

2.3.3.2 Tubulointerstitial nephritis antigen-like protein a pro-angiogenic factor is newly identified in PE pathophysiology

This is the first study reporting the identification of TINAGL1 in human placenta and its expression in pre-eclamptic condition. The conventional protein separation on two-dimensional SDS-PAGE, identified TINAGL1 protein spot with 6.5 isoelectric point and molecular weight of approximately 52kDa. It was down-regulated in the placenta of pre-eclamptic women with a fold change of 1.6 ($p=0.004$) (Table 2.1). Mass spectrometric analysis identified 68 and 54 peptides with a sequence coverage of 61 and 42% in normotensive and pre-eclamptic patients, respectively (Supplemental data 1). Validation of TINAGL1 was performed by western blot of individual normotensive ($n=25$) and pre-eclamptic ($n=25$) patient's placenta. Similar to 2DE results, we observed 1.5 ($p=0.022$) fold decrease of TINAGL1 in the placenta of pre-eclamptic women in Western blot analysis (Figure 2.5).

Human protein atlas shows its maximum RNA expression in placenta. TINAGL1's molecular functions are not well explored in human pregnancy or pre-eclampsia. Most of its biological role is studied in the mouse. Human TINAGL1 shows 90% amino acid sequence identity with mouse protein. TINAGL1 acts as a ligand for integrins $\alpha1\beta1$, $\alpha2\beta1$ and $\alpha5\beta1$, suggesting its role in cell adhesion (195, 196). Expressions of these

integrins are important for trophoblast invasion (197). Recently, *Tinagl1*^{-/-} mice were shown to have impaired fertility during pregnancy (198).

Angiogenesis is one of the major events during pregnancy. Imbalance in angiogenic factors is one of the major events in the pathogenesis of pre-eclampsia (199). The discovery of TINAGL1 as a pro-angiogenic factor in *in-vitro* and *in-vivo* models of angiogenesis (200), has set off its possibility to play a role in angiogenesis during pregnancy. Low level of TINAGL1 in the placenta of pre-eclamptic women might be one of the factors in impaired angiogenesis and cell adhesion which needs to be explored further. Studying its molecular mechanism in earlier stages of gestation in the human will be challenging and one needs to rely on animal models of pre-eclampsia.

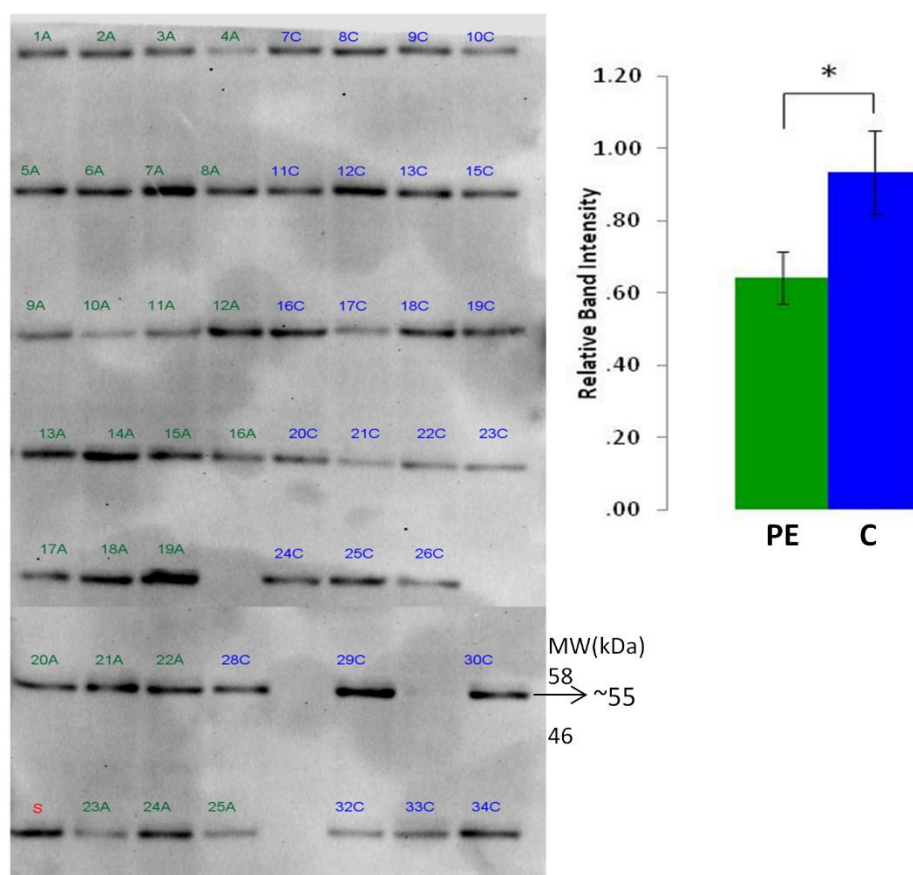


Figure 2.5 Tubulointerstitial nephritis antigen-like protein Western blot analysis
 In the image, PE samples are marked with green (1 to 25A) and normotensive with blue (7 to 34C), and standard sample (S) made by pooling all the individual sample is marked in red. The graph represents relative intensity of normotensive (blue) and pre-eclamptic pregnancies (green) normalized to beta-actin (* $p < 0.05$, ** $p < 0.01$, *** $p < 0.001$, NS- not significant). Negative controls with no primary antibody was used to ascertain specific and non-specific bands.

2.3.3.3 Fragmentation of vimentin in PE

We found vimentin the protein of our interest, as its isoform or fragments were reported less in the case of pre-eclampsia. Vimentin is a major intermediate filament protein in mesenchymal cells. Apart from its normal function in maintaining the structural integrity of cells and tissues, it is also known to play a pivotal role in cell adhesion, migration, signal transduction, apoptosis and immune defense (201). Eight protein spots of vimentin were identified in 2DE gels in which spot 5, 6, 21 and 22 showed down-regulation and spot 8, 17, 18 and 19 showed up-regulation in PE (Figure 2.6). Sequence analysis of protein coverage suggested that these spots contained the central domain peptides with or without either N- or C-terminal peptides. Peptide coverage for spot 21 and 22 was 90-92%, spanning the terminals and central region, while in case of other spots which had more than 40-60% peptide coverage, either N-terminal (spot 5,6 and 8) or C-terminal (spot 18 and 19) or both terminal (spot 17) were missing (Figure 2.6).

To further investigate into the fragments of vimentin, we performed Western blot of 25 each normotensive and pre-eclamptic placental samples individually. In Western blot analysis, anti-vimentin polyclonal antibody identified eight different fragments; however because of limitation of well-separation/similar mobility and for the ease of analysis; fragments 3, 4 and 5 were considered as one band, and fragments 6 and 7 were treated in a similar manner. Protein band I (parent fragment), II and III approximately 58, 46 and 40-30 kDa, respectively, showed no significant fold change, while protein bands IV (~32 kDa) and V (~20 kDa) showed significant fold change of 3.3 ($p < 0.001$) and 2.6 ($p < 0.001$), respectively (Figure 2.7). To normalize the results of western blot we used beta-actin as housekeeping protein (Supplemental data 3).

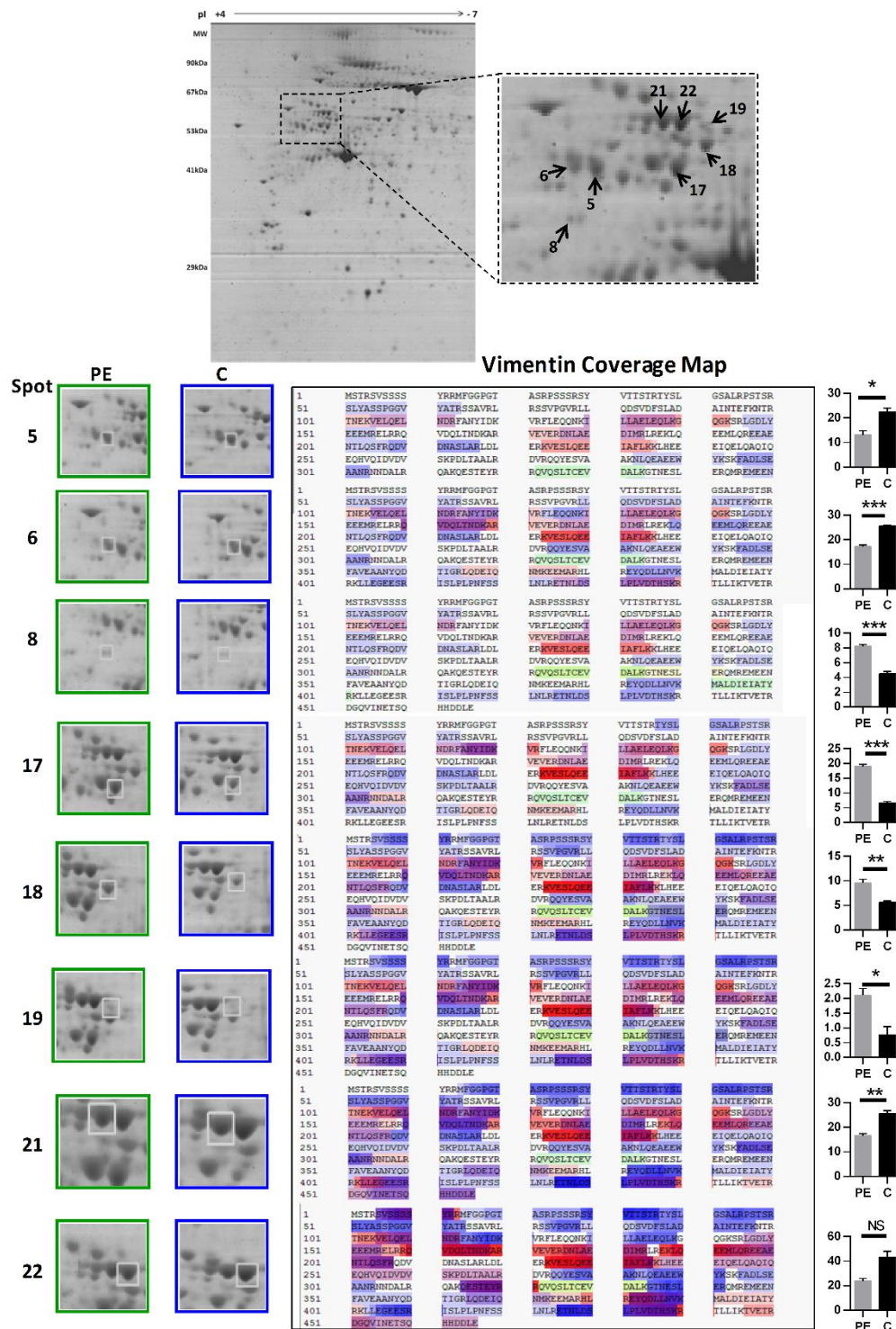


Figure 2.6 2DE gel with the zoomed out image of the region of spots of vimentin Coverage map indicates the protein sequence identified by PLGS software, color code: a blue-matched peptide, red-partially matched peptide, green-modified peptide and yellow- partially modified peptide. Column graph indicates the optical density (y-axis) for spots measured by PDQuest software (fold change and p value for each spot is mentioned in Table 2).

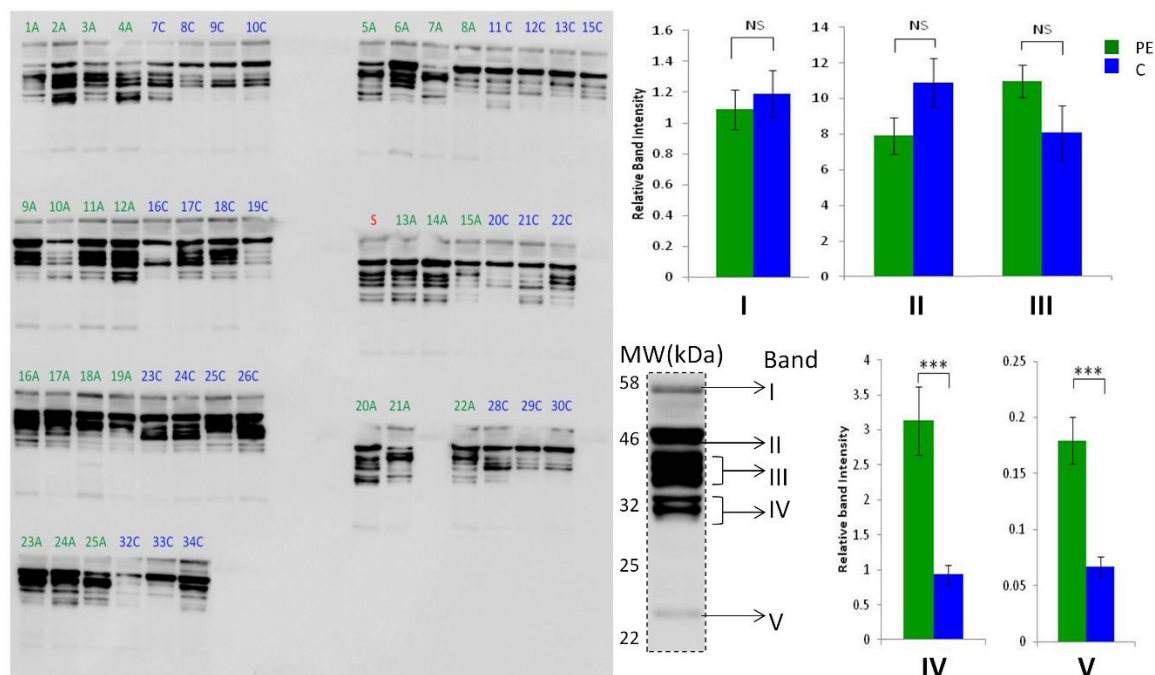


Figure 2.7 Vimentin Western blot analysis

In the image, PE samples are marked with green (1 to 25A) and normotensive with blue (7 to 34C), and standard sample (S) made by pooling all the individual sample is marked in red. The graph represents relative intensity of normotensive (blue) and pre-eclamptic pregnancies (green) normalized to beta-actin (* $p < 0.05$, ** $p < 0.01$, *** $p < 0.001$, NS-not significant).

As most of the intermediate filament proteins, vimentin contains a central rod domain flanked by the N- and C- terminal domains. The central rod consists of four alpha helical segments (1A, 1B, 2A and 2B) linked by the three-linker regions (L1, L1-2 and L2). They are highly dynamic molecules undergoing assembly and disassembly to form a structural organization of IF network. For many decades, vimentin was thought to be a contributor only in the structural integrity of the cell; however research on vimentin knockout $-/-$ mice revealed its role in cell adhesion, signaling and migration (202). Few studies on vimentin $-/-$ mice also showed that loss of vimentin leads to an altered flow-induced remodeling of arteries (203). These studies, in particular, may answer few questions in the pathophysiology of pre-eclampsia wherein there is altered remodeling of spiral arteries.

Most of the functions of vimentin are guided by post-translational modifications such phosphorylation that controls depolymerisation and stability. During apoptosis,

citruination within the head domain has negative effects on its assembly (204). Another level of regulation of vimentin is cleavage by intracellular proteases. Calpains are one of the proteases that cleave vimentin at several sites in the N-terminal region, which leads to a soluble pool of vimentin fragments which plays an important role in angiogenesis, through facilitating translocation metalloproteinase MM1-MMP to the membrane that further allows extracellular matrix degradation for angiogenic sprouting (205).

Our two-dimensional electrophoresis and Western blot for detection of vimentin shows fragmentation of vimentin into lower molecular weight fragments. This fragmentation pattern of vimentin was similar to the one demonstrated by Byun and his co-workers (206). They show that caspase-3 and -7 cleaves vimentin at Asp⁸⁵, while caspase-6 cleaves at Asp²⁵⁹. They also demonstrate that cleavage at Asp⁸⁵ generates truncated vimentin that is sufficient to induce apoptosis. Vimentin fragments are also expressed on cell surfaces of activated platelets (207) and apoptotic neutrophils (208), while activated macrophages secrete vimentin fragments in response to pro-inflammatory cytokine and is probably involved in inflammation (209). Caspases are the key mediator's apoptosis and are known to cleave distinct Asp residues, such as Asp⁸⁵, Asp²⁵⁹ and Asp⁴²⁹ of vimentin, resulting in different molecular weight fragments (Figure 2.8). Most of these fragments were of the similar molecular weight observed in Western blot, suggesting that they are the result of caspase activity during apoptosis. Although vimentin fragmentation studies till date are reported mainly on endothelial cells and various other cell lines, there is no research in placenta tissue.

Apoptosis is an integral part of normal placentation. Beginning from the blastocyst implantation to differentiation and invasion of trophoblast to remodeling of the spiral artery, apoptosis plays a major role [16]. Expression of caspases and endogenous regulators of apoptosis differ in cytotrophoblast and syncytiotrophoblast, which also depends on the trimester of pregnancy (210). During pregnancy complications such as pre-eclampsia, there is altered apoptosis wherein there is an increase in trophoblast cell death (211).

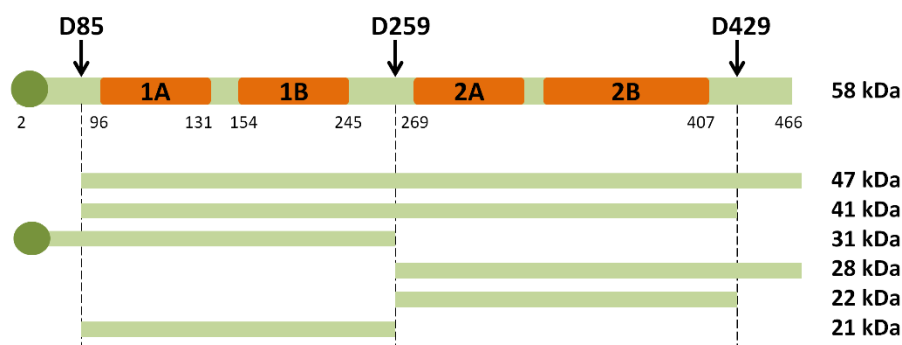


Figure 2.8 Caspase cleaving sites and various fragments of vimentin
(The scales are approximate)

In conclusion, we have used a large number of clinical samples to elucidate the global profile of protein in pre-eclampsia by conventional proteomic method. Though there are certain limitations of 2DE, we were able to observe several proteins that are consistent with the pathophysiological features of pre-eclampsia. Further studies are essential to know the exact role of these proteins, especially, TINAGL1 as pro-angiogenic marker and annexin A6 in pre-eclampsia. The fragments of vimentin observed in our 2DE gels and western blots, suggests that they are the result of apoptosis which happens both in normotensive as well as pre-eclamptic pregnancies. However, the differential expression of these fragments indicates the alteration in apoptosis in pre-eclampsia. Since our study utilizes tissues from various parts of the placenta, it is difficult to predict whether these differential fragments are due to altered apoptosis of cytotrophoblast or syncytiotrophoblast, or from activated macrophages, neutrophils or platelets. Isolation of these cells from the placenta for further studies on vimentin fragment can shed some light on altered apoptosis in pre-eclampsia. Also, studies to find the specific role of these fragment in apoptosis and its secretion into plasma needs to be undertaken for its utility as a marker.

Chapter 3

Biochemical insights into the pathophysiology of pre-eclampsia through placental proteomics- Part 2 (gel free proteomics)

Contents of this chapter is published as research article in Journal of proteome research, 2017, vol 16, 1050-1060.

Chapter 3 Biochemical insights into the pathophysiology of pre-eclampsia through placental proteomics- Part 2 (gel free proteomics)

3.1 Background

2D SDS PAGE is the widely used quantitative proteomic method; however, MS is also emerging as a quantitative proteomic technique. MS quantitative method is based on stable isotope labelling method like SILAC (stable isotope labeling by amino acids in cell culture), ICAT (isotope coded affinity tagging), trypsin-catalyzed ^{18}O labelling, iTRAQ (isobaric tags for relative and absolute quantitation) or semi quantitative label free methods based on ion intensity and spectral count. Quantification by MS techniques have helped in using gel free approach in proteomics.

3.2 Materials and methods

3.2.1 Sample collection

Samples were provided by Department of Obstetrics and Gynaecology, Bharati Hospital, Pune, Maharashtra, India with informed consent from the patients, and the study was approved by the Institutional ethics committee. Inclusive criteria of PE patients were systolic and diastolic blood pressures greater than 140 and 90 mmHg, respectively, with the presence of proteinuria ($>1+$ or 300 mg/24 h) on a dipstick test and repeated recording of the blood pressure with an interval of 6 h. Women with an indication of chronic hypertension, type 1 or 2 diabetes mellitus, renal or liver diseases, and seizure disorder were excluded from the study. Appendix 1 summarizes data on the maternal characteristics of individuals from which placental tissue and plasma were collected and used in the present study. Small sections of tissues from placental cotyledons of normotensive and PE pregnancies were collected immediately after delivery, snap frozen in liquid nitrogen and stored at -80°C until further use. Blood samples (10 mL) were collected in the EDTA vials from each subject during gestational weeks 16-20th (Tri1), 26-30th (Tri2), and 40-at delivery (Tri3) of PE and normotensive women (placenta and plasma were collected from different women). The blood was layered on histopaque (Sigma-Aldrich, St. Louis, MO, USA) and centrifuged at 2000g

for 15 min to separate the plasma, WBCs, and RBCs. The plasma aliquots were stored at -80°C until further analysis.

3.2.2 Protein extraction from placental tissue

Frozen powdered placental tissue (100 mg) from 25 normotensives and 25 preeclamptic was homogenized individually in 250 μ L of lysis buffer containing 1 M urea, 0.2 M thiourea, 70 mM dithiothreitol, 0.1% octyl-beta-thioglucopyranoside, and 0.1% RapigestTM SF (Waters Corporation, Milford, MA, USA). After 30 min of incubation, the homogenate was sonicated for 2 min and centrifuged at 25000 g for 30 min at 25°C. The supernatant was collected and total protein was estimated using Quick StartTM Bradford Protein Assay (Bio-Rad Laboratories, Hercules, CA, USA).

3.2.3 In-solution trypsin digestion and preparation for LC-MS

Placental protein (100 μ g) were digested separately. Each sample was washed twice with Amicon Ultra 3kDa MWCO (Millipore, Billerica, MA, USA) using 50 mM ammonium bicarbonate and the volume was set to 100 μ L with 0.1% of RapigestTM SF for digestion. The protein samples were subjected to heat denaturation (80°C), reduced using 100 mM dithiothreitol for 30 min at 65°C and alkylated with 200 mM iodoacetamide in the dark for 30 min at 25°C. Trypsin (Trypsin Gold, MS grade, Promega, Madison, WI, USA) was added in 1:20 ratio trypsin: protein (w/w) and incubated overnight at 37°C. Rapigest was hydrolyzed by the addition of 2 μ L of formic acid. Each sample was diluted 1:1 with 100fmol/ μ L alcohol dehydrogenase (ADH) standard tryptic digest to give a final protein concentration of 500 ng/ μ L and 50 fmol/ μ L ADH per sample.

3.2.4 Label-free analysis MS^E of placental tissue proteome

Nanoscale LC separation was performed with nanoACQUITY system (Waters Corporation) using nanoACQUITY UPLC 10K-2G -V/M Symmetry C₁₈ trapping column (180 μ m x 20 mm, 5 μ m) and a BEH 130 C₁₈ analytical column (75 μ m x 250 mm, 1.7 μ m). Peptide digest (2 μ L) each sample was injected into trapping, the column was washed with 0.1% solvent A (0.1% formic acid containing water) for 2 min at 10 μ L/min flow rate. Sample elution was performed with a gradient of solvent B (0.1%

formic acid containing acetonitrile) for 180 min (2 to 5%, 2 min; 5 to 27%, 158 min; 27 to 50%, 13 min; 50 to 90%, 2 min; 90 to 2%, 5 min) at a flow rate of 300 nl/min and column temperature at 40°C.

NanoACQUITY system is coupled to SYNAPT Q-TOF High Definition Mass Spectrometer (Waters Corporation) with NanoLockSpray as the ion source. Lockmass calibrant peptide standard [Glu¹]-fibrinopeptide B (Sigma-Aldrich) was infused into ion source at the flow rate of 300 nl/min and sampled every 60 sec. LC-MS^E data was collected over an m/z range of 50 to 2000, the scan time of 0.7 s, a constant low energy of 4V for MS mode and a step from 10 to 45 V of collision energy during high energy MS^E mode scans.

Each LC-MS^E raw data file was uploaded into TransOmicsTM Informatics for Proteomics software (Waters Corporation), developed in collaboration with Nonlinear Dynamics (Newcastle upon Tyne, UK). Transomics data processing involves peak-modelling algorithm to reduce the raw data file by an order of magnitude and create peak model. The LC runs were then aligned to compensate the variation between runs, using a reference run to generate alignment vectors automatically or manually. The aligned runs were then subjected to peak picking algorithm to generate a single map of peptide ions, which is applied to each sample. TransOmics uses a “quantify and then identify” approach, which promotes identification of low abundance peptides, this is done by the ion abundance algorithm as described by Li et al. (212) which allows quantification of peptide ions without MS/MS data. After quantification, each data was normalized using the spiked peptide ions. The quantified peptides were then subjected to identification using statistical tool filters such as ANOVA, power analysis, and q-values (for FDR). Human reviewed proteome database from Uniprot was downloaded and following search parameters were used: trypsin with two allowed missed cleavage, maximum protein mass 1000kDa, carbamidomethyl C as fixed and oxidation M, deamidation NQ, dehydration ST, as variable modification, automatic peptide and fragment tolerance, less than 4% FDR. ADH was used as internal standard for ‘Hi-3’ calibration and relative quantification.

3.2.5 Gene ontology and protein-protein network

Functional annotation of proteome was carried out in DAVID Bioinformatics resource 6.7 (213). STRING 9.1 database (Search Tool for the Retrieval of Interacting Genes) was used to search for protein-protein networks of DEP and later visualized in Cytoscape 2.8.2 (214, 215). BINGO plugin of Cytoscape was used for gene ontology enrichment (216)

3.2.6 Plasma proteome SWATH™ analysis

Plasma samples from PE (n=19) and normotensive (n=19) pregnant women were collected during three different gestational weeks of pregnancy. These samples were subjected to albumin depletion using the protocol mentioned in (217) and trypsin digested as mentioned above. The pool of all the samples (n=109) from Tri1, Tri2 and Tri3 was used for generation of the library. The pooled tryptic digested samples were reconstituted in 2% acetonitrile and 0.1% formic acid and analyzed on a TripleTOF5600 (Sciex, Framingham, MA, USA) MS coupled to an Eksigent NanoLC-Ultra 2D plus system. A total amount 1.5 µg of the sample was loaded onto a reverse phase Eksigent ChromXP trap (200 x 0.5 mm) column and desalted at a flow rate of 2.5 mL per minute for 20 minutes. After desalting, the peptides were separated using an Eksigent C18 column (0.075 x15cm). The peptides were eluted from the column at a flow rate of 300 nl/min using a linear gradient of 5–40% mobile phase B in 75 minutes (mobile phase A was 99.9% water in 0.1% formic acid and mobile phase B was 99.9% ACN in 0.1% formic acid). The LC eluent was analyzed online using a NanoSpray III Source installed on the Triple-TOF 5600 system. Samples were analyzed using a nebulizing gas of 5; a curtain gas of 25, an ion spray voltage of 2500 V and a heater interface temperature of 130°C. For ion library generation, typical data-dependent analysis was performed and the mass spectrometer was operated in a manner where a TOF-MS survey scan was performed in the 350–1250 m/z mass range with an accumulation time of 250 milliseconds, from which the 30 most abundant ions were selected for subsequent MS/MS fragmentation with an accumulation time of 70 milliseconds leading to a cycle time of 2.4 seconds. For this experiment, ions were isolated in quadrupole with a unit resolution (0.7 Da) and rolling collision energy with a spread of 5 V. Only the parent ions with a charge state from +2 to +5 was included in

the MS/MS fragmentation. The threshold precursor ion intensity was set as more than 120 cps and was not present on the dynamic exclusion list. Once an ion had been fragmented by MS/MS, its mass and isotopes were excluded for a period of 10 seconds. The MS/MS spectra were acquired in high sensitivity mode.

For SWATH MS-based experiments, the instrument was specifically operated in a “create swath” mode; wherein it was set to allow a quadrupole resolution of 15 Da/mass selections. Using an isolation width of 16 Da (15 Da of optimal ion transmission efficiency and 1 Da for the window overlap), a set of 60 overlapping windows were constructed covering the 350–1250 Da mass range. The collision energy for each window was determined based on the appropriate collision energy set automatically, with a spread of 5 eV. The total duty cycle was 4.3 seconds (the total of 4.2 seconds for stepping through the 60 isolation windows and 0.1 seconds for the optional survey scan). The MS/MS acquisition was performed using a high-sensitivity mode corresponding to a mass resolution of about 15 000, which also enables the extraction of fragment ions with 10–50 ppm accuracy. Three replicate runs were performed to understand the technical variation.

For the ion library generation, all the Wiff files containing MS and MS/MS spectra generated from Triple TOF 5600 (Sciex) were submitted for database searching using the Protein Pilot v5.0 software (Sciex). For the identification of proteins, the paragon algorithm was employed in a “Thorough ID” search mode against the Uniprot-Human reference dataset (20,191 protein). The search parameters allowed for modifications by IAA as cysteine blocking reagent. We applied 1% global protein level False Determination Rate (FDR) for the identification of proteins. For SWATH analysis, the peaks were extracted using the SWATH Acquisition MicroApp in PeakView v. 2.1 (Sciex) software using group files generated from Protein Pilot v 5.0. In parallel, a sciex SWATH library for plasma proteome was uploaded in PeakView 2.1. For both the ion library files, Retention time (RT) calibration was performed separately in PeakView software using high abundant peptides eluted at different RTs across the gradient and present in both IDA and SWATH run. Group files were extracted using an MS tolerance of 25 ppm and an MS/MS tolerance of 50 ppm, and the following parameters were considered: minimum 2 peptides with 6 transitions, exclude shared peptides, peptide confidence of 99%. These processed. mrkv files from PeakView were then loaded onto

MarkerView v. 1.2.1 (Sciex) for further analysis. This export resulted in the generation of three files containing quantitative information about individual ions, the summed intensity of different ions for a particular peptide and the summed intensity of different peptides for a particular protein. The built-in total ion intensity sum plugin was used for the normalization. Proteins having $p < 0.05$ (calculated among technical replicates of every sample) only considered for further deregulation analysis. Fold change > 2 or < 0.5 for up or down-regulated proteins were considered for relative quantitative analysis for all the samples.

3.2.7 Multiple Reaction Monitoring (MRM) analysis of plasma sample

The plasma samples were further analyzed for relative abundance of four proteins viz apolipoprotein A-I, A-II, haptoglobin and hemopexin using label-free MRM. The plasma samples used for this analysis were digested as described above. Individual samples ($n=10$) from each gestational week of PE and normotensive samples were run in duplicates. LC separation of 15 ug sample was achieved with Shimadzu UHPLC system using X-bridge BEH C18 (2.5 μ m, 1mm i.d.) column with flow rate 0.3mL/min. MRM data were acquired on Sciex 5500 QTRAP operated in the positive ion mode with an ion source temperature of 500°C, GS2 heater gas and GS1 nebulizer gas setting of 45 and a spray voltage of 5500 V. For each protein, 3-5 peptides and 2-5 transitions were monitored. Scheduled MRM transition was performed in Analyst v 1.5.2 using a retention time window of the 60s and dwell time of 20 ms.

The data acquired were analyzed by MultiQuant v3.0.2 (Sciex). The SignalFinderTM integration algorithm within MultiQuant was utilized for peak integration and was also reviewed manually. The raw MRM peak area and retention time obtained for each transition were used for relative quantitation. The assessment of transition, quality and data normalization approaches suggested by Chung et al, 2014 was considered for relative quantitation (218). Finally, for data analysis, we performed split-plot Factorial multivariate analysis of variance (SPANOVA) to understand the between-subjects and within-subjects variations using SPSS v18.0.

3.2.8 Western Blot and Real-Time PCR

Multi-strip Western blotting protocol was performed as mentioned in Edita A. et al, 2007(175). Placental protein (10µg per lane) from normotensive and pre-eclamptic samples (7-gels) was transferred to one single PVDF membrane (Millipore Corporation, Billerica, MA, USA) and blocked overnight at 4°C in 5% skimmed milk or 2% bovine serum albumin. Primary (anti-transferrin receptor and anti-beta actin as loading control) and secondary antibodies incubation was performed as per manufacturer's instructions (Santa Cruz Biotechnology, Santa Cruz, CA, USA). Detection was performed by chemiluminescent ECL reagent (GE Healthcare, Little Chalfont, BUX, UK) and signals were detected with CCD imaging system (Syngene, Cambridge, UK) camera. Analysis of total signal intensity of Western blot bands was performed with Image Studio Lite version 4.0 (Li-Cor Biosciences, Lincoln, NE, USA) using local background subtractions.

Total RNA extraction from placental tissue was performed using RNeasy Plus Mini kit (Qiagen, Valencia, CA, USA) and preparation of cDNA using High-Capacity cDNA Reverse Transcription kit (Applied Biosystems, Foster City, CA, USA) according to manufacturer's protocol. qPCR was performed in 7900 HT Fast Real-time system using SYBR green chemistry using SYBR green Real-time PCR Master mixes (Applied Biosystems). The following gene-specific primers were used: Transferrin receptor1: sense (5'TGAACCAATACAGAGCAGACATAAA3'), antisense (5'CTGGAAGTAGCACGGAAGAAG3') and housekeeping gene betaActin: sense (5'CCATC GTCCACCGCAAAT3'), antisense (5'GCTGTACCTTCACCGTTC3'). All measurements were performed in triplicate and conditions used were as follows: 95°C for 10 min, 40 cycles of 95°C for 3 sec, 60°C for 30 sec. Relative quantitation was performed using Data Assist™ Software (Applied Biosystems).

3.2.9 Experimental design and statistical rationale

For label-free quantification using LC-MS^E of the placental proteome, two technical replicates for each 25 biological replicate were analyzed per normotensive and pre-eclamptic group. The pool of plasma samples for each gestational week (n=19 for each gestational week of PE; n=19, n=16, and n=17 for Tri1, Tri2 and Tri3 of normotensive, respectively) was used for SWATH-MS based experiments. MRM analysis was

performed for 10 biological replicate in each group and each gestational week, with two technical replicates for each sample. Western blot was performed for 25 biological replicates individually for each group, while 18 PE and 27 normotensive samples were used for quantitative real-time PCR. For data analysis, SPSS or GraphPad Prism was used and Student t-test was performed wherever applicable.

3.3 Result and Discussion

3.3.1 Placental proteome profiling of normotensive and pre-eclamptic patients

We selected PE women (n=25) with no previous history of hypertension and normotensive pregnant women (n=25) as a control group (C). To profile the placental proteome, proteins were extracted and peptides after tryptic digestion were analyzed individually by label-free quantitation using ultra-high pressure nano-LC-MS/MS. These experiments resulted in 100 LC-MS/MS datasets that have been submitted to Peptide Atlas database (Identifier: PASS00904). Individual placental protein samples were analyzed in duplicate and reproducibility between technical and biological replicates was uniform across all tissue samples, with average Pearson correlation value of 0.97 and 0.93, respectively (Figure 3.1A). In total 38775 peptides corresponding to 1225 proteins to all the tissue samples were identified by Transomics™ (Supplemental data 4). Uniprot subcellular location enrichment analysis of 1225 proteins resulted in identification of annotated (i) 48.7% cytoplasmic (ii) 38.96% membrane (iii) 35.16% nuclear and (iv) 12.8% secreted. Major organelle such as mitochondrial and endoplasmic reticulum proteins (114 and 90 respectively) was identified (Figure 3.1B).

To find the DEPs, we compared the log₁₀-fold change of the PE to C ratio of all the biological replicates against the corresponding log₁₀ *p*-values on the volcano plot (Figure 3.1C). In total, 224 proteins had *p*-value ≤0.05, which includes 109 down-regulated and 71 up-regulated protein levels in the PE conditions with a fold change cut-off 1.3 (Table 3.1). Principal component analysis (PCA) on the normalized peak intensities for all the differentially expressed protein was performed (Figure 3.1D). The first PC accounted for 30.3% of the total variance while 15.3 and 6.6% variation by PC2 and PC3 respectively.

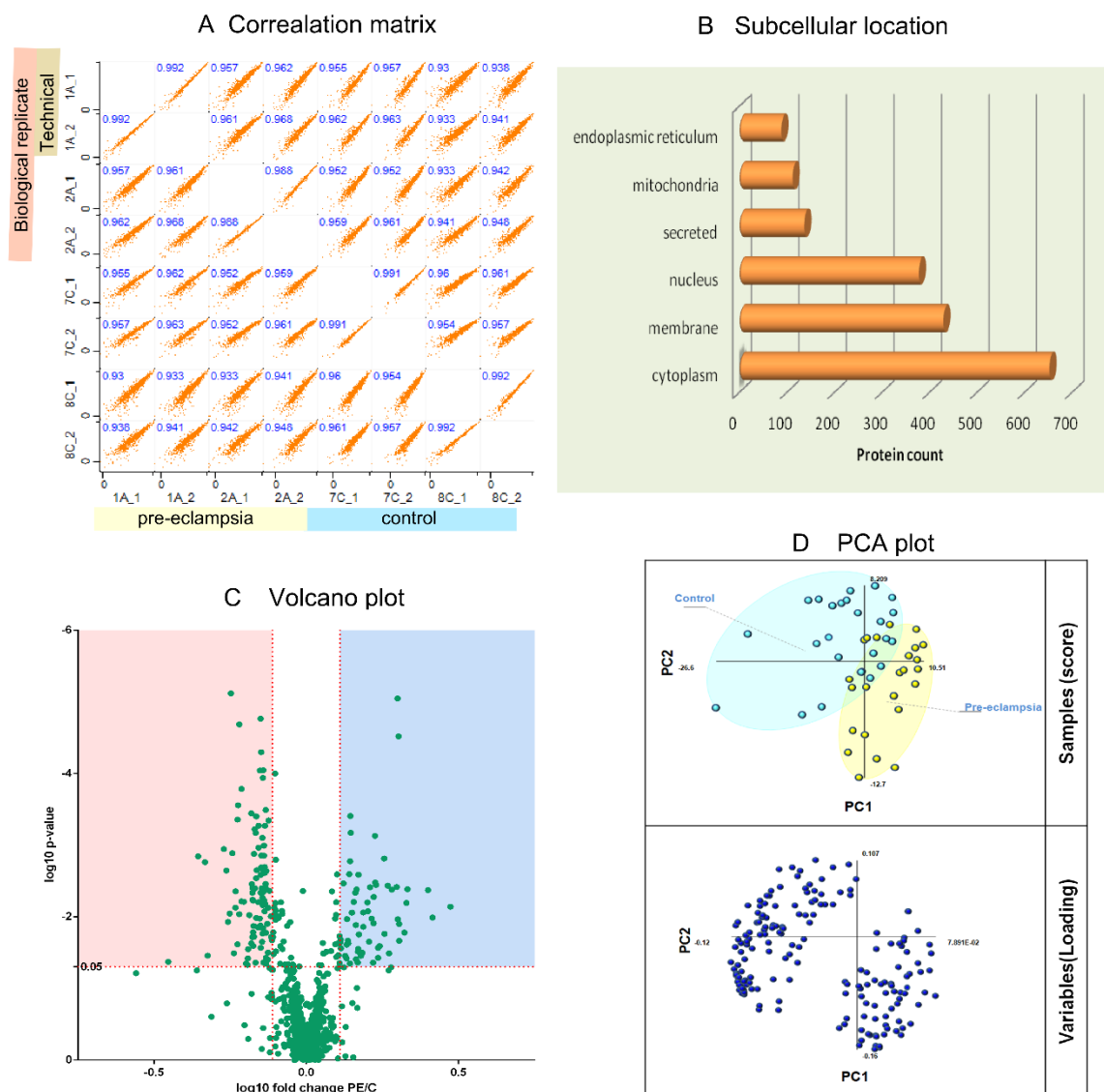


Figure 3.1 Placental proteome

- (A) Scatter plot of protein intensities between the biological and technical replicate of normotensive and pre-eclamptic placental proteome, Pearson correlation coefficient is indicated at the top of each plot. (B) Subcellular localization of the total 1225 proteins identified in the LC-MS^E analysis. Cellular locations were assigned using Uniprot database. (C) Differentially expressed protein's \log_{10} fold changes (x -axis) and the corresponding $\log_{10} p$ values are summarized in volcano plot. The vertical (x -axis) and horizontal (y -axis) dotted lines represents fold change cut-off (0.7, 1.3) and p -value cut-off (<0.05). Proteins in the shaded area represent up-regulation (pink) and down-regulated (blue). (D) Principal component analysis plot of the differentially expressed proteins indicates discrimination between normotensive and pre-eclamptic samples. The score and variable plot represent the relationship between samples and variables.

**Table 3.1 List of Differentially expressed proteins
Up-regulated in pre-eclampsia**

Accession	Description	Max fold change	Anova (p value)
P11021	78 kDa glucose-regulated protein	3.0	0.0072
P08107	Heat shock 70 kDa protein 1A/1B	2.6	0.0102
P02751	Fibronectin	2.5	0.0042
Q12931	Heat shock protein 75 kDa, mitochondrial	2.1	0.0041
Q68CZ2	Tensin-3	2.1	0.0064
P02787	Serotransferrin	2.1	0.0166
P02765	Alpha-2-HS-glycoprotein	2.0	0.0216
P19652	Alpha-1-acid glycoprotein 2	2.0	0.0126
Q9NQC3	Reticulon-4	2.0	0.0000
P14625	Endoplasmic	2.0	0.0108
P18206	Vinculin	2.0	0.0000
P11142	Heat shock cognate 71 kDa protein	1.9	0.0042
P38646	Stress-70 protein, mitochondrial	1.9	0.0507
O15197	Ephrin type-B receptor 6	1.9	0.0038
P54652	Heat shock-related 70 kDa protein 2	1.9	0.0323
P45880	Voltage-dependent anion-selective channel protein 2	1.9	0.0560
P35556	Fibrillin-2	1.9	0.0037
Q92599	Septin-8	1.8	0.0173
P21980	Protein-glutamine gamma-glutamyltransferase 2	1.8	0.0015
Q5U5Z8	Cytosolic carboxypeptidase 2	1.7	0.0256
Q06830	Peroxiredoxin-1	1.7	0.0374
P27824	Calnexin	1.7	0.0272
O75923	Dysferlin	1.7	0.0036
P46940	Ras GTPase-activating-like protein IQGAP1	1.7	0.0033
P98160	Basement membrane-specific heparan sulfate proteoglycan core protein	1.7	0.0007
P02647	Apolipoprotein A-I	1.7	0.0053
P17066	Heat shock 70 kDa protein 6	1.7	0.0123
P30048	Thioredoxin-dependent peroxide reductase, mitochondrial	1.7	0.0435
Q8ND30	Liprin-beta-2	1.6	0.0106
P08133	Annexin A6	1.6	0.0039
P50895	Basal cell adhesion molecule	1.6	0.0223
Q15582	Transforming growth factor-beta-induced protein igh3	1.6	0.0083
P34931	Heat shock 70 kDa protein 1-like	1.6	0.0063
Q96QU1	Protocadherin-15	1.5	0.0138
P06396	Gelsolin	1.5	0.0087
P27487	Dipeptidyl peptidase 4	1.5	0.0318
Q13162	Peroxiredoxin-4	1.5	0.0350
P00367	Glutamate dehydrogenase 1, mitochondrial	1.5	0.0176
P35241	Radixin	1.5	0.0026
P07900-2	Isoform 2 of Heat shock protein HSP 90-alpha	1.5	0.0281
P02649	Apolipoprotein E	1.5	0.0306
P09211	Glutathione S-transferase P	1.5	0.0435
P00747	Plasminogen	1.5	0.0041
Q6ZSZ6-2	Isoform 2 of Teashirt homolog 1	1.5	0.0131
Q5THR3	EF-hand calcium-binding domain-containing protein 6	1.4	0.0046
Q8WV44-2	Isoform 2 of E3 ubiquitin-protein ligase TRIM41	1.4	0.0062
P17948	Vascular endothelial growth factor receptor 1	1.4	0.0087
A6QL64	Ankyrin repeat domain-containing protein 36A	1.4	0.0007
P35221	Catenin alpha-1	1.4	0.0004
P30101	Protein disulfide-isomerase A3	1.4	0.0017
P08238	Heat shock protein HSP 90-beta	1.4	0.0448
Q16181	Septin-7	1.4	0.0025
Q8N4C6	Isoform 5 of Ninein	1.4	0.0234
P32119	Peroxiredoxin-2	1.4	0.0107
P27797	Calreticulin	1.4	0.0245

Accession	Description	Max fold change	Anova (p value)
P02786	Transferrin receptor protein 1	1.4	0.0381
A3KMH1	von Willebrand factor A domain-containing protein 8	1.3	0.0350
Q9BZE9-3	Isoform 3 of Tether containing UBX domain for GLUT4	1.3	0.0507
Q9Y6Q1	Calpain-6	1.3	0.0034
Q8N5G2	Macoilin	1.3	0.0275
Q99469	SH3 and cysteine-rich domain-containing protein	1.3	0.0207
P30041	Peroxiredoxin-6	1.3	0.0227
Q9Y4L1	Hypoxia up-regulated protein 1	1.3	0.0186
Q9H6Q4	Cytosolic Fe-S cluster assembly factor NARFL	1.3	0.0442
Q05209	Tyrosine-protein phosphatase non-receptor type 12	1.3	0.0344
Q7Z4L9	Protein phosphatase 1 regulatory subunit 42	1.3	0.0522
P16104	Histone H2AX	1.3	0.0026
Q16777	Histone H2A type 2-C	1.3	0.0026
P54727	UV excision repair protein RAD23 homolog B	1.3	0.0237
P04040	Catalase	1.3	0.0062
Q9UQB8	Brain-specific angiogenesis inhibitor 1-associated protein 2	1.3	0.0363

Down-regulated in pre-eclampsia

Accession	Description	Max fold change	Anova (p value)
P01009	Alpha-1-antitrypsin	0.35	0.0424
Q9NY27	Serine/threonine-protein phosphatase 4 regulatory subunit 2	0.43	0.0014
Q16352	Alpha-internexin	0.47	0.0017
P01011	Alpha-1-antichymotrypsin	0.47	0.0347
O43707	Alpha-actinin-4	0.52	0.0011
Q5VU43	Myomegalin	0.55	0.0023
P35613-2	Isoform 2 of Basigin	0.55	0.0117
Q8NAN2	Protein FAM73A	0.55	0.0090
P35612	Beta-adducin	0.55	0.0000
P02790	Hemopexin	0.58	0.0013
Q96KP4	Cytosolic non-specific dipeptidase	0.58	0.0323
P23528	Cofilin-1	0.58	0.0074
P05556	Integrin beta-1	0.58	0.0044
Q9H7F0	Probable cation-transporting ATPase 13A3	0.58	0.0242
Q08043	Alpha-actinin-3	0.58	0.0004
P01024	Complement C3	0.58	0.0003
P26038	Moesin	0.58	0.0000
Q13136	Liprin-alpha-1	0.58	0.0092
O96028	Histone-lysine N-methyltransferase NSD2	0.62	0.0061
Q6ZU15	Septin-14	0.62	0.0002
P01023	Alpha-2-macroglobulin	0.62	0.0061
Q8IZU9	Kin of IRRE-like protein 3	0.62	0.0450
P00738	Haptoglobin	0.62	0.0470
P68036-2	Isoform 2 of Ubiquitin-conjugating enzyme E2 L3	0.62	0.0380
O75529	TAF5-like RNA polymerase II p300/CBP-associated factor-associated factor 65 kDa subunit 5L	0.62	0.0282
P13727	Bone marrow proteoglycan	0.66	0.0095
P14210	Hepatocyte growth factor	0.66	0.0004
Q8NBS9	Thioredoxin domain-containing protein 5	0.66	0.0235
Q5VSY0	G kinase-anchoring protein 1	0.66	0.0035
A0MZ66-6	Isoform 6 of Shootin-1	0.66	0.0192
O95954	Formimidoyltransferase-cyclodeaminase	0.66	0.0046
P37802	Transgelin-2	0.66	0.0058
P03951-2	Isoform 2 of Coagulation factor XI	0.66	0.0039
Q9BXJ8-2	Isoform 2 of Transmembrane protein 120A	0.66	0.0059
Q9H201	Epsin-3	0.66	0.0164
P35609	Alpha-actinin-2	0.66	0.0134
P02679-2	Isoform Gamma-A of Fibrinogen gamma chain	0.66	0.0013

Accession	Description	Max fold change	Anova (p value)
O75334	Liprin-alpha-2	0.66	0.0190
Q9C0C2	182 kDa tankyrase-1-binding protein	0.66	0.0006
P35555	Fibrillin-1	0.66	0.0040
P07339	Cathepsin D	0.66	0.0436
P47985	Cytochrome b-c1 complex subunit Rieske, mitochondrial	0.66	0.0007
P09525	Annexin A4	0.66	0.0029
P16284	Platelet endothelial cell adhesion molecule	0.66	0.0004
P23142	Fibulin-1	0.66	0.0103
Q63HQ2	Pikachurin	0.66	0.0022
P05108	Cholesterol side-chain cleavage enzyme, mitochondrial	0.66	0.0255
O75616-2	Isoform HERA-B of GTPase Era, mitochondrial	0.71	0.0140
Q15019	Septin-2	0.71	0.0062
P23229	Integrin alpha-6	0.71	0.0011
P14060	3 beta-hydroxysteroid dehydrogenase/Delta 5>4-isomerase type 1	0.71	0.0005
Q9GZM7	Tubulointerstitial nephritis antigen-like	0.71	0.0105
P04004	Vitronectin	0.71	0.0001
P07237	Protein disulfide-isomerase	0.71	0.0132
O94983-2	Isoform 2 of Calmodulin-binding transcription activator 2	0.71	0.0000
Q14832	Metabotropic glutamate receptor 3	0.71	0.0046
Q8N573-5	Isoform 5 of Oxidation resistance protein 1	0.71	0.0271
P50454	Serpin H1	0.71	0.0026
P08697	Alpha-2-antiplasmin	0.71	0.0021
P13667	Protein disulfide-isomerase A4	0.71	0.0142
P04083	Annexin A1	0.71	0.0001
P49796-6	Isoform 6 of Regulator of G-protein signaling 3	0.71	0.0014
P02675	Fibrinogen beta chain	0.71	0.0040
P01130	Low-density lipoprotein receptor	0.71	0.0224
P11532	Dystrophin	0.71	0.0008
P15311	Ezrin	0.71	0.0054
Q6ZR08-3	Isoform 3 of Dynein heavy chain 12, axonemal	0.71	0.0171
P11166	Solute carrier family 2, facilitated glucose transporter member 1	0.71	0.0022
Q99959	Plakophilin-2	0.71	0.0069
P46776	60S ribosomal protein L27a	0.71	0.0001
P13611	Versican core protein	0.71	0.0143
P02768	Serum albumin	0.71	0.0001
O75083	WD repeat-containing protein 1	0.71	0.0045
Q9H2D6	TRIO and F-actin-binding protein	0.71	0.0435
P00488	Coagulation factor XIII A chain	0.71	0.0010
P02774	Vitamin D-binding protein	0.71	0.0059
P14061	Estradiol 17-beta-dehydrogenase 1	0.71	0.0014
P09630	Homeobox protein Hox-C6	0.71	0.0084
P07355	Annexin A2	0.71	0.0024
P11511	Aromatase	0.71	0.0020
Q5JRA6	Melanoma inhibitory activity protein 3	0.71	0.0005
P0C0L5; P0C0L4	Complement C4-B	0.71	0.0065
Q9P258	Protein RCC2	0.71	0.0039
P22314	Ubiquitin-like modifier-activating enzyme 1	0.71	0.0035
P05120	Plasminogen activator inhibitor 2	0.71	0.0003
Q9NZU7	Calcium-binding protein 1	0.71	0.0375
P37059	Estradiol 17-beta-dehydrogenase	0.71	0.0167
Q03135	Caveolin-1	0.71	0.0452
Q9GZM7-2	Isoform 2 of Tubulointerstitial nephritis antigen-like	0.71	0.0023
P10599-2	Isoform 2 of Thioredoxin	0.76	0.0125
Q92870	Amyloid beta A4 precursor protein-binding family B member 2	0.76	0.0394

Accession	Description	Max fold change	Anova (p value)
Q9Y6U3	Adseverin	0.76	0.0075
Q9NZM1	Myoferlin	0.76	0.0005
Q01995	Transgelin	0.76	0.0043
P80365	Corticosteroid 11-beta-dehydrogenase isozyme 2	0.76	0.0098
Q86UV5	Ubiquitin carboxyl-terminal hydrolase 48	0.76	0.0191
Q9NNX6-6	Isoform 6 of CD209 antigen	0.76	0.0212
Q9HBD1	Roquin-2	0.76	0.0546
P30044	Peroxiredoxin-5, mitochondrial	0.76	0.0192
P38398	Breast cancer type 1 susceptibility protein	0.76	0.0165
P02792	Ferritin light chain	0.76	0.0331
P62158	Calmodulin	0.76	0.0075
Q3SY00	Testis-specific protein 10-interacting protein	0.76	0.0092
Q15084-2	Isoform 2 of Protein disulfide-isomerase A6	0.76	0.0001
Q9BYG3	MKI67 FHA domain-interacting nucleolar phosphoprotein	0.76	0.0303
P01876;	Ig alpha-1 chain C region	0.76	0.0301
P01877			
P59190-2	Isoform 2 of Ras-related protein Rab-15	0.76	0.0111
P00450	Ceruloplasmin	0.76	0.0081
Q7Z3Z0	Keratin, type I cytoskeletal 25	0.76	0.0303

3.3.2 Gene ontology identifies biological processes relevant to pathophysiology of pre-eclampsia

For functional annotation of DEPs, 180 proteins were first listed into STRING for protein–protein interaction (PPI) network and visualized using Cytoscape (Figure 3.2). The network analysis showed 132 nodes and 531 edges, and topological parameter revealed that some nodes in the network had a significant number of connections, the hub nodes with high degree included genes such as ALB, FN1, TF, PLG, APOA1, A2M, CANX, CALM2, CALR, FGG, SERPINF2, ITGB1, HPX, TGFBI, SERPINA1, FGB, VTN, APOE, VCL, ACTN2, CP, HSPA5, HP, AHSG, GC, CAV1, ANXA2, ACTN4, HSP90B1, EZR, TXN, GSN, HSP90AA1, P4HB, BRCA1, PDIA3, PRDX1, PDIA6, C3, LDLR, F13A1, CAT, FTL, HSPA8, TFRC (degree >10) (Figure 3.2).

For gene ontology enrichment analysis of biological process (GOBP), we utilized BINGO plug-in of Cytoscape. GOBP analysis indicated enrichment of many of the physiological processes involved in pathophysiology of PE such as angiogenesis, apoptosis, oxidative stress, hypoxia, placental development, VEGF regulation, cell migration, cell adhesion, coagulation, inflammation, fibrinolysis, iron and calcium ion homeostasis (Hypergeometric test, $p < 0.05$) (Supplemental data 5). Figure 3.3 represents the cluster of DEPs with their regulation pattern in various biological

processes involved in the pathophysiology of PE. Many of these proteins belong to more than one cluster as they play multiple biological functions.

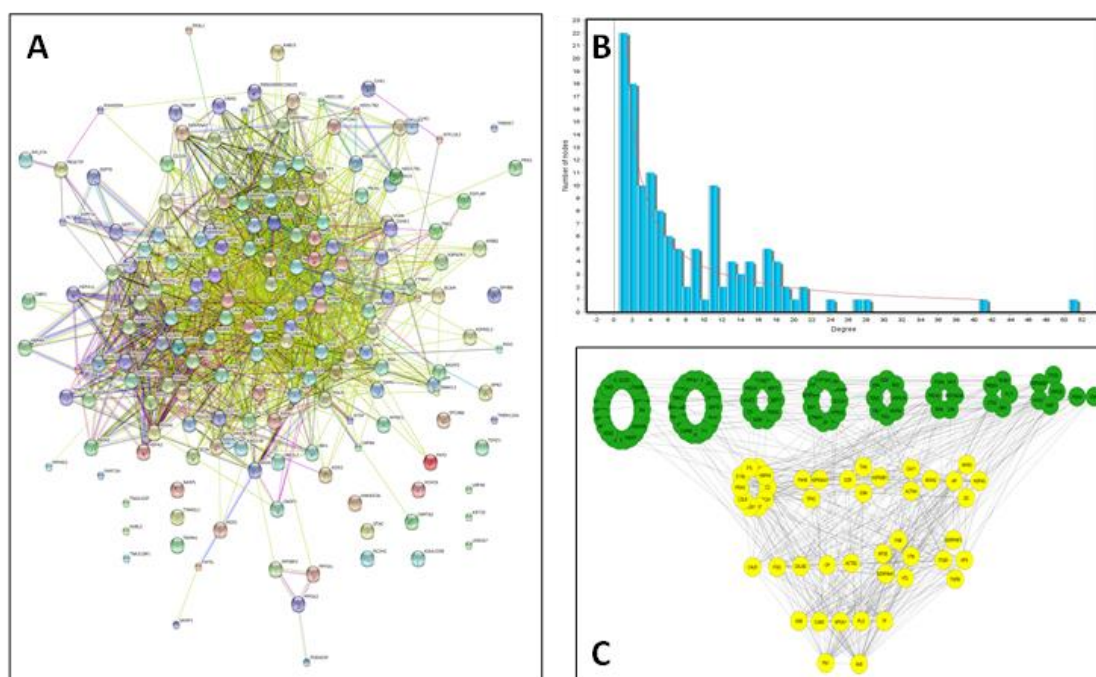


Figure 3.2 Protein- protein interaction network

A) Protein- protein interaction network predicted by STRING. B) Degree node. C) Hub node

3.3.2.1 Abnormal placental apoptosis

Apoptosis was seen to be the largest cluster in the analysis with 31 interacting proteins, of which 19 were negative regulators of apoptosis. In comparison with the normotensive placenta, PE placenta consisted more up-regulated negative regulator proteins of apoptosis such as TF, HSPA1A, PRDX2, PRDX3, HSP90B1, PRDX6, APOE, ALB, TXNDC5, HSPA5, CAT, GSTP1, HSPA9, while down-regulated proteins included ANXA1, PRDX5, HGF, ANXA4, CFL1, SERPINB2. Apoptosis is a major event in the pathophysiology of PE; up-regulation of certain anti-apoptotic protein may be the consequence or secondary effect of the PE condition. Apoptosis releases cell debris which is one of the causes of oxidative stress and inflammation.

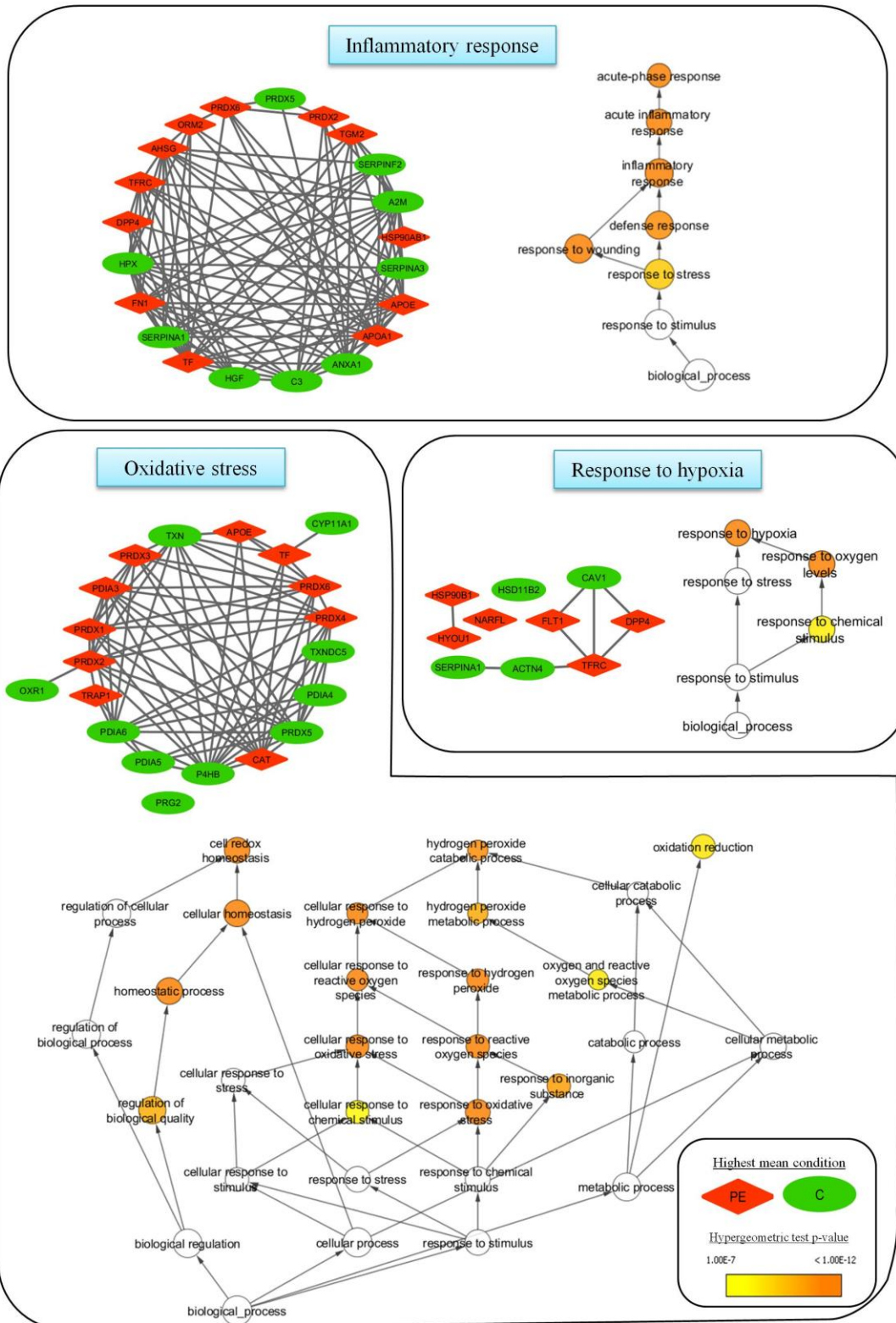


Figure 3.3 (a) Gene ontology and protein-protein interaction networks of differentially expressed proteins (figure continued)

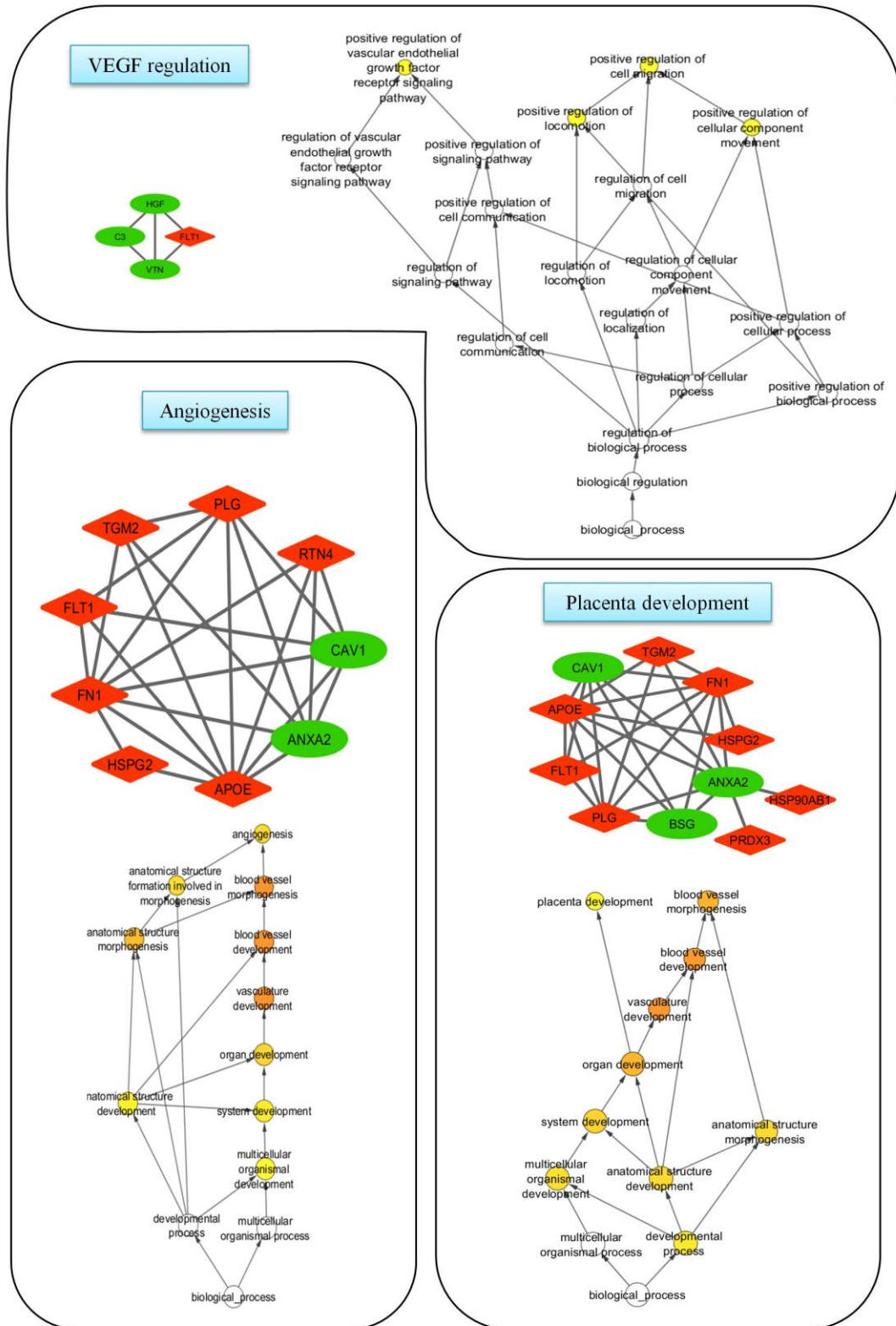


Figure 3.3 (b) Gene ontology and protein-protein interaction networks of differentially expressed proteins (figure continued)

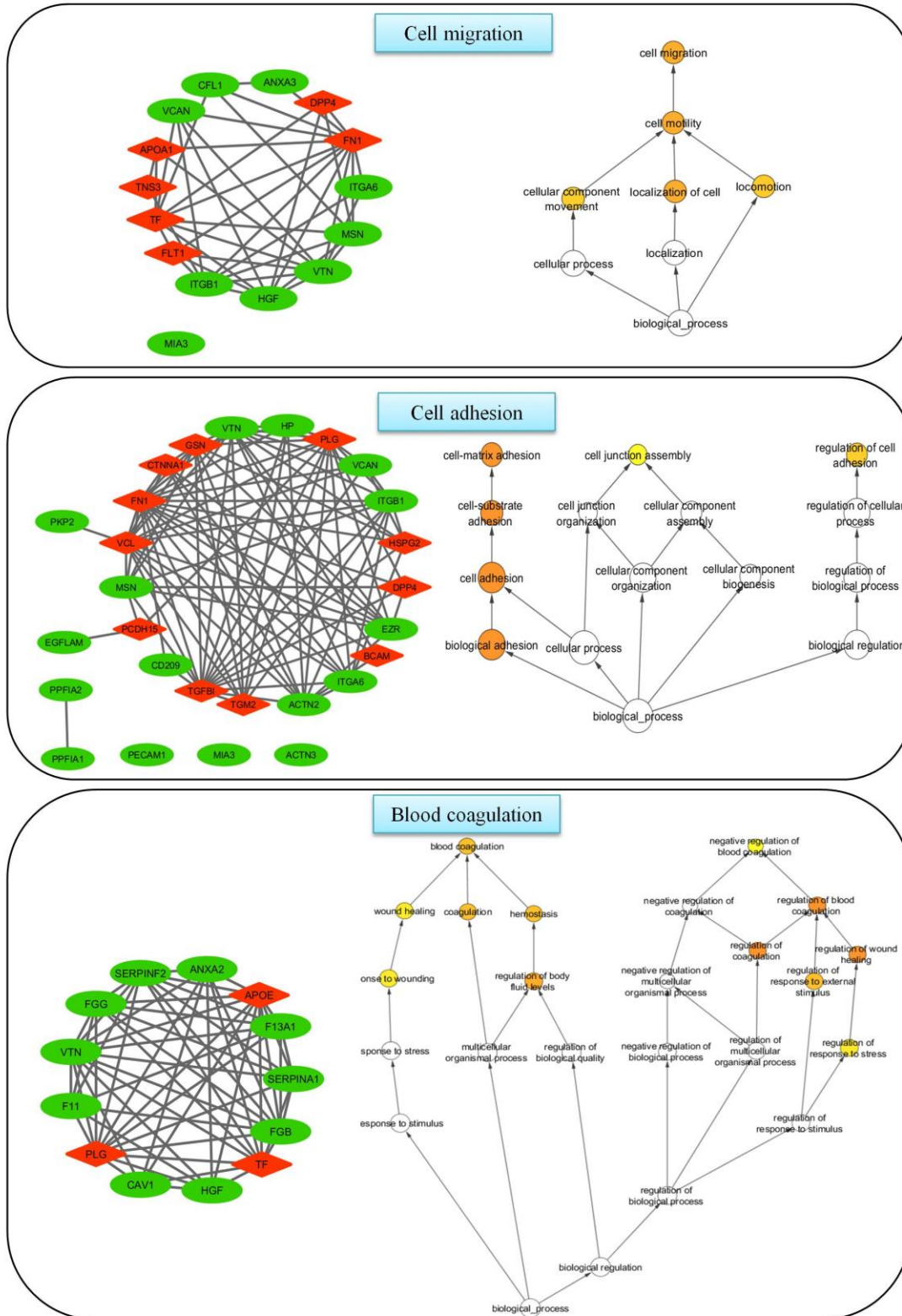


Figure 3.3 (c) Gene ontology and protein-protein interaction networks of differentially expressed proteins (figure continued)

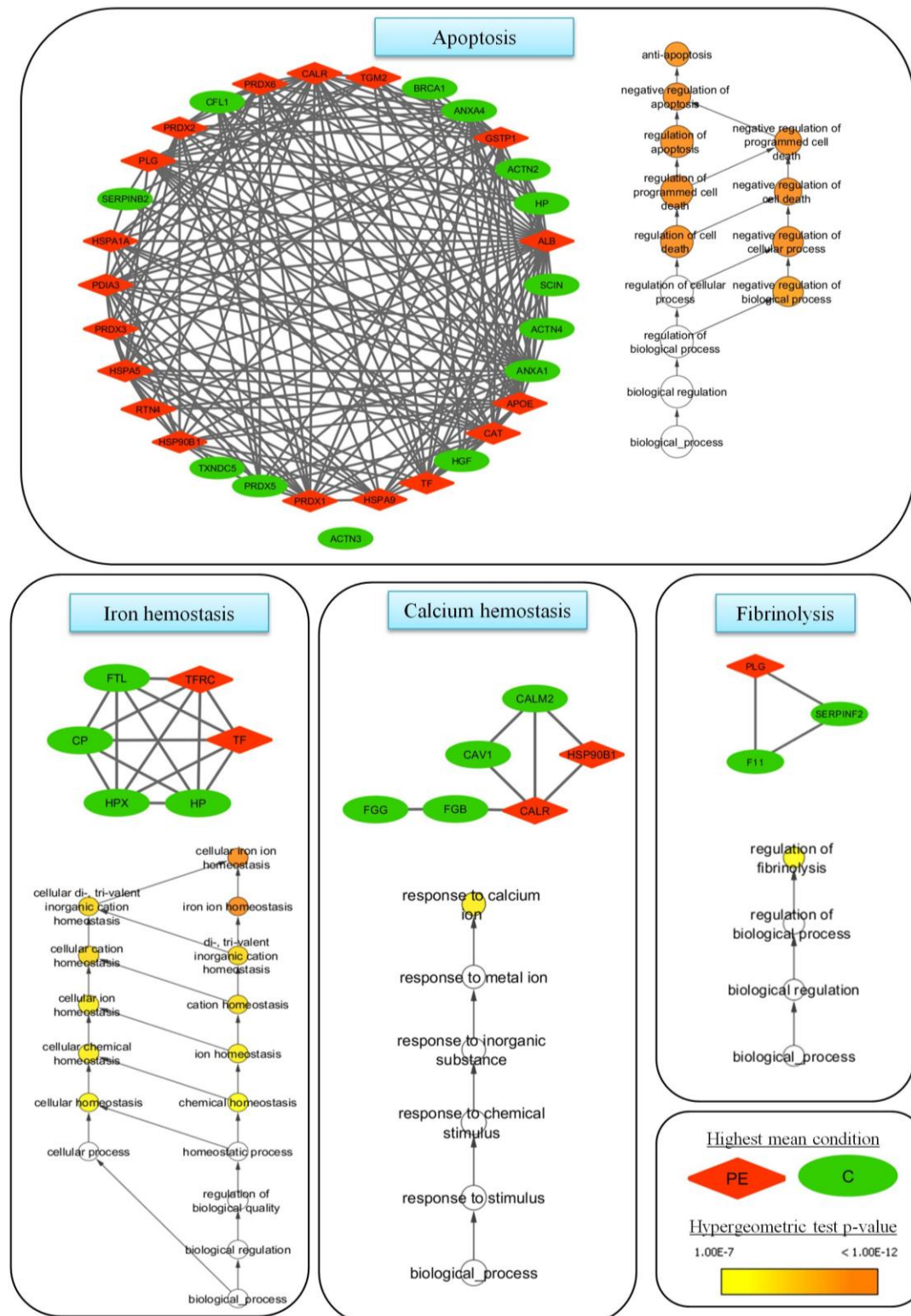


Figure 3.3 (d) Gene ontology and protein-protein interaction networks of differentially expressed proteins

Each cluster represents the enriched molecular or biological process. Nodes represent the proteins and the edges represent the degree of connectivity. Enrichment of the node was done with BINGO 3.0.2, a plugin for Cytoscape. In a cluster, red colored diamond-shaped node indicates the highest mean condition (upregulation) in pre-eclampsia and green colored eclipse shaped node indicates the highest mean condition in normotensive samples.

3.3.2.2 Equilibrium between oxidant-antioxidant factors

We identified 21 DEPs related to oxidative stress, in this cluster, peroxiredoxin (PRDX1, 2, 3, 4, 6) protein family known as antioxidant enzymes is known to be up-regulated in PE except for mitochondrial PRDX5. This increase in antioxidant level might be the consequence of defense mechanism of the cell to reactive oxygen species, while down-regulation of PRDX5 can lead to mitochondrial dysfunction (219-221). Peroxiredoxins are also modulators of redox signaling during inflammation (222). Another important protein that plays a role in oxidative stress, mitochondrial DNA integrity and apoptosis is oxidative resistance 1 (OXR1) protein, found to be down-regulated in PE. This is the first report of OXR1 involvement in PE. Recently an extensive transcriptome study on OXR1 depleted HeLa cells conducted by Yang et al. 2015 reported the role of OXR1 as the key sensor of cellular oxidative stress to regulate the p53 signaling pathway (223). Under-expression of this protein in PE can perhaps lead to increased oxidative stress and apoptosis.

ER stress is evident in pre-eclamptic placenta, which includes an imbalance in protein folding and aggregation of these unfolded proteins. Under oxidative stress, another group of enzymes that helps in proper protein folding are the chaperones, specifically the protein disulfide isomerases (PDIs). Our data indicate this imbalance in the ER resident proteins such as under expression of PDI A4, PDI A6, prolyl 4-hydroxylase subunit beta (P4HB), thioredoxin domain containing 5 (TXNDC5), thioredoxin (TXN) and overexpression of endoplasmic reticulum chaperone protein 1 (HSP90B1), and hypoxia up-regulated protein 1 (HYOU1).

3.3.2.3 Inflammation, fibrinolysis, and coagulation

Systemic inflammation is one of the features of PE. Our data show differential expression of many acute phase proteins. Positive acute phase proteins such as complement C3, C4B, fibrinogen, alpha-2 macroglobulin, alpha-1 antitrypsin, alpha-1 chymotrypsin, ceruloplasmin, haptoglobin, and hemopexin were down-regulated while plasminogen, alpha-1 glycoprotein, and negative acute phase proteins such as transferrin, albumin, alpha-2 HS-glycoprotein and apolipoprotein A1 were up-regulated in PE. Apart from these proteins, many pro- and anti-inflammatory proteins such as apolipoprotein E, fibronectin, tissue transglutaminase, hepatocyte growth factor and

dipeptidyl peptidase IV showed the disparity in expression. Inflammation, fibrinolysis, and coagulation are an integral part of PE pathophysiology (224). PE often results in the hypercoagulable state, which reduced fibrinolysis activity. This is evident in our results wherein plasminogen activator inhibitor-2 (PAI-2) was significantly lower in the PE placenta. This correlates with the previous studies on PAI-2, indicating decreased placental function during PE (225) Other fibrinolysis activator proteins such as annexin A2 (AXNA2), Factor XIa (F11) which helps in activating plasminogen to plasmin, are found to be down-regulated in PE while plasminogen is up-regulated. Annexin family is known to play a role in inflammation, fibrinolysis, and coagulation, and our results show that AXNA1, A2, and A4 are under-expressed while AXN A6 is overexpressed in PE.

3.3.2.4 Proteins involved in angiogenesis are differentially regulated

The pathophysiology of PE is established because of poor trophoblast invasion and impaired angiogenesis which leads to abnormal placentation. The proteins involved in biological processes such as cell migration, cell adhesion, angiogenesis, hypoxia and placental development were also observed as DEP. VEGF receptor-1 (Flt-1) and its soluble form have always been the center of biomarker research in PE regarding impaired angiogenesis. In accordance with others research (226), our data also show overexpression of Flt-1 in PE placenta. Other angiogenic proteins such as vitronectin induce angiogenesis (227), HGF regulates VEGF expression (228); caveolin-1 regulates angiogenesis via VEGF compartmentalization-induced ERK2/1 signaling in the placenta (229) which showed down-regulation in PE.

3.3.3 Plasma proteome profiling of normotensive and pre-eclamptic patients

To verify or validate whether some of these DEPs are secreted into the bloodstream, we carried out plasma proteome analysis during the gestational weeks 16-20th (Tri1), 26-30th (Tri2) and 43 to at delivery (Tri3) of pregnancy. The candidate DEP proteins selected for this analysis were identified by GO term. There were 41 proteins with secreted GO term from DAVID analysis, out of which 17 were up-regulated and 24 down-regulated (Supplemental data 6). Most of these proteins were present in plasma as moderate abundant proteins such as alpha-macroglobulin, fibrinogen, alpha-

antitrypsin, and a few glycoproteins while others were low abundance. We depleted the most abundant albumin protein through precipitation technique to perform SWATH and identified 30 of these secreted proteins in plasma of normotensive and PE patients in three gestational weeks (Supplemental data 7). In addition to these, apolipoprotein A-II was observed to be up-regulated in the PE plasma, which was not found in placenta. Because this forms a complex with the apolipoprotein A-I in HDL complex, we considered it for further validation. Because SWATH analysis was conducted in pooled plasma samples, we then selected the proteins that showed a high fold difference between normotensive and PE in the different gestational week for further investigation in individual plasma samples by MRM. In Swath, depletion of albumin could not reduce its abundance and help identify low abundant protein, and hence in MRM undepleted plasma samples were used.

3.3.3.1 Targeted quantification of Apolipoprotein A-I, Apolipoprotein A-II, Haptoglobin, and Hemopexin by multiple reaction monitoring

For label-free MRM analysis, we selected protein, namely, apolipoprotein A-I, apolipoprotein A-II, haptoglobin, and hemopexin. These proteins belong to lipid and iron metabolism, respectively. However, there are some indirect interactions between them as shown by STRING analysis (Figure 3.4).

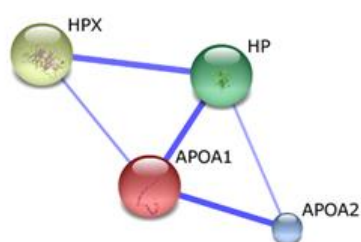


Figure 3.4 Interaction between apolipoprotein A-I, apolipoprotein A-II, hemopexin and haptoglobin analyzed by STRING 9.1

For MRM, at least three peptides and two transitions per peptide were monitored (Table 3.2) (Figure 3.5). Because it was a label-free MRM, it was necessary to assess the quality of data. First, the TIC of all MRM runs was shown to overlap in intensity to prove that there was no difference in amount loaded on a column for all of the samples

(Figure 3.6). Second, the assessment of transition, quality, and data nominalization showed consistency in retention time and peak area across all samples in the experiments. The retention time for all transitions for a given fragment was consistent with a small coefficient of variation (<4%) (Figure 3.7). The raw intensity values of transitions were transformed to log₁₀ scale and quantile-quantile (Q-Q) plot for normality with Shapiro-Wilk *p*-value were plotted for each fragment to check the normality. The Q-Q plot was consistent with normality, with a few outliers that were not considered for further analysis (Supplemental data 8).

Table 3.2 List of peptide and MRM transitions pairs used to detect protein

Protein	Sequence	Q1 (m/z)	Q3 (m/z)	(Charge) Ion Type
Apolipoprotein A1	DLATVYVDVLK	618.4	736.4; 835.5; 936.5; 1007.6	(+2) y6; y7; y8; y9
	DYVSQFEGSALGK	700.8	661.4; 808.4; 936.5; 1023.5; 1122.6	(+2) y7; y8; y9; y10; y11
	LLDNWDSVTSTFSK	806.9	670.3; 769.4; 856.4; 971.5; 1157.6	(+2) y6; y7; y8; y9; y10
	EQLGPVTQEFWDNLEK QGLLPVLESFK	967.0 615.9	618.3; 804.4 623.3; 819.5; 932.6	(+2) y5; y6 (+2) y5; y7; y8
Apolipoprotein A2	EPC[Cmc]VESLVSQYFQTVTDYGK	784.4	783.4; 911.5; 1058.5	(+3) y7; y8; y9
	EQLTPLIK	471.3	373.3; 571.4; 684.5	(+2) y3; y5; y6
Haptoglobin	SPELQAEAK	486.8	659.4; 788.4	(+2) y6; y7
	TEGDGVYTLNNEK	720.3	980.5; 1037.5; 1152.6; 1209.6	(+2) y8; y9; y10; y11
	VVLHPNYSQVDIGLIK	599.0	543.4; 658.4; 757.5; 885.5; 1135.6	(+3) y5; y6; y7; y8; y10
Hemopexin	VTSIQDWVQK	602.3	560.3; 675.4; 803.4; 916.5; 1003.5; 1104.6	(+2) y4; y5; y6; y7; y8; y9
	LLQDEFPGIPSPLDAAVEC[Cmc]HR	789.1	772.3; 843.4; 958.4; 1071.5; 1168.5	(+3) y6; y7; y8; y9; y10
	EWFWDLATGTMK	742.9	537.3; 608.3; 836.5; 1022.5; 1169.5	(+2) y5; y6; y8; y9; y10
	LWWLDLK	487.3	375.2; 488.3; 674.4; 860.5	(+2) y3; y4; y5; y6

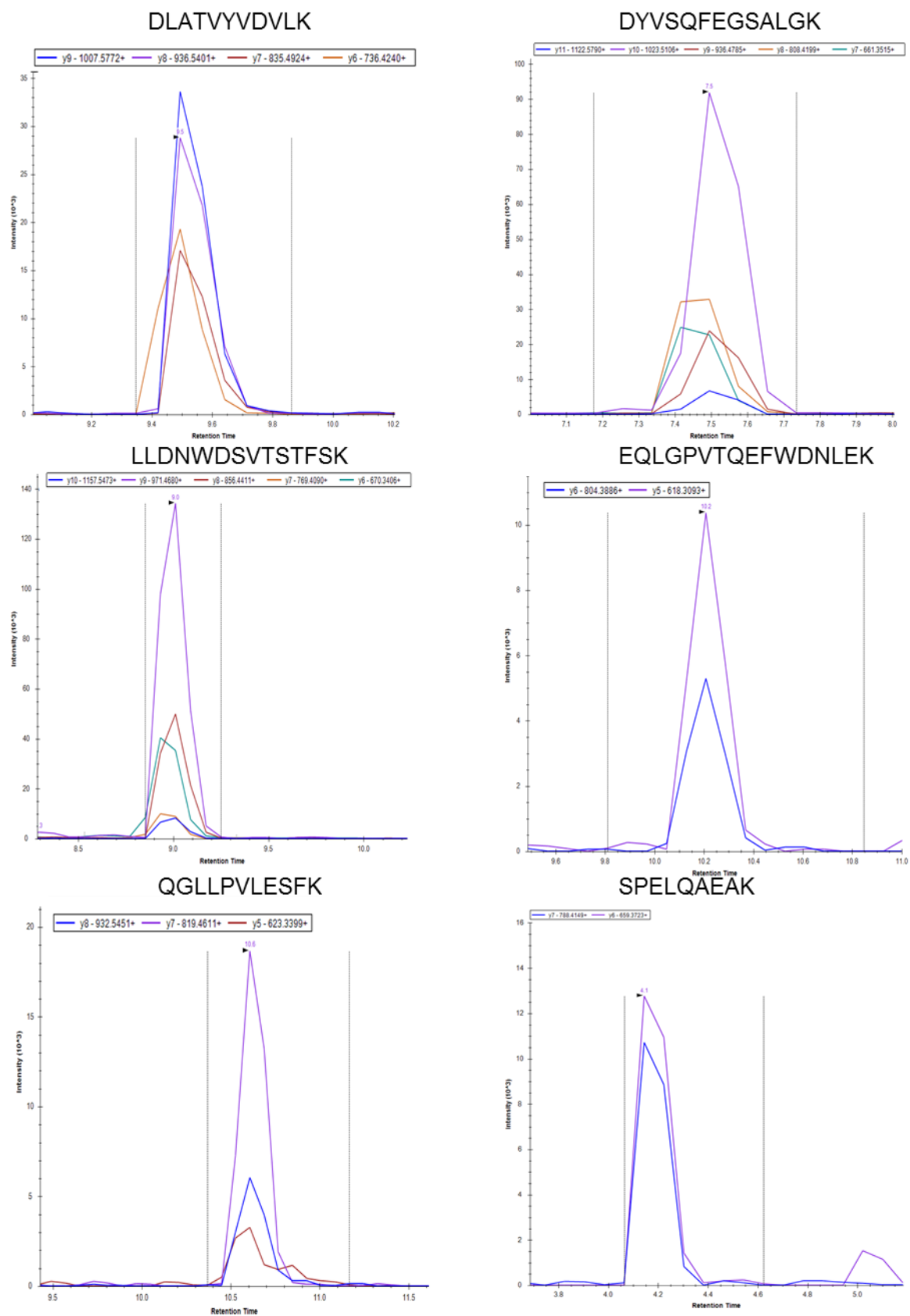


Figure 3.5 (a) MRM transition plots for individual peptides (figure continued)

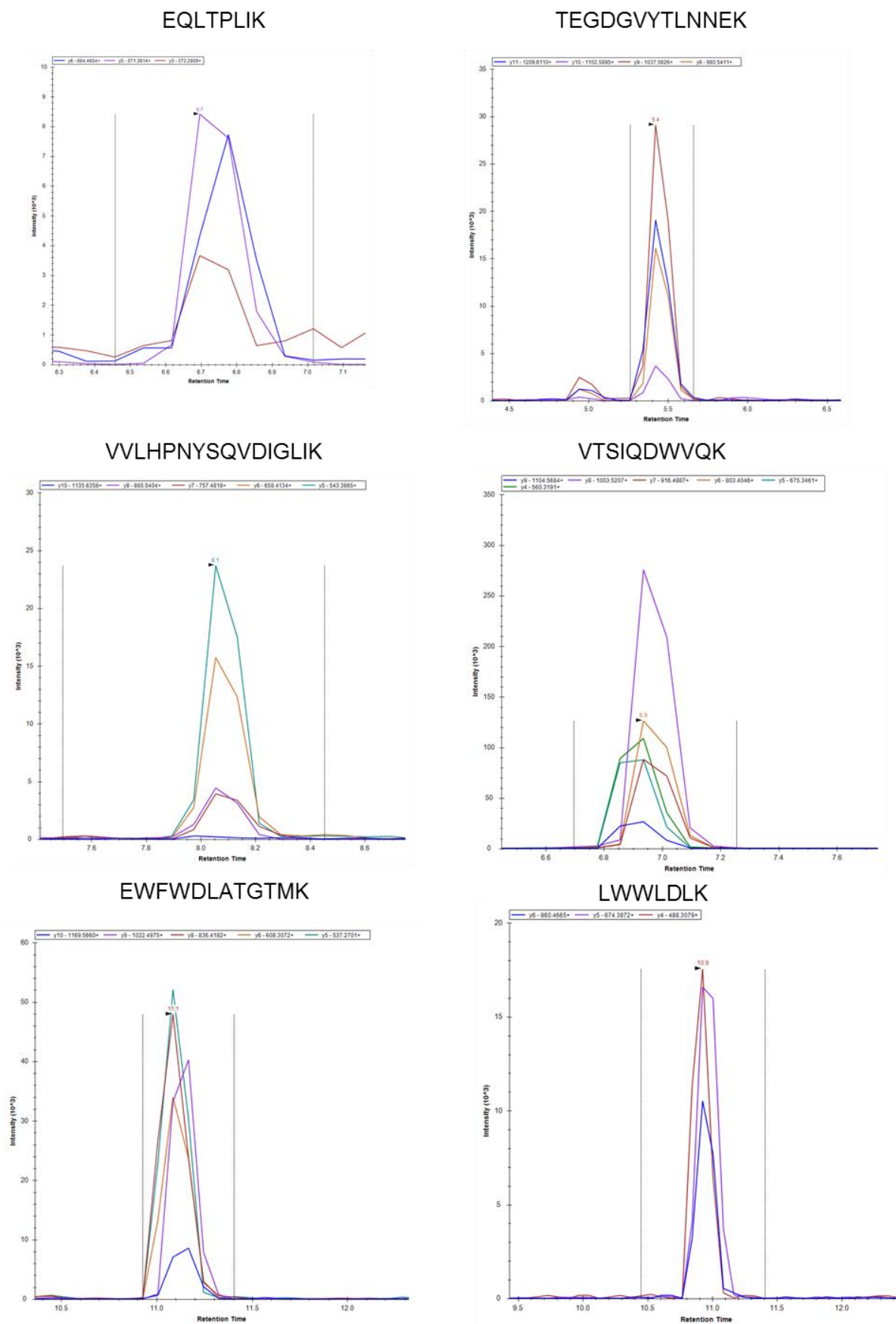


Figure 3.5 (b) MRM transition plots for individual peptides

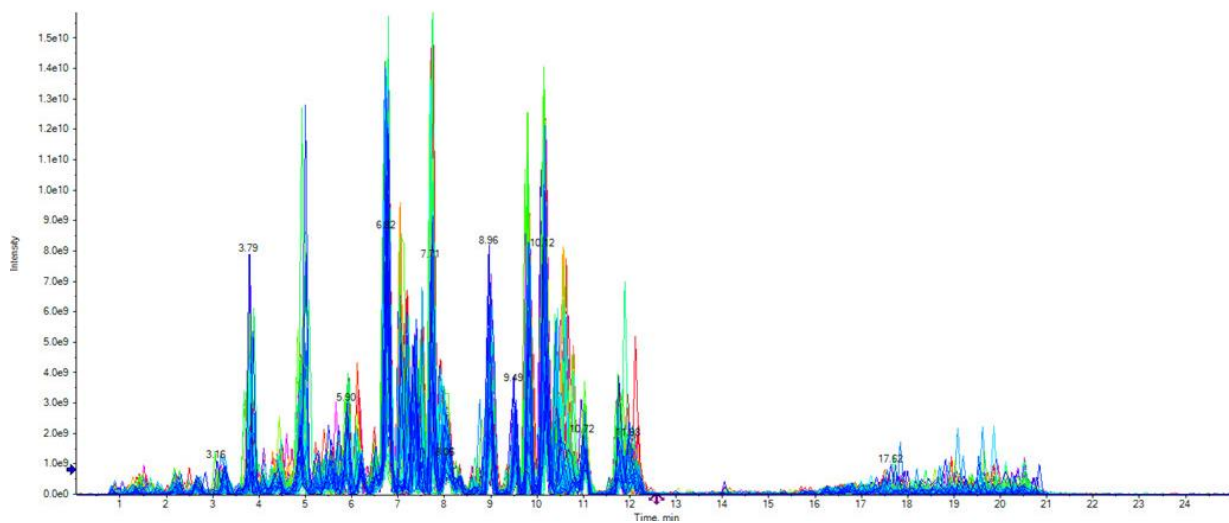


Figure 3.6 Total intensity count of all 120 sample runs (MRM)

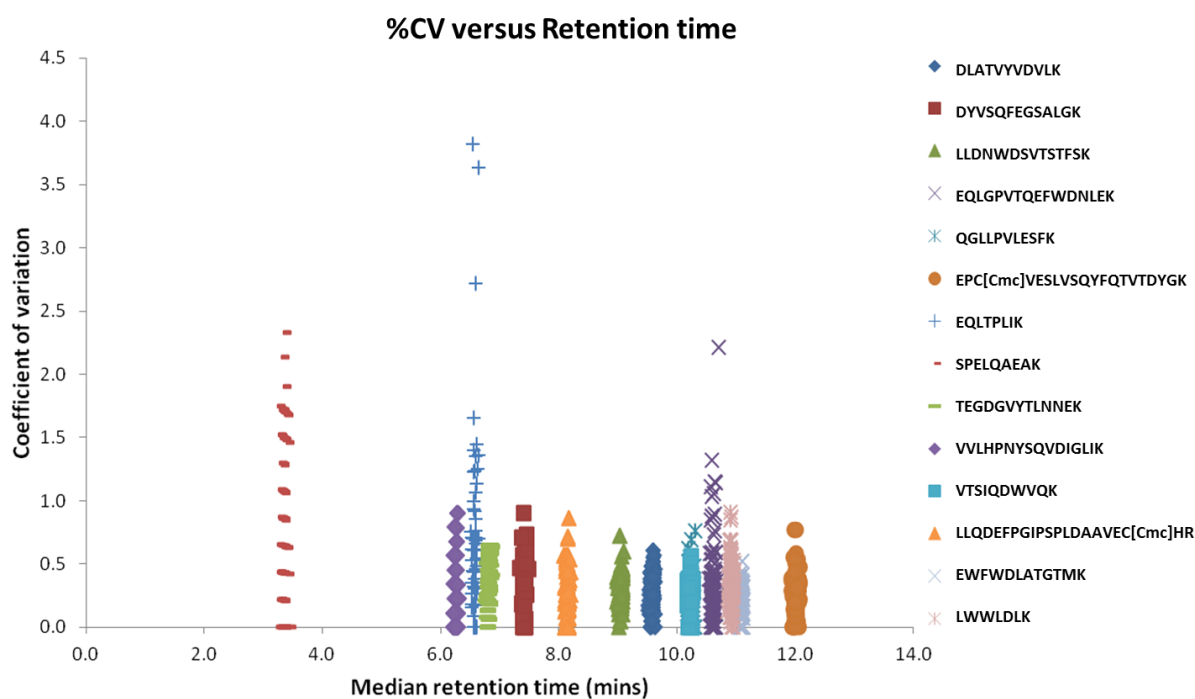


Figure 3.7 Coefficient of variation versus retention time of MRM runs
Transitions have consistent retention time with coefficient of variation less than 4%

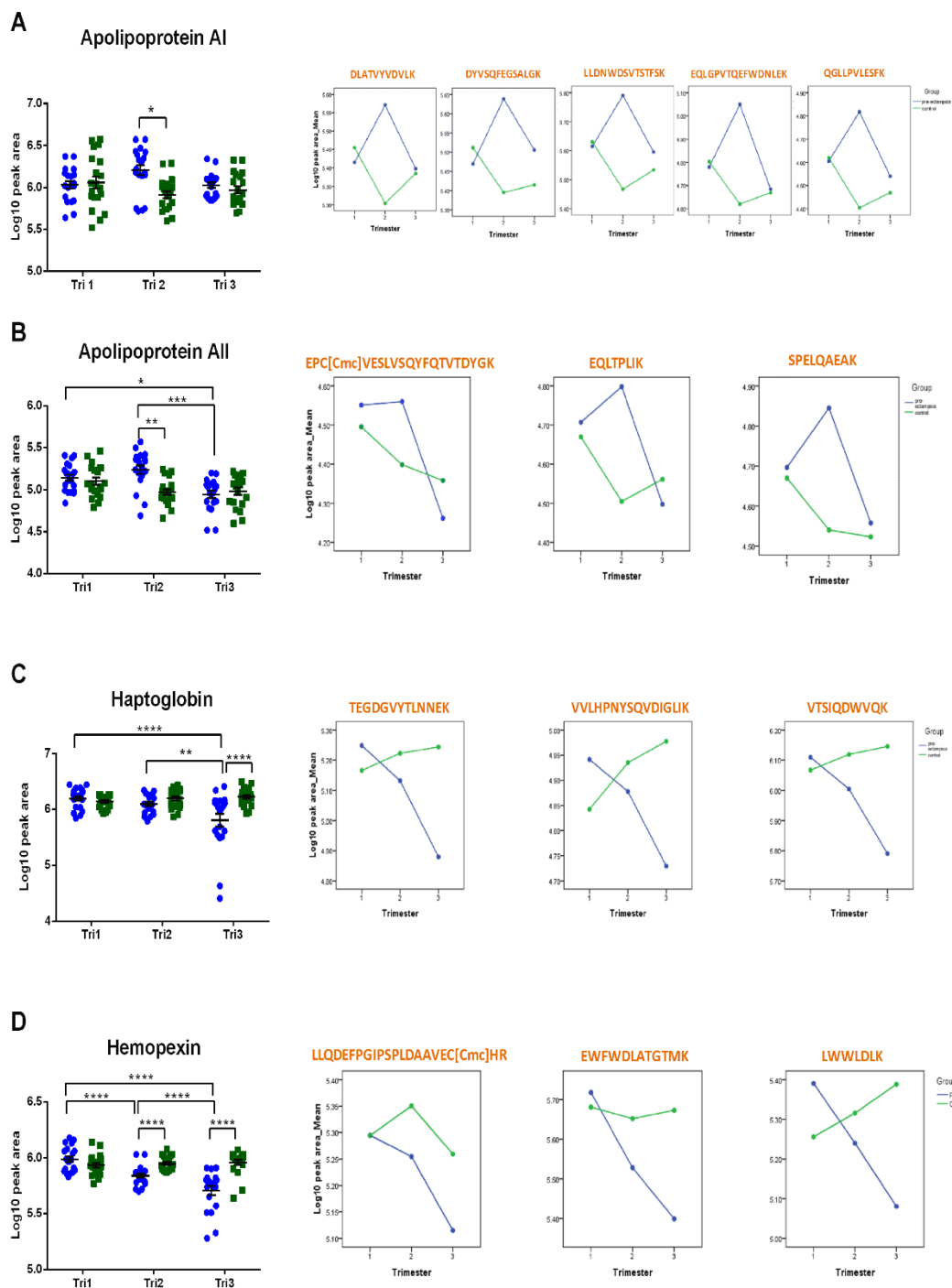


Figure 3.8 Relative abundance of (A) apolipoprotein A-I, (B) apolipoprotein A-II, (C) hemopexin and (D) haptoglobin in plasma of normotensive and pre-eclamptic patients

Dot plot (left side) represents the protein abundance and line graph (right side) represents individual peptide abundance. Throughout the figure green and blue color represent normotensive and pre-eclamptic samples, respectively. The x-axis of graphs represents the three gestational weeks (Tri1, Tri2, and Tri3) and the y-axis represents the mean of Log 10 peak area. Error bars represent SEM and asterisks indicate p -values (* p <0.05, ** p <0.01, *** p <0.001, **** p <0.00001).

Split-plot analysis of variance (SPANOVA) within-subject data analysis showed that all four proteins did not show any variation in normotensive patients throughout the different gestational week while the PE patients showed significant difference within the Tri1, Tri2 and Tri3 in the abundance of ApoA-II, haptoglobin, and hemopexin (Fig. 4). SPANOVA between-subject variation showed a two-fold increase in apolipoprotein A-I and A-II in the Tri2 while haptoglobin and hemopexin decreased in Tri2 and Tri3 (1.8-fold) in PE patients (Figure 3.8).

3.3.3.2 Apolipoprotein A-I and A-II may act as antioxidant in PE

Apolipoprotein A-I and A-II are the major protein components of high-density lipoprotein (HDL). Our data show that there is a significant increase in plasma ApoA-I and A-II during the Tri2 of PE compared with normotensive pregnancy, 2.0 ($p < 0.05$) and 1.9-fold ($p < 0.01$), respectively (Figure 3.8A, B) and it gradually lowers during the Tri3. ApoA-II showed a 2-fold decrease ($p < 0.01$) from Tri2 to Tri3 in PE plasma, while normotensive plasma showed no significant changes (Figure 3.8B).

HDL plays a major role in reverse cholesterol transportation and also as an antioxidant by inhibiting phospholipid oxidation with LDL. Oxidative stress in PE leads to the generation of increased oxidized LDL (230). Oxidized LDL leads to vascular inflammation. The study on transgenic mice reported that overexpression of ApoA-II converts HDL to pro-inflammatory particles (231). The increase in the level of ApoA-I and A-II might be the consequence of the protection of LDL from oxidation. The role of ApoA-II in HDL is less known. However, the study on transgenic mice reported that overexpression of ApoA-II converts HDL to pro-inflammatory particles (231).

3.3.3.3 Iron transport imbalance: haptoglobin, hemopexin, and transferrin receptor -1

Haptoglobin (Hp) is an acute phase protein and an antioxidant that prevents heme-iron oxidative reactions by binding to hemoglobin. It is known to be synthesized in the liver; however, previous studies have suggested that endometrium and decidua also showed increased production of Hp during pregnancy (232). Our data indicate that the Hp level in normotensive plasma samples showed a gradual increase during the gestational week. On the contrary, the PE plasma Hp level decreased with the 1.4-fold difference

in between Tri2 and Tri3 ($p<0.01$) and with the overall 1.7-fold change between Tri1 and Tri3 ($p<0.001$). In Tri3, there is the 1.8-fold difference ($p<0.001$) between normotensive and PE Hp plasma level, which was consistent with the lower expression in placental tissue (Figure 3.8C).

The decrease in the level of Hp may not be able to prevent the oxidative damage caused by free Hb, which is known to be overexpressed in the placenta during PE (233). Hp is also identified as an angiogenic factor in systemic vasculitis (234) and endometriosis (235). However, it is not yet explored as an angiogenic factor in impaired angiogenesis in PE. Previous reports on the role of haptoglobin polymorphism in determining PE are contradictory, wherein Sammour et al., suggest that Hp1-1 phenotype is decreased in PE, while Depypere and coworkers showed its prevalence more in PE patients (236, 237).

Along with Haptoglobin, Hemopexin (Hx) also contributes in neutralizing the heme-iron induced oxidative stress. Hx functions as the heme carrier from the bloodstream to the liver. LDL receptor-related protein-1 (LRP1) is shown to be the endocytic receptor for the heme-Hx complex in liver and placenta (238). LRP1 expression in placental cells suggests its role in heme-Hx uptake by these cells, thus contributing to the Fe pool (238). Baker and coworkers (239) reported plasma hemopexin activity to be decreased in PE in the third trimester as compared to the healthy pregnant and non-pregnant women. Furthermore, they also showed that hemopexin activity in normal pregnant women increases from week 10 onward and downregulates vascular angiotensin II receptor (AT₁) expression, suggesting its role in contracted vascular bed (240). Another study on the level of hemopexin in the serum of PE at third trimester showed no significant difference compared with normal pregnancy (241). Our study shows decreased levels of hemopexin in placenta as well as in plasma of PE patients. We report that Hx level is significantly decreased with 1.2 and 1.7-fold ($p<0.0001$) in Tri2 and Tri3, respectively in PE as compared with the normotensive pregnant women (Figure 3.8D). This decrease in Hx level might be the indicator of oxidative stress contributed by heme-Fe toxicity. The placental proteome data showed an imbalance in the iron transport system, these include upregulation of transferrin and transferrin receptor-1, and downregulation of ceruloplasmin and ferritin light chain.

To further explore the iron transport imbalance, we validated the expression of transferrin receptor-1 (Tfr-1), the major iron receptor in the placenta. Tfr1 showed a 1.7-fold increase ($p < 0.01$) in PE, also anti-Tfr1 antibody detected one more ~81 kDa protein with a fold change of 1.7 ($p < 0.001$), known to be soluble Tfr1 (Figure 3.9 A). This soluble form of transferrin receptor might be formed as a result of increased protease activity due to apoptosis in PE. (Figure 3.9 B) shows the up-regulation of the Tfr1 mRNA by 2.2 fold ($p < 0.001$) in PE, which shows corroboration with protein accumulation pattern. Transferrin receptor (TfR) is a transmembrane dimeric glycoprotein of two identical 95 kDa subunits linked by disulfide bonds. It plays an important role in transporting iron bound to transferrin from mother to fetus. TfR expression in the placenta is observed to be more in the microvillous membrane of syncytiotrophoblasts (242). Although increased sTfR level is considered to be an indicator of Fe deficiency in the case of PE despite generally elevated levels of Fe, up-regulation of TfR raises many questions. Our proteomic and gene expression results show that TfR is overexpressed in PE placenta which is contrary to the immunohistochemical data of showing TfR downregulation (243). In PE, hypoxia and elevated level of iron both are observed. Hypoxia condition upregulates the TfR expression through hypoxia-inducible factor alpha 1 (HIF-1 α) binding to hypoxia regulatory element (HRE) at the transcriptional level, while elevated iron level downregulates its synthesis via binding of iron regulatory protein (IRP) to iron regulatory element (IRE) at the post-transcriptional level (244). Studies show that IRP binding to IRE is dependent not only on the iron level but also on hypoxia and nitric oxide (NO) level. Hypoxia and elevated level of NO both allow the binding of IRP to IRE thus stabilizing and preventing enzymatic degradation of TfR mRNA (245). This gives a possible explanation for its overexpression in PE (Figure 3.9 C). The soluble form of TfR (sTfR) needs to be validated in plasma as a marker of PE.

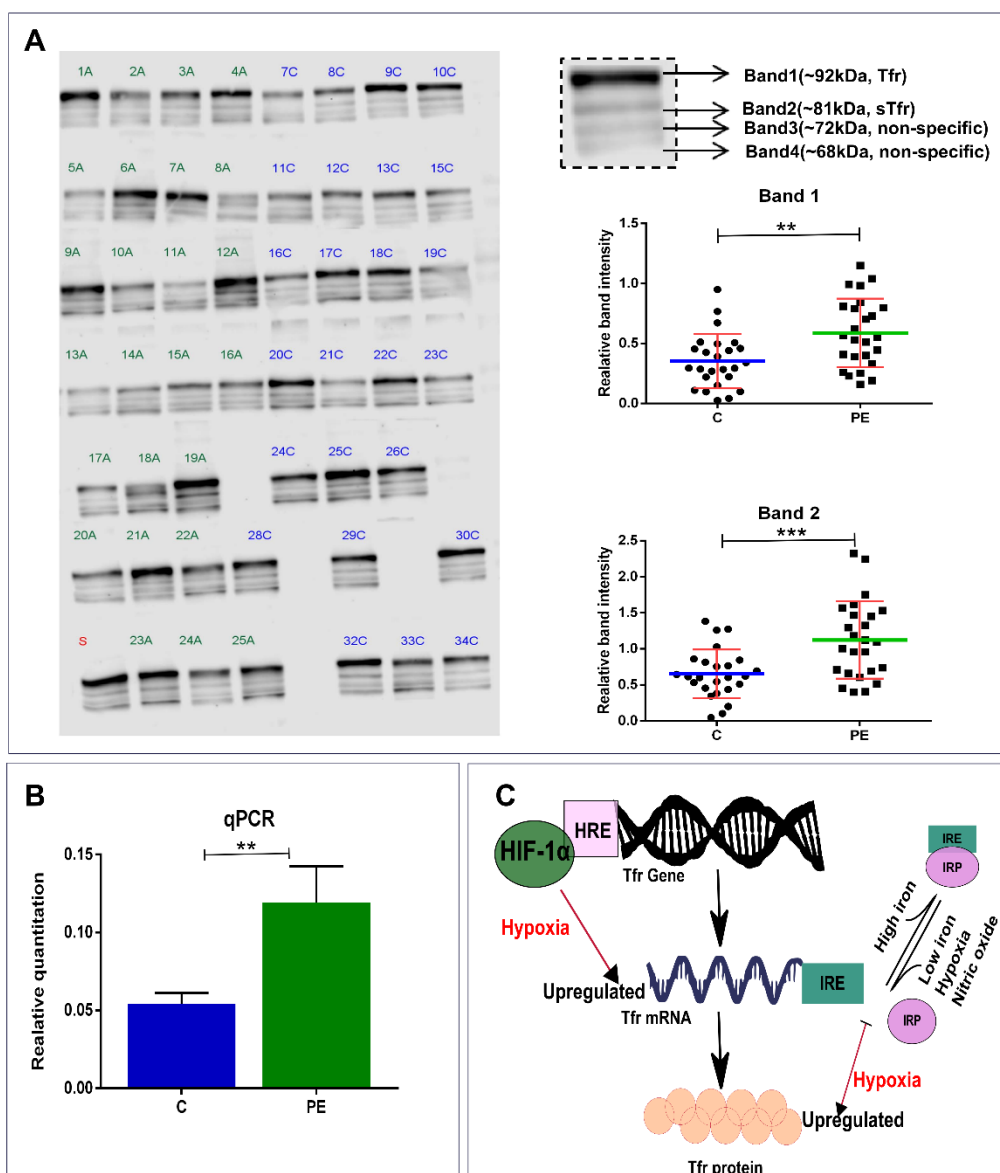


Figure 3.9 Validation of transferrin receptor-1 in placenta tissue

(A) Western blot analysis of normotensive (n=25, blue label) and pre-eclamptic (n=25, green label) samples. Scatter dot plot represents the relative band intensity of Tfr-1 (band 1) and sTfr-1 (band 2). Error bars indicate SEM. (B) Quantitative PCR for Tfr-1 mRNA transcripts. (C) Diagram depicts the hypothesis for overexpression of Tfr-1 under pre-eclamptic condition.

In conclusion, this study of placental proteome to elucidate the pathophysiology and biochemistry related to PE is the first of its kind where we utilized the label-free quantification technique of LC-MS^E individually on 25 PE and 25 normotensive placentae. This is the first study that reports a maximum number of DEP identified from PE placenta, although the total protein number we report is not more than previous studies (246). Elaborative gene ontology analysis of DEP confirms many biological processes that were previously reported are involved in PE along with few novel

proteins. For the first time four differential expressed proteins viz., apolipoprotein A-I and A-II, haptoglobin, and hemopexin were identified throughout the three gestational weeks of pregnancy in PE plasma. These proteins can be further evaluated for the development of potential biomarkers associated with pre-eclampsia pathogenesis.

Chapter 4

**Placental pathophysiology in
pregnant hypertensive rodent model**

Chapter 4 Placental pathophysiology in pregnant hypertensive rodent model

4.1 Background

4.1.1 Rat placenta

Laboratory rats (*Rattus Norvegicus*) have a bicornuate uteri. Depending on the strain, estrus lasts 20h and the gestation lasts 21 to 26 days (average 22 days). The blastocysts arrive in the uterus about 3 to 4 days after mating and implant itself in regularly spaced intervals (247). The blastocyst is encircled with layer of trophoblast (trophectoderm), which proliferates into preplacental cone (ectoplacental cone) by day 8 and forms the placental disk opposite to the implantation site. The placenta develops from the extraembryonic ectoderm derived from the trophoctoderm. The extraembryonic ectoderm proliferates and differentiates into chorionic ectoderm and the ectoplacental cone. The chorionic ectoderm interacts with allantoic mesoderm to give rise to labyrinth zone, while the ectoplacental cone (present only in rodent) forms the junctional zone of the placenta (248). Junctional zone is the site of rodent trophoblast progenitor cells that differentiates into (i) trophoblast giant cells, (ii) spongiotrophoblast cells, (iii) glycogen cells and (iv) invasive trophoblast cells. The invasive trophoblast cells appear by mid gestation and exit the junctional zone to enter the mesometrial uterine compartment where they invade the uterine spiral artery (249).

Similar to humans, the rat placenta is chorioallantoic and also haemochorial in structural organisation (250). Table 4.1 shows the comparison between human and rat placentation.

4.1.2 Hypertensive rodent model-SHRSP

The white Wistar rats are the common laboratory rats used for research. The spontaneously hypertensive rat (SHR) and stroke prone spontaneously hypertensive rat (SHRSP) were obtained by selective inbreeding of Wistar-Kyoto (WKY) rats by Okamoto and colleagues at the Kyoto University Faculty of Medicine, Japan (251).

Table 4.1 Comparison between rat and human placenta

<i>Parameter</i>	<i>Rat</i>	<i>Human</i>
<i>Gestational length</i>	~21 days	~9 months
<i>Placental structure</i>	Chorioallantoic	Chorioallantoic
	Hemochorial	Hemochorial
<i>Maternofetal interdigitation</i>	Discoid	Discoid
	Labyrinthine	Villous
<i>Maternofetal barrier</i>	Hemotrichorial	Hemomonochorial
<i>Uterine-placental interface</i>	Junctional zone	Extravillous trophoblast
<i>Trophoblast invasion</i>	Deep intrauterine: extravascular, interstitial	Deep intrauterine: extravascular, interstitial

The SHRSP has an increased incidence of cardiovascular complications, a higher tendency for stroke, as well as a more rapid onset of hypertension from 5 weeks of age rising to a SBP in male animals of approximately 230 to 250 mmHg (252) relative to the normotensive WKY. SHRSP blood pressure is salt-sensitive, whereby replacing drinking water with a 1% NaCl solution produces a rise in blood pressure of approximately 30 mmHg and accelerates the occurrence of stroke. In contrast, the SHR and WKY are less salt sensitive. (253). The pronounced cardiovascular phenotype and salt-sensitivity of the SHRSP makes it an ideal model to study human hypertension.

The blood pressure profile of the SHRSP during pregnancy is similar to that of women with hypertensive complications of pregnancy. In particular, the SHRSP exhibits the greatest blood pressure difference relative to the WKY from GD 10 to 14, this coincides with the period of rodent placenta development and maturation (Figure 4.1 A-B).

Previous studies by Small et al., showed a significantly impaired outward hypertrophic remodelling of the main uterine artery in SHRSP relative to the WKY (Figure 4.1C). Deficient uterine artery remodelling was associated with a significantly decreased pregnancy-dependent increase in uterine artery diastolic blood flow (254). They also show that significant blood pressure reduction using nifedipine from 6 weeks of age in the SHRSP did not have an effect on the abnormal uterine artery response (254). Therefore, the mechanisms behind this deficient vascular remodelling were not dependent on the presence of pre-existing maternal hypertension.

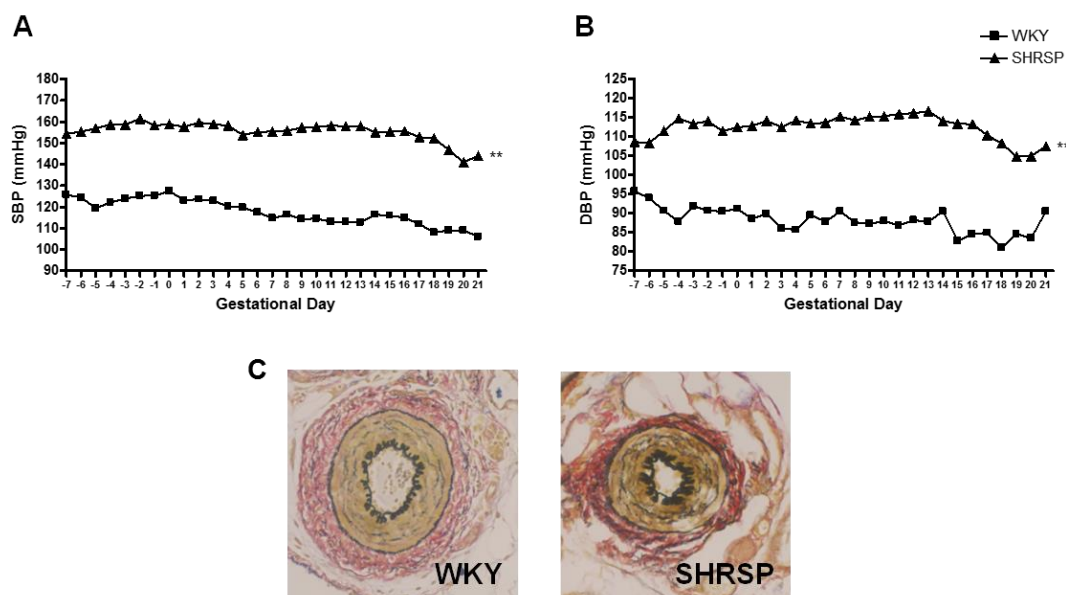


Figure 4.1 Blood pressure profile in the normotensive WKY rat and the SHRSP rats

The SHRSP is hypertensive before and during pregnancy relative to the normotensive WKY (A-B). SBP and DBP represents systolic and diastolic blood pressure. The uterine arteries in SHRSP are constricted compared to WKY (C). Data belongs to University of Glasgow group (254).

4.2 Material and Methods

4.2.1 Sample collection

The work presented in this chapter has used pregnant WKY and SHRSP that were untreated. Females were time mated at 12 weeks of age (± 4 days). Non-pregnant animals were age-matched at 15 weeks ± 4 days (i.e. 12 weeks of age + 21 days of pregnancy). The number of animals and particular gestational day (GD) is given in the associated figure legend.

4.2.2 Protein extraction

Placental tissue was harvested and rinsed in ice cold PBS from WKY and SHRSP, and frozen at -80°C until further use. Frozen tissues were thawed and homogenised in lysis buffer containing 1 M urea, 0.2 M thiourea, 70 mM dithiothreitol, and 0.1% octyl-beta-thioglucopyranoside. The homogenate was centrifuged at 25000 g for 30 min at 25°C . The supernatant was collected and total protein was estimated using Bradford Protein Assay (Bio-Rad Laboratories, Hercules, CA, USA).

4.2.3 In-solution digestion

Placental protein (100 μg) were digested separately. Each sample was washed twice with Amicon Ultra 3kDa MWCO (Millipore, Billerica, MA, USA) using 50 mM ammonium bicarbonate. The protein samples were subjected to heat denaturation (80°C), reduced using 100 mM dithiothreitol for 30 min at 65°C and alkylated with 200 mM iodoacetamide in the dark for 30 min at 25°C. Trypsin (Trypsin Gold, MS grade, Promega, Madison, WI, USA) was added in 1:20 ratio trypsin: protein (w/w) and incubated overnight at 37°C. The reaction was stopped by the addition of 2 μL of formic acid.

4.2.4 Label-free analysis in LTQ orbitrap

LC-MS/MS sequencing was performed on an UltiMate 3000 nano-flow system (Dionex/LC Packings, USA) connected to an LTQ Orbitrap hybrid mass spectrometer (Thermo Fisher Scientific, Bremen, Germany) equipped with a nano-electrospray ion source. After loading (5 μL) onto a Dionex 0.1 \times 20 mm 5 μm C18 nano trap column at a flowrate of 5 $\mu\text{L}/\text{min}$ in 98% water, 0.1% formic acid and 2% acetonitrile, sample was eluted onto an Acclaim PepMap C18 nano column 75 μm \times 50 cm, 2 μm 100 \AA at a flow rate of 0.3 $\mu\text{L}/\text{min}$. The trap and nano flow column were maintained at 35 °C. The samples were eluted with a gradient of solvent A: 98% water, 0.1% formic acid, 2% acetonitrile verses solvent B: 80% acetonitrile, 20% water, 0.1% formic acid starting at 1% B for 5 minutes rising to 20% B after 90 minutes and finally to 40% B after 120 minutes. The column was then washed and re-equilibrated prior to the next injection.

The eluent from the LC were ionized using a Proxeon nano-spray ESI source operating in positive ion mode into an Orbitrap Velos FTMS (Thermo Finnigan, Bremen, Germany). Ionization voltage was 2.6 kV and the capillary temperature was 250°C. The mass spectrometer was operated in MS/MS mode scanning from 380 to 1600 amu. In LC the top 20 multiply charged ions were selected from each scan for MS/MS analysis using HCD at 40% collision energy. The resolution of ions in MS1 was 60,000 and 7,500 for HCD MS2. In CE the top 5 multiply charged ions were selected for MS/MS using a data dependent decision tree method (255) and fragmented by either HCD at 40% or ETD, depending on their mass and charge state.

MS and MS/MS data files were searched, in this case, against the Uniprot rat non-redundant database using MaxQuant (256). Label free quantitation was used for analysis using MaxQuant designed algorithm (257). The statistical analysis was performed using Perseus software (258).

4.2.5 Gene ontology and protein interaction network

Gene ontology and protein interaction network was performed similar to section 3.2.5 in Chapter 3

4.3 Results and Discussion

4.3.1 Comparison of placental proteome of WKY and SHRSP

There was a strong correlation (average Pearson correlation value of 0.96) of label-free quantitation (LFQ) intensities between biological replicates (Figure 4.2A). In total, 944475 peptides were identified at MS1 level and 66597 peptides were sequenced at MS/MS level. 11737 sequenced peptides were assigned to 1593 proteins at a false discovery rate under 1% at the peptide and protein level. 1318 proteins were considered for further analysis after applying filtering criteria such as proteins identified by at least 2 peptides, quantifiable at least in three WKY and/or at least in three SHRSP. Amongst the total proteins identified, 686 are annotated as extracellular exosomes, followed by 663 cytoplasm, 486 nucleus and 383 membrane. Proteins from organelles such as mitochondria (209), endoplasmic reticulum (97) and Golgi apparatus (80) were also annotated (Figure 4.2B). Principal component analysis (PCA) on LFQ intensities for all protein was performed. The PC1 and PC2 accounted for 49.5% and 13.3% of the total variance respectively (Figure 4.2C)

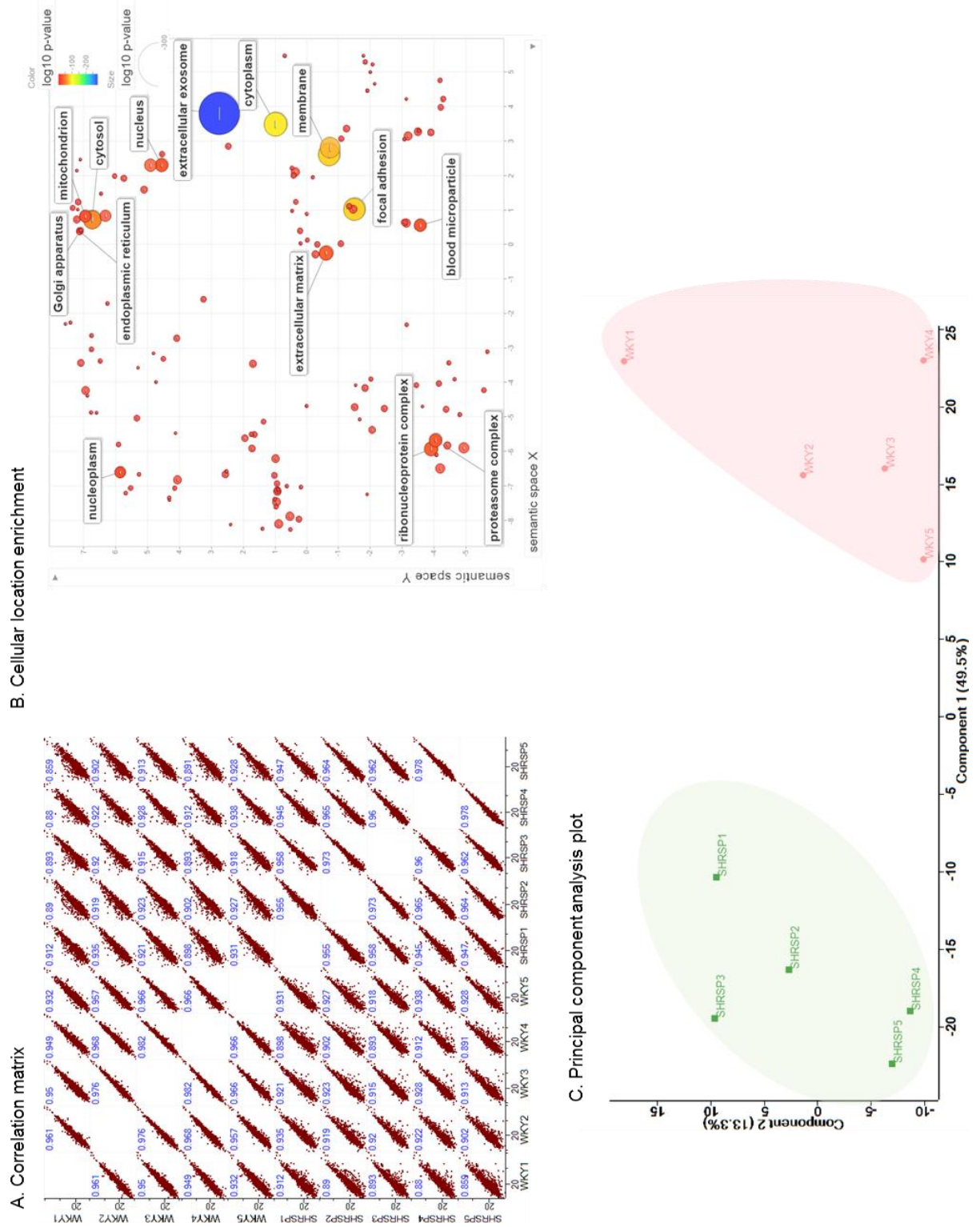


Figure 4.2 Rat placental proteome

(A) Correlation matrix for biological replicates of WKY and SHRSP (B) Scatter plot showing enriched cellular locations of all proteins identified (C) Principal component analysis plot separates the two group at PC1 at 49.5%

The LFQ intensities were \log_2 transformed and missing values were imputed with numbers by normal distribution (width 0.3 and shift 2.5). The LFQ intensities of WKY was compared with SHRSP by two-sample t-test with permutation-based FDR method (250 permutations; FDR 0.05). This resulted in identification of 363 DEP with p value < 0.05 , which was also seen on volcano plot (Figure 4.3). These DEPs included 115 down-regulated and 227 up-regulated protein levels in SHRSP with a fold change cut-off 1.3 (Figure 4.4) (Supplemental data 9). We also found 7 and 14 proteins to be uniquely identified only in WKY and SHRSP respectively with p value < 0.05 (Figure 4.4).

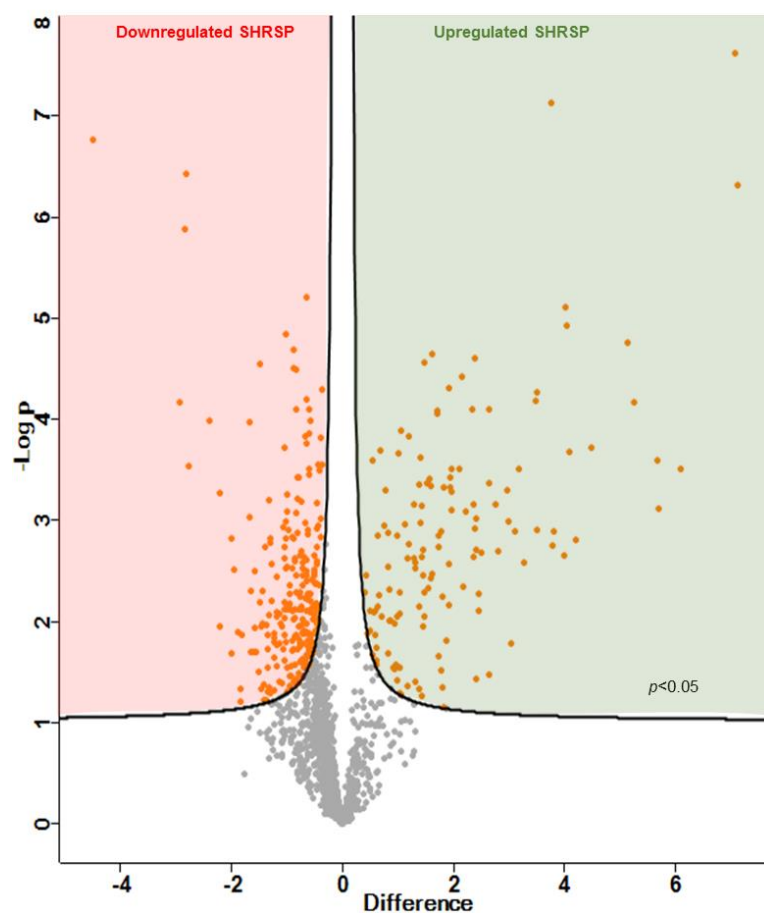


Figure 4.3 Volcano plot for rat placental proteome

Volcano plot showing negative natural log of the p -values plotted against the \log_2 of the change for each of the proteins quantified by label-free proteomic analysis comparing WKY and SHRSP. Significant proteins ($p < 0.05$) are plotted in orange. Many more proteins were down-regulated in SHRSP [negative \log_2 (fold change/difference); red shaded area] than up-regulated [positive \log_2 (fold change/difference); green shaded area]. Fold change/Difference values were scored as SHRSP/WKY.

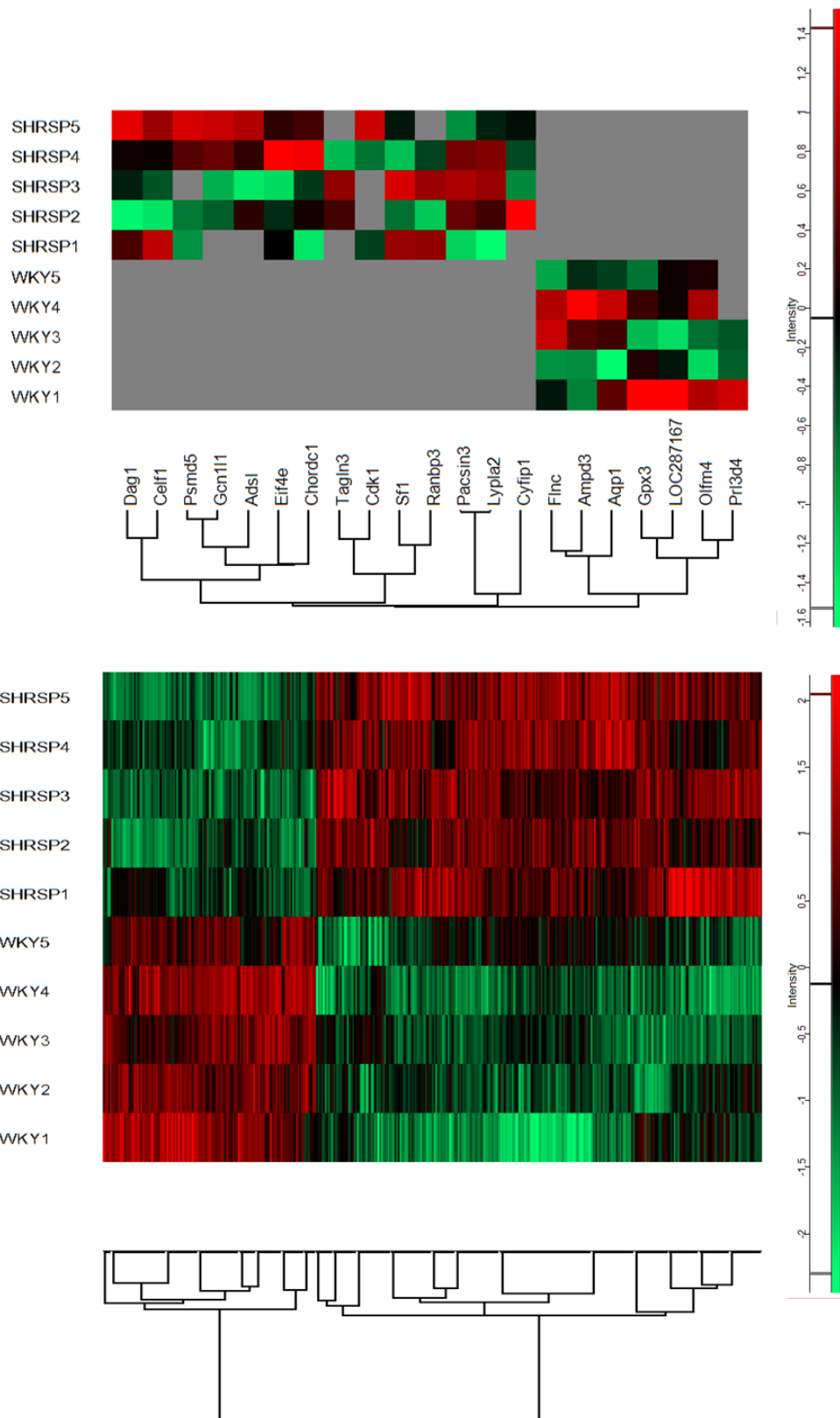


Figure 4.4 Heat map of differentially expressed protein

Clustered heat map of protein LFQ profiles between WKY and SHRSP after t-test analysis. Red, increased protein expression; Green, low relative to the other samples; and Grey represents zero LFQ.

4.3.2 Gene ontology of differentially expressed protein

The 363 DEPs were uploaded to STRING 10.0 for protein interaction network and visualized in Cytoscape 3.4.0. Network analysis showed 367 (363 DEP+isoforms) and 2345 edges, with some nodes with more than 20 degree (number of connections) (Figure 4.5).

Gene ontology enrichment analysis of biological process (GOBP) was performed in BINGO plug-in of Cytoscape. This enrichment resulted in identification of cluster of DEPs involved in physiological processes such as apoptosis, oxidative stress, hypoxia, cell migration, cell adhesion, coagulation, inflammation, fibrinolysis, and iron homeostasis (Hypergeometric test, $p < 0.05$).

Similar to human DEP analysis in Chapter 3, in rat, DEPs associated with apoptosis cluster was found to be the largest, signifying its role in pathophysiology in hypertensive pregnancy. Apoptosis cluster consisted of 48 proteins with 18 negative and 11 positive regulators of apoptosis. The imbalance in inflammation, coagulation and fibrinolysis was clearly visualised with more DEP down-regulated in SHRSP. SERPINE1 or plasminogen activator inhibitor 1 (PAI-1) is a major inhibitor of fibrinolysis pathway was found to be down-regulated in SHRSP, while placental specific PAI-2 was down-regulated in PE (chapter 3). Other fibrinolysis inhibitors and essential for coagulation, heparin cofactor 2 (SERPIND1) and kininogen-1 (KNG1) was down-regulated in SHRSP, this may lead to increased thrombin generation. The hypercoagulable and reduced fibrinolysis state in PE and SHRSP was found similar on the basis of these DEPs.

Another major cluster was of 18 DEPs each belonging to oxidative stress and hypoxia, with 6 DEPs such as AQP1, CAT, CRYAB, HSPD1, LONP1, SERPINE1 common to both the biological process. Major antioxidant from peroxidase protein class viz catalase (CAT), glutathione peroxidase (GPX) 1 and 3 or 6 (isoform) were down-regulated, while peroxiredoxin-4 (PRDX4) was up-regulated in SHRSP compared with WKY. GPX3 a selenium dependent extracellular (plasma) peroxidase was found only in case of WKY. Aquaporin-1 (AQP1) was detected only in the WKY placenta. AQP1 are transmembrane protein that maintain the water haemostasis and reported to be

detected in the endothelium of placental blood vessel and not in trophoblast cells (259). Recently AQP1 was shown to regulate placental development in the mouse (260).

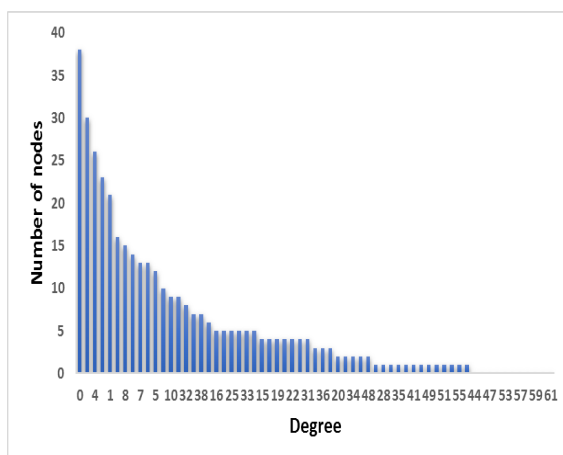
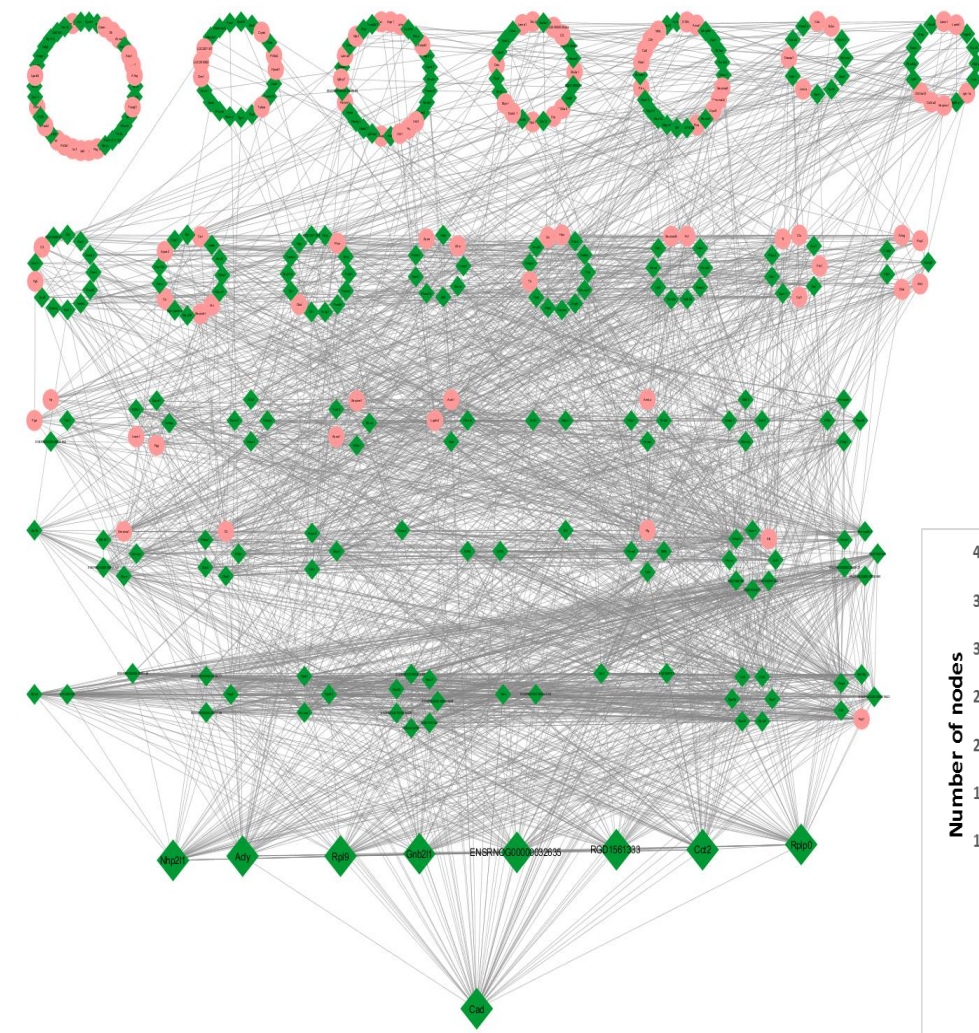


Figure 4.5 Protein interaction network from STRING

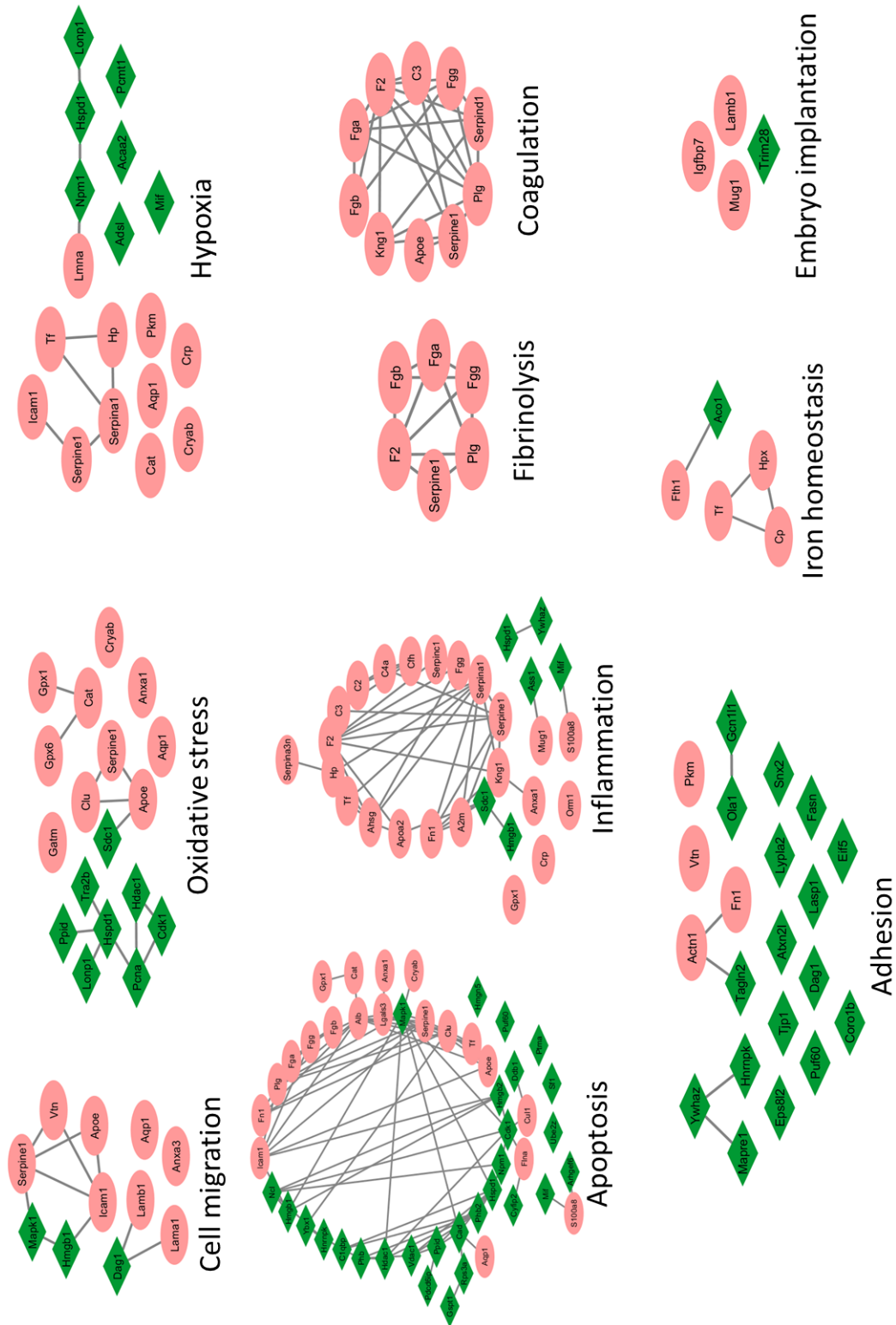


Figure 4.6 Gene ontology biological process enrichment

Each node represent a DEP. Pink oval node represents highest expression in WKY, while green diamond represents highest expression in SHRSP

4.3.3 Comparison of human pre-eclamptic and SHRSP placental physiology

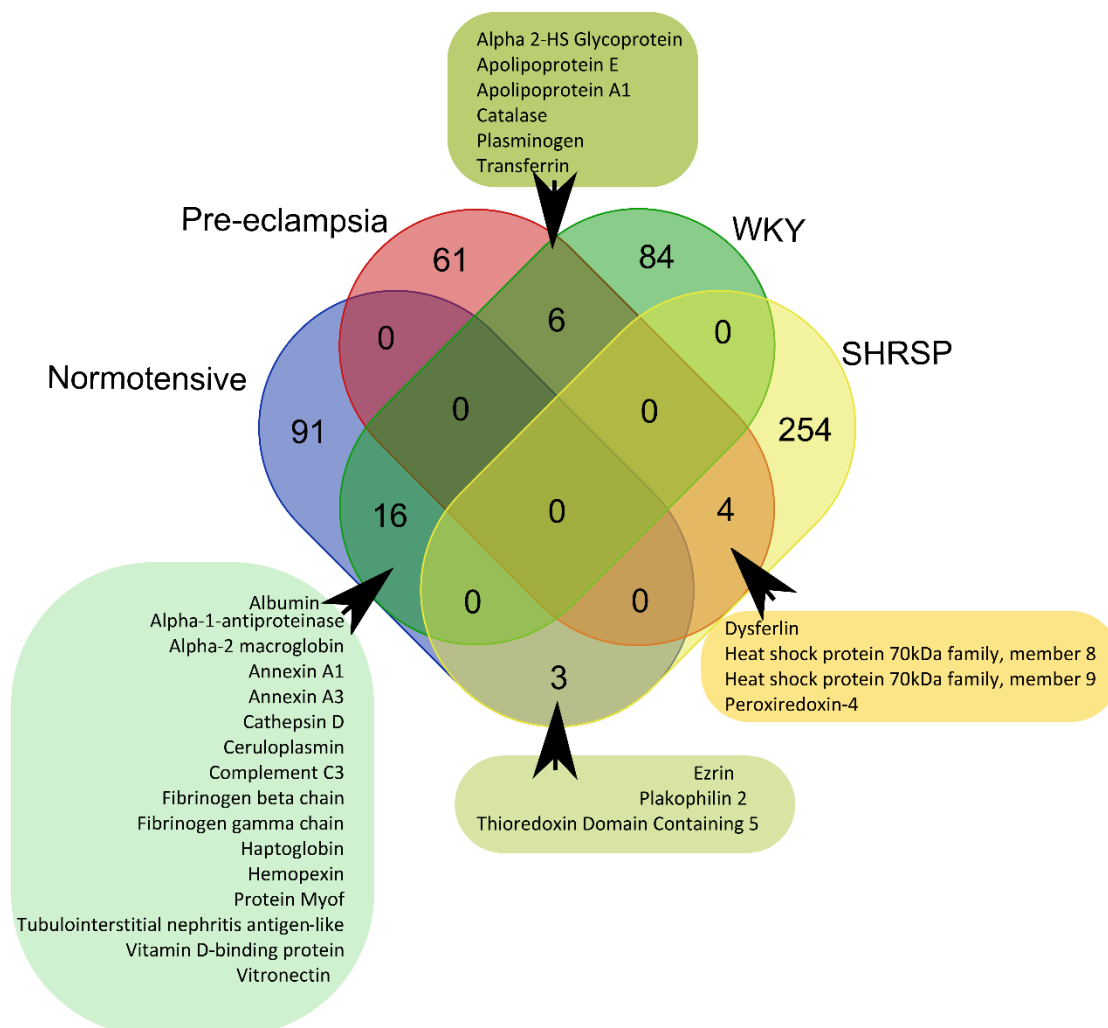


Figure 4.7 Venn diagram with comparison of differentially expressed protein between human and rat model

The DEPs identified in rat placental proteome was twice than in human placenta. Although label free quantitation was used in both cases, yet this variation is seen because of the technological difference in mass spectrometer. This is common problem encountered in proteomic studies. However, it was very interesting to note that approximately 30% of proteome and few DEPs were similar in both the human and rat model. Figure 4.7 depicts the DEPs that were common between normotensive, pre-eclamptic women, WKY and SHRSP rats.

Table 4.2 Comparison of candidate proteins in human and rat

Candidate proteins	Human	Rat
Annexin A6	Up-regulated in PE (Placenta)	Up-regulated in SHRSP (not significant)
Tubulointestinal nephritis antigen like protein-1	Down-regulated in PE (Placenta)	Down-regulated in SHRSP
Transferrin Receptor-1	Up-regulated in PE (Placenta)	Up-regulated in SHRSP (not significant)
Haptoglobin	Down-regulated in PE (placenta & plasma)	Down-regulated in SHRSP
Hemopexin	Down-regulated in PE (placenta & plasma)	Down-regulated in SHRSP
Apolipoprotein AI	Up-regulated in PE (placenta & plasma)	Down-regulated in SHRSP
Apolipoprotein AII	Up-regulated in PE (only plasma)	Down-regulated in SHRSP

When compared to the candidate proteins studied in pre-eclamptic human in previous chapters, we see few of them following the trend in SHRSP rats (Table 4.2). Apolipoprotein AI and AII were found to be up-regulated in PE placenta and plasma, while in SHRSP rats these were found to be down-regulated. Downregulation of HDL components in SHRSP rats correlates with this phenomenon that these rats are known to have pre-existing cardiovascular risk.

Chapter 5

Investigation of urinary peptidome over pregnancy in rodent model of hypertension

Contents of this chapter is published as research article in Hypertension, 2017, DOI:
10.1161/HYPERTENSIONAHA.116.08826

Chapter 5 Investigation of urinary peptidome over pregnancy in rodent model of hypertension

5.1 Introduction

Hypertensive complications are the most common clinical problems encountered during pregnancy (261). Hypertension during pregnancy encompasses a number of pathologies including: pre-eclampsia, pregnancy-induced hypertension and chronic hypertension. Specifically, chronic hypertension during pregnancy poses an increasing clinical problem (262). Pregnant women with chronic hypertension are at an increased risk of maternal and fetal morbidity and mortality as well as a higher incidence of developing super-imposed pre-eclampsia (263). The kidneys play a central role in blood pressure regulation in pregnancy. Women with chronic kidney disease are at increased risk of developing pregnancy complications; where up to 70% experience preterm delivery and up to 40% will develop pre-eclampsia (264, 265). Significant structural and functional changes occur in the kidney during pregnancy including a 1 - 1.5cm increase in size, a 50% increase in glomerular filtration rate, and up to an 80% increase in renal plasma flow (266, 267). These alterations are broadly conserved in rats (268).

The mechanisms which effect pregnancy-related changes in the kidney in normotensive and hypertensive women are incompletely understood. Unbiased screening approaches may have the ability to identify novel pathophysiological pathways. The urinary peptidome provides information about proteins that are involved in local processes in the kidneys and information about other organs obtained through filtration of the dynamic plasma peptidome (269). Peptides derived from processes in the kidney and urogenital tract form the majority of those detected in the urinary peptidome (70%) whilst peptides from the circulation constitute the remainder (270). The small peptides present are generally soluble and due to their size do not require protein digestion before analysis by mass spectrometry (270). Urinary peptidomics has been applied in the field of cardiovascular research to develop biomarker panels for diagnosis, prediction of disease and risk stratification (271). In particular, a number of studies have shown that there are alterations in the urinary peptidome in people with hypertension (272) and in healthy pregnant women compared to those who develop pre-eclampsia (273).

The stroke-prone spontaneously hypertensive rat (SHRSP) obtained by selective inbreeding of the Wistar-Kyoto (WKY) strain is a well-characterised model of cardiovascular disease in general and of maternal chronic hypertension (254). We hypothesized that the urinary peptidome would be altered in both a pregnancy-dependent and strain-dependent manner between the SHRSP and control WKY strain.

5.2 Materials and Methods

5.2.1 Animals

Animals (WKY and SHRSP rats) were housed under controlled lighting (from 0700 to 1900 hours) and temperature ($21 \pm 3^\circ\text{C}$) and received a normal diet (rat and mouse No.1 maintenance diet, Special Diet Services, Grangemouth, UK) provided *ad libitum*. All animal procedures were approved by the Home Office according to regulations regarding experiments with animals in the United Kingdom (Project License Number 60/4286). Females were time mated at 12 weeks of age (± 4 days). Non-pregnant (NP) animals were age-matched at 15 weeks ± 4 days (i.e. 12 weeks of age + 21 days of pregnancy). Day 0 of pregnancy was defined as the day that a coital plug was observed indicative of successful mating having taken place. A subset of SHRSP began nifedipine treatment at 7 weeks of age at 25 mg/kg/day administered in two doses: a 10 mg/kg/day dose mixed in a 1mL aliquot of baby food and a 15 mg/kg/day dose in drinking water in order to maintain lowered blood pressure throughout the 24-hour period. Stock solutions of nifedipine in drinking water were prepared in ethanol and diluted to the appropriate concentration with no more than a 0.8% final ethanol concentration. The number of rats and particular gestational day (GD) is given in the relevant figure legend.

5.2.1.1 Metabolic Cage

The metabolic cage allows individual housing of an animal to collect information on water intake and urine output over 24 hours. A fixed amount of water (200 mL) was given and the food was available *ad libitum* over the 24-hour period. Animals were acclimatized for 4 hours, 3 days prior to measurement. For untreated WKY and SHRSP, urine samples were collected from virgin animals that were housed in the metabolic cage 1 day prior to mating then at GD 12 and 18. For nifedipine treated SHRSP, urine

samples were collected at GD 12 and 18. Urine samples were aliquoted on the ice and stored at -80 °C until use.

5.2.2 Urinary biochemistry

Urinary electrolytes (Cl^- , Na^+ and K^+), albumin, creatinine and urea were measured using commercially available kits (Roche Diagnostics, West Sussex, UK) and analysed using a Roche Cobas® C311 Analyser (Roche Diagnostics, West Sussex, UK).

5.2.3 Histology

Tissues were fixed for 24 hours in 10% formalin at room temperature. After 24 hours, tissues were rinsed and formalin replaced with PBS. Tissues were then placed in histology cassettes (Thermo Fisher, Paisley, UK) and placed in a Citadel 1000 processor (Fisher Scientific, Loughborough, UK) at the following settings: 70% ethanol 30 minutes, 95% ethanol 30 minutes, 100% ethanol 30 minutes, 100% ethanol 30 minutes, 100% ethanol 45 minutes, 100% ethanol 45 minutes, 100% ethanol 60 minutes, 100% ethanol/xylene 30 minutes, xylene 30 minutes, xylene 30 minutes, wax 30 minutes, wax 30 minutes, wax 45 minutes, wax 45 minutes. The total running time was 8 hours and 30 minutes. Tissues were embedded using Shandon Histocentre 3 embedding centre (Fisher Scientific, Loughborough, UK) and Histoplast paraffin (Thermo Fisher, Paisley, UK). Kidneys were cut transversely through the ureter and the cut side was placed face down. Paraffin sections of 2 μm were cut using a Leica Finest 325 Microtome (Fisher Scientific, Loughborough, UK) and baked on to silanised slides at 60 °C overnight. Slides were then stored at room temperature until use. Paraffin blocks were stored at 4 °C. Immediately prior to staining, slides were deparaffinised in histoclear 2 x 7 minutes then rehydrated through an ethanol gradient (100%, 90% and 75%; 5 minutes each) into distilled H₂O for 5 minutes.

5.2.3.1 Periodic acid-Schiff Stain

Sections of 2 μm were used for periodic acid – Schiff stain to stain the basement membrane of the kidney for morphological scoring. Slides were cleared and rehydrated as described in section 2.6.1. Slides were incubated in 0.5% periodic acid (Sigma-Aldrich, Dorset, UK) in dH₂O for 15 minutes to oxidise aldehyde groups followed by

3 changes of dH₂O. Slides were then stained with Schiff's reagent (Sigma-Aldrich, Dorset, UK) for 15 minutes which reacts with the oxidised aldehyde groups to form a magenta dye followed by a wash in warm running tap water for 1 minute and two changes of dH₂O. Sections were counter-stained using Gill's haematoxylin (Sigma-Aldrich, Dorset, UK). This was followed by a 1 minute wash under running tap water and dehydration through an ethanol gradient (95%, 2 x 100%; 5 minutes each). Slides were cleared in histoclear 2 x 5 minutes and mounted using DPX (Sigma-Aldrich, Dorset, UK).

5.2.3.2 Histological analysis of the kidneys

Slides were visualised using an Aperio Slide Scanner (Leica Biosystems, Milton Keynes, UK) at 20x magnification by Clare Orange at the Queen Elizabeth University Hospital pathology unit. Images were downloaded from Leica Digital Image Hub then analysed using Image J by two independent operators who were blinded to the identity of the sections. Measurement of the cortex and medulla area was carried out by drawing around the relevant area and calculating the number of pixels. Glomerular density was counted as the number of glomeruli/ 10x field of view in 25 fields of view/section. Glomerular diameter was measured using 4 lines/glomerulus in 25 glomeruli/section. Glomerular lobule count was conducted manually in 25 glomeruli/section.

5.2.4 Urinary peptidomics

700 μ L of urine was diluted with 700 μ L of 2 M urea and 0.1 M NH₄OH containing 0.02% SDS. A size cut-off for peptides <20 kDa was carried out using Centriscart ultracentrifugation filter devices (Sartorius, Göttingen, Germany) at 3000 x g for 1 hour at 4 °C. To remove urea, electrolytes, and salts the filtrate was then ran through a PD-10 desalting column (Amersham Bioscience, Buckinghamshire, UK) and peptide elution was done using 0.01% aqueous NH₄OH. Finally, all samples were lyophilized, stored at 4°C, and suspended in high-performance liquid chromatography grade H₂O to a final concentration of 2 μ g/ μ L before analysis.

CE-TOF-MS analysis was performed using a P/ACE MDQ CE system (Beckman Coulter, Fullerton, USA) online coupled to a microTOF MS (Bruker Daltonic, Bremen, Germany) as described in (274). Samples were injected with 2 psi for 99 seconds (250 nl) and separation of peptides in the cartridge maintained at 25 °C was attained at 25 kV for 30 minutes and increasing pressure (0.5 psi) for another 35 minutes. The sheath liquid consisted of 30% isopropanol, 0.4% formic acid in HPLC grade water, and running buffer consisted of 79:20:1 (v/v) water, acetonitrile and formic acid. The ESI sprayer (Agilent Technologies, California, USA) was grounded and the ion spray inference potential was set at -4.5 kV. Spectra were accumulated over a mass-to-charge ratio of 350-3000 for every 3 seconds.

Peak picking, deconvolution and deisotoping of mass spectral ion peaks were processed using Mosaiques Visu software (275). The CE-migration time, molecular weight and ion signal intensity were normalized based on the reference signal from internal peptide standards/calibrants (peptides from housekeeping proteins) in rats (276). For calibration, a local and linear regression algorithm was applied with calibrants. The peak list generated for each peptide consisted of molecular weight (kDa), normalized CE migration time (minutes) and normalized signal intensity. The peptide list from all the samples that passed the quality control criteria was compared and annotated in a Microsoft SQL database. The criteria for clustering peptides in different samples were: (i) molecular weight deviation less than ± 50 ppm for small peptide (<800 Da) and gradually increasing to ± 75 ppm for larger peptides (20 kDa) (ii) CE-migration time deviation with linear increase from ± 0.4 to ± 2.5 min in the range from 19-50 minutes. Each peptide was given a unique identification number (Peptide ID). Peptides detected with the frequency of $\geq 70\%$ in at least one group were considered for further analysis.

5.2.5 Liquid chromatography- tandem mass spectrometry (LC-MS/MS) for peptide sequencing

The peptide mixtures extracted for CE-MS were also used for sequencing of the peptides in LC-MS/MS and CE-MS/MS. LC-MS/MS sequencing was performed on an UltiMate 3000 nano-flow system (Dionex/LC Packings, USA) connected to an LTQ Orbitrap hybrid mass spectrometer (Thermo Fisher Scientific, Germany) equipped with a nano-electrospray ion source. After loading (5 μ L) onto a Dionex 0.1 \times 20 mm 5 μ m

C18 nano trap column at a flowrate of 5 $\mu\text{L}/\text{min}$ in 98% water, 0.1% formic acid and 2% acetonitrile, sample was eluted onto an Acclaim PepMap C18 nano column 75 $\mu\text{m} \times 50 \text{ cm}$, 2 μm 100 \AA at a flow rate of 0.3 $\mu\text{L}/\text{min}$. The trap and nano flow column were maintained at 35 $^{\circ}\text{C}$. The samples were eluted with a gradient of solvent A: 98% water, 0.1% formic acid, 2% acetonitrile versus solvent B: 80% acetonitrile, 20% water, 0.1% formic acid starting at 1% B for 5 minutes rising to 20% B after 90 minutes and finally to 40% B after 120 minutes. The column was then washed and re-equilibrated prior to the next injection. Alternatively, samples were injected and separated using a P/ACE MDQ capillary electrophoresis system (Beckman Coulter, Fullerton, USA) as described above for CE-MS.

The eluent from the LC or CE were ionized using a Proxeon nano spray ESI source operating in positive ion mode into an Orbitrap Velos FTMS (Thermo Finnigan, Bremen, Germany). Ionization voltage was 2.6 kV and the capillary temperature was 250 $^{\circ}\text{C}$. The mass spectrometer was operated in MS/MS mode scanning from 380 to 1600 amu. In LC the top 20 multiply charged ions were selected from each scan for MS/MS analysis using HCD at 40% collision energy. The resolution of ions in MS1 was 60,000 and 7,500 for HCD MS2. In CE the top 5 multiply charged ions were selected for MS/MS using a data dependent decision tree method (255) and fragmented by either HCD at 40% or ETD, depending on their mass and charge state.

MS and MS/MS data files were searched, in this case, against the Uniprot rat non-redundant database using SEQUEST (Thermo Proteome Discoverer) with the non-specific enzyme as enzyme specificity. Peptide data were extracted using high peptide confidence and top one peptide rank filters. A peptide mass tolerance of $\pm 10 \text{ ppm}$ and a fragment mass tolerance of $\pm 0.05 \text{ Da}$.

5.2.6 Quantitative PCR for uromodulin expression

Gene expression assay for uromodulin (*Umod*) in kidney tissues was carried out using the following probes from Thermo Fisher, Paisley, UK: *Umod* (Rn01507237_m1) and *Actb* (4352340E). Ct values were analyzed using the $2^{(-\Delta\Delta\text{Ct})}$ method, with ΔCt indicating normalization to the housekeeper β -actin (*Actb*).

5.2.7 Western blot for Umod

Multi-strip blotting was performed as previously described (175). Primary and secondary antibodies were used as per manufacturer's instructions. Primary antibody: Umod: (AF5175, R&D systems, Abingdon, UK) followed by secondary antibody: anti-sheep HRP conjugate (HAF016, R&D systems, Abingdon, UK).

5.2.8 N-deglycosylation of Umod

Umod was N-deglycosylated by PNGase F (New England Biolabs, Beverly, MA) under reducing conditions. 2 µg of Umod was denatured with buffer provided by the manufacture then incubated with PNGase F at 37°C for 1 hour. Protein samples were separated on reducing 4-12% NuPAGE gel and later blotted onto PVDF membrane for Umod detection.

5.2.9 Purification of Umod and polymerization assay

Urine samples from untreated WKY (n=7), SHRSP (n=7) and nifedipine treated SHRSP (n=3) at pre-pregnancy, gestational day (GD) 12 and GD 18 were pooled separately. For purification, 500 µL of urine was filtered using a 3000 Da molecular weight cut-off column (Millipore). Polymerization assay was performed as previously described by Jovine et al.(277). Pellet and supernatant were solubilized in SDS-gel loading buffer and separated on a reducing 10% NuPAGE gel and blotted onto PVDF membrane for Umod detection.

5.2.10 Protease prediction

In order to find the protease that cleaved Umod protein *in vivo*, Proteasix software was used to perform *in silico* protease mapping as described in (278).

5.2.11 Statistical analysis

In urinary peptidomics, peptides were considered significant according to Wilcoxon rank-sum test ($p < 0.05$) followed by adjustment for multiple testing (Benjamini and Hochberg). Later repeated measure ANOVA was used to evaluate significant peptides within different gestational days. Western blot analysis was performed in LICOR Image Studio software and band intensities were made consistent with local background subtraction. Further, either t-test or one-way or two-way ANOVA test were used for statistical significance ($p < 0.05$).

5.3 Results and Discussion

5.3.1 The SHRSP exhibits altered water and electrolyte balance during pregnancy

Water intake and urine output were monitored in WKY and SHRSP over 24-hours using a metabolic cage at three time points: pre-pregnancy (NP), GD12 and GD18 (Figure 5.1A-B). There was a trend for urine output to increase during pregnancy in both strains (Figure 5.1B). Water intake and urine output were significantly less in the SHRSP relative to the WKY at GD18 only (Figure 5.1A-B). Urinary electrolytes (Na^+ , Cl^- , K^+) were reduced in SHRSP relative to WKY in a pregnancy-dependent manner (Figure 5.1C-E).

5.3.2 The SHRSP exhibits increased urinary protein and metabolite excretion during pregnancy

There was no significant difference in urinary albumin between WKY and SHRSP pre-pregnancy however there was a trend for increased albumin in SHRSP at GD12 and 18 (Figure 5.2A). Urinary creatinine measurement was also increased in a pregnancy-dependent manner in SHRSP at GD18 (Figure 5.2B). Urea was found to be increased at GD12 and 18 in SHRSP relative to WKY (Figure 5.2C).

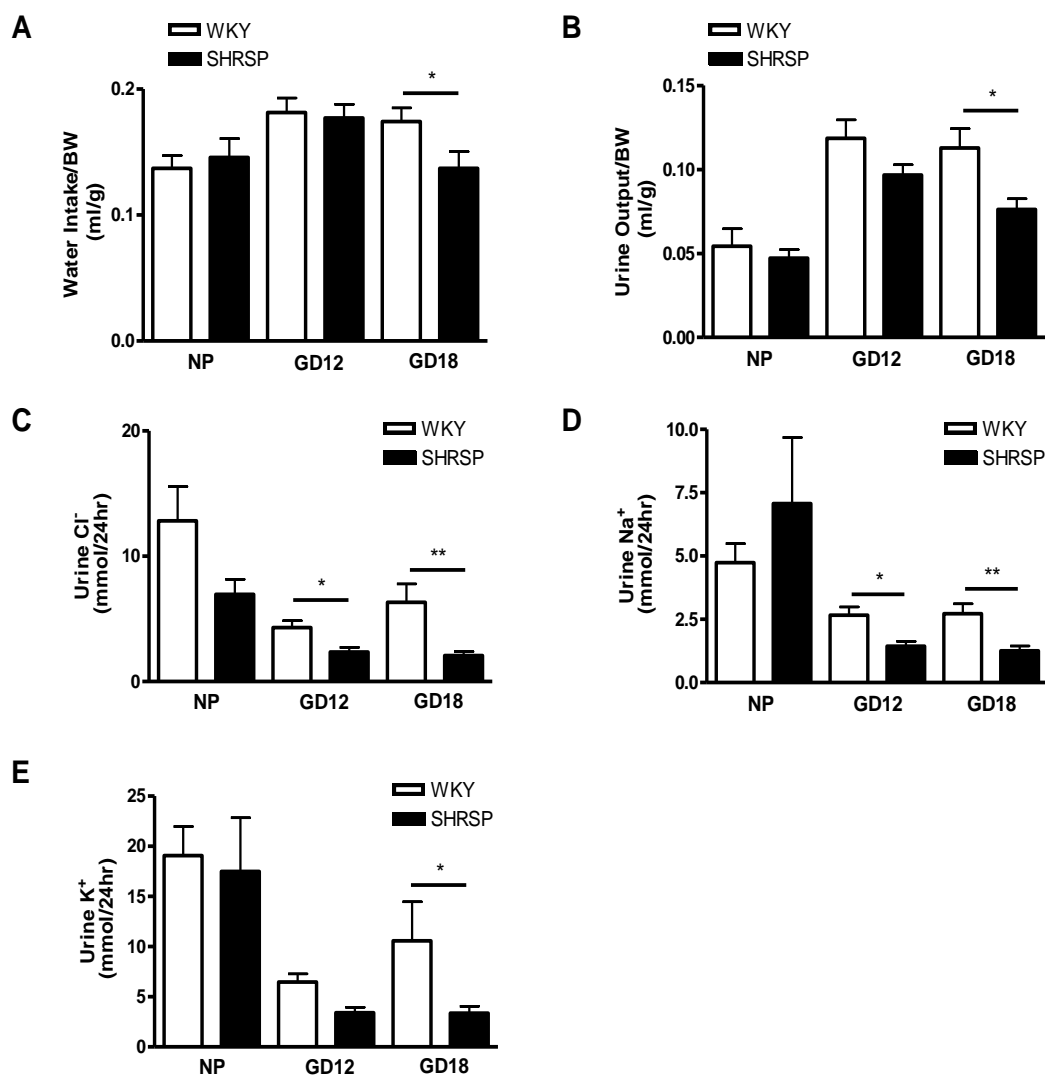


Figure 5.1 Pregnant SHRSP exhibit altered water and electrolyte balance

Water intake and urine output were measured over 24 hours using a metabolic cage in WKY and SHRSP then normalised to bodyweight (n=8). Water intake and urine output were significantly reduced in SHRSP relative to WKY at GD18 (A-B) (* $p < 0.05$ vs. GD18 WKY analysed by student's t test). Electrolytes were measured in urine samples using a Roche Cobas® C311 Analyser and normalised to total urine volume over 24 hours. Pregnant SHRSP showed a significant decrease in chloride (Cl⁻) (C), sodium (Na⁺) (D) and potassium (K⁺) (E) (* $p < 0.05$ ** $p < 0.01$ vs. WKY analysed by student's t-test).

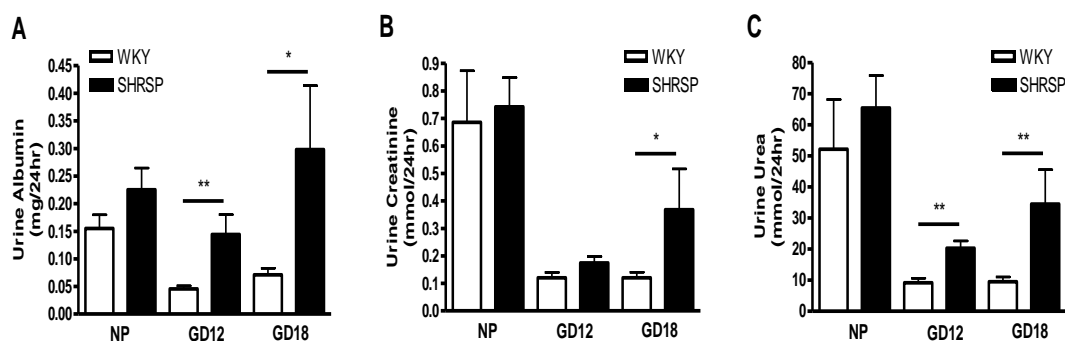


Figure 5.2 Pregnant SHRSP have altered urinary albumin and metabolite levels Urinary albumin (A), creatinine (B) and urea (C) were measured in urine samples using a Roche Cobas® C311 Analyser and normalised to total urine volume over 24 hours from pre-pregnancy, GD12 and GD18 SHRSP and WKY (n=8). Albumin, creatinine and urea were increased in a pregnancy dependent manner in SHRSP relative to WKY (* $p < 0.05$, ** $p < 0.01$ vs. WKY analysed by one way ANOVA followed by post-hoc Tukey test).

5.3.3 The SHRSP Kidney is increased in Size Relative to the WKY but does not Exhibit Histological Abnormalities

Post-mortem kidney weight was increased in both NP and GD18 SHRSP relative to WKY (Figure 5.3A). PAS staining was then used to examine the kidneys histologically (Figure 5.3B). There was a trend towards an increase in the size of the medulla region in NP SHRSP relative to NP WKY ($p = 0.059$); however there was no significant strain difference between pregnant animals (Figure 5.3C). In contrast, cortex size was significantly increased in pregnant SHRSP relative to pregnant WKY but with no difference in NP animals (Figure 5.3D).

Further histological analysis was implemented to examine the glomeruli and for evidence of hypertension-associated pathology. Firstly, the anatomical distribution and structure of the glomeruli was analysed (Figure 5.4A). Glomerular density in the cortex was increased in the SHRSP relative to WKY at both NP and GD18 time points (Figure 5.4B). The number of glomerular lobules was decreased from NP to GD18 WKY but was not significantly different between NP and GD18 SHRSP or between strains (Figure 5.4C). There were no significant strain-dependent or pregnancy-dependent differences in glomerular diameter (Figure 5.4D).

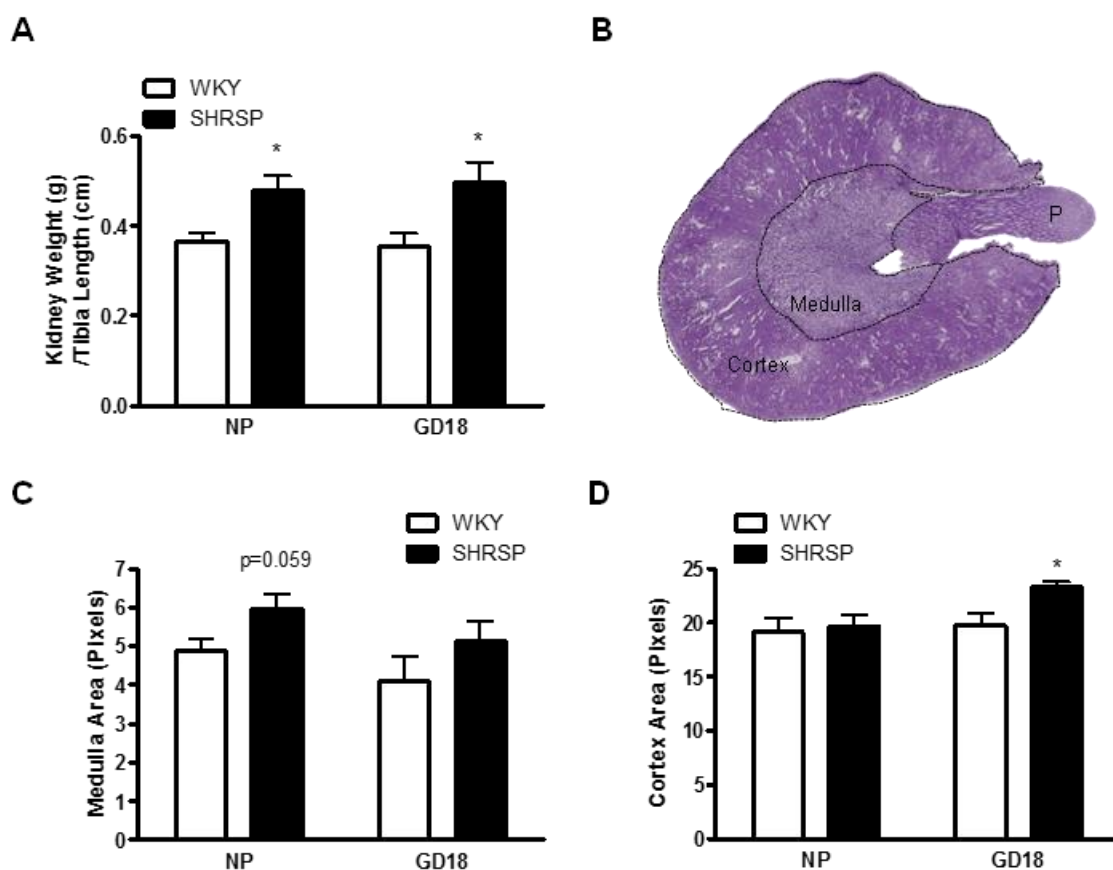


Figure 5.3 Kidney size is increased in non-pregnant and pregnant (GD18) SHRSP relative to WKY

Post-mortem kidney weight was found to be increased in both non-pregnant (NP) and pregnant (GD18) SHRSP relative to WKY (* $p < 0.05$ vs. WKY analysed by student's t test) (A). Kidneys were then analysed histologically using periodic acid-Schiff stain (representative image B) in NP and GD18 WKY and SHRSP ($n = 4-6$). Medulla area showed a trend to be increased in NP SHRSP ($p = 0.059$ analysed by student's t test) but not in pregnant animals (C). Cortex area did not show strain-dependent differences in NP animals but was increased in GD18 SHRSP relative to WKY (* $p < 0.05$ vs. GD18 WKY analysed by student's t-test). P: papilla.

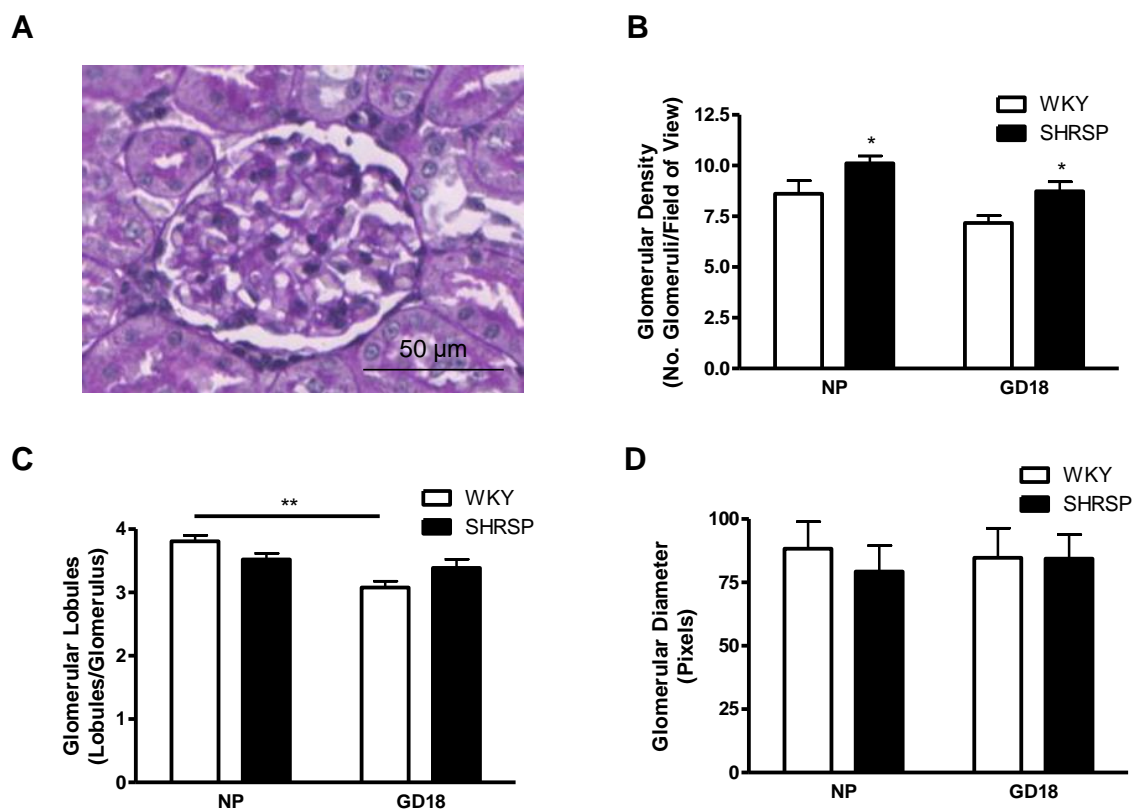


Figure 5.4 Glomeruli distribution is altered in non-pregnant and pregnant (GD18) SHRSP relative to WKY

The distribution and anatomical structure of the glomeruli (A) was quantified in kidney sections from non-pregnant (NP) and GD18 WKY and SHRSP ($n=4-6$). Glomerular density was increased in a strain dependent manner in the SHRSP and was not affected by pregnancy (* $p<0.05$ vs. WKY analysed by student's t-test) (B). Glomerular lobules were decreased from NP to GD18 WKY (** $p<0.01$ vs. GD18 WKY analysed by student's t-test) but this change was not significant in the SHRSP (C). There were no strain-dependent or pregnancy-dependent changes in glomerular diameter (D).

Detailed inspection of the slides was performed to examine pathologies associated with systemic hypertension and hypertensive pregnancy: namely capillary occlusion, protein resorption droplets and vasculopathy. There were no major pathologies detectable in the kidney sections in a strain-dependent or pregnancy-dependent manner (Figure 5.5A-B). There was a trend for the diameter of the vessels supplying the kidney to be increased between NP and pregnant animals in both strains but this could not be formally quantified as these samples were not collected by perfusion-fixation (Figure 5.5B).

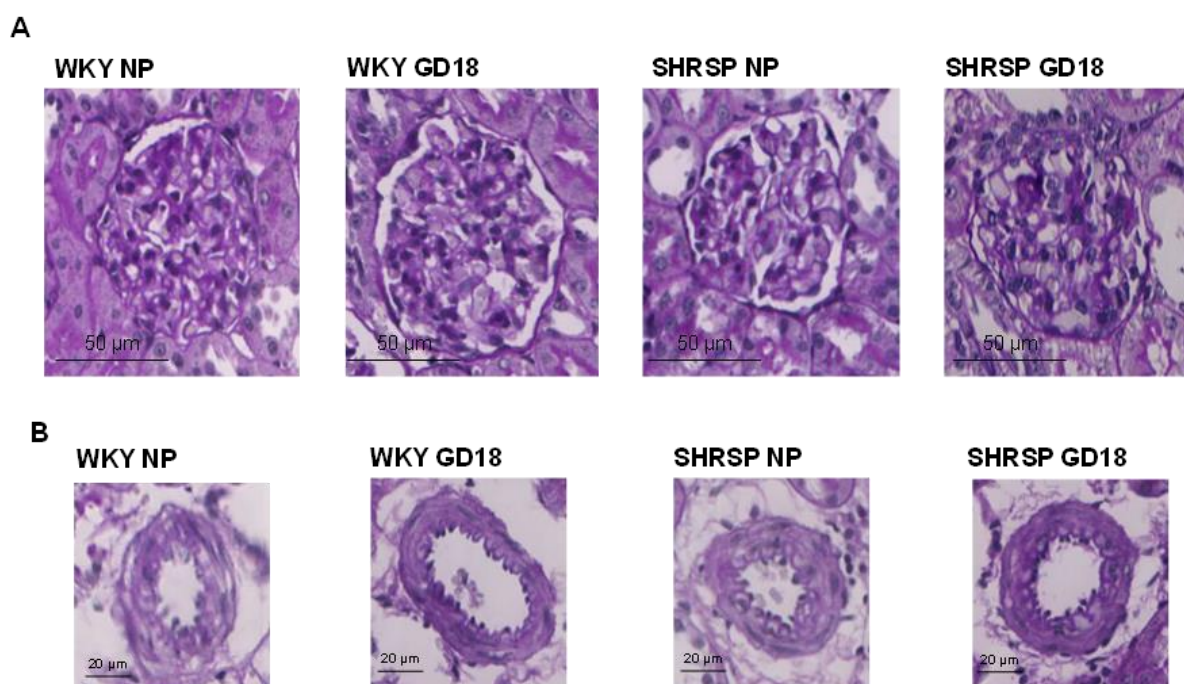


Figure 5.5 The SHRSP does not show histological abnormalities in the glomeruli or vessels of the kidney

Kidney sections from non-pregnant (NP) and GD18 WKY and SHRSP were stained with periodic acid-Schiff stain and inspected for pathology (n=4-6). No notable changes in glomerular structure were detected in a strain or pregnancy dependent manner (A). There was no evidence of vasculopathy; however there was a trend for vessel size to increase during pregnancy in both strains (C).

The initial urine characterisation between WKY and SHRSP showed kidney dysfunction. Urine output is increased in a pregnancy-dependent manner in the WKY. However, in the SHRSP urine output is significantly reduced relative to WKY at GD18. As there was no structural pathology detected in the SHRSP kidney by histology, this reduction in urine output is most likely explained by the reduction in water intake, altered thirst axis or micturition and/or pre-structural alterations in kidney function.

SHRSP showed a pregnancy-dependent increase in urinary creatinine in comparison to pregnant WKY suggesting a reduction in the effectiveness of the glomerular barrier during pregnancy. In order to investigate this change in glomerular function further, a histological analysis was carried out to interrogate kidney structure. The SHRSP kidney weight was increased relative to the WKY in both non-pregnant and pregnant animals suggesting this was a strain-dependent difference; this has also been documented in this model previously (279). It was perhaps not unexpected that there was no detectable glomerular damage by histological evaluation as it has been shown previously that male SHRSP do not develop kidney pathology until 1 year of age or this can be accelerated with salt treatment (280).

5.3.4 The urinary peptidome is altered during pregnancy and between WKY and SHRSP

A peptidome screen was carried out in WKY and SHRSP urine at pre-pregnancy, GD 12 and GD 18 to identify strain, pregnancy and disease-dependent alterations (Figure 5.6). The peptidomic data was subject to a number of comparisons between WKY and SHRSP at different gestational days, such as (i) comparison within rat models at all time points and (ii) comparison between WKY and SHRSP at a given gestational day. The longitudinal comparison (i) within the WKY and SHRSP resulted in the identification of 630 and 739 significant differentially regulated peptides respectively. These were considered to be strain- and pregnancy-dependent alterations. While the comparison between WKY and SHSRP (ii) resulted in 788 significant peptides which were considered to be hypertension-dependent alterations. These disease-specific peptide markers were further evaluated using repeated measures ANOVA. Some peptides were significantly altered at all time points, or at any two or at a single gestational day. The peptides which showed significance at all time points and/or at both GD 12 and GD 18 were considered for further analysis. These 123 peptides were investigated for their regulation pattern with cut-off criteria of ≥ 1.5 fold change and $p \leq 0.05$ (Appendix 2). Compared to WKY, urine from SHRSP consisted of 7 and 39 peptides up- and down-regulated respectively at pre-pregnancy, GD 12 and GD 18. Additionally, 36 peptides were up-regulated and 41 peptides were down-regulated in SHRSP at both GD 12 and GD 18. Sequencing of these differentially expressed

peptides revealed that they belonged to collagen alpha-chains, albumin, pro-thrombin, actin, serpin A3K, pro-epidermal growth factor and Umod (Appendix 3).

In comparison, in urinary peptidomic screens of women with pre-eclampsia the most common constituents are: albumin and tubular proteins which are thought to reflect renal tubule damage(281). However, a characteristic and specific signature for human pre-eclampsia are yet to be determined despite a number of studies (281). The non-biased peptidome screening of urine collected pre-pregnancy, gestational day (GD) 12 and 18 led to the identification of Umod peptides which were increased in a pregnancy-dependent manner in SHRSP relative to WKY.

5.3.5 Umod expression is increased in the urine and kidney of SHRSP during pregnancy

Umod has been extensively studied in association with cardiovascular conditions in humans. Genome-wide association studies (GWAS) have identified *UMOD* variants associated with renal function and hypertension (282). However, the role of Umod in hypertensive pregnancy has not yet been subject to detailed study. All seven of the urinary Umod peptides detected in the present screen were increased in a pregnancy-dependent manner in the SHRSP relative to the WKY. The CE-MS data indicated that Umod peptide expression was greater in SHRSP urine samples relative to WKY with a fold change of 4 ($p<0.05$) and 8 ($p<0.01$) at GD 12 and GD 18 respectively (Figure 5.7). These data were validated in individual urine samples from WKY and SHRSP at pre-pregnancy, GD 12 and GD 18 with western blot where urine from SHRSP showed an increase in Umod protein expression at GD 12 and GD 18 with a fold change of 2.3 ($p<0.05$) (Figure 5.8A).

Gene expression of *Umod* was measured in kidney tissue taken from non-pregnant and GD 18 WKY and SHRSP. *Umod* gene expression was greater in kidney tissue from SHRSP both in non-pregnant and GD 18 samples but the difference only reached statistical significance at GD 18 ($p<0.001$) (Figure 5.8B). This finding was validated at the protein level which showed greater levels of Umod in kidney tissue from GD 18 SHRSP (Figure 5.8C).

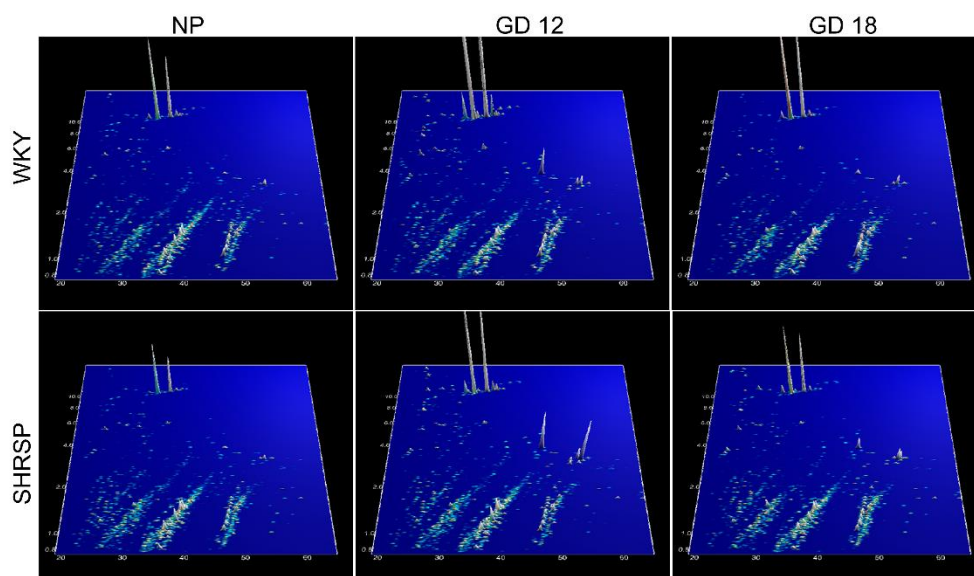


Figure 5.6 Schematic flowchart representing peptidomics data analysis and identification of peptide markers

The counter plot at the top represents the peptide mass fingerprint pattern of WKY (n=7) and SHRSP (n=7) at pre-pregnancy (NP) and gestational day (GD) 12 and 18 observed in CE-MS. On the plot, X-axis represents the CE-migration time, Y-axis mass-to-charge ratio and Z-axis the peptide intensity. Various comparisons were made between strains and gestational days. The numbers above the arrow represents number of peptide identified during the comparison with $p < 0.05$. The strain- and pregnancy-specific peptide markers were not used to for analysis. The disease-specific peptide markers were analysed for pattern of significance i.e at $p < 0.05$ whether the peptide was significant at a given gestational day. Star marked pattern of significance represents peptides that were significant at all GD or GD12-18, and were further used for analysis.

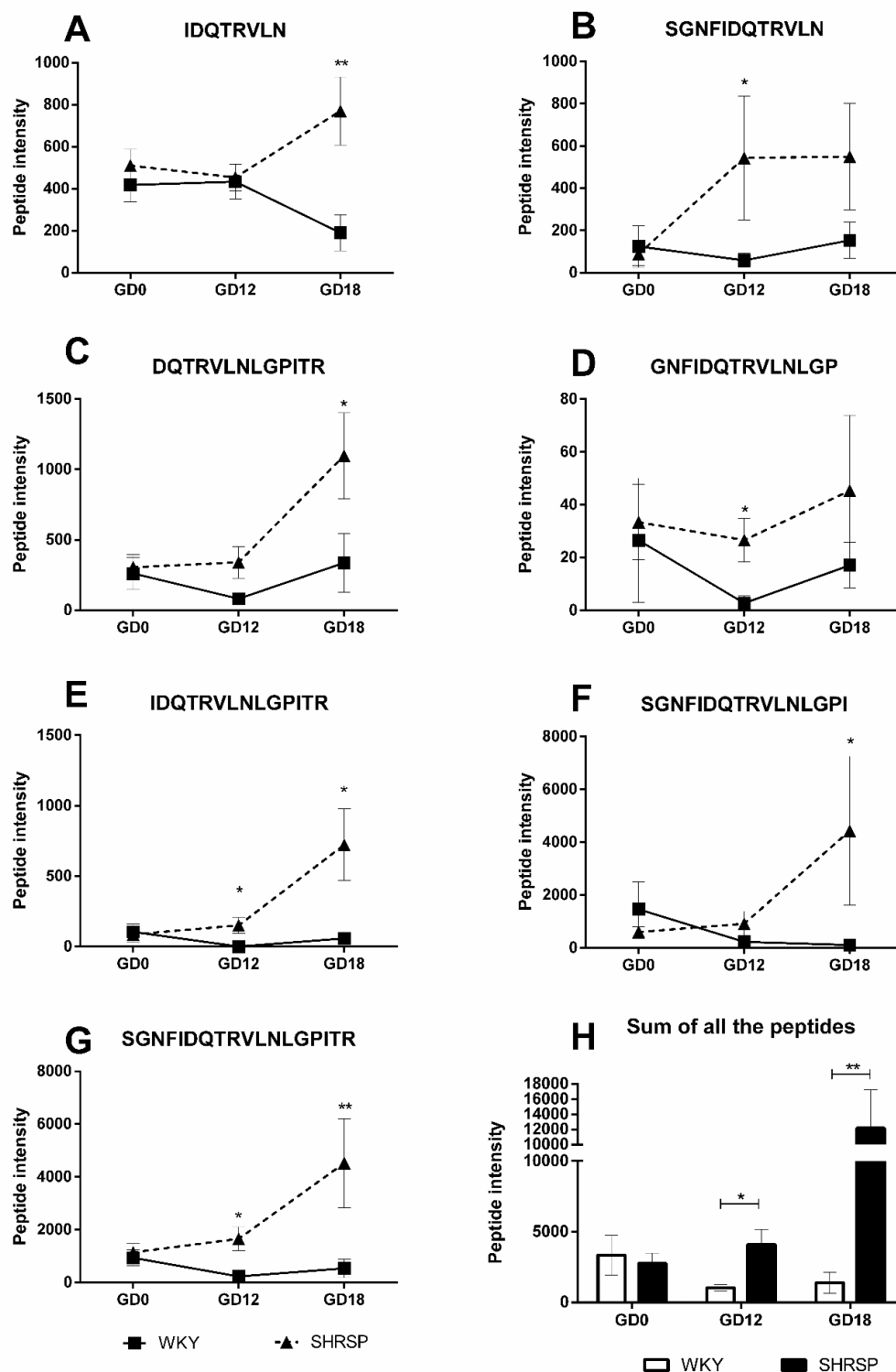


Figure 5.7 Urinary uromodulin peptides are increased in the SHRSP relative to WKY in a pregnancy-dependent manner

Seven peptides detected in the urinary peptidome were derived from uromodulin protein (A-G). Of these peptides, they were all increased in a pregnancy-specific manner in SHRSP (n=7) relative to WKY (n=7) at GD12, GD18 or GD12 and 18. Taking into account the sum of all of the seven peptides (H) showed that uromodulin peptides were increased in a pregnancy-specific manner at GD12 and GD18 in SHRSP relative to WKY (* $p < 0.05$, ** $p < 0.01$ vs. WKY analysed by Wilcoxon-rank test).

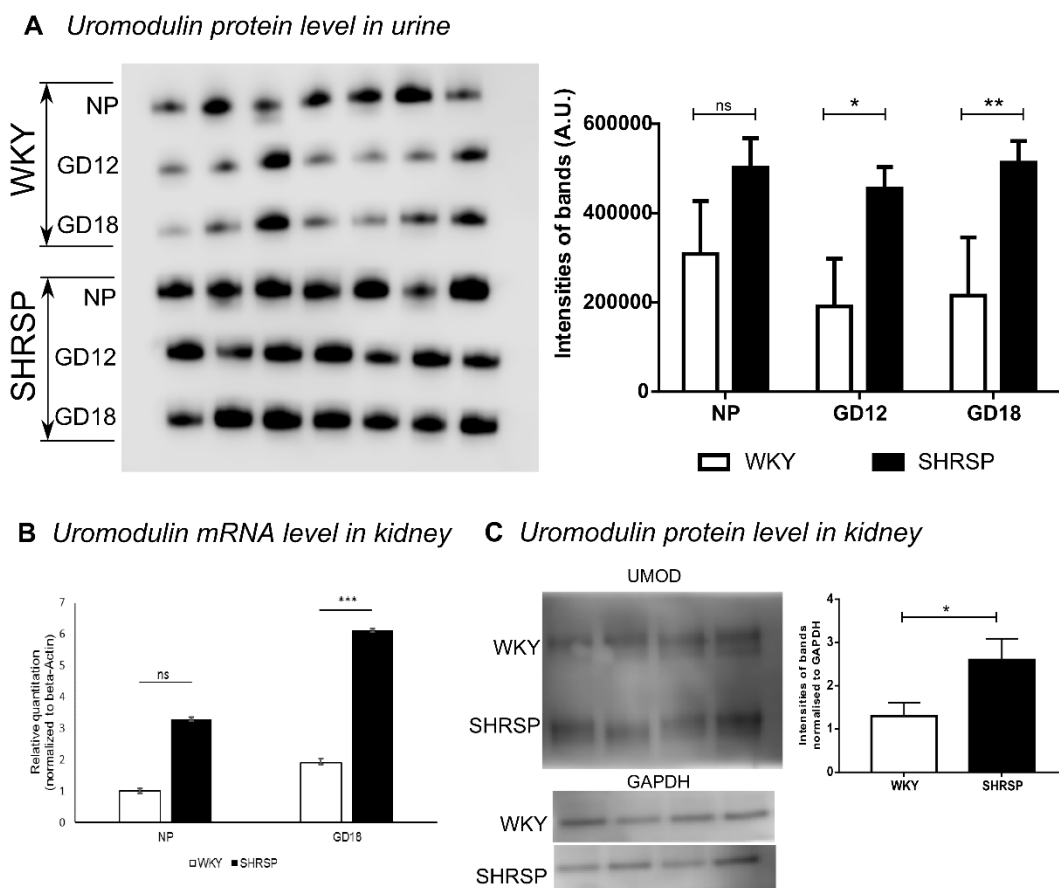


Figure 5.8 Increase in uromodulin in SHRSP validated in urine and kidney tissue (A) Purified UMOD from urine of WKY (n=7) and SHRSP (n=7) was run on 10% NuPAGE gel and blotted onto a single PVDF membrane. UMOD showed increase in SHRSP in pregnancy-dependent manner at GD12 and GD18. (B) Gene expression of *Umod* was measured in kidney tissue from non-pregnant and pregnant (GD18) WKY and SHRSP (n=5). *Umod* expression was increased in kidney tissue from SHRSP at both NP and GD18 time points. (C) UMOD protein was measured from kidney tissue extract of pregnant (GD18) SHRSP (n=4) and WKY (n=4). Pregnant SHRSP showed increased UMOD in kidney tissue. (** $p < 0.01$, *** $p < 0.005$ vs. WKY analysed by one-way ANOVA, T-test).

5.3.6 C-terminal Umod peptides found to be more abundant at GD12 and GD18 in SHRSP urine

CE-MS analysis identified seven peptides of Umod present in the urine samples from WKY and SHRSP. Further sequencing of these peptides using LC-MS/MS revealed that they were exclusively derived from the same C-terminal region (592-609) (Figure 5.7, Figure 5.9). This region of Umod remains membrane-bound after the formation of extracellular polymerization-competent Umod and is also known to have an inhibitory role in Umod polymerization. Expression of these peptides was significantly greater at

either GD 12, GD 18 or both in SHRSP relative to WKY. When compared to our group's previous study which examined urinary peptidomics in women with pre-eclampsia, we found the ortholog peptides of Umod up-regulated in pre-eclampsia (115). In another independent study by Kononikhin et al. which examined the urinary peptidome in mild and severe pre-eclampsia, the same sequence of peptides of Umod were identified as early predictors of pre-eclampsia (283) (Figure 5.9). The presence of these peptides in urine suggests that either they are cleaved by certain proteases from the membrane after the formation of extracellular polymerization-competent Umod or from a longer form of Umod which retains this region. We hypothesized that two forms of Umod exist in the urine of the pregnant rat: a shorter polymerization-competent and a longer polymerization-incompetent form.

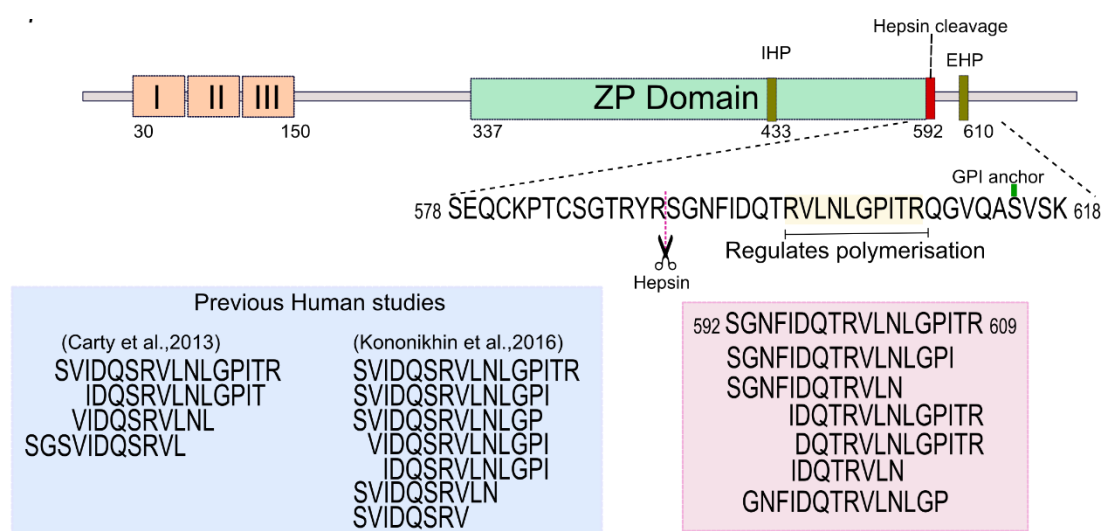


Figure 5.9 Schematic representation of rat UMOD structure

EGF-like domain (orange box I, II, III), the Zona Pellucida (ZP) domain, internal (IHP) and external (EHP) hydrophobic patches, hepsin cleavage site and glycosylphosphatidylinositol (GPI) anchoring site. Zoomed-in sequence represents the C-terminal region identified in mass spectrometry rat data (pink) and previous human studies on pre-eclampsia (blue).

Umod is the most abundant protein in the urine, secreted by the epithelial cells lining the thick ascending limb (TAL) of the loop of Henle in the kidney. The full length Umod in ER gets N-glycosylated and glypiated at its C-terminus, and further modified in Golgi apparatus. The mature Umod with glycosylphosphatidylinositol modification (at S615) is anchored to the apical membrane of TAL facing the tubular lumen. The secreted form of Umod is released by the proteolytic activity of hepsin, a type II transmembrane serine protease (at R591 in rat-evidence by sequence similarity) (284).

Polymerization of secreted Umod helps in formation of a filamentous gel-like structure which acts a physical barrier for ion transport to maintain counter-current gradients in the interstitium (285, 286). Cleavage by hepsin releases the polymerization inhibitory motif (EHP - extracellular hydrophobic patch) that prevents premature intracellular protein assembly (284, 287).

By analyzing peptides of Umod, it is important to understand how these were derived from the full-length protein through the action of various proteases. Proteasix software(278) was used to predict the proteases that might be responsible for cleaving the polymerization-incompetent Umod at the C-terminal. Most of these predicted proteases were classified as either a serine protease or a metalloprotease. Meprin A subunit alpha, a metallopeptidase was predicted with medium confidence, while other proteases such as granzyme A, cathepsin G, matrix metalloprotease (MMP3 and MMP12), plasminogen and neutrophil elastase were predicted with lower confidence (Figure 5.10) (Supplemental data 10).

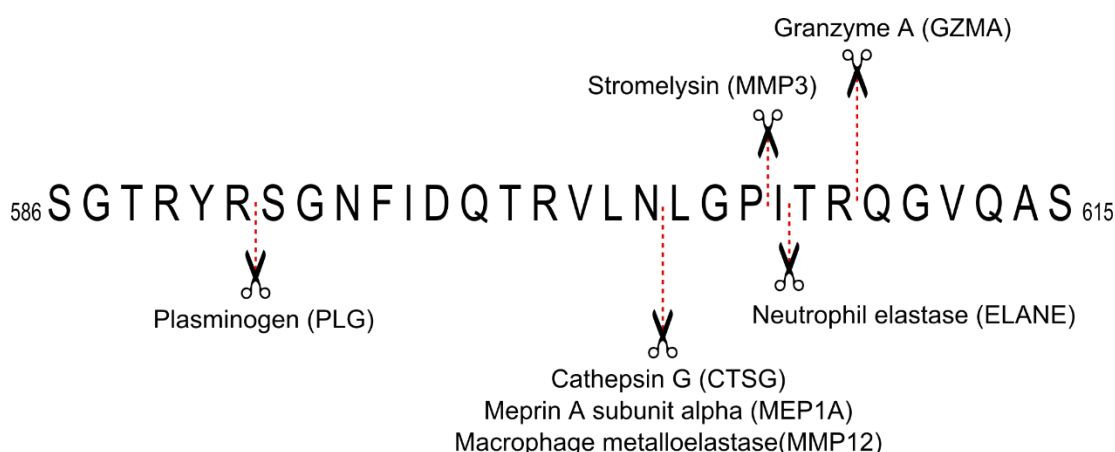


Figure 5.10 Protease prediction

Proteasix software predicted few serine proteases and metalloproteases that might cleave the C-terminal of UMOD, which resulted in the peptides observed in urine.

5.3.7 Polymerization-incompetent Umod is increased in pregnant SHRSP

Urinary peptidomics indicated that the Umod peptide ‘592-SGNFIDQTRVLNLGPITR-609’ and its smaller fragments were released into the urine. This sequence 592-609 consisted of the polymerization inhibitory motif (601-

610); downstream of the hepsin cleavage site (R591) and upstream of GPI anchoring. This led to the question as to whether these peptide fragments were released from the membrane after hepsin cleavage or were these fragments cleaved from a longer form of Umod polypeptide. In order to address this, N-deglycosylation of Umod was performed where two polypeptides were identified.

N-deglycosylation of Umod using PNGase F confirmed the presence of two forms of Umod: a longer polypeptide (~59 kDa) and a shorter polypeptide (~54 kDa) (Figure 5.11A). The presence of the 59 kDa polypeptide of Umod was increased in the urine of SHRSP compared to WKY at all time points (Figure 5.11A). The polymerization assay identified Umod both in the supernatant (polymerization incompetent) and pellet (polymerization-competent) in both strains (Figure 5.11B).

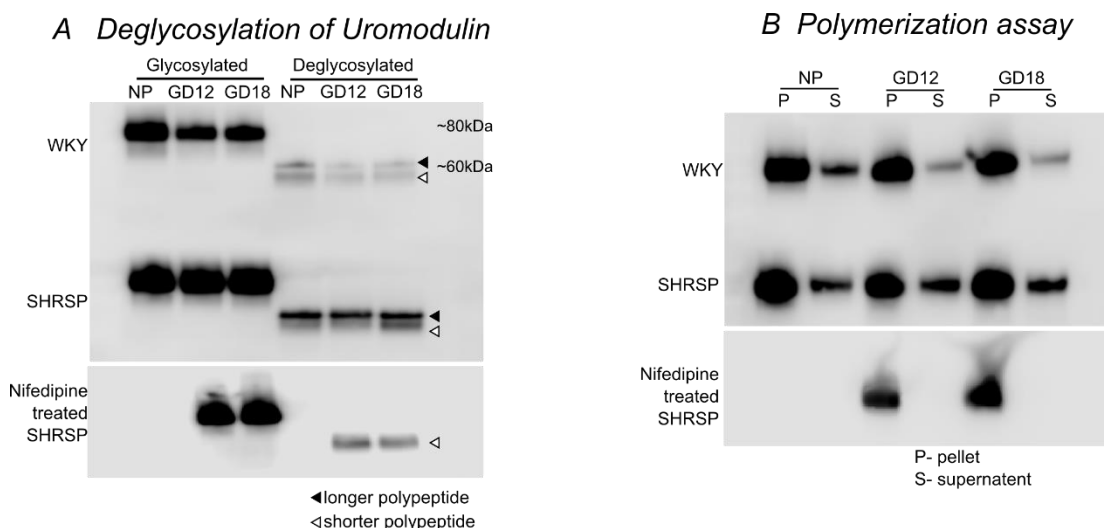


Figure 5.11 Two forms of uromodulin

(A) Deglycosylation of UMOD identified two bands in untreated WKY (pool of n=7) and SHRSP (pool of n=7) at all gestational day, and only single band in nifedipine treated SHRSP (pool of 3) at GD12 and 18. (B) In the polymerisation assay, the pellet fraction (P) represents the polymerization-competent and supernatant (S) the polymerization-incompetent UMOD. Polymerization assay showed polymerization-incompetent UMOD in supernatant (S) of untreated WKY (pool of n=7) and SHRSP (pool of n=7) at all gestational day, while no UMOD bands were observed in nifedipine treated SHRSP (pool of 3). Polymerization-competent UMOD in pellet (P) was observed in untreated WKY and SHRSP, as well as in nifedipine treated SHRSP.

In non-pregnant rats, both polymerisation-competent and polymerisation incompetent Umod were detected in WKY and SHRSP at similar levels (Figure 5.11B). This indicates that the release of longer polypeptide is a common phenomenon in these

strains. However, upon pregnancy, the polymerization-incompetent Umod decreased in a gestation-dependent manner in the WKY. In contrast, the polymerization-incompetent form of Umod increased over pregnancy in the SHRSP (Figure 5.11A-B). This indicates that there is less Umod polymerization in SHRSP. We hypothesize that the longer polypeptides are later cleaved by other as yet unidentified proteases to form the shorter polypeptide, which releases the peptides that were observed in urinary peptidome.

5.3.8 Nifedipine treated pregnant SHRSP showed only polymerization-competent Umod

The correlation between hypertension during pregnancy and release of Umod peptides warrants further investigation. We made an attempt to explore the effect on Umod polymerization when pregnant SHRSP were treated with the antihypertensive drug, nifedipine, from 7 weeks of age. Urine samples from pregnant nifedipine treated SHRSP showed that nifedipine treated rats had only a single band of N-deglycosylated Umod in western blot (Figure 5.11A). In the polymerization assay from these samples, Umod was present only as the polymerization-competent form whereas the polymerization-incompetent form was undetectable at both GD 12 and 18 (Figure 5.11B).

Nifedipine principally acts as a calcium channel blocker and is known to reduce urinary protein excretion rate in patients with renal disease (288) and decrease urinary calcium excretion in women with pre-eclampsia (287). In this study, nifedipine treatment significantly lowered the blood pressure of the pregnant SHRSP (Figure 5.12). The effect of nifedipine indicates two possible mechanisms that drive Umod polymerization. Firstly, the role of calcium in regulating the polymer formation, and secondly, the existence of an indirect unknown mechanism that modulates hypertension and polymer formation. Umod is known to have three EGF-like domains at the N-

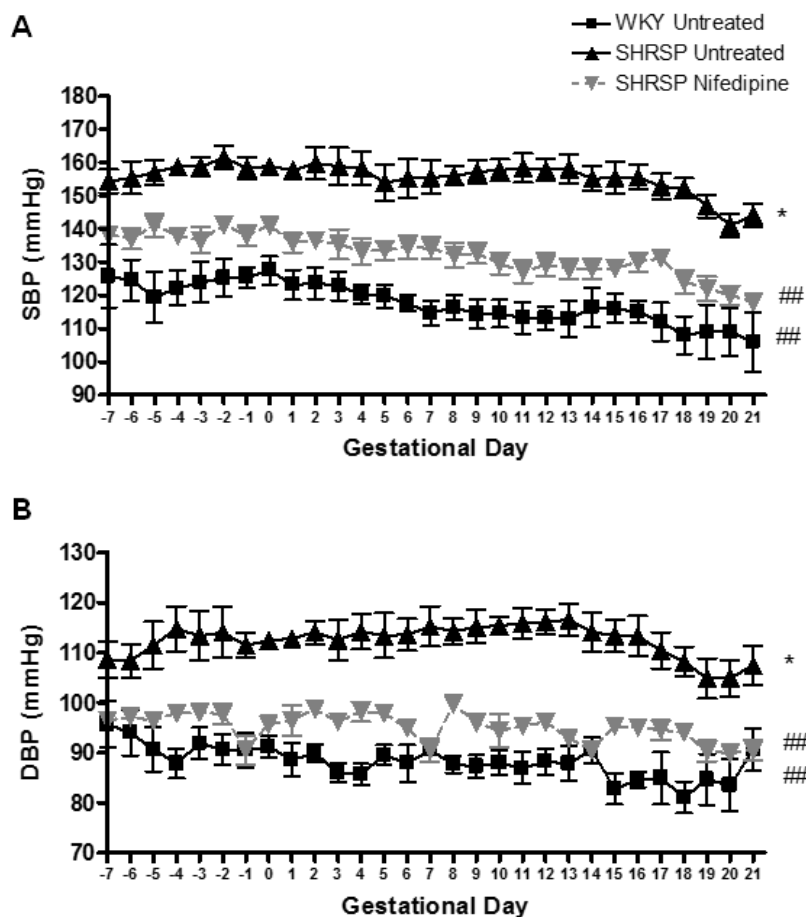


Figure 5.12 Nifedipine significantly inhibits blood pressure elevation in the SHRSP

Systolic (SBP) (A) and diastolic (DBP) (B) blood pressure was monitored in untreated WKY, untreated SHRSP and nifedipine treated SHRSP ($n=6$) using radiotelemetry before day 0 and during pregnancy (gestational day 0 – day 21). SHRSP had significantly increased blood pressure compared to WKY (* $p<0.05$). Nifedipine treatment significantly reduced SHRSP blood pressure (## $p<0.01$ vs. SHRSP). Data analysed by comparing area under the curve values using one way ANOVA and Tukey's *post-hoc* test.

terminus where two of these domains, EGF-like 2 (D67-I108) and EGF-like 3 (D109-E150), are calcium binding domains which have implications in protein-protein interaction. Umod is also known to play a protective role against calcium crystal formation (289). The predicted proteases such as granzyme A, matrix metalloproteinase MMP-3 and 12, metalloendopeptidase, neutrophil elastase, plasmin are all dependent on calcium for their activity, expression or structure (290-294). These proteases were derived from *in silico* analysis in the current study. Future work on determining the expression of each of these proteases and their role in Umod cleavage needs to be undertaken.

List of References

1. Dommissie, J. and Tiltman, A.J., *Placental bed biopsies in placental abruption*. British Journal of Obstetrics and Gynaecology, 1992. 99(8): p. 651.
2. Khong, T.Y., Liddell, H.S., and Robertson, W.B., *Defective haemochorial placentation as a cause of miscarriage: a preliminary study*. British Journal of Obstetrics and Gynaecology, 1987. 94(7): p. 649.
3. Khong, T.Y., De Wolf, F., Robertson, W.B., et al., *Inadequate maternal vascular response to placentation in pregnancies complicated by pre-eclampsia and by small-for-gestational age infants*. British Journal of Obstetrics and Gynaecology, 1986. 93(10): p. 1049.
4. Kim, Y.M., Bujold, E., Chaiworapongsa, T., et al., *Failure of physiologic transformation of the spiral arteries in patients with preterm labor and intact membranes*. American Journal of Obstetrics and Gynecology, 2003. 189(4): p. 1063.
5. Kim, Y.M., Chaiworapongsa, T., Gomez, R., et al., *Failure of physiologic transformation of the spiral arteries in the placental bed in preterm premature rupture of membranes*. American Journal of Obstetrics and Gynecology, 2002. 187(5): p. 1137.
6. Smith, G.C.S., Crossley, J.A., Aitken, D.A., et al., *First-trimester placentation and the risk of antepartum stillbirth*. The Journal of the American Medical Association, 2004. 292(18): p. 2249.
7. Hogberg, U., *The World Health Report 2005: "Make every mother and child count" - Including Africans*. Scandinavian Journal of Public Health, 2005. 33(6): p. 409.
8. Kauma, S., Takacs, P., Scordalakes, C., et al., *Increased endothelial monocyte chemoattractant protein-1 and interleukin-8 in preeclampsia*. Obstetrics and Gynecology, 2002. 100(4): p. 706.
9. *Hypertension in pregnancy. Report of the American College of Obstetricians and Gynecologists' Task Force on Hypertension in Pregnancy*. Obstetrics and Gynecology, 2013. 122(5): p. 1122.
10. Barton, J.R. and Sibai, B.M., *Prediction and prevention of recurrent preeclampsia*. Obstetrics and Gynecology, 2008. 112(2): p. 359.
11. Carr, D.B., Epplein, M., Johnson, C.O., et al., *A sister's risk: Family history as a predictor of preeclampsia*. American Journal of Obstetrics and Gynecology, 2005. 193(3): p. 965.
12. Duckitt, K. and Harrington, D., *Risk factors for pre-eclampsia at antenatal booking: systematic review of controlled studies*. British Medical Journal, 2005. 330(7491): p. 565.
13. Esplin, M.S., *Preterm birth: A review of genetic factors and future directions for genetic study*. Obstetrical and Gynecological Survey, 2006. 61(12): p. 800.
14. Zhang, J. and Patel, G., *Partner change and perinatal outcomes: a systematic review*. Paediatric and Perinatal Epidemiology, 2007. 21: p. 46.
15. Kuklina, E.V., Ayala, C., and Callaghan, W.M., *Hypertensive disorders and severe obstetric morbidity in the United States*. Obstetrics and Gynecology, 2009. 113(6): p. 1299.
16. Organization, W.H., *WHO recommendations for prevention and treatment of pre-eclampsia and eclampsia: summary of recommendations*. 2011.

17. Gilbert, J.S., Ryan, M.J., LaMarca, B.B., et al., *Pathophysiology of hypertension during preeclampsia: linking placental ischemia with endothelial dysfunction*. American Journal of Physiology-Heart and Circulatory Physiology, 2008. 294(2): p. H541.
18. Ilekis, J.V., Reddy, U.M., and Roberts, J.M., *Preeclampsia - A pressing problem: An executive summary of a national institute of child health and human development workshop*. Reproductive Sciences, 2007. 14(6): p. 508.
19. Roberts, J.M., Balk, J.L., Bodnar, L.M., et al., *Nutrient involvement in preeclampsia*. The Journal of Nutrition, 2003. 133(5 Suppl 2): p. 1684S.
20. Brosens, I.A., Robertson, W.B., and Dixon, H.G., *The role of the spiral arteries in the pathogenesis of preeclampsia*. Obstetrics and Gynecology Annual, 1972. 1: p. 177.
21. Zhou, Y., Fisher, S.J., Janatpour, M., et al., *Human cytotrophoblasts adopt a vascular phenotype as they differentiate - A strategy for successful endovascular invasion?* The Journal of Clinical Investigation, 1997. 99(9): p. 2139.
22. Roberts, J.M., *Endothelial dysfunction in preeclampsia*. Seminars in Reproductive Endocrinology, 1998. 16(1): p. 5.
23. Hockel, M. and Vaupel, P., *Biological consequences of tumor hypoxia*. Seminars in Oncology, 2001. 28(2 Suppl 8): p. 36.
24. Wheeler, T., Elcock, C.L., and Anthony, F.W., *Angiogenesis and the placental environment*. Placenta, 1995. 16(3): p. 289.
25. Gerber, H.P., Condorelli, F., Park, J., et al., *Differential transcriptional regulation of the two vascular endothelial growth factor receptor genes. Flt-1, but not Flk-1/KDR, is up-regulated by hypoxia*. The Journal of Biological Chemistry, 1997. 272(38): p. 23659.
26. Shweiki, D., Itin, A., Soffer, D., et al., *Vascular endothelial growth factor induced by hypoxia may mediate hypoxia-initiated angiogenesis*. Nature, 1992. 359(6398): p. 843.
27. Karumanchi, S.A. and Bdolah, Y., *Hypoxia and sFlt-1 in preeclampsia: the "chicken-and-egg" question*. Endocrinology, 2004. 145(11): p. 4835.
28. Burton, G.J., *Oxygen, the Janus gas; its effects on human placental development and function*. Journal of Anatomy, 2009. 215(1): p. 27.
29. Roberts, C.T., *IFPA Award in Placentology Lecture: Complicated interactions between genes and the environment in placentation, pregnancy outcome and long term health*. Placenta, 2010. 31: p. S47.
30. Sargent, I.L., Germain, S.J., Sacks, G.P., et al., *Trophoblast deportation and the maternal inflammatory response in pre-eclampsia*. Journal of Reproductive Immunology, 2003. 59(2): p. 153.
31. Mistry, H.D., Wilson, V., Ramsay, M.M., et al., *Reduced selenium concentrations and glutathione peroxidase activity in preeclamptic pregnancies*. Hypertension, 2008. 52(5): p. 881.
32. Redman, C.W. and Sargent, I.L., *Latest advances in understanding preeclampsia*. Science, 2005. 308(5728): p. 1592.
33. Sikkema, J.M., van Rijn, B.B., Franx, A., et al., *Placental superoxide is increased in pre-eclampsia*. Placenta, 2001. 22(4): p. 304.
34. Walsh, S.W., Vaughan, J.E., Wang, Y., et al., *Placental isoprostane is significantly increased in preeclampsia*. FASEB Journal, 2000. 14(10): p. 1289.

35. Mehendale, S., Kilari, A., Dangat, K., et al., *Fatty acids, antioxidants, and oxidative stress in pre-eclampsia*. International Journal of Gynaecology and Obstetrics, 2008. 100(3): p. 234.
36. Neufeld, G., Cohen, T., Gengrinovitch, S., et al., *Vascular endothelial growth factor (VEGF) and its receptors*. FASEB Journal, 1999. 13(1): p. 9.
37. Sibai, B., Dekker, G., and Kupferminc, M., *Pre-eclampsia*. Lancet, 2005. 365(9461): p. 785.
38. Yancopoulos, G.D., Klagsbrun, M., and Folkman, J., *Vasculogenesis, angiogenesis, and growth factors: ephrins enter the fray at the border*. Cell, 1998. 93(5): p. 661.
39. Maynard, S., Epstein, F.H., and Karumanchi, S.A., *Preeclampsia and angiogenic imbalance*. Annual Review of Medicine, 2008. 59: p. 61.
40. Ahmad, S. and Ahmed, A., *Antiangiogenic effect of soluble vascular endothelial growth factor receptor-1 in placental angiogenesis*. Endothelium : Journal of Endothelial Cell Research, 2005. 12(1-2): p. 89.
41. Schlembach, D., Wallner, W., Sengenberger, R., et al., *Angiogenic growth factor levels in maternal and fetal blood: correlation with Doppler ultrasound parameters in pregnancies complicated by pre-eclampsia and intrauterine growth restriction*. Ultrasound in Obstetrics and Gynecology, 2007. 29(4): p. 407.
42. Rajakumar, A., Powers, R.W., Hubel, C.A., et al., *Novel soluble Flt-1 isoforms in plasma and cultured placental explants from normotensive pregnant and preeclamptic women*. Placenta, 2009. 30(1): p. 25.
43. Muttukrishna, S., Suri, S., Groome, N., et al., *Relationships between TGF beta Proteins and Oxygen Concentrations Inside the First Trimester Human Gestational Sac*. Plos One, 2008. 3(6): p. e2302.
44. Kulkarni, A.V., Mehendale, S.S., Yadav, H.R., et al., *Reduced placental docosahexaenoic acid levels associated with increased levels of sFlt-1 in preeclampsia*. Prostaglandins Leukotrienes and Essential Fatty Acids, 2011. 84(1-2): p. 51.
45. Laskowska, M., Laskowska, K., Leszczynska-Gorzela, B., et al., *Are the maternal and umbilical VEGF-A and SVEGF-R1 altered in pregnancies complicated by preeclampsia with or without intrauterine foetal growth retardation? Preliminary communication*. Medycyna Wieku Rozwojowego, 2008. 12(1): p. 499.
46. Levine, R.J., Lam, C., Qian, C., et al., *Soluble endoglin and other circulating antiangiogenic factors in preeclampsia*. The New England Journal of Medicine, 2006. 355(10): p. 992.
47. Wikstrom, A.-K., Larsson, A., Eriksson, U.J., et al., *Placental growth factor and soluble FMS-like tyrosine kinase-1 in early-onset and late-onset preeclampsia*. Obstetrics and Gynecology, 2007. 109(6): p. 1368.
48. De Vivo, A., Baviera, G., Giordano, D., et al., *Endoglin, PlGF and sFlt-1 as markers for predicting pre-eclampsia*. Acta Obstetrica et Gynecologica Scandinavica, 2008. 87(8): p. 837.
49. Shaarawy, M., Al-Sokkary, F., Sheba, M., et al., *Angiogenin and vascular endothelial growth factor in pregnancies complicated by preeclampsia*. International Journal of Gynaecology and Obstetrics, 2005. 88(2): p. 112.
50. Kulkarni, A.V., Mehendale, S.S., Yadav, H.R., et al., *Circulating angiogenic factors and their association with birth outcomes in preeclampsia*. Hypertension Research, 2010. 33(6): p. 561.

51. Levine, R.J., Maynard, S.E., Qian, C., et al., *Circulating angiogenic factors and the risk of preeclampsia*. The New England Journal of Medicine, 2004. 350(7): p. 672.
52. Robillard, P.Y., Hulsey, T.C., Alexander, G.R., et al., *Paternity patterns and risk of preeclampsia in the last pregnancy in multiparae*. Journal of Reproductive Immunology, 1993. 24(1): p. 1.
53. Salha, O., Sharma, V., Dada, T., et al., *The influence of donated gametes on the incidence of hypertensive disorders of pregnancy*. Human Reproduction, 1999. 14(9): p. 2268.
54. Keelan, J.A. and Mitchell, M.D., *Placental cytokines and preeclampsia*. Frontiers Bioscience, 2007. 12: p. 2706.
55. Kopcow, H.D. and Karumanchi, A., *Angiogenic factors and natural killer (NK) cells in the pathogenesis of preeclampsia*. Journal of Reproductive Immunology, 2007. 76(1-2): p. 23.
56. Moffett, A. and Hiby, S.E., *How Does the maternal immune system contribute to the development of pre-eclampsia?* Placenta, 2007. 28 Suppl A: p. S51.
57. Hiby, S.E., Walker, J.J., O'Shaughnessy, K.M., et al., *Combinations of Maternal KIR and Fetal HLA-C Genes Influence the Risk of Preeclampsia and Reproductive Success*. The Journal of Experimental Medicine, 2004. 200(8): p. 957.
58. Wang, C.C., Yim, K.W., Poon, T.C., et al., *Innate immune response by ficolin binding in apoptotic placenta is associated with the clinical syndrome of preeclampsia*. Clinical Chemistry, 2007. 53(1): p. 42.
59. Wang, Y., Gu, Y., Zhang, Y., et al., *Increased chymotrypsin-like protease (chymase) expression and activity in placentas from women with preeclampsia*. Placenta, 2007. 28(4): p. 263.
60. Quitterer, U., Lothar, H., and Abdalla, S., *AT1 receptor heterodimers and angiotensin II responsiveness in preeclampsia*. Seminars in Nephrology, 2004. 24(2): p. 115.
61. Wallukat, G., Homuth, V., Fischer, T., et al., *Patients with preeclampsia develop agonistic autoantibodies against the angiotensin AT1 receptor*. The Journal of Clinical Investigation, 1999. 103(7): p. 945.
62. Dechend, R., Viedt, C., Muller, D.N., et al., *AT1 receptor agonistic antibodies from preeclamptic patients stimulate NADPH oxidase*. Circulation, 2003. 107(12): p. 1632.
63. Irani, R.A. and Xia, Y., *The functional role of the renin-angiotensin system in pregnancy and preeclampsia*. Placenta, 2008. 29(9): p. 763.
64. Zhou, C.C., Ahmad, S., Mi, T., et al., *Autoantibody from women with preeclampsia induces soluble Fms-like tyrosine kinase-1 production via angiotensin type 1 receptor and calcineurin/nuclear factor of activated T-cells signaling*. Hypertension, 2008. 51(4): p. 1010.
65. Chappell, S. and Morgan, L., *Searching for genetic clues to the causes of pre-eclampsia*. Clinical Science, 2006. 110(4): p. 443.
66. Berends, A.L., Bertoli-Avella, A.M., de Groot, C.J., et al., *STOX1 gene in pre-eclampsia and intrauterine growth restriction*. BJOG: An International Journal of Obstetrics and Gynaecology, 2007. 114(9): p. 1163.
67. van Dijk, M. and Oudejans, C.B., *STOX1: Key player in trophoblast dysfunction underlying early onset preeclampsia with growth retardation*. Journal of Pregnancy, 2011. 2011: p. 521826.

68. Nafee, T.M., Farrell, W.E., Carroll, W.D., et al., *Epigenetic control of fetal gene expression*. BJOG: An International Journal of Obstetrics and Gynaecology, 2008. 115(2): p. 158.
69. Sitras, V., Paulssen, R.H., Gronaas, H., et al., *Differential placental gene expression in severe preeclampsia*. Placenta, 2009. 30(5): p. 424.
70. Sood, R., Zehnder, J.L., Druzin, M.L., et al., *Gene expression patterns in human placenta*. Proceedings of the National Academy of Sciences USA, 2006. 103(14): p. 5478.
71. Waterland, R.A., *Is epigenetics an important link between early life events and adult disease?* Hormone Research, 2009. 71 Suppl 1: p. 13.
72. Chavan-Gautam, P., Sundrani, D., Pisal, H., et al., *Gestation-dependent changes in human placental global DNA methylation levels*. Molecular Reproduction and Development, 2011. 78(3): p. 150.
73. Kulkarni, A., Chavan-Gautam, P., Mehendale, S., et al., *Global DNA methylation patterns in placenta and its association with maternal hypertension in pre-eclampsia*. DNA and cell biology, 2011. 30(2): p. 79.
74. Kulkarni, A., Mehendale, S., Pisal, H., et al., *Association of omega-3 fatty acids and homocysteine concentrations in pre-eclampsia*. Clinical Nutrition, 2011. 30(1): p. 60.
75. Vickery, H.B., *The Origin of the Word Protein*. Yale Journal of Biology and Medicine, 1950. 22(5): p. 387.
76. Sumner, J.B., *The isolation and crystallization of the enzyme urease. Preliminary paper*. The Journal of Biological Chemistry, 1926. 69(2): p. 435.
77. Pauling, L., Corey, R.B., and Branson, H.R., *The structure of proteins; two hydrogen-bonded helical configurations of the polypeptide chain*. Proceedings of the National Academy of Sciences USA, 1951. 37(4): p. 205.
78. Kauzmann, W., *Structural factors in protein denaturation*. Journal of Cell Physiology, 1956. 47(Suppl 1): p. 113.
79. Kauzmann, W., *Some Factors in the Interpretation of Protein Denaturation*. Advances in Protein Chemistry, 1959. 14: p. 1.
80. Sanger, F., *The arrangement of amino acids in proteins*. Advances in Protein Chemistry, 1952. 7: p. 1.
81. Edman, P., *Method for Determination of the Amino Acid Sequence in Peptides*. Acta Chemica Scandinavica, 1950. 4(2): p. 283.
82. Sanger, F., Nicklen, S., and Coulson, A.R., *DNA sequencing with chain-terminating inhibitors*. Proceedings of the National Academy of Sciences USA, 1977. 74(12): p. 5463.
83. Maxam, A.M. and Gilbert, W., *A new method for sequencing DNA*. Proceedings of the National Academy of Sciences USA, 1977. 74(2): p. 560.
84. Beadle, G.W. and Tatum, E.L., *Genetic control of biochemical reactions in neurospora*. Proceedings of the National Academy of Sciences USA, 1941. 27: p. 499.
85. Schmucker, D., Clemens, J.C., Shu, H., et al., *Drosophila Dscam is an axon guidance receptor exhibiting extraordinary molecular diversity*. Cell, 2000. 101(6): p. 671.
86. Wilkins, M.R., Pasquali, C., Appel, R.D., et al., *From proteins to proteomes: Large scale protein identification by two-dimensional electrophoresis and amino acid analysis*. Bio-Technology, 1996. 14(1): p. 61.
87. Pandey, A. and Mann, M., *Proteomics to study genes and genomes*. Nature, 2000. 405(6788): p. 837.

88. Oliver, S.G., Winson, M.K., Kell, D.B., et al., *Systematic functional analysis of the yeast genome*. Trends in Biotechnology, 1998. 16(9): p. 373.
89. Graves, P.R. and Haystead, T.A.J., *Molecular biologist's guide to proteomics*. Microbiology and Molecular Biology Reviews, 2002. 66(1): p. 39.
90. Miyagi, M. and Rao, K.C.S., *Proteolytic 18O-labeling strategies for quantitative proteomics*. Mass Spectrometry Reviews, 2007. 26(1): p. 121.
91. Palmblad, M., Tiss, A., and Cramer, R., *Mass spectrometry in clinical proteomics - from the present to the future*. Proteomics Clinical Applications, 2009. 3(1): p. 6.
92. Alaoui-Jamali, M.A. and Xu, Y.J., *Proteomic technology for biomarker profiling in cancer: an update*. Journal of Zhejiang University. Science. B, 2006. 7(6): p. 411.
93. Andreasen, N., Minthon, L., Davidsson, P., et al., *Evaluation of CSF-tau and CSF-Abeta42 as diagnostic markers for Alzheimer disease in clinical practice*. Archives of Neurology, 2001. 58(3): p. 373.
94. Gerszten, R.E. and Wang, T.J., *The search for new cardiovascular biomarkers*. Nature, 2008. 451(7181): p. 949.
95. Hu, S., Loo, J.A., and Wong, D.T., *Human body fluid proteome analysis*. Proteomics, 2006. 6(23): p. 6326.
96. Nelsestuen, G.L., Harvey, S.B., Zhang, Y., et al., *Top-down proteomic analysis by MALDI-TOF profiling: Concentration-independent biomarkers*. Proteomics Clinical Applications, 2008. 2(2): p. 158.
97. Kolialexi, A., Mavrou, A., and Tsangaris, G.T., *Proteomic analysis of human reproductive fluids*. Proteomics Clinical Applications, 2007. 1(8): p. 853.
98. Underwood, M.A., Gilbert, W.M., and Sherman, M.P., *Amniotic Fluid: Not Just Fetal Urine Anymore*. Journal of Perinatology, 2005. 25(5): p. 341.
99. Cho, C.-K.J., Shan, S.J., Winsor, E.J., et al., *Proteomics Analysis of Human Amniotic Fluid*. Molecular and Cellular Proteomics, 2007. 6(8): p. 1406.
100. Song, H.J., Zhang, P., Guo, X.J., et al., *The proteomic analysis of human neonatal umbilical cord serum by mass spectrometry*. Acta Pharmacologica Sinica, 2009. 30(11): p. 1550.
101. Chien, P.F.W., Arnott, N., Gordon, A., et al., *How useful is uterine artery Doppler flow velocimetry in the prediction of pre-eclampsia, intrauterine growth retardation and perinatal death? An overview*. BJOG: An International Journal of Obstetrics and Gynaecology, 2000. 107(2): p. 196.
102. Podjarny, E., Losonczy, G., and Baylis, C., *Animal models of preeclampsia*. Seminars in Nephrology, 2004. 24(6): p. 596.
103. Abebe, J., Eigbefoh, J., Isabu, P., et al., *Accuracy of urine dipsticks, 2-h and 12-h urine collections for protein measurement as compared with the 24-h collection*. Journal of Obstetrics and Gynaecology, 2008. 28(5): p. 496.
104. Shahbazian, N. and Hosseini-Asl, F., *A comparison of spot urine protein-creatinine ratio with 24-hour urine protein excretion in women with preeclampsia*. Iran Journal of Kidney Diseases, 2008. 2(3): p. 127.
105. Thangaratnam, S., Coomarasamy, A., O'Mahony, F., et al., *Estimation of proteinuria as a predictor of complications of pre-eclampsia: a systematic review*. BMC Medicine, 2009. 7: p. 10.
106. Buhimschi, I.A., Zhao, G., Funai, E.F., et al., *Proteomic profiling of urine identifies specific fragments of SERPINA1 and albumin as biomarkers of preeclampsia*. American Journal of Obstetrics and Gynecology, 2008. 199(5): p. 551 e1.

107. Silverman, G.A., Bird, P.I., Carrell, R.W., et al., *The serpins are an expanding superfamily of structurally similar but functionally diverse proteins. Evolution, mechanism of inhibition, novel functions, and a revised nomenclature.* The Journal of Biological Chemistry, 2001. 276(36): p. 33293.
108. Chelbi, S.T., Mondon, F., Jammes, H., et al., *Expressional and epigenetic alterations of placental serine protease inhibitors: SERPINA3 is a potential marker of preeclampsia.* Hypertension, 2007. 49(1): p. 76.
109. Gupta, S., Agarwal, A., and Sharma, R.K., *The role of placental oxidative stress and lipid peroxidation in preeclampsia.* Obstetrical and Gynecological Survey, 2005. 60(12): p. 807.
110. Auer, J., Camoin, L., Guillonneau, F., et al., *Serum profile in preeclampsia and intra-uterine growth restriction revealed by iTRAQ technology.* Journal of Proteomics, 2010. 73(5): p. 1004.
111. Blumenstein, M., McMaster, M.T., Black, M.A., et al., *A proteomic approach identifies early pregnancy biomarkers for preeclampsia: novel linkages between a predisposition to preeclampsia and cardiovascular disease.* Proteomics, 2009. 9(11): p. 2929.
112. Vascotto, C., Salzano, A.M., D'Ambrosio, C., et al., *Oxidized transthyretin in amniotic fluid as an early marker of preeclampsia.* Journal of Proteome Research, 2007. 6(1): p. 160.
113. Chen, G., Zhang, Y., Jin, X., et al., *Urinary proteomics analysis for renal injury in hypertensive disorders of pregnancy with iTRAQ labeling and LC-MS/MS.* Proteomics Clinical Applications, 2011. 5(5-6): p. 300.
114. Blumenstein, M., Prakash, R., Cooper, G.J., et al., *Aberrant processing of plasma vitronectin and high-molecular-weight kininogen precedes the onset of preeclampsia.* Reproductive Sciences, 2009. 16(12): p. 1144.
115. Carty, D.M., Siwy, J., Brennand, J.E., et al., *Urinary proteomics for prediction of preeclampsia.* Hypertension, 2011. 57(3): p. 561.
116. Karehed, K., Wikstrom, A.K., Olsson, A.K., et al., *Fibrinogen and histidine-rich glycoprotein in early-onset preeclampsia.* Acta Obstetrica et Gynecologica Scandinavica, 2010. 89(1): p. 131.
117. Williams, V.K., Griffiths, A.B., Carbone, S., et al., *Fibrinogen concentration and factor VIII activity in women with preeclampsia.* Hypertension in Pregnancy, 2007. 26(4): p. 415.
118. Dvergsten, J., Manivel, J.C., Correa-Rotter, R., et al., *Expression of clusterin in human renal diseases.* Kidney International, 1994. 45(3): p. 828.
119. Shin, J.K., Han, K.A., Kang, M.Y., et al., *Expression of clusterin in normal and preeclamptic placentas.* The Journal of Obstetrics and Gynaecology Research, 2008. 34(4): p. 473.
120. Calero, M., Rostagno, A., Frangione, B., et al., *Clusterin and Alzheimer's disease.* Subcellular Biochemistry, 2005. 38: p. 273.
121. Watanabe, H., Hamada, H., Yamada, N., et al., *Proteome analysis reveals elevated serum levels of clusterin in patients with preeclampsia.* Proteomics, 2004. 4(2): p. 537.
122. Lim, J.H., Kim, S.Y., Park, S.Y., et al., *Effective prediction of preeclampsia by a combined ratio of angiogenesis-related factors.* Obstetrics and Gynecology, 2008. 111(6): p. 1403.

123. Maynard, S.E., Min, J.-Y., Merchan, J., et al., *Excess placental soluble fms-like tyrosine kinase 1 (sFlt1) may contribute to endothelial dysfunction, hypertension, and proteinuria in preeclampsia*. The Journal of Clinical Investigation, 2003. 111(5): p. 649.
124. Moore Simas, T.A., Crawford, S.L., Solitto, M.J., et al., *Angiogenic factors for the prediction of preeclampsia in high-risk women*. American Journal of Obstetrics and Gynecology, 2007. 197(3): p. 244 e1.
125. Robinson, C.J. and Johnson, D.D., *Soluble endoglin as a second-trimester marker for preeclampsia*. American Journal of Obstetrics and Gynecology, 2007. 197(2): p. 174 e1.
126. Venkatesha, S., Toporsian, M., Lam, C., et al., *Soluble endoglin contributes to the pathogenesis of preeclampsia*. Nature Medicine, 2006. 12(6): p. 642.
127. Bolin, M., Akerud, P., Hansson, A., et al., *Histidine-rich glycoprotein as an early biomarker of preeclampsia*. American Journal of Hypertension, 2011. 24(4): p. 496.
128. Rasanen, J., Girsen, A., Lu, X., et al., *Comprehensive maternal serum proteomic profiles of preclinical and clinical preeclampsia*. Journal of Proteome Research, 2010. 9(8): p. 4274.
129. Blankley, R.T., Gaskell, S.J., Whetton, A.D., et al., *A proof-of-principle gel-free proteomics strategy for the identification of predictive biomarkers for the onset of pre-eclampsia*. BJOG: An International Journal of Obstetrics and Gynaecology, 2009. 116(11): p. 1473.
130. Zhang, H., Zhang, Y., Yang, F., et al., *Complement component C4A and apolipoprotein A-I in plasmas as biomarkers of the severe, early-onset preeclampsia*. Molecular Biosystems, 2011. 7(8): p. 2470.
131. Park, J., Cha, D.H., Lee, S.J., et al., *Discovery of the serum biomarker proteins in severe preeclampsia by proteomic analysis*. Experimental and Molecular Medicine, 2011. 43(7): p. 427.
132. Norwitz, E.R., Tsen, L.C., Park, J.S., et al., *Discriminatory proteomic biomarker analysis identifies free hemoglobin in the cerebrospinal fluid of women with severe preeclampsia*. American Journal of Obstetrics and Gynecology, 2005. 193(3 Pt 2): p. 957.
133. Celik, O., Hascalik, S., Ozerol, E., et al., *Cerebrospinal fluid leptin levels in preeclampsia: relation to maternal serum leptin levels*. Acta Obstetrica et Gynecologica Scandinavica, 2004. 83(6): p. 519.
134. Foyouzi, N., Norwitz, E.R., Tsen, L.C., et al., *Placental growth factor in the cerebrospinal fluid of women with preeclampsia*. International Journal of Gynaecology and Obstetrics, 2006. 92(1): p. 32.
135. Myers, J., Macleod, M., Reed, B., et al., *Use of proteomic patterns as a novel screening tool in pre-eclampsia*. Journal of Obstetrics and Gynaecology, 2004. 24(8): p. 873.
136. Liu, C., Zhang, N., Yu, H., et al., *Proteomic analysis of human serum for finding pathogenic factors and potential biomarkers in preeclampsia*. Placenta, 2011. 32(2): p. 168.
137. Buhimschi, I.A. and Buhimschi, C.S., *Proteomics of the amniotic fluid in assessment of the placenta. Relevance for preterm birth*. Placenta, 2008. 29 Suppl A: p. S95.

138. Romero, R., Espinoza, J., Rogers, W.T., et al., *Proteomic analysis of amniotic fluid to identify women with preterm labor and intra-amniotic inflammation/infection: the use of a novel computational method to analyze mass spectrometric profiling*. The Journal of Maternal-Fetal and Neonatal Medicine 2008. 21(6): p. 367.
139. Park, J.S., Oh, K.J., Norwitz, E.R., et al., *Identification of proteomic biomarkers of preeclampsia in amniotic fluid using SELDI-TOF mass spectrometry*. Reproductive Sciences, 2008. 15(5): p. 457.
140. Page, E.W., *The relation between hydatid moles, relative ischemia of the gravid uterus, and the placental origin of eclampsia*. American Journal of Obstetrics and Gynecology, 1939. 37: p. 291.
141. Centlow, M., Hansson, S.R., and Welinder, C., *Differential proteome analysis of the preeclamptic placenta using optimized protein extraction*. Journal of Biomedicine and Biotechnology, 2010. 2010: p. 458748.
142. Gharesi-Fard, B., Zolghadri, J., and Kamali-Sarvestani, E., *Proteome differences of placenta between pre-eclampsia and normal pregnancy*. Placenta, 2010. 31(2): p. 121.
143. Kim, Y.N., Kim, H.K., Warda, M., et al., *Toward a better understanding of preeclampsia: Comparative proteomic analysis of preeclamptic placentas*. Proteomics Clinical Applications, 2007. 1(12): p. 1625.
144. Mine, K., Katayama, A., Matsumura, T., et al., *Proteome analysis of human placentae: pre-eclampsia versus normal pregnancy*. Placenta, 2007. 28(7): p. 676.
145. Blankley, R.T., Robinson, N.J., Aplin, J.D., et al., *A gel-free quantitative proteomics analysis of factors released from hypoxic-conditioned placentae*. Reproductive Sciences, 2010. 17(3): p. 247.
146. Johnstone, E.D., Sawicki, G., Guilbert, L., et al., *Differential proteomic analysis of highly purified placental cytotrophoblasts in pre-eclampsia demonstrates a state of increased oxidative stress and reduced cytotrophoblast antioxidant defense*. Proteomics, 2011. 11(20): p. 4077.
147. Sun, L.Z., Yang, N.N., De, W., et al., *Proteomic analysis of proteins differentially expressed in preeclamptic trophoblasts*. Gynecologic and Obstetric Investigation, 2007. 64(1): p. 17.
148. Jin, H., Ma, K.D., Hu, R., et al., *Analysis of expression and comparative profile of normal placental tissue proteins and those in preeclampsia patients using proteomic approaches*. Analytica Chimica Acta, 2008. 629(1-2): p. 158.
149. Hoang, V.M., Foulk, R., Clauser, K., et al., *Functional proteomics: examining the effects of hypoxia on the cytotrophoblast protein repertoire*. Biochemistry, 2001. 40(13): p. 4077.
150. Hu, R., Jin, H., Zhou, S., et al., *Proteomic analysis of hypoxia-induced responses in the syncytialization of human placental cell line BeWo*. Placenta, 2007. 28(5-6): p. 399.
151. Sawicki, G., Dakour, J., and Morrish, D.W., *Functional proteomics of neurokinin B in the placenta indicates a novel role in regulating cytotrophoblast antioxidant defences*. Proteomics, 2003. 3(10): p. 2044.
152. Ishioka, S., Ezaka, Y., Umemura, K., et al., *Proteomic analysis of mechanisms of hypoxia-induced apoptosis in trophoblastic cells*. International Journal of Medical Sciences, 2006. 4(1): p. 36.

153. Walther, T., Wallukat, G., Jank, A., et al., *Angiotensin II type 1 receptor agonistic antibodies reflect fundamental alterations in the uteroplacental vasculature*. *Hypertension*, 2005. 46(6): p. 1275.
154. Xia, Y. and Kellems, R.E., *Receptor-activating autoantibodies and disease: preeclampsia and beyond*. *Expert Review of Clinical Immunology*, 2011. 7(5): p. 659.
155. Rauch, J. and Gires, O., *SEREX, Proteomex, AMIDA, and beyond: Serological screening technologies for target identification*. *Proteomics Clinical Applications*, 2008. 2(3): p. 355.
156. Tjalsma, H., Schaeps, R.M., and Swinkels, D.W., *Immunoproteomics: From biomarker discovery to diagnostic applications*. *Proteomics Clinical Applications*, 2008. 2(2): p. 167.
157. Chekir, C., Nakatsuka, M., Noguchi, S., et al., *Accumulation of advanced glycation end products in women with preeclampsia: possible involvement of placental oxidative and nitrative stress*. *Placenta*, 2006. 27(2-3): p. 225.
158. Cooke, C.L., Brockelsby, J.C., Baker, P.N., et al., *The receptor for advanced glycation end products (RAGE) is elevated in women with preeclampsia*. *Hypertension in Pregnancy*, 2003. 22(2): p. 173.
159. Kwon, J.H., Kim, Y.H., Kwon, J.Y., et al., *Clinical significance of serum sRAGE and esRAGE in women with normal pregnancy and preeclampsia*. *Journal of Prenatal Medicine*, 2011. 39(5): p. 507.
160. Webster, R.P. and Myatt, L., *Elucidation of the molecular mechanisms of preeclampsia using proteomic technologies*. *Proteomics Clinical Applications*, 2007. 1(9): p. 1147.
161. Zhang, H.H., Wang, Y.P., and Chen, D.B., *Analysis of nitroso-proteomes in normotensive and severe preeclamptic human placentas*. *Biology of Reproduction*, 2011. 84(5): p. 966.
162. Atkinson, K.R., Blumenstein, M., Black, M.A., et al., *An altered pattern of circulating apolipoprotein E3 isoforms is implicated in preeclampsia*. *Journal of Lipid Research*, 2009. 50(1): p. 71.
163. Ahmad, S., Hewett, P.W., Al-Ani, B., et al., *Autocrine activity of soluble Flt-1 controls endothelial cell function and angiogenesis*. *Vascular Cell*, 2011. 3(1): p. 15.
164. Scioscia, M., Gumaa, K., Kunjara, S., et al., *Insulin resistance in human preeclamptic placenta is mediated by serine phosphorylation of insulin receptor substrate-1 and -2*. *The Journal of Clinical Endocrinology and Metabolism*, 2006. 91(2): p. 709.
165. Shin, J.K., Baek, J.C., Kang, M.Y., et al., *Proteomic analysis reveals an elevated expression of heat shock protein 27 in preeclamptic placentas*. *Gynecologic and Obstetric Investigation*, 2011. 71(3): p. 151.
166. Wilson, C.M., *Staining of Proteins on Gels - Comparisons of Dyes and Procedures*. *Methods in Enzymology*, 1983. 91: p. 236.
167. Yasumitsu, H., Ozeki, Y., Kawsar, S.M.A., et al., *RAMA stain: A fast, sensitive and less protein-modifying CBB R250 stain*. *Electrophoresis*, 2010. 31(12): p. 1913.
168. Neuhoff, V., Arold, N., Taube, D., et al., *Improved staining of proteins in polyacrylamide gels including isoelectric focusing gels with clear background at nanogram sensitivity using Coomassie Brilliant Blue G-250 and R-250*. *Electrophoresis*, 1988. 9(6): p. 255.

169. Candiano, G., Bruschi, M., Musante, L., et al., *Blue silver: A very sensitive colloidal Coomassie G-250 staining for proteome analysis*. Electrophoresis, 2004. 25(9): p. 1327.
170. Yan, J.X., Wait, R., Berkelman, T., et al., *A modified silver staining protocol for visualization of proteins compatible with matrix-assisted laser desorption/ionization and electrospray ionization-mass spectrometry*. Electrophoresis, 2000. 21(17): p. 3666.
171. Dunn, M.J., *Detection of Proteins in Polyacrylamide Gels by Fluorescent Staining*. The Protein Protocols Handbook, 2009: p. 547.
172. Unlu, M., Morgan, M.E., and Minden, J.S., *Difference gel electrophoresis: a single gel method for detecting changes in protein extracts*. Electrophoresis, 1997. 18(11): p. 2071.
173. Tonge, R., Shaw, J., Middleton, B., et al., *Validation and development of fluorescence two-dimensional differential gel electrophoresis proteomics technology*. Proteomics, 2001. 1(3): p. 377.
174. Steinberg, T.H., Chernokalskaya, E., Berggren, K., et al., *Ultrasensitive fluorescence protein detection in isoelectric focusing gels using a ruthenium metal chelate stain*. Electrophoresis, 2000. 21(3): p. 486.
175. Aksamitiene, E., Hoek, J.B., Kholodenko, B., et al., *Multistrip Western blotting to increase quantitative data output*. Electrophoresis, 2007. 28(18): p. 3163.
176. Huang, D.W., Sherman, B.T., and Lempicki, R.A., *Systematic and integrative analysis of large gene lists using DAVID bioinformatics resources*. Nature Protocols, 2009. 4(1): p. 44.
177. Supek, F., Bosnjak, M., Skunca, N., et al., *REVIGO summarizes and visualizes long lists of gene ontology terms*. PLoS One, 2011. 6(7): p. e21800.
178. Hall, L. and Martinus, R.D., *Hyperglycaemia and oxidative stress upregulate HSP60 & HSP70 expression in HeLa cells*. Springerplus, 2013. 2: p. 431.
179. Ozawa, K., Kuwabara, K., Tamatani, M., et al., *150-kDa oxygen-regulated protein (ORP150) suppresses hypoxia-induced apoptotic cell death*. The Journal of Biological Chemistry, 1999. 274(10): p. 6397.
180. Cho, S.Y., Lee, J.H., Bae, H.D., et al., *Transglutaminase 2 inhibits apoptosis induced by calcium- overload through down-regulation of Bax*. Experimental and Molecular Medicine, 2010. 42(9): p. 639.
181. Honda, K., Yamada, T., Endo, R., et al., *Actinin-4, a novel actin-bundling protein associated with cell motility and cancer invasion*. The Journal of Cell Biology, 1998. 140(6): p. 1383.
182. Magdolen, U., Schroeck, F., Creutzburg, S., et al., *Non-muscle alpha-actinin-4 interacts with plasminogen activator inhibitor type-1 (PAI-1)*. Biological Chemistry, 2004. 385(9): p. 801.
183. Burton, G.J. and Yung, H.W., *Endoplasmic reticulum stress in the pathogenesis of early-onset pre-eclampsia*. Pregnancy Hypertension, 2011. 1(1-2): p. 72.
184. Eletto, D., Dersh, D., Gidalevitz, T., et al., *Protein disulfide isomerase A6 controls the decay of IRE1alpha signaling via disulfide-dependent association*. Molecular Cell, 2014. 53(4): p. 562.
185. Horna-Terron, E., Pradilla-Dieste, A., Sanchez-de-Diego, C., et al., *TXNDC5, a newly discovered disulfide isomerase with a key role in cell physiology and pathology*. International Journal of Medical Sciences, 2014. 15(12): p. 23501.

186. Sullivan, D.C., Huminiecki, L., Moore, J.W., et al., *EndoPDI, a novel protein-disulfide isomerase-like protein that is preferentially expressed in endothelial cells acts as a stress survival factor*. The Journal of Biological Chemistry, 2003. 278(47): p. 47079.
187. Wojcik, C., Rowicka, M., Kudlicki, A., et al., *Valosin-containing protein (p97) is a regulator of endoplasmic reticulum stress and of the degradation of N-end rule and ubiquitin-fusion degradation pathway substrates in mammalian cells*. Molecular Biology of the Cell, 2006. 17(11): p. 4606.
188. Staron, M., Yang, Y., Liu, B., et al., *gp96, an endoplasmic reticulum master chaperone for integrins and Toll-like receptors, selectively regulates early T and B lymphopoiesis*. Blood, 2010. 115(12): p. 2380.
189. Ikeda, J., Kaneda, S., Kuwabara, K., et al., *Cloning and expression of cDNA encoding the human 150 kDa oxygen-regulated protein, ORP150*. Biochemical and Biophysical Research Communications, 1997. 230(1): p. 94.
190. Ozawa, K., Kondo, T., Hori, O., et al., *Expression of the oxygen-regulated protein ORP150 accelerates wound healing by modulating intracellular VEGF transport*. The Journal of Clinical Investigation, 2001. 108(1): p. 41.
191. Cornely, R., Rentero, C., Enrich, C., et al., *Annexin A6 is an organizer of membrane microdomains to regulate receptor localization and signalling*. IUBMB Life, 2011. 63(11): p. 1009.
192. Rambotti, M.G., Spreca, A., and Donato, R., *Immunocytochemical localization of annexins V and VI in human placentae of different gestational ages*. Cell and Molecular Biology Research, 1993. 39(6): p. 579.
193. Koese, M., Rentero, C., Kota, B.P., et al., *Annexin A6 is a scaffold for PKC α to promote EGFR inactivation*. Oncogene, 2013. 32(23): p. 2858.
194. Bolnick, J., Albitar, L., Laidler, L.L., et al., *Blocking Epidermal Growth Factor Receptor Signaling in HTR-8/SVneo First Trimester Trophoblast Cells Results in Dephosphorylation of PKB α /AKT and Induces Apoptosis*. Obstetrics and Gynecology International, 2011. 2011: p. 896896.
195. Tajiri, Y., Igarashi, T., Li, D., et al., *Tubulointerstitial nephritis antigen-like 1 is expressed in the uterus and binds with integrins in decidualized endometrium during postimplantation in mice*. Biology of Reproduction, 2010. 82(2): p. 263.
196. Li, D., Mukai, K., Suzuki, T., et al., *Adrenocortical zonation factor 1 is a novel matricellular protein promoting integrin-mediated adhesion of adrenocortical and vascular smooth muscle cells*. FASEB Journal, 2007. 27(10): p. 2506.
197. Damsky, C.H., Librach, C., Lim, K.H., et al., *Integrin switching regulates normal trophoblast invasion*. Development, 1994. 120(12): p. 3657.
198. Takahashi, A., Rahim, A., Takeuchi, M., et al., *Impaired female fertility in tubulointerstitial antigen-like 1-deficient mice*. The Journal of Reproduction and Development, 2016. 62(1): p. 43.
199. Wang, A., Rana, S., and Karumanchi, S.A., *Preeclampsia: the role of angiogenic factors in its pathogenesis*. Physiology (Bethesda), 2009. 24: p. 147.
200. Brown, L.J., Alawoki, M., Crawford, M.E., et al., *Lipocalin-7 is a matricellular regulator of angiogenesis*. PLoS One, 2010. 5(11): p. e13905.
201. Ivaska, J., Pallari, H.M., Nevo, J., et al., *Novel functions of vimentin in cell adhesion, migration, and signaling*. Experimental Cell Research, 2007. 313(10): p. 2050.
202. Mendez, M.G., Kojima, S., and Goldman, R.D., *Vimentin induces changes in cell shape, motility, and adhesion during the epithelial to mesenchymal transition*. FASEB Journal, 2010. 24(6): p. 1838.

203. Schiffers, P.M., Henrion, D., Boulanger, C.M., et al., *Altered flow-induced arterial remodeling in vimentin-deficient mice*. *Arterioscler Thromb Vasc Biol*, 2000. 20(3): p. 611.
204. Dave, J.M. and Bayless, K.J., *Vimentin as an Integral Regulator of Cell Adhesion and Endothelial Sprouting*. *Microcirculation*, 2014. 21(4): p. 333.
205. Kwak, H.I., Kang, H., Dave, J.M., et al., *Calpain-mediated vimentin cleavage occurs upstream of MT1-MMP membrane translocation to facilitate endothelial sprout initiation*. *Angiogenesis*, 2012. 15(2): p. 287.
206. Byun, Y., Chen, F., Chang, R., et al., *Caspase cleavage of vimentin disrupts intermediate filaments and promotes apoptosis*. *Cell Death and Differentiation*, 2001. 8(5): p. 443.
207. Podor, T.J., Singh, D., Chindemi, P., et al., *Vimentin exposed on activated platelets and platelet microparticles localizes vitronectin and plasminogen activator inhibitor complexes on their surface*. *J Biol Chem*, 2002. 277(9): p. 7529.
208. Moisan, E. and Girard, D., *Cell surface expression of intermediate filament proteins vimentin and lamin B1 in human neutrophil spontaneous apoptosis*. *J Leukoc Biol*, 2006. 79(3): p. 489.
209. Mor-Vaknin, N., Punturieri, A., Sitwala, K., et al., *Vimentin is secreted by activated macrophages*. *Nat Cell Biol*, 2003. 5(1): p. 59.
210. Straszewski-Chavez, S.L., Abrahams, V.M., and Mor, G., *The role of apoptosis in the regulation of trophoblast survival and differentiation during pregnancy*. *Endocr Rev*, 2005. 26(7): p. 877.
211. Longtine, M.S., Chen, B., Odibo, A.O., et al., *Villous trophoblast apoptosis is elevated and restricted to cytotrophoblasts in pregnancies complicated by preeclampsia, IUGR, or preeclampsia with IUGR*. *Placenta*, 2012. 33(5): p. 352.
212. Li, G.Z., Vissers, J.P., Silva, J.C., et al., *Database searching and accounting of multiplexed precursor and product ion spectra from the data independent analysis of simple and complex peptide mixtures*. *Proteomics*, 2009. 9(6): p. 1696.
213. Huang da, W., Sherman, B.T., and Lempicki, R.A., *Systematic and integrative analysis of large gene lists using DAVID bioinformatics resources*. *Nature Protocols*, 2009. 4(1): p. 44.
214. Szklarczyk, D., Franceschini, A., Kuhn, M., et al., *The STRING database in 2011: functional interaction networks of proteins, globally integrated and scored*. *Nucleic Acids Research*, 2011. 39(Database issue): p. D561.
215. Smoot, M.E., Ono, K., Ruscheinski, J., et al., *Cytoscape 2.8: new features for data integration and network visualization*. *Bioinformatics*, 2011. 27(3): p. 431.
216. Maere, S., Heymans, K., and Kuiper, M., *BiNGO: a Cytoscape plugin to assess overrepresentation of gene ontology categories in biological networks*. *Bioinformatics*, 2005. 21(16): p. 3448.
217. Chen, Y.Y., Lin, S.Y., Yeh, Y.Y., et al., *A modified protein precipitation procedure for efficient removal of albumin from serum*. *Electrophoresis*, 2005. 26(11): p. 2117.
218. Chung, L.M., Colangelo, C.M., and Zhao, H., *Data Pre-Processing for Label-Free Multiple Reaction Monitoring (MRM) Experiments*. *Biology* 2014. 3(2): p. 383.

219. Banmeyer, I., Marchand, C., Clippe, A., et al., *Human mitochondrial peroxiredoxin 5 protects from mitochondrial DNA damages induced by hydrogen peroxide*. FEBS Letters, 2005. 579(11): p. 2327.
220. De Simoni, S., Linard, D., Hermans, E., et al., *Mitochondrial peroxiredoxin-5 as potential modulator of mitochondria-ER crosstalk in MPP⁺-induced cell death*. Journal of Neurochemistry, 2013. 125(3): p. 473.
221. Sabharwal, S.S., Waypa, G.B., Marks, J.D., et al., *Peroxiredoxin-5 targeted to the mitochondrial intermembrane space attenuates hypoxia-induced reactive oxygen species signalling*. The Biochemical Journal, 2013. 456(3): p. 337.
222. Knoops, B., Argyropoulou, V., Becker, S., et al., *Multiple Roles of Peroxiredoxins in Inflammation*. Molecules and Cells, 2016. 39(1): p. 60.
223. Yang, M., Lin, X., Rowe, A., et al., *Transcriptome analysis of human OXR1 depleted cells reveals its role in regulating the p53 signaling pathway*. Scientific Reports, 2015. 5: p. 17409.
224. Dusse, L.M., Rios, D.R., Pinheiro, M.B., et al., *Pre-eclampsia: relationship between coagulation, fibrinolysis and inflammation*. Clinica Chimica Acta, 2011. 412(1-2): p. 17.
225. Nakashima, A., Kobayashi, T., and Terao, T., *Fibrinolysis during normal pregnancy and severe preeclampsia relationships between plasma levels of plasminogen activators and inhibitors*. Gynecologic and Obstetric Investigation, 1996. 42(2): p. 95.
226. Maynard, S.E., Min, J.Y., Merchan, J., et al., *Excess placental soluble fms-like tyrosine kinase 1 (sFlt1) may contribute to endothelial dysfunction, hypertension, and proteinuria in preeclampsia*. The Journal of Clinical Investigation, 2003. 111(5): p. 649.
227. Li, R., Luo, M., Ren, M., et al., *Vitronectin regulation of vascular endothelial growth factor-mediated angiogenesis*. Journal of Vascular Research, 2014. 51(2): p. 110.
228. Matsumura, A., Kubota, T., Taiyoh, H., et al., *HGF regulates VEGF expression via the c-Met receptor downstream pathways, PI3K/Akt, MAPK and STAT3, in CT26 murine cells*. International Journal of Oncology, 2013. 42(2): p. 535.
229. Liao, W.X., Feng, L., Zhang, H., et al., *Compartmentalizing VEGF-induced ERK2/1 signaling in placental artery endothelial cell caveolae: a paradoxical role of caveolin-1 in placental angiogenesis in vitro*. Molecular Endocrinology, 2009. 23(9): p. 1428.
230. Qiu, C., Phung, T.T., Vadachkoria, S., et al., *Oxidized low-density lipoprotein (Oxidized LDL) and the risk of preeclampsia*. Physiological Research, 2006. 55(5): p. 491.
231. Castellani, L.W., Navab, M., Van Lenten, B.J., et al., *Overexpression of apolipoprotein AII in transgenic mice converts high density lipoproteins to proinflammatory particles*. The Journal of Clinical Investigation, 1997. 100(2): p. 464.
232. Berkova, N., Lemay, A., Dresser, D.W., et al., *Haptoglobin is present in human endometrium and shows elevated levels in the decidua during pregnancy*. Molecular Human Reproduction, 2001. 7(8): p. 747.
233. Centlow, M., Carninci, P., Nemeth, K., et al., *Placental expression profiling in preeclampsia: local overproduction of hemoglobin may drive pathological changes*. Fertility and Sterility, 2008. 90(5): p. 1834.

234. Cid, M.C., Grant, D.S., Hoffman, G.S., et al., *Identification of haptoglobin as an angiogenic factor in sera from patients with systemic vasculitis*. The Journal of Clinical Investigation, 1993. 91(3): p. 977.
235. Sharpe-Timms, K.L., Ricke, E.A., Piva, M., et al., *Differential expression and localization of de-novo synthesized endometriotic haptoglobin in endometrium and endometriotic lesions*. Human Reproduction 2000. 15(10): p. 2180.
236. Sammour, R.N., Nakhoul, F.M., Levy, A.P., et al., *Haptoglobin phenotype in women with preeclampsia*. Endocrine, 2010. 38(2): p. 303.
237. Depypere, H.T., Langlois, M.R., Delanghe, J.R., et al., *Haptoglobin polymorphism in patients with preeclampsia*. Clinical Chemistry and Laboratory Medicine, 2006. 44(8): p. 924.
238. Hvidberg, V., Maniecki, M.B., Jacobsen, C., et al., *Identification of the receptor scavenging hemopexin-heme complexes*. Blood, 2005. 106(7): p. 2572.
239. Bakker, W.W., Donker, R.B., Timmer, A., et al., *Plasma hemopexin activity in pregnancy and preeclampsia*. Hypertension in Pregnancy, 2007. 26(2): p. 227.
240. Bakker, W.W., Henning, R.H., van Son, W.J., et al., *Vascular contraction and preeclampsia: downregulation of the Angiotensin receptor 1 by hemopexin in vitro*. Hypertension, 2009. 53(6): p. 959.
241. Rayman, M.P., Barlis, J., Evans, R.W., et al., *Abnormal iron parameters in the pregnancy syndrome preeclampsia*. American Journal of Obstetrics and Gynecology, 2002. 187(2): p. 412.
242. Loh, T.T., Higuchi, D.A., van Bockxmeer, F.M., et al., *Transferrin receptors on the human placental microvillous membrane*. The Journal of Clinical Investigation, 1980. 65(5): p. 1182.
243. Khatun, R., Wu, Y., Kanenishi, K., et al., *Immunohistochemical study of transferrin receptor expression in the placenta of pre-eclamptic pregnancy*. Placenta, 2003. 24(8-9): p. 870.
244. Toth, I., Yuan, L., Rogers, J.T., et al., *Hypoxia alters iron-regulatory protein-1 binding capacity and modulates cellular iron homeostasis in human hepatoma and erythroleukemia cells*. The Journal of Biological Chemistry, 1999. 274(7): p. 4467.
245. Tacchini, L., Bianchi, L., Bernelli-Zazzera, A., et al., *Transferrin receptor induction by hypoxia. HIF-1-mediated transcriptional activation and cell-specific post-transcriptional regulation*. The Journal of Biological Chemistry, 1999. 274(34): p. 24142.
246. Wang, F., Shi, Z., Wang, P., et al., *Comparative proteome profile of human placenta from normal and preeclamptic pregnancies*. PLoS One, 2013. 8(10): p. e78025.
247. Davies, J. and Glasser, S., *Histological and fine structural observations on the placenta of the rat*. Cells Tissues Organs, 1968. 69(4): p. 542.
248. Caluwaerts, S., Verduyck, L., Luyten, C., et al., *Endovascular trophoblast invasion and associated structural changes in uterine spiral arteries of the pregnant rat*. Placenta, 2005. 26(7): p. 574.
249. Soares, M., Chapman, B., Rasmussen, C., et al., *Differentiation of trophoblast endocrine cells*. Placenta, 1996. 17(5-6): p. 277.
250. Carter, A.M. and Enders, A.C., *Comparative aspects of trophoblast development and placentation*. Reproductive Biology and Endocrinology, 2004. 2(1): p. 46.
251. Okamoto, K. and Aoki, K., *Development of a strain of spontaneously hypertensive rats*. Japanese circulation journal, 1963. 27(3): p. 282.

252. Yamori, Y., Tomimoto, K., Ooshima, A., et al., *Developmental course of hypertension in the SHR-substrains susceptible to hypertensive cerebrovascular lesions*. Japanese Heart Journal, 1974. 15(2): p. 209.
253. Yamori, Y., Nara, Y., Kihara, M., et al., *Sodium and other dietary factors in experimental and human hypertension: The Japanese experience*, in *Frontiers in Hypertension Research*. 1981, Springer. p. 46.
254. Small, H.Y., Morgan, H., Beattie, E., et al., *Abnormal uterine artery remodelling in the stroke prone spontaneously hypertensive rat*. Placenta, 2016. 37: p. 34.
255. Swaney, D.L., McAlister, G.C., and Coon, J.J., *Decision tree-driven tandem mass spectrometry for shotgun proteomics*. Nat Methods, 2008. 5(11): p. 959.
256. Cox, J. and Mann, M., *MaxQuant enables high peptide identification rates, individualized p.p.b.-range mass accuracies and proteome-wide protein quantification*. Nature Biotechnology, 2008. 26(12): p. 1367.
257. Cox, J., Hein, M.Y., Lubner, C.A., et al., *Accurate proteome-wide label-free quantification by delayed normalization and maximal peptide ratio extraction, termed MaxLFQ*. Molecular and Cellular Proteomics, 2014. 13(9): p. 2513.
258. Tyanova, S., Temu, T., Sinitcyn, P., et al., *The Perseus computational platform for comprehensive analysis of (prote)omics data*. Nature Methods, 2016. 13(9): p. 731.
259. Zhu, X.Q., Jiang, S.S., Zhu, X.J., et al., *Expression of aquaporin 1 and aquaporin 3 in fetal membranes and placenta in human term pregnancies with oligohydramnios*. Placenta, 2009. 30(8): p. 670.
260. Guo, J., He, H., Liu, H., et al., *Aquaporin-1, a New Maternally Expressed Gene, Regulates Placental Development in the Mouse*. Biology of Reproduction, 2016. 95(2): p. 40.
261. Mammaro, A., Carrara, S., Cavaliere, A., et al., *Hypertensive disorders of pregnancy*. Journal of Prenatal Medicine, 2009. 3(1): p. 1.
262. Seely, E.W. and Ecker, J., *Chronic hypertension in pregnancy*. Circulation, 2014. 129(11): p. 1254.
263. Bramham, K., Parnell, B., Nelson-Piercy, C., et al., *Chronic hypertension and pregnancy outcomes: systematic review and meta-analysis*. British Medical Journal, 2014. 348: p. g2301.
264. Jones, D.C. and Hayslett, J.P., *Outcome of pregnancy in women with moderate or severe renal insufficiency*. N Engl J Med, 1996. 335(4): p. 226.
265. Imbasciati, E., Gregorini, G., Cabiddu, G., et al., *Pregnancy in CKD stages 3 to 5: fetal and maternal outcomes*. Am J Kidney Dis, 2007. 49(6): p. 753.
266. Dunlop, W., *Serial Changes in Renal Hemodynamics during Normal Human-Pregnancy*. Brit J Obstet Gynaec, 1981. 88(1): p. 1.
267. Cheung, K.L. and Lafayette, R.A., *Renal Physiology of Pregnancy*. Adv Chronic Kidney Dis, 2013. 20(3): p. 209.
268. Davison, J.M. and Lindheimer, M.D., *Changes in renal haemodynamics and kidney weight during pregnancy in the unanaesthetized rat*. J Physiol, 1980. 301: p. 129.
269. Norden, A.G.W., Rodriguez-Cutillas, P., and Unwin, R.J., *Clinical urinary peptidomics: Learning to walk before we can run*. Clin Chem, 2007. 53(3): p. 375.
270. Decramer, S., de Peredo, A.G., Breuil, B., et al., *Urine in Clinical Proteomics*. Mol Cell Proteomics, 2008. 7(10): p. 1850.

271. Delles, C., Diez, J., and Dominiczak, A.F., *Urinary proteomics in cardiovascular disease: Achievements, limits and hopes*. *Proteom Clin Appl*, 2011. 5(5-6): p. 222.
272. Carty, D.M., Schiffer, E., and Delles, C., *Proteomics in hypertension*. *J Hum Hypertens*, 2013. 27(4): p. 211.
273. Kolialexi, A., Mavreli, D., Tounta, G., et al., *Urine proteomic studies in preeclampsia*. *Proteom Clin Appl*, 2015. 9(5-6): p. 501.
274. Albalat, A., Bitsika, V., Zurbig, P., et al., *High-resolution proteome/peptidome analysis of body fluids by capillary electrophoresis coupled with MS*. *Methods in Molecular Biology*, 2013. 984: p. 153.
275. Neuhoff, N., Kaiser, T., Wittke, S., et al., *Mass spectrometry for the detection of differentially expressed proteins: a comparison of surface-enhanced laser desorption/ionization and capillary electrophoresis/mass spectrometry*. *Rapid Communications in Mass Spectrometry*, 2004. 18(2): p. 149.
276. Rouse, R., Siwy, J., Mullen, W., et al., *Proteomic candidate biomarkers of drug-induced nephrotoxicity in the rat*. *PLoS One*, 2012. 7(4): p. e34606.
277. Jovine, L., Qi, H., Williams, Z., et al., *The ZP domain is a conserved module for polymerization of extracellular proteins*. *Nat Cell Biol*, 2002. 4(6): p. 457.
278. Klein, J., Eales, J., Zurbig, P., et al., *Proteasix: a tool for automated and large-scale prediction of proteases involved in naturally occurring peptide generation*. *Proteomics*, 2013. 13(7): p. 1077.
279. Graf, C., Maserluth, C., Keizer, W.D., et al., *Sodium Retention and Hypertension after Kidney-Transplantation in Rats*. *Hypertension*, 1993. 21(5): p. 724.
280. Griffin, K.A., Churchill, P.C., Picken, M., et al., *Differential salt-sensitivity in the pathogenesis of renal damage in SHR and stroke prone SHR*. *American Journal of Hypertension*, 2001. 14(4): p. 311.
281. Hladunewich, M., Karumanchi, S.A., and Lafayette, R., *Pathophysiology of the clinical manifestations of preeclampsia*. *Clin J Am Soc Nephrol*, 2007. 2(3): p. 543.
282. Padmanabhan, S., Melander, O., Johnson, T., et al., *Genome-wide association study of blood pressure extremes identifies variant near UMOD associated with hypertension*. *PLoS Genetics*, 2010. 6(10): p. e1001177.
283. Kononikhin, A.S., Starodubtseva, N.L., Bugrova, A.E., et al., *An untargeted approach for the analysis of the urine peptidome of women with preeclampsia*. *J Proteomics*, 2016. 149: p. 38.
284. Brunati, M., Perucca, S., Han, L., et al., *The serine protease hepsin mediates urinary secretion and polymerisation of Zona Pellucida domain protein uromodulin*. *eLife*, 2015. 4: p. e08887.
285. Matthey, M. and Naftalin, L., *Mechanoelectrical transduction, ion movement and water stasis in uromodulin*. *Experientia*, 1992. 48(10): p. 975.
286. Wiggins, R.C., *Uromuroid (Tamm-Horsfall glycoprotein) forms different polymeric arrangements on a filter surface under different physicochemical conditions*. *Clinica Chimica Acta*, 1987. 162(3): p. 329.
287. Barton, J.R., Mercer, B.M., and Sibai, B.M., *The effect of nifedipine on urinary excretion of calcium in preeclampsia*. *American Journal of Perinatology*, 1997. 14(10): p. 609.
288. Kloke, H.J., Wetzels, J.F., Koene, R.A., et al., *Effects of low-dose nifedipine on urinary protein excretion rate in patients with renal disease*. *Nephrology Dialysis Transplantation*, 1998. 13(3): p. 646.

289. Mo, L., Huang, H.Y., Zhu, X.H., et al., *Tamm-Horsfall protein is a critical renal defense factor protecting against calcium oxalate crystal formation*. *Kidney International*, 2004. 66(3): p. 1159.
290. Gossas, T. and Danielson, U.H., *Characterization of Ca²⁺ interactions with matrix metalloproteinase-12: implications for matrix metalloproteinase regulation*. *The Biochemical Journal*, 2006. 398(3): p. 393.
291. Wilhelm, S.M., Shao, Z.H., Housley, T.J., et al., *Matrix Metalloproteinase-3 (Stromelysin-1) - Identification as the Cartilage Acid Metalloprotease and Effect of Ph on Catalytic Properties and Calcium Affinity*. *J Biol Chem*, 1993. 268(29): p. 21906.
292. Velotti, F., Palmieri, G., Dambrosio, D., et al., *Differential Expression of Granzyme-a and Granzyme-B Proteases and Their Secretion by Fresh Rat Natural-Killer-Cells (Nk) and Lymphokine-Activated Killer-Cells with Nk Phenotype (Lak-Nk)*. *Eur J Immunol*, 1992. 22(4): p. 1049.
293. Kokot, K., Teschner, M., Schaefer, R.M., et al., *Stimulation and inhibition of elastase release from human neutrophil-dependence on the calcium messenger system*. *Mineral and Electrolyte Metabolism*, 1987. 13(3): p. 189.
294. Nakamura, K., Kimura, M., Fenton, J.W., 2nd, et al., *Duality of plasmin effect on cytosolic free calcium in human platelets*. *The American Journal of Physiology*, 1995. 268(4 Pt 1): p. C958.

Appendix

Appendix1: Maternal characteristic

Parameter	Normotensive (n=25)	Pre-eclamptic (n=25)
Age, yrs	24.08 ± 3.92	23.44 ± 2.69
Weight, kg	59.18 ± 9.06	64.67 ± 11.33
Height, cm	152.56 ± 8.87	154.84 ± 4.90
Gestation, wks	39.25 ± 1.15	38.46 ± 1.38
Systolic blood pressure, mmHg	120.00 ± 8.16	144.40 ± 12.27 ***
Diastolic blood pressure, mmHg	77.20 ± 4.58	98.56 ± 10.00 ***
Haemoglobin, g/dL	11.66 ± 1.51	11.86 ± 1.20 ^{NS}

Values are mean ± standard deviation

*** p<0.001 and NS- not significant when compared to normotensive

Appendix 2: 123 urinary peptides altered between WKY and SHRSP at all time points (NP, GD12 and GD18) or GD12 & GD18 only

PeptideID	Mass [Da]	Migration time [Min]	Log2 peptide intensity						Fold change (WKY/ SHRSP)		
			WKY NP	SHRSP NP	WKY GD12	SHRSP GD12	WKY GD18	SHRSP GD18	NP	GD12	GD18
929	857.4815	28.15	5.93	6.28	6.35	7.03	5.97	7.12	0.94	0.90	0.84
1054	862.4315	22.67	6.57	8.10	8.11	6.86	6.86	6.36	0.81	1.18	1.08
1304	874.4576	34.49	7.49	6.14	7.73	5.75	6.64	3.95	1.22	1.34	1.68
4119	1009.498	37.80	12.33	13.33	12.23	12.91	11.82	13.09	0.92	0.95	0.90
4706	1046.479	47.56	5.75	6.67	5.57	7.32	6.13	4.75	0.86	0.76	1.29
5098	1073.363	46.52	13.04	13.67	13.11	13.83	13.28	14.25	0.95	0.95	0.93
5254	1083.533	36.50	11.96	11.35	12.24	11.21	12.08	11.42	1.05	1.09	1.06
5474	1099.53	36.52	8.98	7.83	9.31	7.72	9.86	8.23	1.15	1.21	1.20
5497	1100.587	28.83	7.31	5.11	8.58	7.67	8.52	6.09	1.43	1.12	1.40
5661	1111.608	30.47	7.52	4.06	8.29	5.98	7.90	5.15	1.85	1.39	1.53
6367	1155.575	29.05	6.57	4.10	7.14	3.41	8.39	4.48	1.60	2.09	1.87
6546	1167.54	47.90	4.49	5.59	4.63	3.92	5.08	4.30	0.80	1.18	1.18
7006	1196.367	47.02	12.07	12.79	12.42	13.09	12.91	13.48	0.94	0.95	0.96
7982	1255.65	26.25	6.73	4.55	7.88	3.90	6.75	5.44	1.48	2.02	1.24
8591	1295.622	29.62	8.05	3.67	8.18	3.00	9.73	4.23	2.19	2.73	2.30
9325	1341.649	38.48	6.65	5.63	6.62	5.30	7.52	5.21	1.18	1.25	1.44
10270	1407.682	48.28	7.91	9.23	8.50	9.14	8.91	6.45	0.86	0.93	1.38
10772	1444.684	40.04	4.60	5.84	4.28	3.39	7.37	4.59	0.79	1.26	1.61
11141	1471.739	39.49	4.27	4.30	4.99	4.22	5.34	4.74	0.99	1.18	1.13
12407	1564.769	39.41	7.19	5.89	8.34	6.64	8.90	5.66	1.22	1.26	1.57
12582	1579.76	26.34	8.60	7.18	10.10	8.95	9.86	6.87	1.20	1.13	1.44
12628	1584.553	47.97	10.32	12.13	11.42	12.12	11.48	12.24	0.85	0.94	0.94
12969	1611.795	40.17	5.59	7.54	5.92	6.83	5.78	7.19	0.74	0.87	0.80
13270	1635.838	33.09	6.11	4.45	6.30	3.66	7.01	4.56	1.37	1.72	1.53
13543	1659.818	39.66	8.96	6.90	9.43	6.79	9.41	5.46	1.30	1.39	1.72
13580	1663.806	40.59	8.70	5.54	9.39	4.19	8.92	4.80	1.57	2.24	1.86

PeptideID	Mass [Da]	Migration time [Min]	Log2 peptide intensity						Fold change (WKY/ SHRSP)		
			WKY NP	SHRSP NP	WKY GD12	SHRSP GD12	WKY GD18	SHRSP GD18	NP	GD12	GD18
13742	1679.814	40.76	7.82	6.23	8.45	5.75	7.40	5.22	1.25	1.47	1.42
14788	1780.881	28.09	6.98	4.44	9.02	2.89	9.26	4.33	1.57	3.12	2.14
14896	1790.854	33.26	6.62	4.42	8.29	5.42	8.28	4.66	1.50	1.53	1.78
15819	1885.854	28.11	9.79	4.57	10.90	3.50	11.42	4.68	2.14	3.12	2.44
100383	1139.544	28.69	9.92	6.65	10.46	7.06	10.89	6.37	1.49	1.48	1.71
100433	1173.604	26.22	6.30	4.47	7.69	3.67	6.06	4.87	1.41	2.10	1.24
100744	1417.721	26.35	5.87	4.27	7.21	4.15	6.42	4.65	1.37	1.74	1.38
100773	1433.684	32.66	7.07	5.52	7.79	6.11	7.93	6.28	1.28	1.28	1.26
100916	1532.692	39.51	6.33	8.34	8.62	9.19	7.00	9.06	0.76	0.94	0.77
100954	1554.759	26.62	6.33	4.60	7.18	3.57	6.80	4.57	1.38	2.01	1.49
100964	1561.754	28.12	7.59	4.19	8.80	3.89	8.20	4.91	1.81	2.26	1.67
101001	1584.787	27.29	7.10	4.52	8.12	3.52	8.32	4.83	1.57	2.31	1.72
101201	1713.872	28.25	7.19	4.43	8.82	3.54	9.03	4.84	1.62	2.49	1.87
101224	1726.832	28.14	5.34	4.55	5.81	3.76	6.37	4.69	1.17	1.54	1.36
101391	1832.94	33.34	6.33	4.54	6.28	3.54	7.78	4.94	1.39	1.77	1.57
101392	1833.646	48.36	5.17	6.55	4.94	6.58	6.78	4.81	0.79	0.75	1.41
101695	2013.958	25.17	8.05	4.63	8.93	3.74	9.39	5.05	1.74	2.39	1.86
102001	2196.056	25.43	7.54	4.18	9.66	3.76	9.26	4.61	1.80	2.57	2.01
102056	2239.077	26.87	8.01	4.65	9.33	3.52	8.34	5.06	1.72	2.65	1.65
106356	1418.602	48.47	7.81	4.70	7.40	3.86	8.73	5.14	1.66	1.92	1.70
880	855.4258	35.91	9.61	10.94	9.42	10.64	8.86	11.32	0.88	0.88	0.78
1512	883.4193	35.35	7.59	8.27	7.77	6.69	8.43	6.66	0.92	1.16	1.27
1615	888.4502	34.67	7.05	6.27	8.22	5.97	7.04	4.86	1.13	1.38	1.45
2684	931.5043	27.26	7.97	7.67	7.49	9.31	7.82	8.83	1.04	0.80	0.89
2981	947.4504	34.20	7.66	7.31	7.23	5.09	7.51	5.79	1.05	1.42	1.30
3258	960.5006	29.69	5.54	6.03	7.14	5.88	5.93	4.99	0.92	1.21	1.19
3668	982.5227	36.14	10.42	10.22	10.41	9.58	10.30	8.68	1.02	1.09	1.19
3784	989.4635	47.52	6.51	6.42	6.74	7.99	7.02	5.54	1.01	0.84	1.27
3791	989.5253	28.87	8.40	9.05	7.80	9.24	6.99	8.98	0.93	0.84	0.78

PeptideID	Mass [Da]	Migration time [Min]	Log2 peptide intensity						Fold change (WKY/ SHRSP)		
			WKY NP	SHRSP NP	WKY GD12	SHRSP GD12	WKY GD18	SHRSP GD18	NP	GD12	GD18
3930	998.4752	34.70	10.08	9.68	9.56	8.17	9.43	6.41	1.04	1.17	1.47
4042	1004.478	47.47	7.44	8.21	7.72	8.92	8.85	6.97	0.91	0.87	1.27
4680	1044.505	36.33	6.11	7.63	6.18	5.59	6.53	5.53	0.80	1.11	1.18
4824	1055.523	36.37	9.66	9.55	9.44	8.94	9.49	8.91	1.01	1.06	1.06
5014	1068.567	29.18	5.30	4.67	5.62	3.91	5.66	4.84	1.14	1.44	1.17
5114	1073.515	36.41	6.52	5.76	5.98	3.96	6.25	5.09	1.13	1.51	1.23
5789	1119.531	48.01	4.82	5.38	4.67	5.91	6.64	5.91	0.90	0.79	1.12
6058	1134.515	47.95	6.16	4.69	4.99	5.56	7.18	5.16	1.31	0.90	1.39
6252	1148.544	48.13	4.93	4.99	4.94	5.90	6.36	5.00	0.99	0.84	1.27
6545	1167.564	29.66	8.30	5.88	5.88	7.50	5.67	9.18	1.41	0.78	0.62
7181	1206.626	25.61	6.64	5.38	6.25	7.93	7.04	5.14	1.23	0.79	1.37
7302	1214.566	37.03	11.12	11.34	11.69	11.14	11.60	12.04	0.98	1.05	0.96
7534	1227.606	37.47	10.57	10.37	10.26	9.45	10.65	9.95	1.02	1.09	1.07
8404	1283.405	47.36	6.44	6.77	7.21	3.99	8.16	6.39	0.95	1.81	1.28
8590	1295.61	37.80	5.85	5.95	6.53	4.29	7.54	5.62	0.98	1.52	1.34
8661	1300.715	39.78	5.99	4.46	7.22	3.86	8.35	4.88	1.34	1.87	1.71
9006	1321.704	32.99	6.65	6.20	6.63	5.18	7.11	5.92	1.07	1.28	1.20
9090	1324.681	29.94	7.57	7.03	9.26	7.61	9.05	6.34	1.08	1.22	1.43
9131	1326.631	39.17	8.23	9.06	8.20	5.14	7.11	5.30	0.91	1.60	1.34
9601	1358.66	32.35	7.02	7.36	5.34	6.53	6.96	5.43	0.95	0.82	1.28
9863	1378.668	39.11	10.44	10.55	10.86	10.08	10.22	9.15	0.99	1.08	1.12
9871	1378.731	31.31	6.94	6.50	8.40	7.60	8.35	6.65	1.07	1.11	1.26
10013	1388.717	39.15	9.66	9.21	10.47	9.54	9.82	8.04	1.05	1.10	1.22
10393	1415.706	39.41	5.71	5.70	5.80	6.85	6.18	5.72	1.00	0.85	1.08
10625	1434.691	48.95	4.71	7.65	6.15	8.04	7.28	7.07	0.62	0.76	1.03
11179	1474.77	26.54	4.98	4.51	5.79	4.18	5.51	4.64	1.10	1.38	1.19
11487	1497.745	31.62	4.91	4.49	5.23	3.61	5.03	4.42	1.09	1.45	1.14
11667	1511.678	39.29	5.95	6.83	6.13	5.35	6.38	5.45	0.87	1.14	1.17
11737	1515.825	32.86	4.71	6.21	6.72	5.36	4.86	5.78	0.76	1.25	0.84

PeptideID	Mass [Da]	Migration time [Min]	Log2 peptide intensity						Fold change (WKY/ SHRSP)		
			WKY NP	SHRSP NP	WKY GD12	SHRSP GD12	WKY GD18	SHRSP GD18	NP	GD12	GD18
12757	1594.92	33.72	6.04	5.80	4.70	6.45	5.86	8.83	1.04	0.73	0.66
12958	1610.734	38.89	6.83	6.16	8.06	4.90	7.45	4.53	1.11	1.65	1.65
13079	1620.735	32.13	5.06	4.48	5.99	3.96	6.87	4.57	1.13	1.51	1.50
13290	1636.792	40.73	10.05	10.03	10.51	9.77	9.67	8.59	1.00	1.08	1.13
13458	1650.839	33.29	5.19	4.89	6.68	4.79	5.98	4.59	1.06	1.39	1.30
13670	1671.9	28.18	7.11	6.31	8.28	6.70	6.81	4.66	1.13	1.24	1.46
13740	1679.77	32.30	9.18	9.20	9.07	8.01	9.78	8.75	1.00	1.13	1.12
13819	1687.84	41.42	5.26	4.85	5.32	4.24	5.58	4.59	1.08	1.25	1.22
14020	1706.866	41.37	7.12	8.04	8.11	7.12	7.37	5.42	0.89	1.14	1.36
14404	1743.872	33.58	6.88	6.17	7.60	6.29	6.51	5.11	1.11	1.21	1.27
15228	1825.811	40.93	6.65	7.42	7.23	6.53	6.96	5.55	0.90	1.11	1.25
16047	1905.941	34.11	8.35	7.80	9.16	7.25	6.44	5.27	1.07	1.26	1.22
16054	1906.927	42.64	8.95	9.25	8.80	7.90	8.12	5.89	0.97	1.11	1.38
16851	1992.943	42.36	8.77	9.29	9.21	8.36	8.20	7.30	0.94	1.10	1.12
16914	2000.106	35.84	8.97	9.41	7.33	9.83	7.61	11.52	0.95	0.75	0.66
17594	2072.013	40.74	6.32	6.90	7.02	5.83	6.98	5.04	0.92	1.20	1.38
17878	2099.082	42.32	6.14	7.02	6.11	4.23	5.76	5.15	0.88	1.45	1.12
20566	2420.078	44.61	7.04	7.68	7.16	5.77	6.39	4.77	0.92	1.24	1.34
21602	2566.11	44.92	5.86	6.61	6.42	5.13	5.45	4.77	0.89	1.25	1.14
29610	3981.973	38.00	5.17	4.45	7.19	4.64	6.16	4.40	1.16	1.55	1.40
33289	5452.868	24.75	11.77	11.77	10.45	12.70	12.27	8.41	1.00	0.82	1.46
100000	800.3959	33.34	8.16	7.23	7.97	6.08	8.15	6.32	1.13	1.31	1.29
100026	828.4175	33.50	6.76	7.59	7.67	6.31	7.10	5.33	0.89	1.22	1.33
100111	902.4517	29.35	6.53	5.56	5.89	4.96	5.69	4.71	1.18	1.19	1.21
100343	1095.353	47.05	7.70	5.81	5.62	8.58	7.54	5.58	1.32	0.66	1.35
100542	1253.576	37.28	6.04	5.74	6.71	3.38	7.61	5.45	1.05	1.98	1.40
100572	1274.494	47.99	5.81	5.64	7.80	5.10	7.87	5.09	1.03	1.53	1.55
100806	1456.767	27.87	4.88	4.34	6.49	3.77	6.23	4.55	1.12	1.72	1.37
100913	1529.64	29.08	5.58	5.96	7.43	9.05	7.38	8.35	0.94	0.82	0.88

PeptideID	Mass [Da]	Migration time [Min]	Log2 peptide intensity						Fold change (WKY/ SHRSP)		
			WKY NP	SHRSP NP	WKY GD12	SHRSP GD12	WKY GD18	SHRSP GD18	NP	GD12	GD18
101148	1675.841	41.45	5.90	5.66	6.60	3.80	6.44	4.69	1.04	1.74	1.37
101272	1753.899	50.19	5.49	5.94	5.60	3.57	7.09	4.92	0.92	1.57	1.44
101403	1837.903	28.25	5.91	4.33	8.18	3.73	8.58	4.47	1.37	2.19	1.92
101420	1849.971	29.18	5.92	4.96	7.31	5.51	5.86	4.90	1.19	1.33	1.20
101782	2060.054	42.88	5.29	6.96	6.97	4.05	6.43	4.22	0.76	1.72	1.52
101946	2165.127	30.74	5.07	4.46	5.74	3.55	5.90	5.22	1.14	1.62	1.13
102676	3411.458	28.83	5.13	5.84	5.77	5.83	5.64	4.81	0.88	0.99	1.17
102804	4113.821	47.13	4.65	4.25	6.77	3.70	4.98	4.50	1.09	1.83	1.11
102868	4816.223	32.08	5.01	4.66	5.19	3.56	5.06	4.41	1.08	1.46	1.15
107005	1694.835	33.02	5.52	4.25	6.85	4.44	6.47	4.44	1.30	1.54	1.46

Appendix 3: Sequenced peptides list

PeptideID	Mass [Da]	Sequence	Protein name	Theoretical Mass	Start AA	Stop AA	Rat. Protein Accessions
12757	1594.92	IDQTRVLNLGPITR	Uromodulin	1594.91549	596	609	P27590
16914	2000.106	SGNFIDQTRVLNLGPITR	Uromodulin	2000.080323	592	609	P27590
9131	1326.631	TVDETYVPKEF	Serum albumin	1326.634348	516	526	P02770
11179	1474.77	SVIHEDVYEEKK	RCG32337, isoform CRA_a	1474.730374	47	58	D3ZJA4
14788	1780.881	DKTEKELLDSYIDGR	Prothrombin	1780.884309	345	359	P18292
3668	982.5227	VPSYPGPpGP	Protein Col19a1	982.569898	76	84	D3ZCQ0
8590	1295.61	DPVESKIYFAQ	Pro-epidermal growth factor	1295.639768	522	532	P07522
11667	1511.678	AGPpGpPpGpPGSIGHpG	procollagen, type IX, alpha 3 (predicted), isoform CRA_a	1511.700471	555	571	D3ZX71

PeptideID	Mass [Da]	Sequence	Protein name	Theoretical Mass	Start AA	Stop AA	Rat. Protein Accessions
12958	1610.734	LAQLmANEWPHSQA	NACHT, leucine rich repeat and PYD containing 5	1610.751105	69	82	D3ZDM5
9006	1321.704	DGILGRDTLPHE	Contrapsin-like protease inhibitor 1	1321.662629	21	32	P05545
11141	1471.739	ALYQAEAFVADFK	Contrapsin-like protease inhibitor 1	1471.734731	155	167	P05545
11487	1497.745	GPPGpPGDPGKPGAPGK	Collagen alpha-1(IX) chain	1497.757592	68	84	F1LQ93
13742	1679.814	GMpGSpGGPGNDGKPGpG	Collagen alpha-1(III) chain	1679.720948	536	554	P13941
14896	1790.854	GESGRpGPpGPSGPRGQpG	Collagen alpha-1(III) chain	1790.829588	557	575	P13941
16851	1992.943	QGIpGTSGPpGENGKpGEpGP	Collagen alpha-1(III) chain	1992.902478	640	660	P13941
4706	1046.479	GppGPpGPpGPG	Collagen alpha-1(II) chain	1046.466889	1139	1150	P05539
9863	1378.668	ApGEDGRpGPpGPQ	Collagen alpha-1(II) chain	1378.611322	512	525	P05539
10625	1434.691	GPpGPpGPpGPPSGGY	Collagen alpha-1(I) chain	1434.641559	1170	1185	P02454
3784	989.4635	GppGPpGPpGP	Collagen alpha-1(I) chain	989.445425	131	141	P02454
4042	1004.478	GPpGPpGPPSGG	Collagen alpha-1(I) chain	1004.456324	1173	1184	P02454
4119	1009.498	GRVGPpGPSGN	Collagen alpha-1(I) chain	1009.494075	870	880	P02454
6546	1167.54	GPpGPpGPPSGGY	Collagen alpha-1(I) chain	1167.519653	1173	1185	P02454
4680	1044.505	ApGFpGARGPS	Collagen alpha-1(I) chain	1044.498815	397	407	P02454
5254	1083.533	GVVGLpGQRGE	Collagen alpha-1(I) chain	1083.483267	828	839	P02454
5789	1119.531	GPpGPTGPTGPpG	Collagen alpha-1(I) chain	1119.519653	321	333	P02454
6252	1148.544	GLpGPpGApGPQG	Collagen alpha-1(I) chain	1148.546202	177	189	P02454
9090	1324.681	GLpGpKGDGRDAGP	Collagen alpha-1(I) chain	1324.637142	726	739	P02454
10013	1388.717	RpGEVGPpGPpGPAG	Collagen alpha-1(I) chain	1388.668442	907	921	P02454
11737	1515.825	GPpGPpGPVgKEGGKGP	Collagen alpha-1(I) chain	1515.768157	882	898	P02454

PeptideID	Mass [Da]	Sequence	Protein name	Theoretical Mass	Start AA	Stop AA	Rat. Protein Accessions
13079	1620.735	DGVAGPKGPAGERGSpGP	Collagen alpha-1(I) chain	1620.785598	488	505	P02454
13290	1636.792	GSpGSpGPDGKTGPpGPAG	Collagen alpha-1(I) chain	1636.732893	531	549	P02454
13670	1671.9	PpGPpGPVGKEGGKPRG	Collagen alpha-1(I) chain	1671.869268	882	899	P02454
14020	1706.866	TGPIGPpGPAGApGDKGET	Collagen alpha-1(I) chain	1706.811144	755	773	P02455
13543	1659.818	GAPGAKGNVGppGEPGPpG	Alpha 4 type V collagen	1659.785263	620	638	P68136
4824	1055.523	NELRVAPEE	Actin, alpha skeletal muscle	1055.524738	94	102	P68136

REVIEW

Dynamic proteome in enigmatic preeclampsia: An account of molecular mechanisms and biomarker discovery

Sheon Mary¹, Gouri V. Patil¹, Asmita V. Kulkarni², Mahesh J. Kulkarni^{1*}, Sadhana R. Joshi^{2*}, Savita S. Mehendale³ and Ashok P. Giri¹

¹Division of Biochemical Sciences, National Chemical Laboratory (CSIR), Pune, Maharashtra, India

²Department of Nutritional Medicine, Interactive Research School for Health Affairs, Bharati Vidyapeeth University, Pune, Maharashtra, India

³Department of Gynecology, Bharati Vidyapeeth Medical College, Pune, Maharashtra, India

The coevolution of genomics and proteomics has led to advancements in the field of diagnosis and molecular mechanisms of disease. Proteomics is now stepping into the field of obstetrics, where early diagnosis of pregnancy complication such as preeclampsia (PE) is imperative. PE is a multifactorial disease characterized by hypertension with proteinuria, which is a leading cause of maternal and neonatal morbidity and mortality occurring in 5–7% of pregnancies worldwide. This review discusses the probable molecular mechanisms that lead to PE and summarizes the proteomics research carried out in understanding the pathogenicity of PE, and for identifying the candidate biomarker for diagnosis of the disease.

Received: October 5, 2011

Revised: November 30, 2011

Accepted: December 1, 2011

Keywords:

Hypertension / Oxidative stress / Pregnancy complication / Proteinuria

1 Pregnancy and related complications

Pregnancy is a complex state involving physiological changes in various maternal organs to support the development of fetus and these changes determine the overall success of a pregnancy. Yet, a continuum of complications are associated with pregnancy such as unexplained miscarriage [1], preeclampsia (PE) and intrauterine growth restriction (IUGR) [2], placental abruption [3], preterm labor with intact membranes [4], premature rupture of the membranes [5], and stillbirth [6], caused by either changes in intrauterine environment, impaired trophoblast invasion, and maternal nutrition. PE is a unique hypertensive disorder in pregnancy that complicates approximately 5–7% of pregnancies and is associated with significant fetal/neonatal morbidity and mortality [7]. In 2000, the National High Blood Pressure Education Program (NHBPEP)

Working Group [8] defined the criteria for diagnosis of PE as (i) systolic blood pressure ≥ 140 mmHg or diastolic blood pressure ≥ 90 mmHg that occurs after 20 weeks of gestation in a woman with previously normal blood pressure and (ii) proteinuria defined as urinary excretion of 0.3 g protein or higher in a 24-h urine specimen. PE untreated can lead to eclampsia or hemolysis, elevated liver enzymes and low platelet count (HELLP) syndrome. The known risk factors for PE include pre-existing hypertension, diabetes, autoimmune diseases, family history of PE, obesity, and increased maternal age [9–13]. There is a pressing need to better understand the mechanisms of the disease, with the ultimate goal of preventing the disorder especially since the incidence of PE and rates of adverse outcomes are increasing [14–16].

2 PE: Pathophysiology and etiological factors

PE involves changes in both placental and maternal physiology. Placentation is the process by which the placental

Correspondence: Dr. Ashok P. Giri, Division of Biochemical Sciences, National Chemical Laboratory, Homi Bhabha Road, Pune 411008, Maharashtra, India

E-mail: ap.giri@ncl.res.in

Fax: +91-20-25902648

Abbreviations: AF, amniotic fluid; PE, preeclampsia; PIGF, placental growth factor; RAS, renin-angiotensin system; sFlt-1, soluble vascular endothelial growth factor receptor 1; TTR, transthyretin; VEGF, vascular endothelial growth factor

*Additional corresponding authors:

Dr. Mahesh J. Kulkarni, E-mail: mj.kulkarni@ncl.res.in;

Dr. Sadhana R. Joshi, E-mail: srjoshi62@yahoo.com

Placental Proteomics Provides Insights into Pathophysiology of Pre-eclampsia and Predicts Possible Markers in Plasma

Sheon Mary,[†] Mahesh J. Kulkarni,^{*,†} Dipankar Malakar,[‡] Sadhana R. Joshi,[§] Savita S. Mehendale,^{||} and Ashok P. Giri^{*,†}

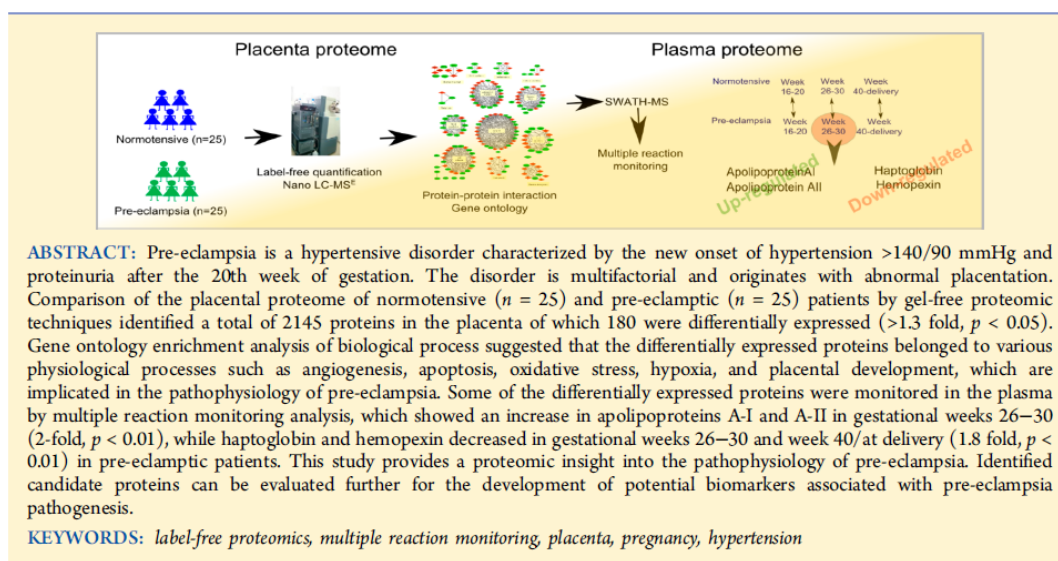
[†]Division of Biochemical Sciences, CSIR-National Chemical Laboratory, Homi Bhabha Road, Pune, Maharashtra 411008, India

[‡]Sciex, 121 Udyog Vihar, Gurgaon, Haryana 122015, India

[§]Department of Nutritional Medicine, Interactive Research School for Health Affairs, Pune, Dhankawadi 411043, India

^{||}Department of ObGy, Bharati Hospital, Pune, Maharashtra 411043, India

Supporting Information



INTRODUCTION

The state of pregnancy is a complex phenomenon that involves major changes in the physiology of maternal organs, especially in the newly developed organ, the placenta. The majority of pregnancies are successful with slight discomforts such as mild nausea, while marginal women suffer from complications. These pregnancy complications include placental abruption, ectopic pregnancy, hypertensive pregnancy, miscarriage, and so on. Under severe conditions, these complications lead to long-term maternal health problems or maternal or fetal deaths. Pre-eclampsia (PE) is a hypertensive disorder characterized by the new onset of hypertension of >140/90 mmHg and proteinuria after the 20th week of gestation. As per the task force report issued by American College of Obstetricians and Gynecologists, in the absence of proteinuria, a new onset of hypertension with either thrombocytopenia or renal insufficiency or impaired liver function or pulmonary edema or cerebral or visual symptoms is also suggested to be used as diagnostic criteria for PE.¹

Worldwide, 10 million women develop PE, of which >76 000 women die per year.²

Author: During normal pregnancy, the blastocyst adheres and invades the endometrium. This process takes place with the help of extravillous trophoblasts. This invasive cytotrophoblast breaks through the maternal deciduas to reach spiral arteries in the myometrium.³ The next stage is remodeling of uterine spiral arteries to low resistance and high caliber arteriolar system, which requires the release of vasodilators (e.g., nitric oxide and carbon monoxide) and angiogenic factors (e.g., vascular endothelial growth factor, placental growth factors) by trophoblast. Moreover, pseudovasculogenesis occurs by transformation to endothelial phenotype via expression of various cell adhesion molecules (e.g., vascular cell-adhesion molecule 1, integrins).⁴ The primary defect in PE is the failure of invasion by trophoblast

Received: November 4, 2016

Published: December 28, 2016

RESEARCH

Open Access



Tubulointerstitial nephritis antigen-like 1 protein is downregulated in the placenta of pre-eclamptic women

Sheon Mary¹, Mahesh J. Kulkarni^{1*}, Savita S. Mehendale², Sadhana R. Joshi³ and Ashok P. Giri^{1*}

Abstract

Background: Tubulointerstitial nephritis antigen-like 1 protein (TINAGL1), is a matricellular protein, known to play role in cell adhesion and cell receptor interaction. Research related to TINAGL1 is limited to cell culture and animal models. Demonstration of TINAGL1 as a positive regulator of angiogenesis and its expression in the decidua of post-implantation mouse uterus, prompted us to validate its expression in human placenta during impaired angiogenesis in pre-eclamptic condition.

Methods: Placental tissue from normotensive (n = 25) and pre-eclamptic (n = 25) pregnancies were used to study the differentially expressed proteins by two-dimensional gel electrophoresis and TINAGL1 protein was validated with Western blotting.

Results: A total of 55 protein spots were differentially expressed (fold change >1.5, p < 0.05), of which 27 were upregulated and 28 were downregulated in the pre-eclamptic placenta. TINAGL1 was found to be downregulated in pre-eclamptic compared to normotensive pregnant women.

Conclusion: This is the first study reporting TINAGL1 to be present in human placenta and differentially expressed in pre-eclamptic condition. The functional role of TINAGL1 in association to human pregnancy needs to be explored further.

Keywords: Pre-eclampsia, Tubulointerstitial nephritis antigen-like 1 protein, Human placenta, Matricellular protein, Proteomics

Background

Tubulointerstitial nephritis antigen-like 1 protein (TINAGL1) also known as Lipocalin 7 (LCN7) or adrenocortical zonation factor-1 (AZ1) or tubulointerstitial nephritis antigen related protein (TIN-ag-RP) is a matricellular protein. TINAGL1 is similar to tubulointerstitial nephritis antigen (TINAGL) in its protein domain composition, i.e. two EGF-like domains and a proteolytically inactive cathepsin B-like domain [1]. Unlike TINGAL, its expression is not limited to kidney, but found in a variety of organs, such as vascular smooth muscle [1], glomerular basement membrane [1], uterine capillaries [2],

adrenocortical cells [3] and lung capillary endothelium [4]. As a matricellular protein, it interacts with other structural matrix proteins such as laminin, collagen, and fibronectin and plays a role of a ligand for cell integrins receptors such as $\alpha_1\beta_1$, $\alpha_2\beta_1$ and $\alpha_5\beta_1$ [3]. Brown et al. [5], using murine endothelial cell lines and zebrafish embryo demonstrated that TINGAL1 is a positive regulator of angiogenesis that increases endothelial cell invasion, angiogenic sprouting and sensitivity of TGF- β . The demonstration of marked expression of TINGAL1 in the decidua of postimplantation mouse uterus [2] and the blastocoelic surface of trophoctoderm [6] has instigated the possible role of this protein in pregnancy.

Pre-eclampsia (PE) complicates 5–8% pregnancies and is a leading cause of maternal and perinatal morbidity and mortality worldwide. PE is diagnosed by the

*Correspondence: mj.kulkarni@nccl.res.in; ap.giri@nccl.res.in

¹ Division of Biochemical Sciences, CSIR-National Chemical Laboratory, Pune, Maharashtra 411008, India

Full list of author information is available at the end of the article



© The Author(s) 2017. This article is distributed under the terms of the Creative Commons Attribution 4.0 International License (<http://creativecommons.org/licenses/by/4.0/>), which permits unrestricted use, distribution, and reproduction in any medium, provided you give appropriate credit to the original author(s) and the source, provide a link to the Creative Commons license, and indicate if changes were made. The Creative Commons Public Domain Dedication waiver (<http://creativecommons.org/publicdomain/zero/1.0/>) applies to the data made available in this article, unless otherwise stated.

Polymerization-Incompetent Uromodulin in the Pregnant Stroke-Prone Spontaneously Hypertensive Rat

Sheon Mary,* Heather Yvonne Small,* Justyna Siwy, William Mullen, Ashok Giri, Christian Delles

Abstract—The kidney is centrally involved in blood pressure regulation and undergoes extensive changes during pregnancy. Hypertension during pregnancy may result in an altered urinary peptidome that could be used to indicate new targets of therapeutic or diagnostic interest. The stroke-prone spontaneously hypertensive rat (SHRSP) is a model of maternal chronic hypertension. Capillary electrophoresis-mass spectrometry was conducted to interrogate the urinary peptidome in SHRSP and the control Wistar–Kyoto strain at three time points: prepregnancy and gestational days 12 and 18. The comparison within and between the Wistar–Kyoto and SHRSP peptidome at all time points detected 123 differentially expressed peptides (fold change >1.5; $P<0.05$). Sequencing of these peptides identified fragments of collagen α -chains, albumin, prothrombin, actin, serpin A3K, proepidermal growth factor, and uromodulin. Uromodulin peptides showed a pregnancy-specific alteration in SHRSP with a 7.8-fold ($P<0.01$) and 8.8-fold ($P<0.05$) increase at gestational days 12 and 18, respectively, relative to the Wistar–Kyoto. Further investigation revealed that these peptides belonged to the polymerization-inhibitory region of uromodulin. Two forms of uromodulin (polymerization competent and polymerization incompetent) were found in urine from both Wistar–Kyoto and SHRSP, where the polymerization-incompetent form was increased in a pregnancy-specific manner in SHRSP. Nifedipine-treated pregnant SHRSP showed only polymerization-competent uromodulin, indicating that calcium may be mechanistically involved in uromodulin polymerization. This study highlights, for the first time, a potential role of uromodulin and its polymerization in hypertensive pregnancy. (*Hypertension*. 2017;69:00-00. DOI: 10.1161/HYPERTENSIONAHA.116.08826.)

• Online Data Supplement

Key Words: hypertension ■ kidney ■ Nifedipine ■ pregnancy ■ uromodulin

Hypertensive complications are the most common clinical problems encountered during pregnancy.¹ Hypertension during pregnancy encompasses many pathologies including preeclampsia, pregnancy-induced hypertension, and chronic hypertension. Specifically, chronic hypertension during pregnancy poses an increasing clinical problem.² Pregnant women with chronic hypertension are at an increased risk of maternal and fetal morbidity and mortality, as well as a higher incidence of developing superimposed preeclampsia.³ The kidneys play a central role in blood pressure regulation in pregnancy. Women with chronic kidney disease are at increased risk of developing pregnancy complications, where up to 70% experience preterm delivery and up to 40% will develop preeclampsia.^{4,5} Significant structural and functional changes occur in the kidney during pregnancy including a 1- to 1.5-cm increase in size, a 50% increase in glomerular filtration rate, and up to an 80% increase in renal plasma flow.^{6,7} These alterations are broadly conserved in rats.⁸

The mechanisms that affect pregnancy-related changes in the kidney in normotensive and hypertensive women are incompletely understood. Unbiased screening approaches may have the ability to identify novel pathophysiological pathways. The urinary peptidome provides information about proteins that are involved in local processes in the kidneys and information about other organs obtained through filtration of the dynamic plasma peptidome.⁹ Peptides derived from processes in the kidney and urogenital tract form the majority of those detected in the urinary peptidome (70%), whereas peptides from the circulation constitute the remainder.¹⁰ The small peptides present are generally soluble and because of their size do not require protein digestion before analysis by mass spectrometry.¹⁰ Urinary peptidomics has been applied in the field of cardiovascular research to develop biomarker panels for diagnosis, prediction of disease, and risk stratification.¹¹ In particular, many studies have shown that there are alterations

Received December 1, 2016; first decision December 20, 2016; revision accepted March 1, 2017.

From the BHF Glasgow Cardiovascular Research Centre, Institute of Cardiovascular and Medical Sciences, University of Glasgow, Scotland (S.M., H.Y.S., W.M., C.D.); Department of Biochemical Sciences, CSIR-National Chemical Laboratory, Pune, India (S.M., A.G.); and Mosaiques Diagnostics GmbH, Hannover, Germany (J.S.).

*These authors contributed equally to this work.

The online-only Data Supplement is available with this article at <http://hyper.ahajournals.org/lookup/suppl/doi:10.1161/HYPERTENSIONAHA.116.08826/-/DC1>.

Correspondence to Christian Delles, BHF Glasgow Cardiovascular Research Centre, Institute of Cardiovascular and Medical Sciences, University of Glasgow, 126 University Pl, Glasgow G12 8TA. E-mail Christian.Delles@glasgow.ac.uk

© 2017 The Authors. *Hypertension* is published on behalf of the American Heart Association, Inc., by Wolters Kluwer Health, Inc. This is an open access article under the terms of the Creative Commons Attribution License, which permits use, distribution, and reproduction in any medium, provided that the original work is properly cited.

Hypertension is available at <http://hyper.ahajournals.org>

DOI: 10.1161/HYPERTENSIONAHA.116.08826

Sheon Mary Samji

Address: Pune, Maharashtra, India, 411008

Date of Birth: July 31,1986

Nationality: Indian

Email ID: sheonmary@gmail.com

Phone no.: +91 9049046207



Education

- | | |
|---------------------|---|
| 2011-Present | PhD in Biotechnology, CSIR-National Chemical Laboratory, Pune, India |
| 2008-2010 | Masters in Biotechnology, Modern College, Pune University, India |
| 2004-2008 | Bachelors in Biotechnology, Dr. D.Y Patil Arts Science Commerce College, Pune University, India |

Research Experience

- | | |
|---------------------|---|
| 2015-2016 | Visiting research fellow
University of Glasgow, Glasgow, Scotland, UK
Advisor: Prof. Christian Deltas, Dr. Willam Mullen
Project: (1) Investigation of urinary peptidome in hypertensive pregnant rat model. (2) Study of placental proteome of hypertensive pregnant rat model. (3) Investigation of urinary peptidome in diabetic patients. (4) Investigation of urinary peptidome in cardiovascular rat model |
| 2011-present | Doctoral fellow
CSIR-National Chemical Laboratory, Pune, India
Advisor: Dr. Ashok P. Giri, Dr.Mahesh J. Kulkarni
Project: Proteomic pattern in Pre-eclampsia. Studying differential expression of proteins in placenta of pre-eclamptic and normotensive pregnancy using gel based and gel free proteomics |
| 2008-2010 | Master's Internship
CSIR-National Chemical Laboratory, Pune, India
Advisor: Dr. Ashok P. Giri
Project: Development of recombinant proteinase inhibitor incorporated microemulsion for plant protection against insect pest |
| 2007-2008 | Bachelor's project
Dr. D. Y. Patil ACS college, Pune, India
Advisor: Dr. Uttam Bodake |

Project: Biodegradation of Low Density Poly Ethylene (LDPE) by microorganisms *Pseudomonas putida* and *Pseudomonas aeruginosa*

Skills and Techniques

- Proteomic techniques: one and two dimensional electrophoresis, Western blot and ELISA
- Mass spectrometry: Protein digestion techniques, identification and label free quantification of proteins by mass spectrometer. Handled Bruker- CE- TOF MS, Waters- SYNAPT HDMS (LC-QTOF) and AB SCIEX TOF/TOF 5800 system. Mass spectrometry related software Mascot, Protein lynx Global Server, Transomics, Progenesis, Maxquant, Protein Pilot and Isoquant
- Molecular biology: mRNA isolation and cDNA preparation, PCR techniques and Real time PCR
- Bioinformatics: protein- protein interaction networks
- Animal handling license: small animals (mice and rat)
- Histology of kidney and placenta

Teaching Experience

2013	Guest lecturer, Ahmednagar college, Masters level; Proteomics
2012	Guest lecturer, Fergusson College Pune, Masters level subjects: Genetic Engineering and proteomics
2007-2013	Tutoring in Institute of Mathematics and Science Subjects: Biology, Physics and Chemistry for Class X

Awards and Fellowship

2015	Commonwealth split-site scholarship for UK
2011	Council of Scientific and Industrial Research-Junior research fellowship (CSIR-JRF) with 192 th national rank for five years Ph.D fellowship
2010	Graduate Aptitude Test in Engineering (GATE) Biotechnology fellowship

2010	Council of Scientific and Industrial Research-National eligibility Test (CSIR-NET) fellowship with 26 th national rank for lectureship
2010	Pune University 2 nd rank for Masters in Biotechnology
2008	Pune University 4 th rank for Bachelors in Biotechnology

Conferences

- British Society for Proteome Research, 2016, Glasgow, UK: Proteomic Approaches to Health and Disease. Oral presentation. Best Poster award.
- Lumps and bumps conference, 2016, Nottingham, UK: Placentation and Cancer. Poster presentation.
- 26th European meeting on hypertension and cardiovascular protection, 2016, Paris, France. Poster presentation. Travel Grant.
- 6th Annual meeting of the Proteomics Society of India PSI, 2014, Bombay, India.
- 4th Annual meeting of the Proteomics Society of India PSI, 2012, Pune, India.
- Food Safety Issues with specific emphasis on GM food crops, India, 2010, Pune, India

Publications

- **Mary, S.**, Kulkarni, M. J., Malakar, D., Joshi, S. R., Mehendale, S. S., Giri, A. P. (2017) Placental proteomics provides insights into pathophysiology of pre-eclampsia and predicts possible markers in plasma. *Journal Proteome Research* 16, 1050-1060.
 - **Mary, S.**, Kulkarni, M. J., Mehendale, S. S., Joshi, S. R., Giri, A. P. (2017) Tubulointerstitial nephritis antigen-like 1 protein is downregulated in the placenta of pre-eclamptic women. *Clinical Proteomics*. (DOI : 10.1186/s12014-017-9144-2, In press)
 - **Mary, S.**, Small, H. Y., Siwy, J., Mullen, W., Giri, A. P., Delles, C., (2017) Polymerization-incompetent Uromodulin in the Pregnant Stroke Prone Spontaneously Hypertensive
-

Rat. *Hypertension*. (DOI: 10.1161/HYPERTENSIONAHA.116.08826, In Press)

- **Mary, S.**, Kulkarni, M. J., Mehendale, S. S., Joshi, S. R., Giri, A. P. (2017) Differential accumulation of vimentin fragments in pre-eclamptic placenta. (manuscript submitted)
 - Bhat, S., **Mary, S.**, Banarjee, R., Giri, A. P., Kulkarni, M. J. (2014). Immune response to chemically modified proteome. *Proteomics Clinical Applications* 8, 19-34.
 - Kulkarni, M. J., Korwar, A., **Mary, S.**, Bhonsle, H. (2013). Glycated Proteome: From reaction to intervention. *Proteomics Clinical Applications* 7, 155-170.
 - **Mary, S.**, Patil, G. V., Kulkarni, A. V., Kulkarni, M. J., Joshi, S. R., Mehendale, S. S., Giri, A. P. (2012). Dynamic proteome in enigmatic preeclampsia: An account of molecular mechanisms and biomarker discovery. *Proteomics Clinical Applications* 6, 79-90.
-